U.S. Department
of Commerce

Volume 115
Number 3
July 2017

Fishery Bulletin

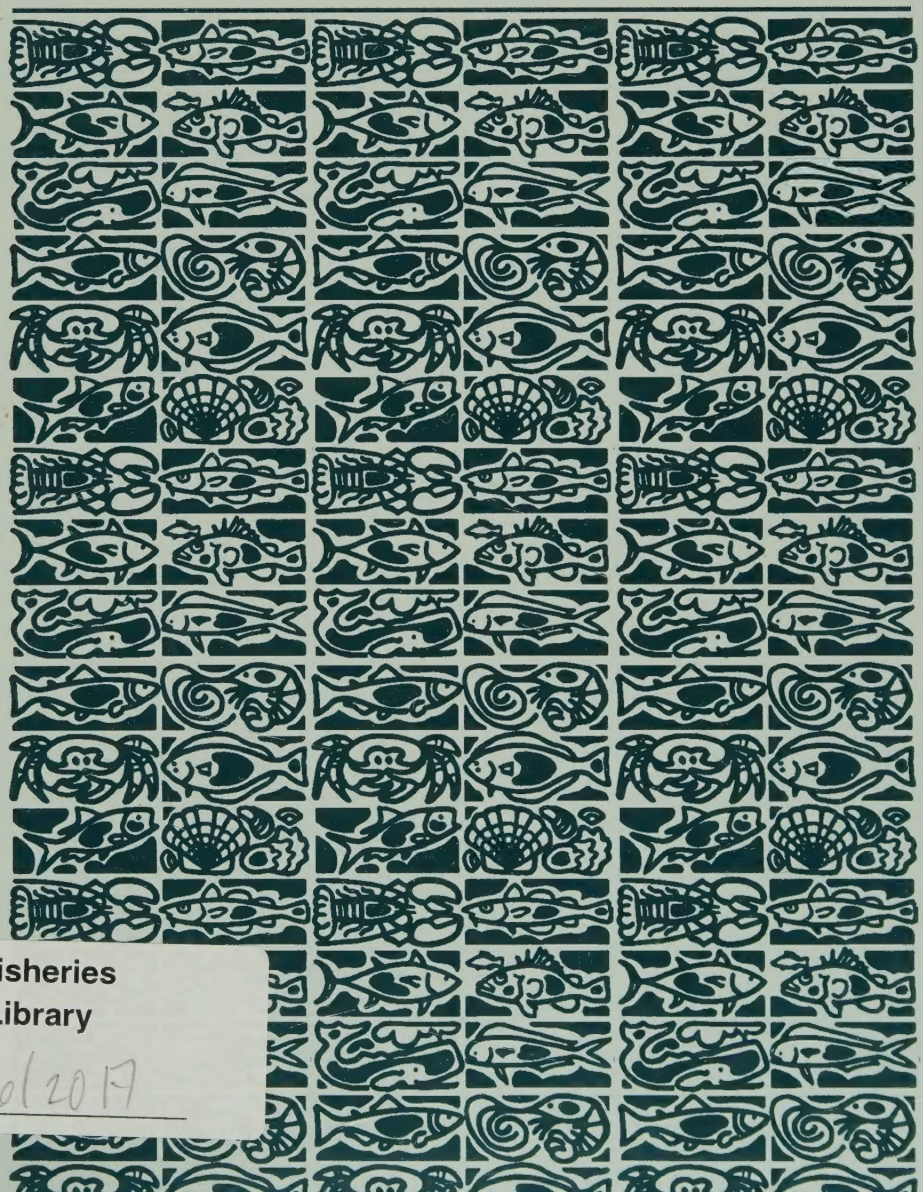

Pacific Islands Fisheries
Science Center Library

Received on: 11/6/2017

U.S. Department of Commerce
Wilbur Ross
Secretary

National Oceanic and Atmospheric Administration
Benjamin Friedman
Acting NOAA Administrator

National Marine Fisheries Service
Chris Oliver
Assistant Administrator for Fisheries

The *Fishery Bulletin* (ISSN 0090-0656) is published quarterly by the Scientific Publications Office, National Marine Fisheries Service, NOAA, 7600 Sand Point Way NE, Seattle, WA 98115-0070.

Although the contents of this publication have not been copyrighted and may be reprinted entirely, reference to source is appreciated.

The Secretary of Commerce has determined that the publication of this periodical is necessary according to law for the transaction of public business of this Department. Use of funds for printing of this periodical has been approved by the Director of the Office of Management and Budget.

For Sale by the Superintendent of Documents, U.S. Government Printing Office, Washington, DC 20402. Subscription price per year: $32.00 domestic and $44.80 foreign. Cost per single issue: $19.00 domestic and $26.60 foreign. **See back for order form.**

Fishery Bulletin

Scientific Editor
Richard Langton

National Marine Fisheries Service
Northeast Fisheries Science Center
Maine Field Station
17 Godfrey Drive, Suite 1
Orono, ME 04473

Managing Editor
Sharyn Matriotti

National Marine Fisheries Service
Scientific Publications Office
7600 Sand Point Way NE
Seattle, Washington 98115-0070

Associate Editor
Kathryn Dennis

National Marine Fisheries Service
Office of Science and Technology
1845 Wasp Blvd., Bldg. 176
Honolulu, Hawaii 96818

Editorial Committee

Richard Brodeur	National Marine Fisheries Service, Newport, Oregon
John Carlson	National Marine Fisheries Service, Panama City, Florida
Kevin Craig	National Marine Fisheries Service, Beaufort, North Carolina
John Graves	Virginia Institute of Marine Science, Gloucester Point, Virginia
Rich McBride	National Marine Fisheries Service, Woods Hole, Massachusetts
Rick Methot	National Marine Fisheries Service, Seattle, Washington
Bruce Mundy	National Marine Fisheries Service, Honolulu, Hawaii
David Sampson	Oregon State University, Newport, Oregon
Michael Simpkins	National Marine Fisheries Service, Woods Hole, Massachusetts
Dave Somerton	National Marine Fisheries Service, Seattle, Washington
Mary Yoklavich	National Marine Fisheries Service, Santa Cruz, California

***Fishery Bulletin* web site: www.fisherybulletin.noaa.gov**

The *Fishery Bulletin* carries original research reports on investigations in fishery science, engineering, and economics. It began as the Bulletin of the United States Fish Commission in 1881; it became the Bulletin of the Bureau of Fisheries in 1904 and the *Fishery Bulletin* of the Fish and Wildlife Service in 1941. Separates were issued as documents through volume 46; the last document was no. 1103. Beginning with volume 47 in 1931 and continuing through volume 62 in 1963, each separate appeared as a numbered bulletin. A new system began in 1963 with volume 63 in which papers are bound together in a single issue. Beginning with volume 70, number 1, January 1972, *Fishery Bulletin* became a periodical, issued quarterly. In this form, it is available by subscription from the Superintendent of Documents, U.S. Government Printing Office, Washington, DC 20402. It is also available free in limited numbers to libraries, research institutions, state and federal agencies, and in exchange for other scientific publications.

U.S. Department of Commerce
Seattle, Washington

Volume 115
Number 3
July 2017

Fishery Bulletin

Contents

Articles

273–283 **Walden, John B., Rolf Färe, and Shawna Grosskopf**

Measuring changes in productivity of a fishery with the Bennet–Bowley indicator

284–299 **Brown-Peterson, Nancy J., Robert T. Leaf, Amy M. Schueller, and Michael J. Andres**

Reproductive dynamics of Gulf menhaden (*Brevoortia patronus*) in the northern Gulf of Mexico: effects on stock assessments

300–325 **Kuykendall, Kelsey M., Eric N. Powell, John M. Klinck, Paula T. Moreno, and Robert T. Leaf**

Management strategy evaluation for the Atlantic surfclam (*Spisula solidissima*) using a spatially explicit, vessel-based fisheries model

326–342 **Hulson, Peter-John F., Dana H. Hanselman, and S. Kalei Shotwell**

Investigations into the distribution of sample sizes for determining age composition of multiple species

343–354 **Somerton, David A., Kresimir Williams, and Matthew D. Campbell**

Quantifying the behavior of fish in response to a moving camera vehicle by using benthic stereo cameras and target tracking

355–364 **López Quintero, Freddy O., Javier E. Contreras-Reyes, and Rodrigo Wiff**

Incorporating uncertainty into a length-based estimator of natural mortality in fish populations

The National Marine Fisheries Service (NMFS) does not approve, recommend, or endorse any proprietary product or proprietary material mentioned in this publication. No reference shall be made to NMFS, or to this publication furnished by NMFS, in any advertising or sales promotion which would indicate or imply that NMFS approves, recommends, or endorses any proprietary product or proprietary material mentioned herein, or which has as its purpose an intent to cause directly or indirectly the advertised product to be used or purchased because of this NMFS publication.

The NMFS Scientific Publications Office is not responsible for the contents of the articles.

365–379 Molina, Juan M., Gabriela E. Blasina, and Andrea C. Lopez Cazorla

Age and growth of the highly exploited narrownose smooth-hound (*Mustelus schmitti*) (Pisces: Elasmobranchii)

380–395 Tolotti, Mariana, Robert Bauer, Fabien Forget, Pascal Bach, Laurent Dagorn, and Paulo Travassos

Fine-scale vertical movements of oceanic whitetip sharks (*Carcharhinus longimanus*)

396–407 Macchi, Gustavo J., Karina Rodrigues, Marina V. Diaz, and María I. Militelli

Effects of skipped spawning on the reproductive potential of Argentine hake *(Merluccius hubbsi)*

408–418 Cullen, Daniel W., and Bradley G. Stevens

Use of an underwater video system to record observations of black sea bass (*Centropristis striata*) in waters off the coast of Maryland

419–432 Harter, Stacey L., Heather Moe, John K. Reed, and Andrew W. David

Fish assemblages associated with red grouper pits at Pulley Ridge, a mesophotic reef in the Gulf of Mexico

433–436 Guidelines for authors

National Marine
Fisheries Service
NOAA

Fishery Bulletin
established in 1881

Spencer F. Baird
First U.S. Commissioner
of Fisheries and founder
of *Fishery Bulletin*

Measuring change in productivity of a fishery with the Bennet–Bowley indicator

John B. Walden (contact author)[1]
Rolf Färe[2,3]
Shawna Grosskopf[4,5]

Email address for contact author: john.walden@noaa.gov

[1] Northeast Fisheries Science Center
National Marine Fisheries Service, NOAA
166 Water Street
Woods Hole, Massachusetts 02543

[2] Department of Economics and
Department of Applied Economics
Oregon State University
Ballard Extension Hall
Corvallis, Oregon 97331

[3] Department of Agricultural and
Resource Economics
University of Maryland
College Park, Maryland 20742

[4] Department of Economics
Oregon State University
Bexell Hall
Corvallis, Oregon 97331

[5] Centre for Environmental and Resource
Economics (CERE)
Department of Economics
Umeå University
S-901 87, Umeå, Sweden

Abstract—The U.S. National Marine Fisheries Service has undertaken to measure the economic performance of fisheries that have implemented catch shares as a management strategy. Among the metrics used, change in productivity was identified as important, and considerable research has been conducted to construct metrics and to measure this change. We introduce the Bennet–Bowley (BB) indicator as another tool to measure change in productivity, show how to construct the indicator, and apply it to the northeast multispecies fishery, which adopted a catch share system in 2010. The BB indicator is then used to show the contribution of vessels entering, continuing within, and exiting the fishery to overall fleet productivity. Results showed that after catch share management, fleet productivity declined and that vessels continuing in the fishery as a group contributed the most to a decline in aggregate productivity. On a per-vessel basis, a core group of vessels continuing in the fishery and that were present throughout the study period showed a decline in productivity after catch share management was implemented. These declines were caused by reduced outputs (i.e. catch) in relation to use of inputs (e.g. labor, fuel, materials) after catch shares were implemented.

Manuscript submitted 5 August 2016.
Manuscript accepted 16 March 2017.
Fish. Bull. 115:273–283 (2017)
Online publication date: 25 April 2017.
doi: 10.7755/FB.115.3.1

The views and opinions expressed or implied in this article are those of the author (or authors) and do not necessarily reflect the position of the National Marine Fisheries Service, NOAA.

Management of commercial and recreational fisheries has long been a topic of interest in public policy circles. This interest is due to the common pool nature of the resource, and the human dimension of the various user groups that rely on the resource for food, income, and recreational opportunities. Policy choices for the management of the resource are typically multidimensional, and involve a variety of regulatory instruments to control catch. Because management decisions are usually tied to the status of fish stocks, governments typically monitor and assess changes in the fish biomass on a regular basis. However, there is often not an equivalent monitoring system to track changes in the socio-economic status and well-being of resource users who depend on the fishery for part, or all, of their livelihood.

Gradually, there has been a shift in terms of assessing changes which take place among marine fishery user groups, particularly after important management modifications have taken place. In the United States, this shift in appraisal has been partially due to further adoption of "rights based management" in fisheries, also known as "catch shares," which secures a certain share of the total allowable catch (TAC) from a fishery for an individual vessel owner, community or association. Although catch shares have existed in some form since 1990 in U.S. fisheries, recent interest in expanding catch shares to multiple fisheries has generated interest in creating a consistent set of socio-economic performance indicators for these fisheries (Clay et al., 2014; Murphy et al., 2015). Currently, the same effort has not taken place for recreational fisheries. Consequently, the focus in our study will be on commercial fishing vessels.

The interest in evaluating economic and social changes centered on fishing fleets and communities is a positive development. It recognizes

that a more complete evaluation of management success includes changes that occur in the harvesting sector and how the people who depend on the resource for their livelihood are impacted by management choices. An initial set of indicators developed in the U.S. northeast region were broken into 5 broad groupings: financial viability, distributional outcomes (i.e. distibution of benefits and costs of a program among individuals, groups and communities), governance, stewardship, and well-being of fishermen and fishing communities (Clay et al., 2014). The choice of these categories was the result of a collaborative effort among economists and other social scientists in the northeast region.

Among the indicators of financial improvement, a change in productivity, hereafter "productivity change," has been the focus of a concerted effort within the U.S. National Marine Fisheries Service (Walden et al., 2012, 2015; Thunberg et al., 2015). Simply put, productivity change describes how the landings from fishing vessels, and the inputs (fuel, labor, materials) used to produce those landings change through time. This indicator is important because productivity change is directly tied to profit change. If, for example, prices for the fish landed are stable, and the inputs such as fuel used on a fishing trip do not change, profits can increase if vessels are able to produce more landings (outputs) for a given level of inputs.

Because fishing vessels typically land more than one species of fish and use several different inputs such as fuel, labor, and vessel capital to land fish, in order to measure productivity, both landings and inputs need to be aggregated into single values. Combining input and outputs into single values is typically done with aggregators, which are determined by either nonparametric or parametric programming methods, or by prices. In this article, we use prices to aggregate inputs and outputs. Once the landings produced (noted as 'Y') and the inputs used (noted as 'X') are aggregated into a single value, in any time period, productivity can be viewed as either the ratio of the output value aggregate Q(Y) to the input value aggregate Q(X) (i.e., $TFP=Q(Y)/Q(X)$), or the difference between the 2 quantities (i.e., $TFP=Q(Y)-Q(X)$). According to Diewert (2005), if the ratio measure of TFP is used (i.e. $Q(Y)/Q(X)$), the resulting measure is called an index, whereas if the second additive definition is used, the measure is called an indicator. In order to assess how productivity has changed between time periods, referred to as *t and 0*, productivity change is then either TFP_t/TFP_0, or $TFP_t - TFP_0$.

There have been a large number of studies in which an index number is used to measure change in productivity in fisheries (Squires, 1992; Jin et al., 2002; Fox et al., 2003; Brandt, 2007; Stephen and Vieira, 2013; Walden and Kitts, 2014; Pan and Walden, 2015). The difference between these studies was usually in the way in which the index number was constructed, and in the prices used to weight the inputs and outputs. In recent reports by the U.S. and Australian governments, index numbers were used to track trends over different time periods for multiple fisheries (Stephen and Vieira, 2013; Walden et al., 2015). However, there have been no studies that we are aware of in which an indicator has been used to measure changes in productivity in a commercial fishery.

In this study, we introduce and measure change in productivity on the basis of differences with the Bennet–Bowley (BB) indicator. The BB indicator is an attractive method to measure productivity change because it can be easily constructed in spreadsheet software and it has additive properties that allow one to construct the indicator at the vessel level and then aggregate results to the overall fishery level. It does not require complex statistical or aggregation methods to measure a change in productivity. Our work contributes to fisheries productivity studies by showing how the BB indicator can be constructed to examine change in productivity, and how it can then be aggregated to the fleet or fishery level. Therefore, the BB indicator becomes another measure of productivity that can be added to the growing toolbox of techniques used to measure a change in productivity in commercial fisheries. We also show how a simple volume indicator can be constructed to measure changing biomass, which can then be combined with the productivity measure to arrive at a measurement of biomass-adjusted productivity. As far as we know, our study is the first that specifically uses the BB indicator to assess change in productivity in a commercial fishery.

The BB indicator is used to measure change in productivity in the northeast multispecies fishery (i.e., groundfish fishery) over a period covering the transition to catch share management. It is used to examine both the contribution of vessels entering, exiting, and continuing within the groundfish fishery to productivity change, and also the impact of changing species mix and quantities of inputs used on productivity. Results show a significant decline in productivity after conversion to catch shares—a decline caused by declines in output quantities, and an overall decline in productivity among "continuing" vessels. Because continuing vesssels composed the largest vessel group, they had the most influence over total change in productivity. Breakdown of the BB indicator into groups of outputs and inputs showed that declines in quantities of outputs overwhelmed declines quantities of inputs after the catch share system was incorporated. Although vessels were able to reduce their use of inputs somewhat, the influence of declining outputs was greater and resulted in negative productivity. Until there is further growth in outputs resulting from improved biomass, or consolidation of the fleet, increases in productivity are unlikely to occur.

Materials and methods

We are interested in measuring both the overall productivity change at the fishery level, and the contribution of different segments of a fishing fleet to a change

in overall productivity. Specifically, we wish to examine how the productivity of vessels entering, exiting, and continuing within the fishery taken together influences the aggregate productivity measure. In order to accomplish both tasks, we use the BB indicator, which is a price-weighted arithmetic mean of the difference in the change in output quantities and input quantities used by firms (i.e., vessels) (Färe et al., 2008; Balk, 2010). First, we show how to derive the BB indicator, and then how it can be decomposed into 3 components: 1) the productivity of exiting vessels, 2) the productivity of entering vessels, and 3) the productivity of continuing vessels within the fishery. This decomposition will allow us to assess the contribution of each group to overall productivity. A similar approach was used to assess productivity gains in the mid-Atlantic individual transferable quota (ITQ) fishery for the Atlantic surfclam (Spisula solidissima) and ocean quahog (Arctica islandica) over a 30-year time period by using the Färe–Primont index (Färe et al., 2015). However, that approach required weighting individual productivity scores by input distance functions. The BB indicator differs because it requires no weighting of individual productivity measures, and it can be constructed in spreadsheets. Therefore, it is easier than the Färe-Primont approach for constructing the overall indicator. After examining the influence of entering and exiting vessels, we then extend the analysis in a different direction and use the additive nature of the BB indicator to determine how the composition of outputs produced and inputs used have influenced productivity change. The additive nature of the BB indicator allows us to see how landings mix and how changing input use have influenced productivity change.

In terms of notation, let $x^1 \in \Re^N_+$ be an input vector at time τ and let $y^1 \in \Re^M_+$ be an output vector, t=t,t+1. Let the corresponding prices be $w^1 \in \Re^N_+$ and $p^1 \in \Re^M_+$. The BB indicator takes the following form:

$$BB_t^{t+1} = \frac{1}{2}\left[\frac{p^t}{p^t g_y + w^t g_x} + \frac{p^{t+1}}{p^{t+1} g_y + w^{t+1} g_x}\right]\left[y^{t+1} - y^t\right] - \frac{1}{2}\left[\frac{w^t}{p^t g_y + w^t g_x} + \frac{w^{t+1}}{p^{t+1} g_y + w^{t+1} g_x}\right]\left[x^{t+1} - x^t\right] \quad (1)$$

$$= \frac{1}{2}\sum_{m=1}^{M}\left[\frac{p_m^t}{p^t g_y + w^t g_x} + \frac{p_m^{t+1}}{p^{t+1} g_y + w^t g_x}\right]\Delta y_m - \frac{1}{2}\sum_{n=1}^{N}\left[\frac{w_n^t}{p^t g_y + w^t g_x} + \frac{w_n^{t+1}}{p^{t+1} g_y + w^{t+1} g_x}\right]\Delta x_n, \quad (2)$$

which is a price-weighted difference between output change $y^t1 - y^t$ and input change $x^t1 - x^t$. The weights used, which are the terms in the square brackets are formed by using directional vectors (g_x, g_y), $g_x \in \Re^N_+$ and $g_y \in \Re^M_+$. Values need to be chosen for these vectors, and one possible choice is to set the directional vectors (g_x, g_y) equal to the observed input and output levels. Doing so makes the denominators in the bracketed term equal to the sum of total revenue and total cost. Instead, we set the value of the directional vectors equal to (1,1), which restricts the sum of the weights found in Equation 1 to equal one, and is consistent with share-valued weights.

Note that the weights include both outputs and input prices—a consequence of the fact that the indicator is derived from profit maximization. A useful property of the BB indicator is additivity, i.e., that the vessel-level BB indicators can be added together and it will be equivalent to the industry-level calculated BB indicator. We assume that each group and each unit member face the same prices which gives us our desired decomposition, namely the ability to group our fleet into 3 different sets of entering (N), continuing (C), and exiting (E) vessels, and the sum of the indicator for each group will equal the total indicator:

$$BB_t^{t+1} = (BB^C)_t^{t+1} + (BB^N)_t^{t+1} + (BB^E)_t^{t+1}. \quad (3)$$

To illustrate how the decomposition works, for new units the indicator equals

$$(BB^N)_t^{t+1} = \frac{1}{2}\left[\frac{p^t}{p^t g_y + w^t g_x} + \frac{p^{t+1}}{p^{t+1} g_y + w^{t+1} g_x}\right]\left(\sum_{k=1}^{K_n} y_k^{t+1}\right) - \frac{1}{2}\left[\frac{w^t}{p^t g_y + w^t g_x} + \frac{w^{t+1}}{p^{t+1} g_y + w^{t+1} g_x}\right]\left(\sum_{k=1}^{K_n} x_k^{t+1}\right). \quad (4)$$

Because these "new" units did not exist in period t, their inputs and outputs are zero at t. For the exiting units, inputs and outputs are zero in period t+1 and therefore the indicator equals

$$(BB^E)_t^{t+1} = \frac{1}{2}\left[\frac{p^t}{p^t g_y + w^t g_x} + \frac{p^{t+1}}{p^{t+1} g_y + w^{t+1} g_x}\right]\left(-\sum_{k=1}^{K_E} y_k^t\right) - \frac{1}{2}\left[\frac{w^t}{p^t g_y + w^t g_x} + \frac{w^{t+1}}{p^{t+1} g_y + w^{t+1} g_x}\right]\left(-\sum_{k=1}^{K_E} x_k^t\right). \quad (5)$$

Adjusting for a change in biomass with a volume indicator

Fishing vessels produce landed fish that are extracted from a stock, and changes in productivity between 2 periods are linked to the changes in fish stocks. For example, if a fish stock declines between years, a fishing vessel may still be able to maintain the same level of landings as those of the prior year by increasing effort, which means a greater use of inputs. Consequently, a productivity indicator such as the BB indicator would decline between years because the quantity of outputs would stay the same, whereas the quantity of inputs would increase. The relationship between productivity change and biomass change has been recognized for some time now. Failing to account for a change in biomass results in a measure of productivity that has been called "biased" in the past (Squires, 1992). More recent studies have used the terms "biomass adjusted" and "biomass unadjusted" productivity change (Walden

et al., 2015). What is usually important to managers and others is how policy changes have impacted productivity separately from changes in biomass, which is why a biomass-adjusted measure is desired.

Because we wish to isolate the change in productivity that is associated with changing outputs and inputs from a productivity change associated with changing fish biomass, a method needs to be used to separate productivity change from the change in biomass in the overall productivity metric. We follow the approach used by Jin et al. (2002) and construct an indicator of change in biomass which is then subtracted from the overall BB indicator. In this way, we are treating biomass as an input, recognizing that biomass is then transformed into an output by the fishing vessel. However, the biomass measure is subtracted from the overall BB indicator, rather than at the individual vessel level. From a social planner's perspective, biomass that is not harvested by the fleet during the current production period, has the potential to be transformed into an output in the next period. In our paradigm, the biomass is not under control of the vessel, and improvements in biomass in subsequent periods do not directly translate into increased future harvests because managers set the total allowable catch for each period.

The biomass indicator we choose has been developed previously and is called a "volume indicator" (VI) (Moosberg et al.[1]). The VI is calculated as follows:

$$VI = \frac{1}{2}(p^{t+1} + p^{t})(s^{t+1} - s^{t}) = \frac{1}{2}\left(\sum_{b=1}^{B} p_b^{t+1}s_b^{t+1} - p_b^{t+1}s_b^{t} + p_b^{t}s_b^{t+1} - p_b^{t}s_b^{t}\right), \quad (6)$$

where s = the spawning stock biomass of species b in period t or t+1; and
p = the price of species b in period t or t+1.

The VI is needed for multispecies fisheries so that all species in the multispecies complex can be included in a single composite indicator. However, the same formula can also be used for a single species fishery. After VI has been calculated, it is then subtracted from the unadjusted BB indicator to arrive at what we term a "biomass adjusted" indicator of productivity:

$$BB_{BA}^{t} = BB_{BU}^{t} - VI^{t}, \quad (7)$$

where subscript BA = biomass adjusted;
subscript BU = biomass unadjusted; and
t = time period.

The northeast multispecies fishery

Before describing the data that are used in the BB indicator, a brief description of the fleet and fishery are in order. There are 13 fish species included in the fishery management plan for what is commonly referred to as the New England groundfish fishery; additional species are caught as bycatch and are not considered part of the fishery management plan. The species included in the New England groundfish fishery are the American plaice (*Hippoglossoides platessoides*), Atlantic cod (*Gadus morhua*), Atlantic halibut (*Hippoglossus hippoglossus*), pollock (*Pollachius virens*), Atlantic wolffish (*Anarhichas lupus*), haddock (*Melanogrammus aeglefinus*), ocean pout (*Zoarces americanus*), Acadian redfish (*Sebastes fasciatus*), white hake (*Urophycis tenuis*), windowpane (*Scophthalmus aquosus*), winter flounder (*Pseudopleuronectes americanus*), witch flounder (*Glyptocephalus cynoglossus*), and yellowtail flounder (*Limanda ferruginea*). Atlantic wolffish, ocean pout, and windowpane are currently prohibited from being landed. The fishing fleet operates between Cape Hatteras, North Carolina, and the U.S.–Canadian border. In fishing year 2013 (1 May 2013–30 April 2014), the total exvessel value of landings from groundfish species landed in the fishery was approximately $55.2 million (U.S $2010), although revenue from both groundfish and non-groundfish species landed on groundfish trips was approximately $270 million. Revenue was estimated on the basis of 327 vessels that completed a designated groundfish trip.

In May 2010, Amendment 16 to the northest multispecies plan (available at website, accessed March 31, 2017) was implemented, which expanded the use of catch shares within a voluntary sector system. Vessel owners were allocated a share of the total allowable catch (TAC) for 9 different groundfish species[2] on the basis of their historical landings.[3] However, vessel owners were only allowed to catch their quota if they operated within a harvest cooperative (i.e., approved fishing sector). The amount of each species that could be potentially harvested by a sector (allowable catch entitlement, or ACE) is the sum of individual shares that each vessel brings into the sector. Sector management then set the rules for managing their portfolio of species for the benefit of sector members. Vessel owners wishing to buy, lease, or sell their ACE are subject to the trading rules for their respective sector. These rules may specify that trades take place within the sector before transactions are made with owners in a different sector. Thus, the ACE is not as freely tradable as an ITQ. Additionally, vessels are still subject to year round area closure regulations, which were retained from the prior plan, but fishermen may request exemptions from seasonal closures and trip limits.

[1] Moosberg, H. J., R. Färe, S. Grosskopf, and P. Roos, 2007. Volume and price indicators: decomposition and revenue with an application to Swedish pharmacies, 8 p. Department of Economics. Oregon State Univ., Corvallis, Oregon.

[2] Species included the Atlantic redfish, pollock, white hake, witch flounder,American plaice, winter flounder, yellowtail flounder, Atlantic cod, and haddock. Additionally, some species had TAC assigned by stock area. The qualifying period for determining each owner's TAC was 1996–2006.

[3] Under the prior Amendment 13, 2 small sectors had been allowed to form which both harvested Atlantic cod from Georges Bank. Amendment 16 substantially expanded the number of allowed sectors.

Each sector must hold an ACE (which includes both landings and discards) for all species in an area where a vessel is to fish. Because different species are often caught together in a single area, stocks for which where there is a low overall quota have the potential to shut off fishing of more abundant stocks, and are referred to as "choke" stocks. Once an ACE is exhausted for a single species in a sector, no further fishing in the stock area can take place by sector members, thereby limiting fishing for other species for which sectors have an available ACE. Essentially, there is not enough available supply of ACE for these stocks to satisfy demand for an ACE within the sector. Depending on the trading rules for a given sector, members can go outside their own sector to lease additional ACE if it is available and needed.

Before Amendment 16, vessels did not operate under hard quotas for most stocks, but rather under target TACs, which were set for the fishery as a whole. Under a target TAC, fishing could continue even if the TAC was exceeded, and then additional fishing restrictions would be put in place the following fishing year to adjust the harvest to an appropriate level given the excess harvest. In some respects, the catch share system is more restrictive than the past controls of fishing effort, although sector members can request waivers from some of the individual regulations on fishing effort that still exist. We also note that the hard quotas imposed would still be part of any management system chosen. When sectors were proposed as a management option, there was a great deal of uncertainty about future quotas. Nevertheless, it was hoped that the sector system would help stabilize a fleet that had been in a state of decline for several years. There was a sense that the system would allow the fishing fleet to get away from the "regulatory treadmill" that had plagued it for years with continually changing regulations to control fishing effort (Lee and Thunberg, 2013).

During the first year of the plan, roughly 98% of the ACE was held by vessels that joined sectors (Lee and Thunberg, 2013). It should be noted that each sector acts independently to further the self-interest of its members. Generally, vessel owners within a sector have been treating the quota they bring into a sector as their own allocation, such as they would have done within an ITQ system. Each sector member is jointly liable with other sector members if the sector exceeds its allocation for any stock. A large amount of monitoring takes place within sectors to ensure that allocation for any species is not exceeded.

Vessel owners that elected not to join a sector are allowed to use their vessels under the "common pool" system, where they are subject to regulations on fishing effort, along with an aggregate allowable catch limit (ACL) for each species. Under this system, each vessel is allocated a number of fishing days for the entire fishing year, and vessels are allowed to lease, buy, or sell days with other members of the common pool. However, trading is highly restricted because vessels can trade only with other vessels of similar size. This restriction was meant to prevent days from being transferred from vessels with low fishing power to those with higher fishing power. Vessels under the common pool system are also subject to the same year round area closures as are vessels fishing in the catch share system; moreover they are subject to seasonal closures from which sector vessels may obtain an exemption. The ACL applies to all vessels in the common pool and could potentially lead to fishing derbies as vessels try to fish their days as quickly as possible before the fishery is shut down. Currently, the ACLs for the common pool are divided into 3 trimesters to smooth catch levels over the year.

There are several different types of fishing vessels that harvest species managed in the fishery, but we limit this study to vessels which used otter trawl, gillnet, or longline gear and landed catch on identified groundfish trips. These gear groups are used to harvest the majority of the landings in this fishery and are consistent with the methods used by others to assess productivity change in this fishery (Murphy et al., 2015). Otter trawl nets are towed behind a vessel to catch fish and are considered a mobile gear. Fixed panels of nets are used with gillnet vessels and baited hooks on set lines in the water column are used with longline vessels, and both types of vessels then retrieve the fishing gear after a certain amount of time. Both gears are considered fixed gear. Between 2007 and 2013, the number of vessels in these gear groups declined dramatically, from 585 to 283 (Table 1). On average, the size of the vessels (by tonnage and horsepower) increased over the same time period, whereas the average number of trips declined and average days at sea increased. During 2013, the average number of trips was quite low (28.9), whereas the average days spent fishing increased to 55.2, the highest level during the time period. Average revenue, which was based on all species caught on trips which were identified as a multispecies trips, peaked in 2011 at $298,400 (U.S. $2010, Table 1). After 2011, revenue declined for the following 2 years. After implementation of the catch share system, revenues earned were higher than the 3 years before implementation of the management plan (2007–2009).

Data

In order to derive the BB indicator, data on quantities landed, inputs used to produce the corresponding landings, prices paid for the landings, and prices paid for the inputs used in the production process are needed. Because of the large number of species landed by groundfish vessels, the groundfish speices were separated into 6 different groups. Additionally, monkfish (*Lophius americanus*) was included in one of the groupings and the barndoor skate (*Dipturus laevis*), rosetta skate (*Leucoraja garmani*), winter skate (*Leucoraja ocellata*), clearnose skate (*Raja eglanteria*), thorny skate (*Amblyraja radiata*), little skate (*Leucoraja erinacea*), and smooth skate (*Malacoraja senta*) were broken out into their own category. These species are caught as bycatch on groundfish trips. The species groupings

Table 1

Number of vessels, mean physical characteristics, effort, and revenue for vessels used to derive the Bennet–Bowley productivity indicator in this study to measure productivity change before and after the implementation of a catch share system in 2010 for the northeast groundfish fishery.

Year	Vessels	Mean weight (metric tons)	Mean length (m)	Mean horsepower (hp)	Trips	Mean number of days fished	Mean value ($1000s U.S. 2010)
2007	585	54	16.2	426	39.9	44.4	210.2
2008	535	54	16.2	429	43	46.6	214.2
2009	489	52	16.2	428	45.8	47	209.8
2010	371	54	16.2	446	28	43	239.5
2011	344	57	16.5	455	34.9	54.6	298.3
2012	338	58	16.5	460	33	53.6	246.1
2013	283	59	16.8	467	28.9	55.2	241.6

were Atlantic cod, haddock, roundfish (pollock, white hake, and monkfish), flatfish (yellowtail flounder, witch flounder, winter flounder, American plaice), skates (barndoor, rosetta, winter, clearnose, thorny, little, and smooth skates), and an "other" category which was all other species.

Inputs included fuel, ice (for storing fish), bait (only on vessels using hook-and-line gear), crew services, and capital user cost. The quantity of fuel used on each trip was calculated from trip level regression models (Walden and Kitts, 2014). Fuel price ($2010, GDP implicit price deflator) was an average yearly price calculated from fuel prices collected on trips with an observer present (i.e., sampling trips). Crew services were the product of crew size obtained from vessel logbooks multiplied by the corresponding days the vessel spent at sea. Because crew members in this fishery are usually compensated by sharing in the proceeds from the trip, there is no observed wage rate (i.e., price of labor) to use in the index. Instead, the average hourly earnings for construction workers obtained from the Bureau of Labor Statistics (Current Employment Statistics, website, accessed March 2015) was used as a proxy for hourly crew wages because crews need to be compensated at least as much as they be for labor in other industries (i.e., opportunity cost). Although the choice of opportunity cost data may seem arbitrary, past studies have used similar approaches although the choice of alternative occupations has varied. For example, Squires (1992) used the average hourly wage in the retail, transportation, and manufacturing sectors in his study of the Pacific coast trawl fishery. Skirtun and Vieira (2012) used the hourly wages of agricultural workers in Australia in their study of profit drivers in Australian fisheries. Given the wide geographic distribution of vessels in our study (Maine to Virginia), we consider the wage rate for construction workers to be an appropriate measure for wages. Hourly wages multiplied by 8 was considered the daily opportunity cost of crew labor. The daily cost of food per crew member, calculated from sampling trips, was then added to the daily wage rate to obtain a total daily cost per crew member per day at sea.

In past studies, fishing vessel performance was mearsured by using the concept of capital services to measure the flow of capital (Squires, 1992; Dupont et al., 2005). In this study, we need both a price for capital and a quantity of capital for each time period. To calculate the price of capital during each period, we adopt the "capital user cost" concept (Balk, 2011), which is a per unit (vessel) cost constructed from 3 components: 1) the opportunity cost of capital, which reflects the the price which must be paid to an owner of an asset to prevent the asset from being sold (Balk, 2011); 2) the value change of the asset, which reflects both depreciation and re-investment in the asset (for the vessels in this study, only depreciation will be considered, because investment value is generally not available); and 3) the specific taxes levied on the use of an asset, which are not relevant to the fishing vessels in this study. We note that this approach is essentially the same method outlined by Christensen and Jorgenson (1969). However, we are limited in our ability to carry out these calculations because of a lack of data on investment value and because vessel values likely changed after the switch to sector management.

The value of capital was set at $5053 per meter of vessel length (Pan and Walden, 2015), and the interest rate used was the yield for BAA-rated bonds (Squires, 1992; Walden and Kitts, 2014) deflated to 2010 levels by using the GDP implicit price deflator. Depreciation was set at 6%, which was based on rates established by the U.S. Bureau of Economic Analysis. The quantity of capital used is the the percentage of recorded fishing time a vessel has spent in the groundfish fishery. A vessel that operates 100% of the time in the fishery has a value of 1. By making this adjustment, the entire capital user cost is not charged to the groundfish

Table 2

Bennet-Bowley (BB) productivity indicators, biomass volume indicator, and biomass-adjusted BB productivity indicator for the period 2007–2013. The BB indicator is based on 2 years of data; therefore, the values for the row labeled 2008, for example, are results for the time period 2007–2008.

Year	Output indicator	Input indicator	BB indicator[1]	Biomass indicator	Biomass-adjusted BB indicatior
2008	0.30	−0.07	0.37	−0.07	0.44
2009	0.11	−0.06	0.17	−0.21	0.38
2010	−0.94	−0.16	−0.79	−0.27	−0.52
2011	0.09	0.08	0.01	−0.06	0.07
2012	−0.79	−0.04	−0.75	−0.36	−0.39
2013	−0.25	−0.07	−0.18	−0.09	−0.09

[1]A BB indicator >0 indicates improvement, whereas a value <0 indicates decline.

fishery if the vessel operated part of the year in other fisheries (Färe et al., 2015).

In addition to fuel, labor, and capital, the quantity of ice used per trip was also included as an input category. Vessels that used longline gear included one additional input category, which was bait. Total bait cost was obtained from observer data, but it was only an aggregate cost with no price or quantity data. In order to include the quantity of bait, an average cost per day at sea for bait was calculated from sea sampling trips. Bait cost was then multiplied by days spent at sea (as recorded in the vessel logbooks) to obtain the total cost of bait for each trip. In the bait price and quantity components, days at sea were used as the quantity input, and the cost per day at sea for bait was the price component.

Results

The constructed BB indicator is shown with its component parts, namely the output indicator and input indicator, in Table 2. These are all normalized values ($1000s) where the normalization factor was the 2007 value of the overall quota (TAC) for most of the groundfish species (Table 2).[4] The 2007 TAC value was picked as a normalization factor so that both the BB indicator and the VI used to measure changes in biomass would be normalized by the same factor. The BB indicator is based on 2 years of data, consequently when interpreting the results in Table 2, the row labeled 2008 provides results for the time period 2007–2008. Unlike a ratio-based index number, the BB indicator can be either positive, or negative, with positive values indicating productivity increase and negative productivity decline.

The biomass-adjusted BB indicator showed increases in both 2008 and 2009, before dropping sharply in 2010, which was the first year of the new catch share system (Table 2)[5]. The drop-off was expected because the management system adopted strict catch limits and accountability measures for all participants. It was also consistent with the trend seen in the previously published Lowe index that was calculated for the annual performance report for this fishery (Murphy et al, 2015).[6] Although the Lowe index and BB indicator are not directly comparable, overall the trends were generally consistent with one another. Between 2011 and 2013, the biomass-adjusted BB indicator continued to decline.

Entry and exit

As the BB indicator has been constructed, vessels that exit the fishery and do not fish in a year will always contribute negatively to the overall indicator, whereas entering vessels will always contribute positively. Vessels continuing within the fishery may either contribute positively or negatively to the indicator. Results show that productivity changes in any year are primarily being driven by vessels continuing withing the fishery (Table 3). Only in 2011 did entering vessels contribute

[4] The species and stock areas included in the TAC value were Georges Bank Atlantic cod, Gulf of Maine Atlantic cod, Gulf of Maine haddock, southern New England yellowtail flounder, Gulf of Maine yellowtail flounder, American plaice, witch flounder, Georges Bank winter flounder, southern New England/mid-Atlantic winter flounder, white hake, and pollock.

[5] The species included in the biomass indicator were Georges Bank Atlantic cod, Gulf of Maine Atlantic cod, Gulf of Maine haddock, southern New England yellowtail flounder, Gulf of Maine yellowtail flounder, American plaice, witch flounder, Georges Bank winter flounder, southern New England/mid-Atlantic winter flounder, white hake, and pollock.

[6] The productivity estimates in the annual groundfish report were based on a 2007 base year, and were converted to annual changes to be consistent with the Bennet-Bowley indicator method.

Table 3

Bennet-Bowley productivity indicator values unadjusted for biomass change for continuing, entering, and exiting vessels for the period 2007–2013 in the northeast groundfish fishery. Note: 2010 was the year in which the catch share system was implemented for this fishery.

	Entering vessels		Continuing vessels		Exiting vessels		
Year	Indicator	No. of vessels	Indicator	No. of vessels	Indicator	No. of vessels	Total value of BB indicator
2008	0.06	51	0.39	484	−0.08	101	0.37
2009	0.03	49	0.21	440	−0.07	95	0.17
2010	0.04	36	−0.47	335	−0.36	154	−0.79
2011	0.10	52	0.04	292	−0.13	79	0.01
2012	0.07	52	−0.75	286	−0.08	58	−0.75
2013	0.02	27	−0.10	256	−0.09	82	−0.18

more to the indicator than vessels continuing within the fishery when both values were positive. However, the number of vessels in the group continuing within the fishery each year was far greater than the number of entering vessels, and the additive nature of the indicator means that they should be contributing more to the indicator unless entering vessels were much more productive than continuing vessels. Even if entering vessels are more productive, their low numbers mean that, in aggregate, they do not contribute as much to the metric of fleet productivity. The large contribution by continuing vessels in the aggregate measure is consistent with that of other studies, which show that continuing vessels were the largest group after a change to a catch share system and contributed the most to aggregate productivity change (Walden et al., 2012; Färe et al., 2015). A catch share system, whether it is a cooperative system or an ITQ system, creates a barrier to entry owing to limited quotas and the initial rules for allocation. Entering vessels may need to buy or lease a quota, and therefore be more productive to offset the quota cost.

There was a core group of vessels within the fleet in our study that was present in all 6 years. In order to determine whether the move to a catch share system changed the productivity of these vessels, a nonparametric Kruskal-Wallis test was used to compare their normalized BB indicators before and after catch shares were implemented on an individual vessel basis. Results from the Kruskal–Wallis test indicated that the distributions were not equal (chi-square: 94.9, df=1), and examination of the BB indicator showed that the postcatch share, the median value of the BB indicator (−0.003), was lower than the precatch share (0.002). This result was consistent with the results for the whole fleet, which showed productivity declines after the catch shares were implemented. It is also consistent with separate findings for this fishery, which showed declines in productivity after the catch share system was put in place (Murphy et al., 2015).

A final question regarding these core vessels—a question that existed throughout the entire study period—was whether there were persistent differences in performance between the vessels within this group. In order to examine this question, vessels were separated into quartiles depending on unadjusted productivity (i.e., without biomass considered) in 2008. Unadjusted productivity was used because the VI used to measure a change in biomass affected all vessels equally. In other words, it did not shift a vessel into a different quartile. Productivity for each group was then tracked for the remaining years in the study (Fig. 1). Tracking of vessel groups allowed us to see whether the vessesl with higher productivity contributed the most to the indicator throughout the remaining years.

Vessels that were in the top quartile (i.e., with a higher degree of productivity) during 2008 contributed positively to the overall productivity gain in both 2008 and 2009, and, as a group, contributed more than the other 3 quartiles combined. In 2010, this same group of vessels contributed the most to productivity decline. Interestingly, the bottom quartile group in 2008 was the only group that showed a positive productivity gain in 2010. In 2011, the top 2008 quartile contributed negatively to overall productivity gain, whereas the other 3 quartiles contributed positively. In 2012 the top 2008 quartile group contributed the most to productivity decline, although there was little difference among all 4 groups. In 2013, all 4 groups had a negative productivity gain, and the third quartile group contributed the most to productivity decline. Summarizing these findings in terms of the top 2008 vessels shows that productivity gains for these vessels before catch shares turned into productivity declines after the switch to the catch share system.

The reversal in economic status for the top quartile indicates that, before the implementation of catch shares, those vessels were successful within the framework of regulations controlling fishing effort that existed during that time period and perhaps aided by permission to lease fishing days and the lack of hard

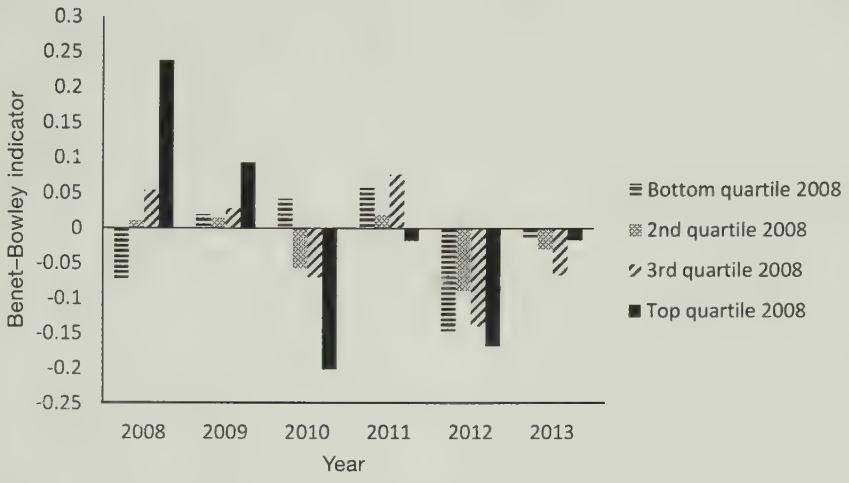

Figure 1

Bennet–Bowley (BB) productivity indicator values unadjusted for biomass change during 2008–2013 and shown by quartile (where the "top quartile" represents vessels with the highest degree of productivity in 2008). The BB indicator was used to measure a change in productivity before and after the implementation of a catch share system in 2010 in the northeast groundfish fishery.

quotas on several species. During the catch share era (2010–2013), negative productivity gains occurred for these vessels in all 4 years. Unlike procedures of the precatch share era (2008–2009), the inability to continue fishing because of concerns about the proportion of bycatch in relation to target species in catches, and a lack of ACE for key species, may be hindering the ability of fishing crews to post productivity gains. Over time, these vessels may again be leaders in productivity gain, but it may take time for new trading arrangements and other institutional changes to allow these gains to occur.

Changes in outputs and inputs

Vessels could also improve their productivity by changing their input use, or switching their output targets, and harvesting a different mix of species. The output and input portions of the BB indicator can be examined separately, and doing so showed that, in both 2008 and 2009 before catch shares were implemented, the output indicator increased, whereas the input indicator decreased (Table 2). The years 2008 and 2009 were years before catch shares were implemented, and all vessels were under an input control system. The ability to reduce input use and increase outputs led to productivity gains during that time period. In the first year of the new management regine (2010), both the output and input indicators decreased. In the following year, 2011, the input indicator increased, and this year was the only one in the time series when this increase occurred. This gain is consistent with gain in the data seen in Table 1, where both days at sea and the number of trips increased in 2011, along with an increase in the average size of vessels operating in the fishery. Generally, in years where both the output indicator and input indicator declined, the declining use of inputs was not enough to offset the declining outputs, and productivity declined.

One possible reason for the continuing decline in the output indicator could be deterioration of the fish stock biomass. Because the biomass indicator developed above is an additive measure, it can be used to both adjust the productivity metric and to examine trends in the species-specific components of overall biomass. A negative value in the biomass indicator indicates reduced fish biomass. Between 2008 and 2013, the biomass indicator was negative in all years (Table 2). The year 2010, which was the first year of the catch share plan, showed a particularly large drop in the VI (–0.27).

Although the biomass indicator is used to adjust the BB indicator, it does not give a complete picture of how biomass is impacting vessel output. Specifically, if there are species interactions among the various stocks where they are caught jointly, the most constraining stock would likely be limiting catches of other stocks. Availability of species may also change if there is a spatial shift in the distribution of species. For example, species may shift more offshore to deeper colder water because of environmental changes. With a catch share system where quotas can be "unbundled" and leased on a species basis, it may be possible for quotas to be traded in a manner such that vessels that are specialists in one species can lease or buy quota that will not constrain their activities. The trading arrangements which would facilitate "unbundling" of quotas, however, may take some time to evolve.

There is also a question of how the use of inputs changes after the transition to catch shares is implemented. Again, the additive property of the indicator shows how vessels altered their use of inputs after the transition to the new catch share plan (Table 2). With the exception of 2011, the total amount of inputs used by the fleet declined. The largest decline in the use of inputs occurred in 2010, the first year of the catch share plan. This drop in inputs was expected because the catch share plan gave vessels the opportunity to use their inputs differently as their output mix changed, or to exit the fishery. In an output-constrained fishery, reducing the use of inputs and the cost of fishing leads to increasing profitability (Squires et al., 2016).

Discussion

The BB indicator is a powerful tool that can be used to assess productivity change in commercial fisheries. The additive nature of the indicator allows it to be used for examining productivity change starting at the individual vessel level and then aggregating the individual results to the fleet or fishery level. Individual vessels can be grouped into different categories for comparison, such as entering, continuing, and exiting vessels, and it is possible to determine which groups are contributing the most to productivity change. Moreover, grouping vessels into different fleet segments can give managers additional insight into changes that have occurred in response to regulatory actions.

We applied the BB indicator to measure productivity change in the northeast multispecies fishery and found that productivity declined after catch shares were implemented because outputs declined more than inputs declined. There are a number of plausible reasons why outputs declined so much, but it is likely to have occurred because of lower quotas for key stocks. Because catches usually include a mixture of species, lower quotas for key species would constrain the catch of other more abundant species. These key species are usually referred to as "choke" species.

The BB indicator was used to examine the contribution of entering, continuing, and exiting vessels to productivity change. Results showed that continuing vessels contributed the most to productivity change each year because they were the largest fleet segment. This specific catch share system allows incumbent vessels some degree of protection from new entrants with no catch history because incumbent vessels are guaranteed a portion of the overall quota for each species for which they have catch history. As long as they can fish that quota profitably, they need not exit the fishery. The lack of improved productivity is similar to findings from studies of 2 other fisheries after implementation of ITQ systems in other parts of the world. In the first, gains in economic efficiency in a Norwegian purse-seine fishery did not occur after transition to an ITQ, and this outcome was attributed partially to the grandfathering of fishing rights (Nøstbakken, 2012). In a different study, after an ITQ system was implemented for the Peruvian anchovy fishery, productivity gains did not occur, but price increases did occur (Natividad, 2015). Over time, there may be productivity gains both in these 2 fisheries and the fishery we highlighted, but such gains are still uncertain. Although we expect less productive vessels to exit over time, externalities still exist that work against productivity gains. For example, vessels can still be displaced spatially by other vessels. If this displacement occurs, some crews (i.e., vessels) may have to use more inputs to reach new fishing areas, and overall vessel productivity may decline depending on how all the vessels adjust their fishing patterns.

An important part of any exercise that examines productivity trends for fisheries is adjustment for biomass change. Managers wish to know the impact of their policies on productivity of the fleet separately from any changes caused by differences in biomass. A volume indicator was constructed, which is similar to the BB indicator, to adjust for biomass in the fishery. The value of the volume indicator was subtracted from the BB indicator to arrive at a biomass-adjusted BB indicator. Declining biomass leads to a negative volume indicator, and subtracting this value means the adjusted BB indicator will be greater than the unadjusted BB indicator. In other words, productivity apart from biomass would increase. In this study, the biomass adjustment did not change the sign of the BB indicator, but it did change the magnitude. Negative productivity changes were still negative, but not as negative as the unadjusted productivity indicator. The issue of adjusting the productivity metric by biomass change is important, and further research needs to be conducted on making adjustments at the vessel level to account for biomass change. Because the fleet BB indicator is an aggregate value, subtracting the biomass indicator is an acceptable approach.

Productivity change is an important economic metric for managers to track when gauging economic performance, and the BB indicator is a very easy to construct and flexible measure. However, productivity change is just one metric and needs to be combined with other metrics, such as price changes, profitability, and fleet size to give meaningful signals to managers. The northeast groundfish fishery is still in a transition phase in terms of vessels fully adjusting to the catch share system, and productivity gains may not be seen for several years, particularly if stock conditions do not improve. However, productivity change in a fishery will be limited because the vessels are harvesting a finite resource, and in any year total output is capped by the allowable harvest. Fishery regulations are designed to limit output, and productivity gains will eventually peak even with full transferability of quota. Ultimately, managers may want to move toward a measure of profitability, rather than productivity, if there are enough cost data available to gauge economic performance. Profitability would give a better indication of the health of the fishing fleet than productivity by itself.

Acknowledgments

We thank E. Thunberg, M. Simpkins, and 2 anonymous reviewers for helpful comments and suggestions. This research was funded by the Office of Science and Technology, National Marine Fisheries Service. The views in this article are the authors alone and do not represent those of Oregon State University.

Literature cited

Balk, B. M.
2010. An assumption-free framework for measuring productivity channge. Rev. incone wealth 56:S224–S256.
2011. Measuring and decomposing capital input cost. Rev. Income Wealth 57:490–512.

Brandt, S.
2007. Evaluating tradable property rights for natural resources: the role of strategic entry and exit. J. Econ. Behav. Organ. 63:158–176.

Christensen, L. R., and D. W. Jorgenson.
1969. The measurement of U.S. real capital input, 1929–1967. Rev. Income Wealth 15:293–320.

Clay, P. M., A. Kittts, and P. Pinto da Silva.
2014. Measuring the social and economic performance of catch share programs: definition of metrics and application to the U.S. Northeast Region groundfish fishery. Mar. Policy 44:27–36.

Diewert, W. E.
2005. Index number theory using differences rather than ratios. Am. J. Econ. Sociol. 64:311–360.

Dupont, D. P., K. J. Fox, D. V. Gordon, and R. Q. Grafton.
2005. Profit and price effects of multi–species individual transferable quotas. J. Agric. Econ. 56:31–57.

Färe, R., S. Grosskopf, and D. Margaritis.
2008. Efficiency and productivity: Malmquist and more. *In* The measurement of productive efficiency and productivity growth (H. O. Fried, C. A. K. Lovell, and S. S. Schmidt, eds.) p. 522–621. Oxford Univ. Press, New York.

Färe, R., S. Grosskopf, and J. Walden.
2015. Productivity change and fleet restructuring after transition to individual transferable quota management. Mar. Policy 62:318–325.

Fox, K. J., R. Q. Grafton, J. Kirkley, and D. Squires.
2003. Property rights in a fishery: regulatory change and firm performance. J. Environ. Econ. Manage. 46: 156–177.

Jin, D., E. Thunberg, H. Kite-Powell, and K. Blake.
2002. Total factor productivity change in the New England groundfish fishery: 1964–1993. J. Environ. Econ. Manage. 44:540–556.

Lee, M.-Y. A., and E. M. Thunberg.
2013. An inverse demand system for New England groundfish: welfare analysis of the transition to catch share management. Am. J. Agric. Econ. 95:1178–1195.

Murphy, T., A. Kitts, C. Demarest, and J. Walden.
2015. 2013 final report on the performance of the northeast multispecies (groundfish) fishery (May 2013–April 2014). U.S. Dep. Commerce, Northeast Fish. Sci. Cent. Ref. Doc. 15-02, 106 p. Document

Natividad, G.
2015. Quotas, productivity, and prices: the case of anchovy fishing. J. Econ. Manage. Strategy 25:220–257.

Nøstbakken, L.
2012. Investment drivers in a fishery with tradable quotas. Land Econ. 88:400–424.

Pan, M., and J. Walden.
2015. Measuring productivity in a shared stock fishery: a case study of the Hawaii longline fishery. Mar. Policy 62:302–308.

Skirtun, M., and S. Vieira.
2012. Understanding the drivers of profitability in Commonwealth fisheries electronic resource. ABARES Tech. Rep. 12.4, 46 p. Aust. Bur. Agric. Res. Econ. Sci., Canberra, Australia.

Squires, D.
1992. Productivity measurement in common property resource industries: an application to the Pacific coast trawl fishery. RAND J. Econ. 23:221–236.

Squires, D., M. Maunder, N. Vestergaard, V. Restrepo, R. Metzner, S. Herrick Jr., I. del Valle, and P. Andersen.
2016. Effort rights in fisheries management: General principles and case studies from around the world. *In* Effort rights in fisheries management: general principles and case studies from around the world; Bilbao, Spain, 17–20 September 2012 (D. Squires, M. Maunder, N. Vestergaard, V. Restrepo, R. Metzner, S. Herrick Jr., R. Hannesson, I. del Valle, and P. Andersen, eds.), p. 1–9. FAO Fish. Aquac. Proc. 34. FAO, Rome.

Stephan, M., and S. Vieira.
2013. Productivity analysis of key Commonwealth fisheries. ABARES Tech. Rep. 13.09, 44 p. Aust. Bur. Agric. Res. Econ. Sci., Canberra, Australia. [Available from website.]

Thunberg, E., J. Walden, J. Agar, R. Felthoven, A. Harley, S. Kasperski, J. Lee, T. Lee, A. Mamula, J. Stephen, and A. Strelcheck.
2015. Measuring changes in multi-factor productivity in U.S. catch share fisheries. Mar. Policy 62:294–301.

Walden, J. B., and N. Kitts.
2014. Measuring fishery profitability: an index number approach. Mar. Policy 43:321–326.

Walden, J. B., J. E. Kirkley, R. Färe, and P. Logan.
2012. Productivity change under an individual transferable quota management system. Am. J. Agric. Econ. 94:913–928.

Walden, J., B. Fissel, D. Squires, and N. Vestergaard.
2015. Productivity change in commercial fisheries: an introduction to the special issue. Mar. Policy 62:289–293.

National Marine
Fisheries Service
NOAA

Fishery Bulletin
established in 1881

Spencer F. Baird
First U.S. Commissioner
of Fisheries and founder
of *Fishery Bulletin*

Reproductive dynamics of Gulf menhaden (*Brevoortia patronus*) in the northern Gulf of Mexico: effects on stock assessments

Nancy J. Brown-Peterson (contact author)[1]
Robert T. Leaf[1]
Amy M. Schueller[2]
Michael J. Andres[1]

Email address for contact author: nancy.brown-peterson@usm.edu

[1] Division of Coastal Sciences
School of Ocean Science and Technology
The University of Southern Mississippi
703 East Beach Drive
Ocean Springs, Mississippi 39564
Present address for contact author: Center for Fisheries Research and Development
Gulf Coast Research Laboratory
The University of Southern Mississippi
703 East Beach Drive
Ocean Springs, Mississippi 39564

[2] Beaufort Laboratory
Southeast Fisheries Science Center
National Marine Fisheries Service, NOAA
101 Pivers Island Road
Beaufort, North Carolina 28516

Abstract—Gulf menhaden (*Brevoortia patronus*) produce one of the largest U.S. fisheries, yet information on reproductive dynamics of the stock is sparse. Males and females reach 50% maturity at 140.8 and 137.2 mm fork length, respectively and recruit into the commercial fishery at this size. Analysis of fishery-dependent data from 1964 through 2014 indicated that somatic condition was lower during the late 1980s and late 2000s and that reproductively active fish from 2014 were significantly larger and had greater gonadosomatic index values than those from 1964 through 1970. Histological analysis performed on fish from 2014 through 2016 revealed spawning-capable and actively spawning fish of both sexes from early October through mid-March. Females have indeterminate fecundity, are batch spawners, and spawn every 2.1–4.3 days, although oocyte recruitment shows some characteristics of determinate fecundity. Mean relative batch fecundity was 107.8 eggs/g ovary-free body weight (standard error 17.1). Estimates from age-structured assessment models based on updated fecundity and maturity measures resulted in a 100–1000× greater production of eggs than previous estimates. Model output, including the number-at-age, age-specific fishing-induced mortality, and spawners-per-recruit are sensitive to alterations in age-specific annual fecundity. Therefore, updated estimates of Gulf menhaden reproductive dynamics can affect assessments of the stock.

Manuscript submitted 1 August 2016.
Manuscript accepted 28 March 2017.
Fish. Bull. 115:284–299 (2017).
Online publication date: 9 May 2017.
doi: 10.7755/FB.115.3.2.

The views and opinions expressed or implied in this article are those of the author (or authors) and do not necessarily reflect the position of the National Marine Fisheries Service, NOAA.

Gulf menhaden (*Brevoortia patronus*), family Clupeidae, are exploited by an industrial purse seine fleet and a smaller purse-seine bait fleet in the northern Gulf of Mexico (GOM). The fishery comprises the largest catches, by weight, of any fishery in the lower contiguous United States (Vaughn et al., 2007; VanderKooy and Smith[1]). The majority of the commercial landings (>99%) are harvested for the reduction fishery at 3 facilities based along the GOM coast (Moss Point, Mississippi, and Empire and Abbeville, Louisiana), which operates from the third Monday in April through October 31 (Vaughan et al., 2007). Harvest data for Gulf menhaden are estimated from daily catch records. The most recent Gulf menhaden stock assessment was completed in 2013 (SEDAR[2]) and updated in October 2016 (Schueller[3]). Although the fishery has economic and ecological importance, changes in the biological aspects of the stock in the past 5 decades of exploitation have not been described, particularly those related to reproduction.

[1] VanderKooy, S. J., and J. W. Smith (eds.). 2015. The menhaden fishery of the Gulf of Mexico, United States: a regional management plan, 2015 rev. Gulf States Mar. Fish. Comm., No. 240, 200 p. Gulf States Mar. Fish. Comm., Ocean Springs, MS. [Available from website, accessed June 2016].

[2] SEDAR (Southeast Data, Assessment, and Review). 2013. SEDAR 32A—Gulf of Mexico menhaden stock assessment report, 422 p. SEDAR, North Charleston, SC. [Available from website, accessed June 2016].

[3] Schueller, A. 2016. GDAR 02—Gulf menhaden stock assessment: 2016 update. Gulf States Mar. Fish. Comm., GSMFC No. 254, 65 p. GSMFC, Ocean Springs, MS. [Available from website.]

Relatively little recent work has been done to describe the reproductive dynamics of Gulf menhaden. Gulf menhaden spawn offshore in high-salinity waters (Fore, 1970; Sogard et al., 1987). Larvae are transported to estuaries from late winter through early spring (Shaw et al., 1985; Govoni, 1997), and juveniles remain in the estuary until they move offshore the following fall. Females in spawning condition have been documented to occur from September to April, but the reported peak spawning season occurs between December and February (Combs, 1969; Lewis and Roithmayr, 1981). Gulf menhaden are batch spawners (Lewis and Roithmayr, 1981), but the duration of the spawning season, the frequency with which an individual spawns, and annual fecundity are not well known, but are likely age- and length-dependent (see Lowerre-Barbieri et al., 2011). Because accurate age-specific spawning seasonality, batch fecundity (BF), and estimates of spawning frequency have not been reported for Gulf menhaden, the fecundity estimates reported by Lewis and Roithmayr (1981), currently employed in the stock assessment model used for Gulf menhaden, may be inaccurate. Such inaccuracies can lead to a biased understanding of the reproductive capability of the stock.

Our objective is to determine the characteristics of the reproductive biology of Gulf menhaden in order to assess their effects on stock assessments and to understand historical patterns of reproductive output. We provide information on the reproductive biology of Gulf menhaden, including size-at-maturity, the duration and timing of the spawning season, individual ovarian and testicular dynamics, BF, and spawning frequency, and incorporate age-specific fecundity data into an age-structured stock assessment model to understand how updated estimates can change our understanding of the Gulf menhaden stock. Finally, we evaluate historic changes in the demographic characteristics of the Gulf menhaden stock by comparing data collected from the commercial fishery from 1964 through 2014. This research is intended to improve a general understanding of the dynamics of the Gulf menhaden stock and provide information for management.

Materials and methods

Collection of samples

Gulf menhaden were collected from Mississippi and Louisiana coastal waters of the northern GOM from August to October 2014, from January to June 2015, November 2015, and from January to February 2016. Samples were obtained opportunistically from purse-seine boats at the Omega Protein reduction facility at Moss Point, Mississippi, during the commercial fishing season (from April to October) and from commercial shrimp trawls in February 2015. Gulf menhaden were also obtained during trawl and gillnet sampling by the Louisiana Department of Wildlife and Fisheries (LDWF) and the University of Southern Mississippi (USM) Center for Fisheries Research and Development (CFRD) in the winter and early spring. When possible, biological data were collected from fish within 24 h of capture from fresh fish stored on ice. All collections obtained from LDWF, and some collections from Omega Protein, were frozen upon capture, and these specimens remained fully or partially frozen during the recording of biological data.

Fish were measured for fork length (FL) in millimeters and weighed (W) in grams, and scales were removed from along the lateral line, below the insertion of the dorsal fin, rinsed, and stored in paper coin envelopes for age determination, consistent with current fishery age-sampling methods. Sex was macroscopically determined, and gonads were removed and weighed (GW) to the nearest 0.01 g. The gonadosomatic index (GSI) and condition factor (K) were calculated as:

$$GSI = (GW/(W - GW)) \times 100 \quad (1)$$

$$\text{and } K = (W/FL^3) \times 100{,}000. \quad (2)$$

Gonads were macroscopically classified into reproductive phases according to the terminology of Brown-Peterson et al. (2011), and a portion of the left gonad from each fish was placed into individually labeled cassettes and preserved in 10% neutral buffered formalin for histological analysis. Gonadal tissue from frozen specimens was placed in cold (4°C) formalin and allowed to thaw in the refrigerator in the fixative to minimize damage to the frozen tissues and improve the histological preparations.

Age determination

Individual ages were determined by methods consistent with the Gulf menhaden stock assessments (VanderKooy[4]). Collected scales were rinsed in warm tap water, dried, and mounted onto glass slides (n=10 scales/fish). Age estimates were determined by counting annuli on images that were projected by using an Eberbach[5] macro-projector (Eberbach Corp., Ann Arbor, MI) at 48× magnification. A birthdate of 1 January was assigned for all fish (SEDAR[2]). Fish captured in January and February that had scales with a large margin beyond the last annulus were classified as a year older.

Reproductive biology

Histological processing of gonadal tissues followed standard techniques. Tissues were fixed for a minimum of 1 week, rinsed overnight in running tap water, dehydrated in a series of graded ethanols, and embed-

[4] VanderKooy, S. (ed.) 2009. A practical handbook for determining the ages of Gulf of Mexico fishes, 2nd ed. Gulf States Mar. Fish. Comm., Publ. No. 167, 136 p. Gulf States Mar. Fish. Comm., Ocean Spring, MS. [Available from website, accessed June 2016].

[5] Mention of trade names or commercial companies is for identification purposes only and does not imply endorsement by the National Marine Fisheries Service, NOAA.

ded in paraffin. Tissues were cross sectioned at 4 µm and stained with hematoxylin and eosin. Microscopic inspection of testicular and ovarian tissues and evaluation of spermatogenesis and oogenesis followed the method of Brown-Peterson et al. (2011). Reproductive phases were assigned to males and females (Brown-Peterson et al., 2011), and included immature, developing (with the early developing subphase), spawning capable (with the actively spawning sub-phase for females), regressing, and regenerating. Additionally, broad reproductive descriptors of males and females were defined as reproductively active (including the developing, spawning capable, and actively spawning phases) or reproductively inactive (including the immature, early developing, regressing, and regenerating phases).

Females assessed macroscopically to be in the actively spawning subphase were sampled for fecundity by placing a weighed portion (0.01 g) of the ovary into Gilson's fixative or 10% neutral buffered formalin. Ovarian tissue fixed in Gilson's fixative remained in solution for a minimum of 3 months prior to analysis; tissue fixed in 10% formalin remained in solution 1 month before analysis. Tissues were rinsed overnight in running water and oocytes remaining attached to ovarian tissue were teased apart. The volumetric method (Bagenal and Braum, 1971) was used to determine BF (number of eggs), and 6 replicate samples of all oocytes ≥500 µm, representing oocytes undergoing oocyte maturation (OM), were counted. To determine the correct size of oocytes to count for fecundity determinations, all oocytes >80 µm from an actively spawning fish were counted and measured in a 1-mL subsample. Oocyte size-frequency graphs were constructed, and only oocytes ≥500 µm that presented a distinct mode at the end of the distribution were counted. This largest batch of oocytes was verified histologically to be either hydrated or undergoing OM for each sample analyzed. Additionally, the oocyte size-frequency distribution of secondary growth oocytes (>80 µm) of fish in the actively spawning sub-phase at the beginning (October) and end (March) of the reproductive season was plotted to identify the fecundity pattern (determinate or indeterminate) of Gulf menhaden, following procedures described by Lowerre-Barbieri et al. (2011).

Spawning frequency of females was determined by calculating the percentage of females in the spawning capable phase (including the actively spawning subphase) with 1) ≤24 h postovulatory follicle complex (POF) or 2) oocytes undergoing OM after procedures as outlined in Brown-Peterson and Warren (2001). Spawning frequency data were used in combination with BF data to estimate total annual fecundity.

Using fecundity data in the stock assessment

The Beaufort Assessment Model (BAM) is the primary assessment model used for the federal stock assessment of Gulf menhaden (Williams and Shertzer, 2015). Data inputs include a suite of fishery-independent and fishery-dependent data, and the model is age structured. Aging error was included in the model, as in the "base" formulation of the BAM during the last benchmark assessment (see SEDAR[2] for the aging error matrix). Natural mortality was assumed to be time invariant, but age varying. The sex ratio was fixed at 1:1 and the parameters of the von Bertalanffy growth function were estimated internally and constant. Fish were assumed to spawn on 1 January, and therefore all reproductive values in the stock assessment correspond to 1 January. The maturity ogive was fixed such that 0% of individuals were mature at age 0 and age 1 and 100% were mature at age 2. Mean lengths at age on 1 January were used to calculate mean fecundity at age on 1 January. Recruitment was modeled with a Beverton–Holt stock recruitment curve and steepness was fixed at 0.75. Selectivity for the commercial reduction fishery was assumed to be dome shaped and only age-1 selectivity was estimated. Constant catchability was estimated for each of the 2 fishery-independent gears (gill and seine nets) used to sample the stock. Gillnet sampling targets age-1 to 4+ fish, whereas seine net sampling targets predominately age-0 fish.

We compared the estimates from the "base" formulation of the BAM, that incorporates age-specific fecundity estimates from Lewis and Rothymayr (1981) and the maturity schedule described above, with BAM-derived estimates based on alternative formulations from reproductive dynamics described in this work. We incorporated 2 changes to the input variables in the BAM model: the magnitude of individual egg production and the maturity schedule. We used "high" and "low" estimated annual fecundity that were based on the mean length-specific egg production of each age class, given length-at-age on 1 January, and the minimum and maximum estimated number of annual spawns for each age class. The high annual fecundity scenario assumes more frequent spawning for each individual relative to the low annual fecundity scenario. We also altered the age-specific maturity schedule based on the length-specific maturity relationship we developed. We evaluated the temporal trends in the magnitude of egg production of the stock and the maximum proportion of spawners-per-recruit of the stock for each scenario. We also evaluated the year-specific percent difference in number at age and instantaneous annual fishing mortality (F) at age between the base model used in the 2012 stock assessment and the base model used in the 2013 stock assessment, using the logistic relationship described in this work.

Comparisons of historical data

To assess historic changes in the Gulf menhaden stock in the northern Gulf of Mexico (Mississippi and Louisiana) we used data (NMFS[6]) obtained from the com-

[6] NMFS (National Marine Fisheries Service). 2015. Unpubl. data. Gulf menhaden biostatistical database. [Available from Beaufort Laboratory, Southeast Fish. Sci. Center., Natl. Mar. Fish. Serv., 101 Pivers Island Rd., Beaufort, NC 28516.]

mercial fishery from 1964 to 2014 and archived at the National Marine Fisheries Service (NMFS) Beaufort Laboratory. At each commercial reduction plant operating during these years, a sample of fish was taken from the top of the fish hold. Ten (1971–2014) or 20 (1964–1970) fish were haphazardly selected from that sample. Each fish was weighed (in grams), measured for FL (Schueller et al., 2012), and a scale patch was removed for aging. For fish collected from 1964 to 1970, sex was determined, and gonads were weighed (in grams) and macroscopically classified according to NMFS criteria (Huntsman and Chapoton, 1973). For these data, females were considered reproductively active with a GSI≥1.0 and males were considered reproductively active with a GSI≥0.5.

Data analyses

Reproductive biology Precision of macroscopic in contrast to histological assessment of gender, as well as reproductive phase assessment for both males and females, was compared by calculating percent agreement (Klibansky and Scharf, 2015) and testing with a chi-square test, where differences were considered significant at $P<0.05$. When only 2 phases were compared, the Yates corrected chi-square test was used. The sex ratio was calculated for each month and overall and was analyzed with a chi-square test. The size-at-50%-maturity for males and females was determined with a logistic regression in R software (vers. 3.1.3; R Core Team, 2015).

Distribution of males and females in each reproductive phase for each age were compared among months when fish were reproductively active by using the Kolmogorov–Smirnov 2-sample test with a Bonferroni adjustment to determine whether a significant difference existed in reproductive potential among months. Relative batch fecundity (RBF), expressed as number of eggs/g of fish weight, was calculated as BF/ovary-free fish weight. The relationship of BF and RBF to fish size (FL, W, age) and K was determined by using linear and nonlinear regression analyses. Data were $\log_{10}$-transformed where necessary to meet assumptions and provide a better linear fit. Analyses were performed with IBM SPSS Statistics software, vers. 18 (IBM, Armonk, NY) and differences were considered significant if $P<0.05$.

Comparisons of historical data Annual length–weight relationships were determined (1964–2014). Both length and weight were log-transformed and standardized for each year:

$$g = \frac{(x - \bar{x})}{SD_x} \quad (3)$$

$$\text{and } h = \frac{(y - \bar{y})}{SD_y}, \quad (4)$$

where x = the log-transformed length;
$\bar{x}$ = the mean log-transformed length; and
SD_x = the standard deviation of x, y was the log-transformed weight;
$\bar{y}$ = the mean log-transformed weight; and
SD_y = the standard deviation of y (Kruschke, 2014).

Standardizing the data was necessary given the correlation between the parameters in the length–weight relationship.

Length-weight relationships were fitted by using Bayesian methods for linear regression in R and the program JAGS (Plummer, 2003):

$$h = \beta_0 + \beta_1 g, \quad (5)$$

where length, g, was related to weight, h, through a slope, β_1, and intercept, β_0.

Priors for the slope and intercept parameters were normally distributed N(0, 0.1). A total of 30,000 chains were run for each year and a 10,000-chain burn-in period.

Comparisons of FL, GSI, and K of reproductively active males and females collected in September and October during 1964–1970 and 2014–2015 were made with t-tests; equality of variance was assessed with Levene's test. These analyses were performed with IBM SPSS Statistics software (vers. 18) and considered significant at $P<0.05$.

Results

Age determination

Age estimates were determined from scales of 539 Gulf menhaden (269 females, 213 males, 57 fish of unknown sex) collected from 2014 through 2015 and used in our analyses of reproductive biology. Age estimates ranged from 1 through 4 years, with the majority of males and females in the age-2 class. Most fish of unidentified sex were age-1, corresponding to immature or young-of-year individuals. There was a large overlap in length-at-age, likely owing to the extended spawning season and variability in length-at-age.

Reproductive biology

A total of 697 Gulf menhaden were collected from 2014 through 2016 for reproductive analysis, composed of 337 females, 294 males, and 66 fish of unknown sex, of which 22 were <130 mm FL and sexually immature. Macroscopic differentiation of gender was particularly difficult for fish that were reproductively inactive or were frozen before analysis. Overall, there was 80% agreement between macroscopic and histological gender assignment for females and 84% agreement for males. Chi-square analysis showed a significant misclassification of gender based on macroscopic observations for males and females ($\chi^2_{593}=239.1$, $P<0.001$), suggesting histological analysis is necessary to accurately determine gender of Gulf menhaden, particularly with frozen specimens.

Overall, the sex ratio of Gulf menhaden was not significantly different from 1:1. Females dominated the collections in February, June, September, October, and for all months combined, and significantly more females than males were sampled in September (P=0.019). Relatively equal sex ratios suggested that fish of both sexes are equally susceptible to fishing pressure and there is no difference in mortality associated with gender.

Size at sexual maturity was found to be virtually identical for males and females. Length-at-50%-maturity was calculated as 137.2 mm FL and 140.0 mm FL for females (Fig. 1A) and males (Fig. 1B), respectively. Fish this size typically recruit into the commercial fishery in the late summer and early fall and were considered to be late age-1.

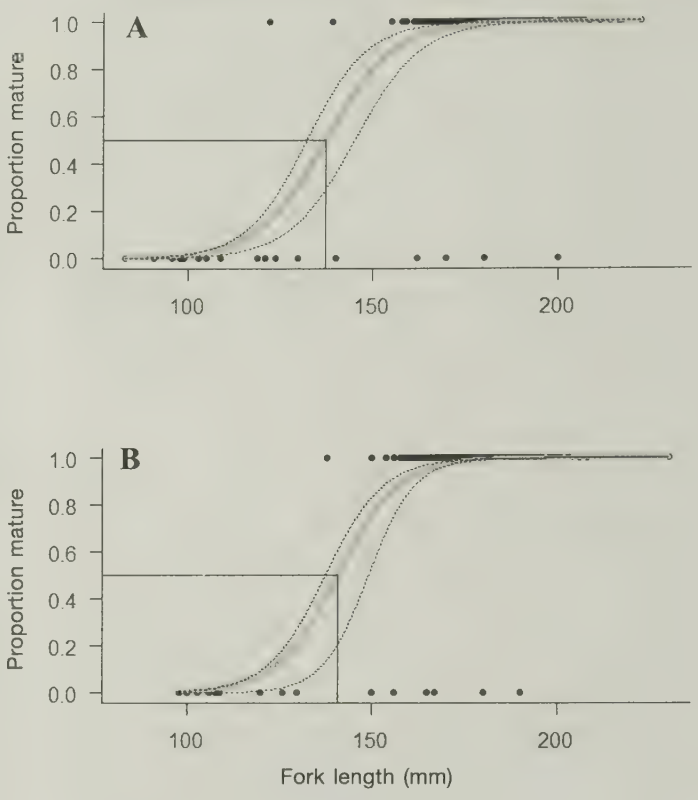

Figure 1

Logistic regression of maturity at size for (**A**) female and (**B**) male Gulf menhaden (*Brevoortia patronus*) collected from the northern Gulf of Mexico during 2014 through 2016. Solid black lines indicate size at 50% maturity. The gray line is the mean prediction, and the dotted lines are the 95% confidence intervals.

Histological analysis There was poor agreement between macroscopic and histological assessment of reproductive phase for female Gulf menhaden (χ^2_{318}=198.2, P<0.001). However, the Yates corrected chi-square test for comparison of histological and macroscopic agreement in reproductive assessments of the spawning capable and actively spawning phases showed there was not a significant difference in misclassification between these 2 phases (Yates χ^2_{72}=3.44, P=0.064). There was also poor agreement between macroscopic and histological assessment of reproductive phase for male Gulf menhaden (χ^2_{275}=137.0, P<0.001). However, agreement between macroscopic and histological assessments of reproductive phase improved when Gulf menhaden were classified as either reproductively active or inactive. For females, 99% of fish macroscopically assessed as reproductively inactive remained in that classification after histological inspection and there was an 82% agreement between macroscopic and histological assessment for reproductively active females. Similarly, males showed a 98% agreement for reproductively active fish and a 93% agreement for reproductively inactive fish when macroscopic and histological classifications were compared.

Gulf menhaden ovarian tissue showed asynchronous oocyte development and evidence of batch spawning. Females in the spawning capable phase had oocytes in all stages of development, and there was evidence of POFs in some ovaries in early October (Fig. 2A). Females in the actively spawning subphase (Fig. 2B) had oocytes undergoing OM or hydrated oocytes, as well as vitellogenic oocytes in various stages of development (Fig. 2B). The immature phase was histologically distinguished from the regenerating phase by the smaller size of the primary growth oocytes, lack of space among oocytes, and the large amount of interstitial tissue present in the immature ovary.

The testis of Gulf menhaden is an anastomosing tubular type, characterized by highly branched germinal compartments that do not terminate at the testis periphery. Testicular tissue showed differences in the number of spermatocysts along the tubules as the reproductive season progressed. Active spermatogenesis was evident in males in the early germinal epithelium (GE) subphase of the spawning capable phase (Fig. 2C), and spermatogonia, spermatocytes and spermatids present within cysts completely lined the tubules; additionally, tubules were filled with spermatozoa. In the late GE subphase, typical of the end of the reproductive period, the tubules were still swollen with spermatozoa, but little active spermatogenesis was taking place, and few spermatocysts were seen lining the tubules (Fig. 2D). The regenerating phase was histologically distinguished from the immature phase in males by the presence of some residual spermatozoa (Sz) within the tubules. Testicular tissue from males collected in September and October showed microspoordian infection, although this was not a common occurrence.

Spawning seasonality The GSI values increased in early October for both males and females, and reached peak values for females by the second half of October (Fig. 3).

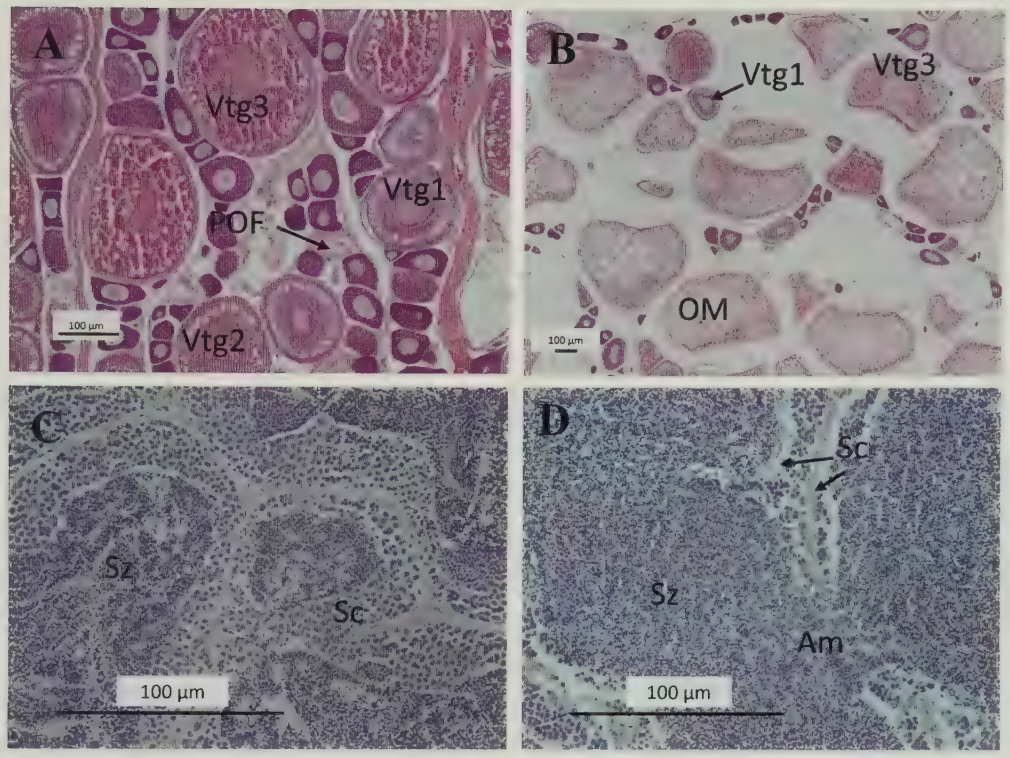

Figure 2

Histological sections of gonadal tissue in the spawning capable phase from Gulf menhaden (*Brevoortia patronus*) collected from the northern Gulf of Mexico in 2014. (**A**) Female in spawning capable phase, showing asynchronous oocyte development and evidence of batch spawning (postovulatory follicle [POF] complex); fish captured 6 October 2014. (**B**) Female in actively spawning sub-phase, showing asynchronous oocyte development and a distinct batch of oocytes in the germinal vesicle migration stage of oocyte maturation (OM), just prior to spawning; fish captured 28 October 2014. (**C**) Male in early germinal epithelium (GE) sub-phase of spawning capable reproductive phase, with the tubules outlined by a continuous GE undergoing active spermatogenesis; fish captured 6 October 2014. (**D**) Male in late GE sub-phase of spawning capable reproductive phase (note that spermatocysts are uncommon along tubules as spermatogenesis decreases); fish captured 28 October 2014. Am=anastomosing tubules; St=spermatid; Sz=spermatozoa; Vtg1=primary vitellogenic oocyte; Vtg2=secondary vitellogenic oocyte; Vtg3=tertiary vitellogenic oocyte.

Female GSI remained elevated but gradually decreased from late October through March, whereas male GSI remained elevated from early October through March and there was no gradual decline during the reproductive season (Fig. 3). Mean male and female GSI values suggest a spawning season extending from early October through the end of March.

Histological analysis allowed refinement of the Gulf menhaden spawning season. All females captured in late August were in the regenerating phase, and females first began to exhibit gonadal recrudescence in mid-September (Table 1A). By early October, >50% of females were spawning capable (Table 1A). Histological evidence that Gulf menhaden begin spawning in early October includes the presence of some females in the actively spawning subphase, as well as 22% of spawning capable females having POF (Fig. 2A). By late October through late February, all sexually mature females captured were spawning capable, with 41% and 35% of these actively spawning in October and January, respectively (Table 1A). Although many females were in the regenerating reproductive phase by March (Table 1A), some remained spawning capable in mid-March, and 66% of those were actively spawning. Thus, histological analysis showed that female Gulf menhaden were actively spawning from early October through mid-March, a 5.5-month spawning season that was similar to that seen in the GSI data (Fig. 3).

Male Gulf menhaden began gonadal recrudescence sooner than females; active spermatogenesis was occurring in 49% of males captured in late August as they entered the early developing or developing phases

(Table 1B). By mid-September, some males were in the spawning capable reproductive phase, and 72% of males were spawning capable by early October (Table 1B). Spawning capable males dominated collections from October through March. Males in the regressing and regenerating phases were first seen in early March, and by mid-April all males had ceased spawning (Table 1B). During the early portion of the spawning season (October and November), most males were found in the early GE (Fig. 2C) subphase of the spawning-capable reproductive phase, indicating active spermatogenesis throughout the testis. Active, although somewhat reduced, spermatogenesis continued during January and February (mid GE subphase). At the end of the spawning season in March, all males were in the late GE subphase (Fig. 2D) and reduced spermatogenesis, but abundant spermatozoa, were still present in the tubules. Histological analysis showed that most males were spawning capable during the same 5.5-month period when females were spawning capable.

Age-based differences in gonadal recrudescence were evident in both females and males at the beginning of the reproductive season. Although there was no significant difference in the distribution of reproductive phases between age-1 and age-2 females in September (P=0.088), no age-1 females were in the developing phase (Fig. 4). There was a significant difference between age-1 and age-2 females in October (P=0.047, Fig. 4), with a much higher percentage of age-1 fish in the immature, early developing, and developing phases compared with age-2 females. There was no difference in distribution across all 3 ages, or between ages-2 and -3 (P=0.165 and 0.875, respectively; Fig. 4) in October. Therefore, younger female Gulf menhaden appeared to have a delayed beginning of the reproductive season.

Age-1 and age-2 males did not exhibit a significant difference (P=0.514) in the distribution of reproductive phases (Suppl. Fig. 1) (online only) in August at the beginning of gonadal recrudescence. However, in September a significant difference (P=0.017) in phase distribution was seen (Suppl. Fig. 1). A high percentage of age-1 males were in the immature and early developing phases and no spawning capable individuals were observed, whereas immature age-2 males were not present in September, a high percentage of age-2 males were present in the developing phase, and some age-2 males were spawning capable (Suppl. Fig. 1). Although there was no significant difference in reproductive phase distribution between ages-1, -2, and -3 in October (P=0.056), the percentage of males in the developing phase decreased with increasing age, and all age-3 fish captured were spawning capable (Suppl. Fig. 1). Therefore, younger male Gulf menhaden also exhibited a delayed beginning of the reproductive season when compared to older males.

Spawning frequency Spawning frequency varied depending on the method used (Table 2). The OM method provided a more consistent estimation of spawning frequency than the POF method (Table 2) with the exception of the early October sample, when Gulf menhaden were just beginning to spawn. Spawning frequency estimates from February and March should be viewed with caution because of low sample sizes. Combining fish from all months, spawning frequency ranged from every 2.1 to 4.3 days, depending on the method used. Assuming a 5.5-month spawning season, these spawning frequency estimates suggest that an individual female Gulf menhaden has the potential to spawn 38–79 times during the reproductive season. Smaller, age-1 females likely have fewer potential spawns than older, larger females during the reproductive season (35–71 times) because of the delay in reaching the actively spawning subphase in early October (Fig. 4).

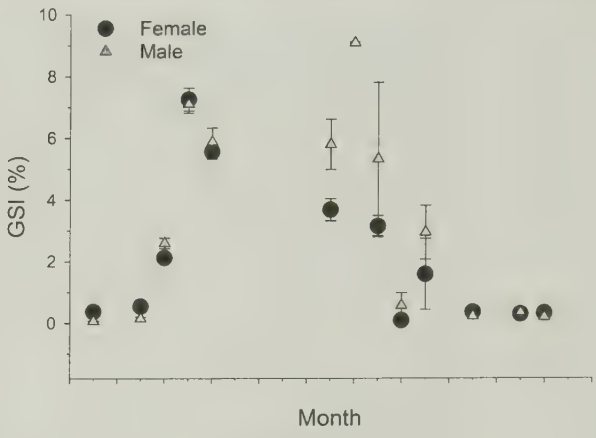

Figure 3

Mean bimonthly gonadosomatic index (GSI) values of male and female Gulf menhaden (*Brevoortia patronus*) collected from the northern Gulf of Mexico in 2014 through 2016. Error bars indicate standard errors of the means.

Fecundity Samples were analyzed from 16 actively spawning Gulf menhaden from late October through March. Fish ranged in size from 165 to 203 mm FL and were primarily age 2. Batch fecundity ranged from 2829 to 59,423 eggs per individual, with an overall mean BF of 15,367 eggs (standard error [SE] 3260; median: 11,577). The RBF ranged from 31.1–328.3 eggs/g ovary-free body weight with an overall mean of 107.8 eggs/g ovary-free body weight (SE 17.1; median: 101.7). Batch fecundity was significantly ($F_{1,15}$=5.629, P=0.033), positively related to FL, although this relationship explained only 28.7% of the variation in BF (Fig. 5). Batch fecundity was also significantly positively related to weight ($F_{1,15}$=5.278, P=0.038, coefficient of determination [r^2]=0.274). Log_{10} transformation of the data resulted in the best predictive fit for BF and FL; the predictive equation was:

$$\log BF = 4.695(\log FL) - 6.547. \quad (6)$$

Table 1

Bimonthly percentages of (**A**) female and (**B**) male Gulf menhaden (*Brevoortia patronus*), collected from Mississippi and Louisiana coastal waters of the northern Gulf of Mexico during 2014–2016, in reproductive phases determined by histological examination. The phases include immature (Imm), early developing subphase (EDev), developing (Dev), spawning capable (SC), early germinal epithelium (GE) subphase (EGE), mid GE subphase (MGE), late GE subphase (LGE), actively spawning subphase (AS), regressing (Rgs), and regenerating (Rgn).

(A) Females

Date	*n*	Imm	EDev	Dev	SC	AS	Rgs	Rgn
16–31 Aug	46	0	0	0	0	0	0	100
16–30 Sep	80	5	6	3	0	0	0	86
1–15 Oct	56	2	11	20	57	3	0	7
16–31 Oct	64	1	0	0	58	41	0	0
1–15 Nov	14	0	0	0	100	0	0	0
16–31 Jan	17	0	6	0	59	35	0	0
1–15 Feb	4	100	0	0	0	0	0	0
16–28 Feb	6	0	0	0	100	0	0	0
1–15 Mar	1	0	0	0	0	0	100	100
16–31 Mar	7	14	0	0	14	29	0	43
16–30 Apr	5	0	0	0	0	0	0	100
1–15 May	15	7	0	0	0	0	0	93
1–15 Jun	23	4	0	0	0	0	0	96

(B) Males

						SC subphase				
Date	*n*	Imm	EDev	Dev	SC	EGE	MGE	LGE	Rgs	Rgn
16–31 Aug	50	4	41	8	0	0	0	0	0	47
16–30 Sep	54	6	37	36	4	0	0	0	0	17
1–15 Oct	50	0	0	28	72	83	17	0	0	0
16–31 Oct	56	0	0	0	100	59	37	4	0	0
1–15 Nov	14	0	0	0	100	60	30	10	0	0
16–31 Jan	16	0	6	0	94	31	69	0	0	0
1–15 Feb	3	0	0	0	100	0	100	0	0	0
16–28 Feb	2	0	0	0	100	0	0	0	0	0
1–15 Mar	4	0	25	0	25	0	0	100	25	25
16–31 Mar	4	0	0	0	75	0	0	100	25	0
16–30 Apr	12	0	0	0	0	0	0	0	33	67
1–15 May	16	6	6	0	0	0	0	0	6	82
1–15 Jun	13	0	8	0	0	0	0	0	15	77

Batch fecundity was not significantly related to age (P=0.698) nor K (P=0.768). Additionally, RBF was not significantly related to length (P=0.282), weight (P=0.615), or K (P=0.546), suggesting the RBF calculation removes the effects of fish size and can therefore be used to accurately compare fecundity of different-size fishes. Thus, based on RBF and spawning frequency, an average size female of 150 g may produce as many as 614,460–1,277,430 eggs during the 5.5-month reproductive season.

The oocyte dynamics of Gulf menhaden offer an unclear picture as to whether this species has determinate or indeterminate fecundity. Oocyte size-frequency distributions of secondary growth oocytes in Gulf menhaden from October and March show a dramatic reduction in the number of small vitellogenic oocytes in March than in October (Fig. 6), suggesting that new oocytes are not recruited into vitellogenesis at the end of the spawning season—a pattern typical of determinate fecundity but also seen in some species with indeterminate fecundity. The gap in oocyte distribution between primary and secondary growth oocytes typically seen in species with determinate fecundity is not seen in Gulf menhaden, although that is not unexpected in this instance because only secondary growth oocytes were counted. Histological observations of females from February and March showed a lower percentage of primary and secondary vitellogenic oocytes in the ovary than from October and November, suggestive of determinate fecundity. However, the percentage of atresia in

Table 2

Estimates of spawning frequency of spawning capable Gulf menhaden (*Brevoortia patronus*) collected from Mississippi and Louisiana coastal waters during 2014 through 2016. Estimates were derived by using 2 different calculation methods: postovulatory follicle (POF) and oocyte maturation (OM), including hydrated oocytes.

Month	*n*	POF method	OM method
Early October	32	22%, 4.5 days	6.25%, 16 days
Late October	63	6.3%, 15.9 days	41.3%, 2.4 days
All October	95	4.6%, 8.6 days	29.5%, 3.4 days
Early November	14	21%, 4.76 days	0.0%
Late January	16	43.8%, 2.3 days	37.5%, 2.6 days
Late February	6	83%, 1.2 days	0.0%
Late March	3	0	66.6%, 1.5 days
All combined	134	23.1%, 4.3 days	47.8%, 2.1 days

females in the regressing reproductive phase ranged from 2.3 to 13.9%; atresia percentages >10% are suggestive of indeterminate fecundity. Similarly, calculations of total annual fecundity present conflicting evidence of determinate or indeterminate fecundity. Total fecundity of a 181-g female was 473,370 eggs, based on total oocytes at the beginning of the season but 1,658,316 eggs based on BF and spawning frequency (suggestive of indeterminate fecundity), whereas total fecundity of a 132-g female was 204,347 eggs based on total oocytes at the beginning of the season and 174,958 eggs based on BF and spawning frequency (suggestive of determinate fecundity). Finally, although a steady decrease in GSI values as the season progresses (Fig. 3) is typical of species with determinate fecundity, this decrease can also occur in species with indeterminate fecundi-

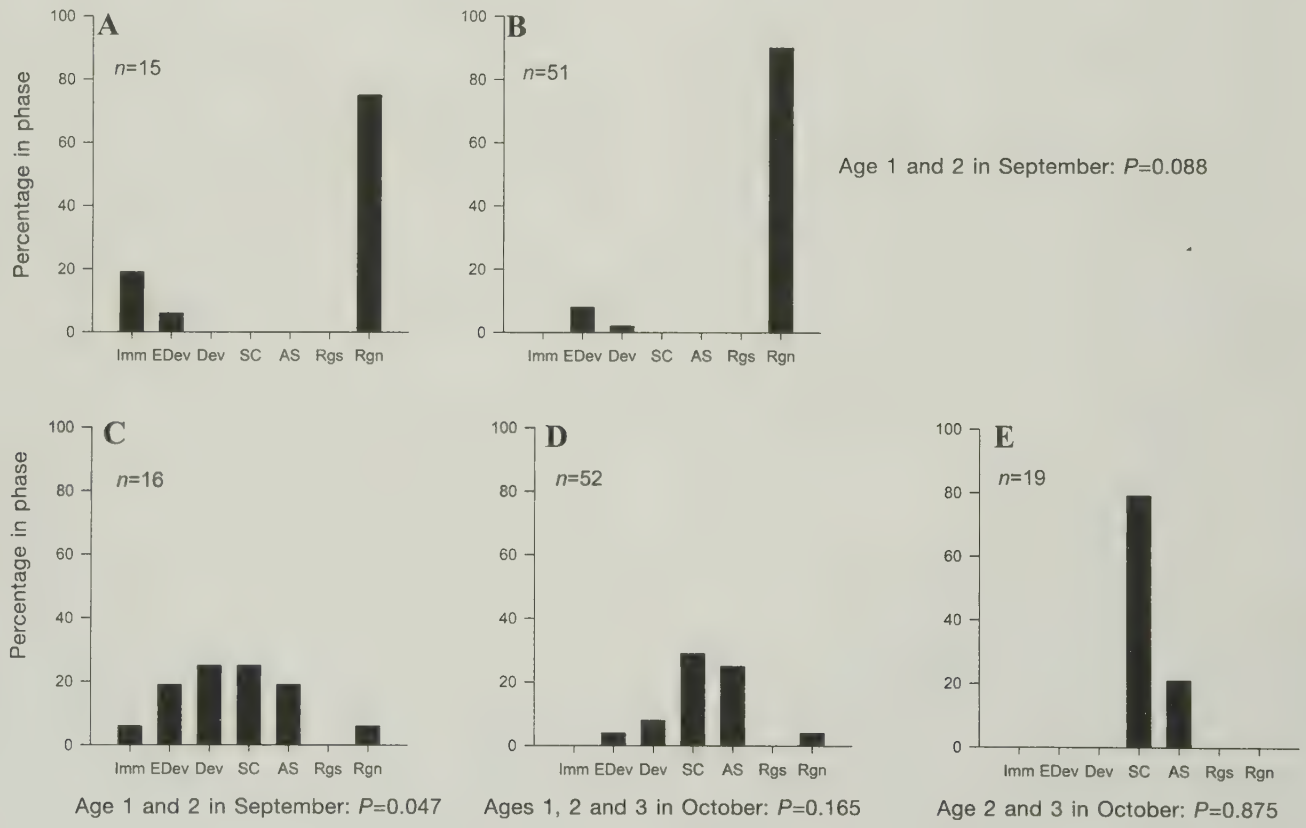

Figure 4

Distribution of female reproductive phases for Gulf menhaden (*Brevoortia patronus*) collected from the northern Gulf of Mexico during 2014 through 2016, by age at the beginning of the reproductive season: (**A**) age-1 and (**B**) age-2 females in September and (**C**) age-1, (**D**) age-2, and (**E**) age-3 females in October. The probabilities (*P*) from the results of a Kruskall–Wallace 2-sample test of similarity of distributions within a month are provided. The reproductive phases are immature (Imm), early developing (EDev), developing (Dev), spawning capable (SC), actively spawning (AS), regressing (Rgs), and regenerating (Rgn).

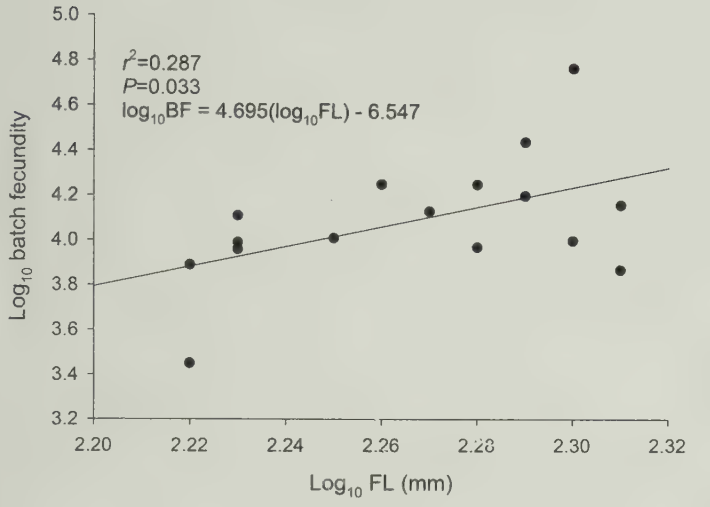

Figure 5

Batch fecundity of Gulf menhaden (*Brevoortia patronus*) collected from the northern Gulf of Mexico during 2014 through 2016 (n=16). $\log_{10}$ transformation resulted in a significant relationship between fork length (FL) and batch fecundity (BF). r^2=coefficient of determination.

ty and an extended spawning season. These conflicting lines of evidence lead us to conclude that Gulf menhaden likely have indeterminate fecundity, but also show some characteristics of determinate fecundity.

Modeling stock assessments

The incorporation of "high" estimates of annual fecundity (based on age-1 with 71 spawnings/year and age-2+ with 79 spawnings/year), "low" estimates of annual fecundity (based on age-1 with 35 spawnings/year and age-2+ with 38 spawns/year), and alternative maturity schedules affected stock-level estimates. Altering the fecundity estimate in the high and low scenarios increased estimated annual egg production 100- to 1000-fold for each year of the assessment model (Fig. 7A). Altering the maturity schedule to include age-1 reproduction (68% of age-1 individuals capable of spawning) resulted in an approximately 10-fold increase in stock-level egg production for each fecundity scenario (Fig. 7A) but reduced the proportion of maximum spawning per recruit in each of the scenarios (Fig. 7B). The percent change in estimated numbers-at-age between the scenarios that included age-1 reproduction and base model estimates indicated that there was a greater number of individuals in each age class for all years examined, particularly in the age-3 and age-4+ groups (Suppl. Fig. 2A) (online only). In 2012, the estimated percent decrease in number at age was small for the age classes 1 and 2 (<1%) but was reduced 9.3%, 4.2% and 9.8% for ages-0, 3 and 4, respectively. The estimated increase in annual F was small and generally consistent across age classes for each year, with an observed increase in F in age classes 0, 2, 3, and 4 of ~1.5% and an increase in the estimated F rate for age-1 of <0.5% (Suppl. Fig. 2B). Estimated selectivity of age-1 fish in the commercial reduction fishery for the updated fecundity estimates was marginally greater than that estimated in the base model formulation (0.050 vs. 0.051). Estimated log-transformed catchability of the 2 fishery-independent gears (gill and seine nets) used to sample the stock exhibited minor differences in the base model formulation (1.251 and 1.177 for the high and low estimates, respectively). Catchability of the seine gear was reduced from 0.127 to 0.125.

Comparisons of historical data

Annual sample sizes from the Gulf menhaden fishery during 1964 through 2014 ranged from 4611 in 2010 to 16,823 fish in 1994 (Suppl. Table) (online only). Low sample size in 2010 was the result of closures of fishing areas due to the Deepwater Horizon oil spill. Mean estimated slope and intercept for the length–weight relationships varied over time (Suppl. Fig. 3) (online only). The highest slope was 3.98 in 1991 and the lowest slope was 2.52 in 1986. Slope translates into how heavy a fish is compared with its length. Slopes of 3.0 indicate a proportional fish; slopes <3.0 indicate a skinnier fish and slopes >3.0 indicate a heavier fish. Intercept values varied between −15.92 in 1991 to −8.39 in 1986. Variability in the slope and intercept values was generally random, but there were 2 time periods (late 1980s and late 2000s) that had about 5 years of lower than average slope, therefore indicating Gulf menhaden were less robust during those times.

We found significant differences in reproduction-related measures in both males and females between 1964–1970 and 2014. Reproductively active females in October 2014 were significantly larger (t_{146}=2.22, P=0.03), had a higher K (t_{146}=2.708, P=0.008), and a greater GSI (t_{146}=4.143, P<0.001) than those from 1964 through 1970 (Table 3). However, no significant difference existed between years in September for any of these measures. Reproductively active males in October 2014 showed significantly greater FL (t_{108}=2.387, P=0.019) and GSI (t_{108}=2.319, P=0.047) than those from 1964 through 1970 (Table 3); whereas no significant difference in male condition was found in October, fish from 2014 had higher K than those from 1964 through 1970.

Discussion

Gulf menhaden continues to be one of the most ecologically and economically important stocks in the northern GOM and plays an important role in the trophic structure of the region (Sagarese et al., 2016). We provide new reproductive information and document

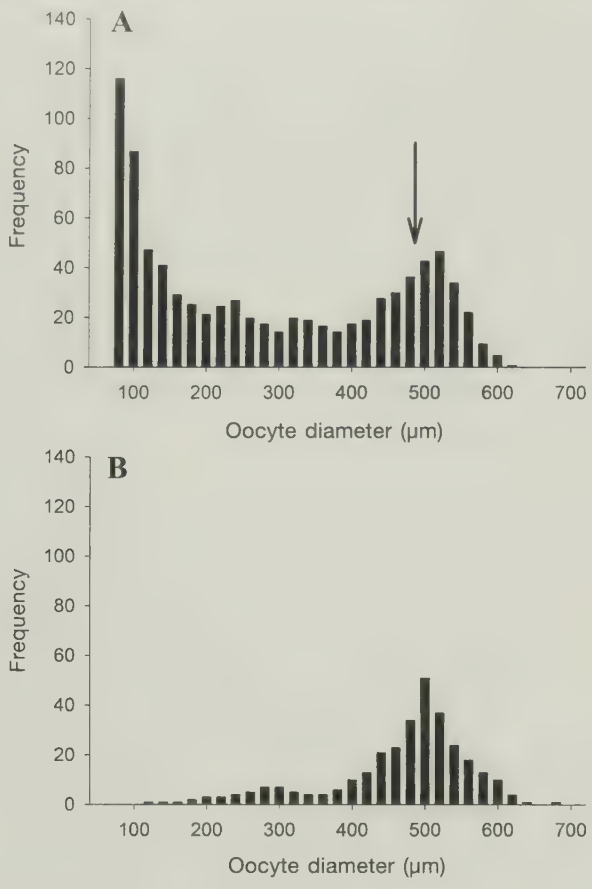

Figure 6

Distributions of oocyte sizes of female Gulf menhaden (*Brevoortia patronus*) collected from the northern Gulf of Mexico during 2014 through 2016, showing an indeterminate fecundity pattern with lack of recruitment of secondary vitellogenic oocytes at the end of the spawning season. (**A**) Fish captured 31 October 2014, 186 mm FL. Arrow indicates oocytes undergoing oocyte maturation; only oocytes ≥500 μm were counted for fecundity estimates. (**B**) Fish captured 18 March 2015, 165 mm FL. Note lack of vitellogenic oocytes from 80 to 350 μm in the March sample.

how these new data address critical needs for stock assessments and for understanding the ecological dynamics of the stock. The results of our work indicate that Gulf menhaden have greater fecundity than that previously reported, and the characteristics of the reproductive dynamics are different than previously thought. Specifically, we found that egg production is greater and that the reproductive season is protracted, lasting 5.5-months. We also found that Gulf menhaden are batch spawners that spawn every 2.1–4.3 days and that although they show indeterminate fecundity, they have several traits typically associated with determinate fecundity.

The 5.5-month reproductive season (October–March) for Gulf menhaden from the north-central GOM described here is slightly longer than that previously reported. Combs (1969) found the spawning season occurred from late October to February or early March according to histological analysis, whereas Lewis and Roithmayr (1981) found peak spawning, determined from GSI, to occur from November through January, and that a few spawning capable females were present in February and none after that time. Not only is the Gulf menhaden spawning season longer than previously reported, our data indicate that a high percentage of fish are spawning in October, and these fish are vulnerable to capture by the commercial purse-seine fishery that operates through the end of October.

Smaller and younger Gulf menhaden have a shorter reproductive season than older, larger fish. Although data were not previously available for size-at-sexual-maturity for Gulf menhaden, sexual maturity was assumed to have been reached when fish approach their second birth date (VanderKooy and Smith[1]). Indeed, we found that 50% maturity is reached at 137–140 mm FL, and fish of this size are found in the fall as they approach their second birth date. However, smaller age-1 fish in the fall have lower GSI values and delayed gonadal development than those of larger fish. Furthermore, our analysis of historic Gulf menhaden data suggests that the reproductive season may have shifted to a slightly earlier start in 2014 than during 1964–1970, possibly as a result of 2014 fish being slightly larger and in better condition. It is well established that older, larger females begin spawning earlier in the reproductive season and that smaller individuals may have a longer time between spawning events than larger individuals of the same species (Lowerre-Barbieri et al., 2011; Fitzhugh et al., 2012). These variations among different-size fish must be taken into account when calculating annual fecundity estimates and estimating spawning stock biomass. Our analysis has taken this variation into account by including a 1-month delay in the spawning season for age-1 fish, although we have insufficient data to estimate differences in spawning frequency between females age-1 and older.

This study is the first to examine GSI and histology of male Gulf menhaden. Males began gonadal recrudescence about 1 month before females do but, like females, were reproductively inactive by mid-April. Male Gulf menhaden exhibit an anastomosing tubular type of testes typical of other clupeids (Grier and Uribe Aranzábal, 2009). Male and female GSI values were similar in Gulf menhaden, particularly at the beginning of the spawning season, as also seen in another clupeid, the Pacific sardine (*Sardinops sagax* [Stewart et al.[7]]). In contrast, some male sardines have higher GSI values than females (Tsikliras and Antonopoulou, 2006; Tsikliras et al., 2010), although male marine te-

[7] Stewart, J., G. Ballinger, and D. Ferrell. 2010. Review of the biology and fishery for Australian sardines (*Sardinops sagax*) in New South Wales—2010. Industry & Investment NSW, Fish. Res. Rep. Ser. 26, 57 p. [Available from website.]

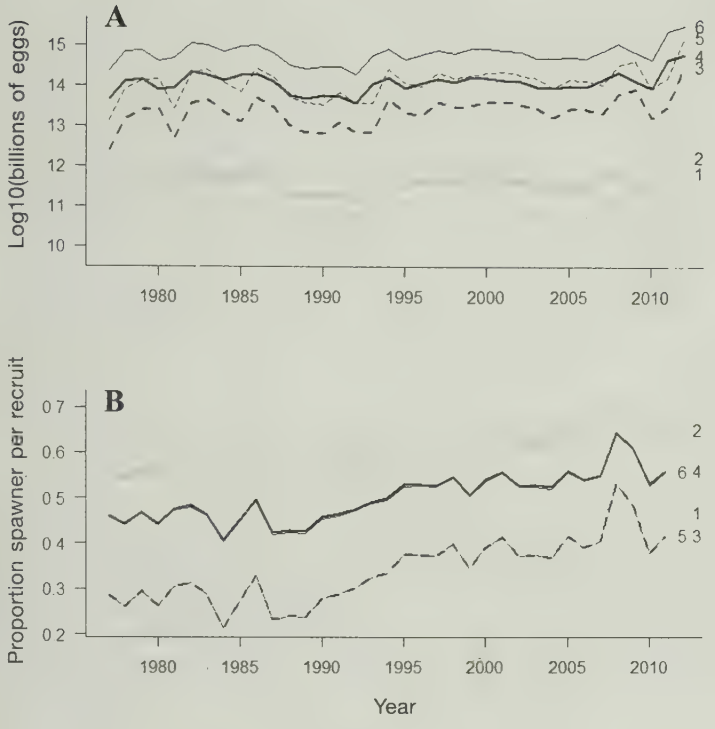

Figure 7

Estimates of (**A**) annual egg production of the stock and (**B**) the maximum proportion of spawners-per-recruit of Gulf menhaden (*Brevoortia patronus*) based on collections from the northern Gulf of Mexico during 2014 through 2016. For each panel, fecundity from Lewis and Roithmayr (1981, lines 1 and 2) and the low (lines 3 and 4) and high (lines 5 and 6) estimates of fecundity derived in this study are displayed with 2 different age-specific maturity patterns (dashed and solid lines). Lines 1, 3, and 5 display the expected temporal patterns when the age at first maturity is 2 years. Lines 2, 4, and 6 display the expected temporal pattern in maximum proportion of spawners-per-recruit when maturity is modeled with the logistic relationship described in this work (proportion of age-1 spawners is 0.68).

leosts typically have notably lower GSI values than females (Wootton, 1998). The high male GSI values of Gulf menhaden and other clupeids may be related to increased sperm competition in the pelagic environment (Stockley et al., 1997), which is common with species that spawn in groups (Erisman and Allen, 2006) such as Gulf menhaden.

Lack of concordance between macroscopic and histological assessment of reproductive phase in Gulf menhaden was unexpected. Although histological assessment remains the best method to accurately identify specific reproductive phases (West, 1990; Brown-Peterson et al., 2011), we found that broadly assessing fish as reproductively active or inactive by macroscopic inspection is sufficiently accurate, as did Klibansky and Scharf (2015). Thus, macroscopic assessments could allow biologists, managers, and industry personnel to determine reproductive seasonality of Gulf menhaden.

The fecundity pattern of Gulf menhaden has not previously been reported, although Combs (1969) documented asynchronous oocyte development and suggested Gulf menhaden are batch spawners. Fish with determinate fecundity recruit all oocytes to be spawned during the year into vitellogenesis at the beginning of the reproductive season before the first spawing and can be either batch or total spawners, whereas fish with indeterminate fecundity continually recruit oocytes into vitellogenesis throughout the reproductive season and are batch spawners (Murua and Saborido-Rey, 2003). Marine clupeids exhibit both types of fecundity patterns; cold water species, such as Atlantic and Pacific herring (*Clupea harengus* and *C. pallasii*), show determinate fecundity and total spawning, whereas many temperate and subtropical batch spawning clupeids (such as species of *Sardinella* and *Sardinops*) tend to have indeterminate fecundity (Ganias, 2013). However, American shad (*Alosa sapidissima*) have recently been shown to have determinate fecundity in northern populations and indeterminate fecundity in southern populations (McBride et al., 2016), as predicted for species with wide geographic ranges by Ganias et al. (2015). The subtropical/tropical clupeid Spanish sardine (*Sardinella aurita*) has been shown to have determinate fecundity but is likely to be a batch spawner (Tsikliras and Antonopoulou, 2006) while the Brazilian menhaden (*Brevoortia aurea*) is a batch spawner reported to have indeterminate fecundity (Macchi and Acha, 2000; Lajud et al., 2016). Our data indicate that Gulf menhaden are likely to have indeterminate fecundity, but have some traits more typical of fish with determinate fecundity, such as high GSI values at the beginning of the spawning season, a reduction in secondary growth oocytes as the spawning season progresses, and the lack of massive atresia at the end of the spawning period in at least some individuals. Indeed, Ganias et al. (2017) showed that some species with indeterminate fecundity can cease recruiting new oocytes during the spawning season; this is likely the case for Gulf menhaden. The variations in fecundity patterns among clupeids show the importance of assessing determinate or indeterminate fecundity for each species and of not relying solely on geographic location or spawning strategy. Understanding fecundity patterns, as well as spawning dynamics, is also important for estimating total annual fecundity.

Our mean BF estimates of 15,367 eggs (SE 3260) are much lower than the previous fecundity estimates for age-2 Gulf menhaden of 47,900 eggs (SE 5038)

Table 3

Comparisons of historic and current mean fork length (FL), in millimeters, mean condition (K), and mean gonadosomatic index (GSI) with standard errors (SEs) in parentheses, of reproductively active male and female Gulf menhaden (*Brevoortia patronus*) collected from the northern Gulf of Mexico at the beginning of the reproductive season. Historic data are for 1964 through 1970; current data are from 2014. Reproductively active fish are defined as GSI≥1.0 for females and ≥0.5 for males. Significant differences are in bold.

	Month	Date	n	FL (SE)	t-value	P
Fork length						
Female	September	Current	2	202.0 (9.0)	−1.93	0.086
		Historic	9	217.3 (3.3)		
	October	Current	105	192.0 (1.17)	2.22	**0.03**
		Historic	43	184.9 (3.0)		
Male	October	Current	103	185.9 (1.1)	2.38	**0.019**
		Historic	7	175.7 (4.8)		
Condition						
Female	September	Current	2	2.098 (0.086)	0.197	0.848
		Historic	9	2.069 (0.064)		
	October	Current	105	2.094 (0.027)	2.708	**0.008**
		Historic	43	2.073 (0.022)		
Male	October	Current	103	2.156 (0.013)	1.620	0.108
		Historic	7	2.070 (0.054)		
Gonadosomatic index						
Female	September	Current	2	1.63 (0.59)	−0.348	0.726
		Historic	9	2.02 (0.50)		
	October	Current	105	5.44 (0.32)	4.143	**<0.001**
		Historic	43	3.75 (0.25)		
Male	October	Current	103	5.12 (0.28)	2.319	**0.047**
		Historic	7	3.53 (0.63)		

(Lewis and Roithmayr, 1981), and the low r^2 value for the fecundity-size relationship is typical among batch spawning fish species. We counted only oocytes ≥500 µm for fecundity estimates—sizes that correspond to oocytes about to be spawned (i.e., hydrated oocytes or oocytes undergoing OM), whereas Lewis and Roithmayr (1981) counted all oocytes >360 µm, which included vitellogenic oocytes that would not be released in a batch. Although there are no previous estimates of RBF for Gulf menhaden for comparison purposes, Lajud et al. (2016) reported RBF ranged from 50–381 eggs/g ovary-free body weight in the Brazilian menhaden, within the RBF range of 60–212 eggs/g ovary-free body weight previously reported by Macchi and Acha (2000) for the same species; both values are similar to our estimates of 31–328 eggs/g ovary-free body weight for Gulf menhaden.

Despite the lower estimate of BF presented here, the total annual estimated fecundity is 11–23 times greater than the values provided by Lewis and Roithmayr (1981) for fish of all sizes (Fig. 8) as a result of combining BF estimates with spawning frequency estimates. The methods we used to determine spawning frequency could result in either underestimation of spawning frequency (due to degradation or destruction of POF due to sample treatment) or an overestimation (due to congregation of females undergoing OM in the sampled area), and for this reason we provide a high and low range which results in a more accurate estimation of total annual fecundity than that of previous reports. Our spawning frequency estimates are higher than those of the only other report of spawning frequency for a species of menhaden (Brazilian menhaden, every 8 days [Macchi and Acha, 2000]). Gulf menhaden appear to spawn more frequently than European pilchard (*Sardina pilchardus*, every 11–12 days) and Pacific sardine (every 10 days)—batch spawning clupeids with indeterminate fecundity and group synchronous oocyte development (Ganias et al., 2004; Lo et al., 2010). However, Brazilian sardinella (*Sardinella brasiliensis*) spawn as frequently as every 2 days during the peak spawning season (Isaac-Nahum et al., 1988)—a frequency that is similar to ours for Gulf menhaden.

Estimates produced from the re-analysis of the stock assessment indicate that some model output, including the number-at-age, age-specific fishing mortality, and spawners-per-recruit are sensitive to alterations in age-specific annual fecundity. A primary use for determining length- and age-specific fecundity is for inclusion in assessment models for determination of

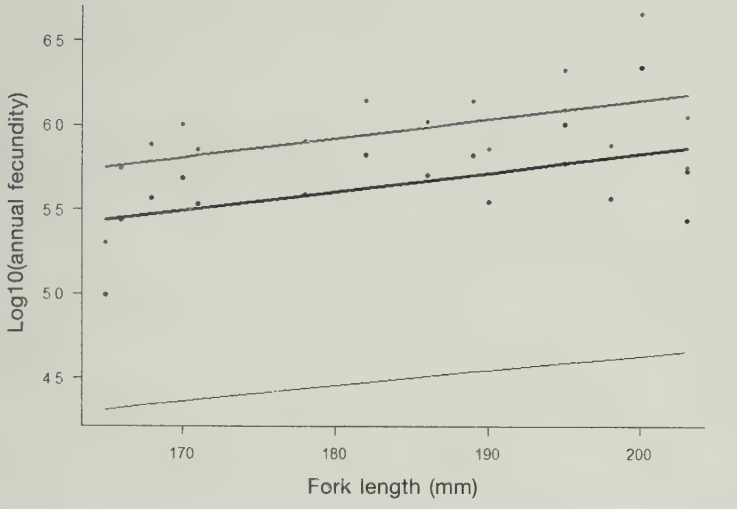

Figure 8

Fork length in relation to specific annual fecundity of Gulf menhaden (*Brevoortia patronus*) collected from the northern Gulf of Mexico during 2014 through 2016. Thick lines are fitted to gray (high estimate, spawning frequency of 2.1 days) and black (low estimate, spawning frequency 4.3 days) points. The thin line is the length-specific fecundity estimate from Lewis and Roithmayr (1981).

stock status. Our results indicate that even in the face of the intense fishing pressure during the early and mid-1980s, the proportion of spawners-per-recruit has remained near 30% or less for the duration of the assessment history. Selectivity and catchability parameters changed only a small amount. The small reduction in the estimated catchability parameters for each gear followed the estimated increases for numbers-at-age observed throughout the time series.

Overall, the condition of the Gulf menhaden stock has remained relatively constant over the past 50 years despite heavy fishing pressure because the 95% Bayesian credible intervals of the historical length–weight relationships generally encompass the constant slope and intercept values from Schueller et al. (2012). Although growth has been variable over time, the data indicate that there has not been a directional change in growth with harvest pressure over time. The stock seems to be resilient to changes in harvest pressures—a feature that adds to its sustainability (Schueller[3]).

We note that the effects on the ecosystem of the estimated increase in fecundity could be profound, although it was not evaluated in this work. Forage fish biomass is often considered to be critical in ecosystem structure and function and have beneficial effects on higher trophic levels (Cury et al., 2011). Research by Fuiman et al. (2015) has highlighted the potential importance of "egg boons" in marine systems; eggs rich in lipids and containing essential free fatty acids that are not able to be synthesized by fish but are consumed by predators likely play an important role in food webs. Thus, the new data provided here suggests that the dramatically greater estimated reproductive output of Gulf menhaden not only has potentially positive impacts at the ecosystem level, but also helps explain a continued robust Gulf menhaden stock despite high fishing pressure.

Acknowledgments

We thank K. Herbert (Omega Protein), T. Bui (Louisiana Cooperative Extension Service), C. Dean (Louisiana Department of Wildlife and Fisheries), and W. Dempster (USM CFRD) for assistance in obtaining Gulf menhaden, C. Jones (USM) for data collection, E. Hall and J. Potts (NMFS Beaufort Laboratory) for providing ages, and J. W. Smith (NMFS Beaufort Laboratory) for project facilitation and oversight. This research was funded by Cooperative Research Program grant #NA14NMF4540064 from the NMFS to the senior author and R. Leaf.

Literature cited

Bagenal, T. B., and E. Braum.
1971. Eggs and early life history. *In* Methods for assessment of fish production in fresh waters, IBP Handbook 3, 2nd ed. (W. E. Ricker, ed.), p. 159–181. Blackwell Scientific Publishing, Oxford, UK.

Brown-Peterson, N. J., and J. W. Warren.
2001. The reproductive biology of spotted seatrout, *Cynoscion nebulosus*, along the Mississippi Gulf Coast. Gulf Mex. Sci. 2001:61–73.

Brown-Peterson, N. J., D. M. Wyanski, F. Saborido-Rey, B. J. Macewicz, and S. K. Lowerre-Barbieri.
2011. A standardized terminology for describing reproductive development in fishes. Mar. Coast. Fish. 3:52–70.

Combs, R. M.
1969. Embryogenesis, histology and organology of the ovary of *Brevoortia patronus*. Gulf Res. Rep. 2:333–434.

Cury, P. M., I. L. Boyd, S. Bonhommeau, T. Anker-Nilssen, R. J. M. Crawford, R. W. Furness, J. A. Mills, E. J. Murphy, H. Österblom, M. Paleczny, et al.
2011. Global seabird response to forage fish depletion—one-third for the birds. Science 334:1703–1706.

Erisman, B. E., and L. G. Allen.
2006. Reproductive behaviour of a temperate serranid fish, *Paralabrax clathratus* (Girard), from Santa Catalina Island, California, U.S.A. J. Fish Biol. 68:157–184.

Fitzhugh, G. R, K. W. Shertzer, G. T. Kellison, and D. M. Wyanski.
2012. Review of size- and age-dependence in batch spawning: implications for stock assessment of fish species exhibiting indeterminate fecundity. Fish. Bull. 110:413–425.

Fore, P. L.
1970. Eggs and larvae of the Gulf menhaden. *In* Report of the Bureau of Commercial Fisheries Biology Laboratory, Beaufort, N.C., for the fiscal year ending June 30, 1968. U.S. Fish Wildl. Serv., Circ. 341 (K. A. Henry, J. H. Kutkuhn, and staff), p. 11–13. Bur. Commer. Fish., U.S. Fish Wildl. Serv., U.S. Dep. Interior, Washington, DC.

Fuiman, L. A., T. L. Connelly, S. K. Lowerre-Barbieri, and J. W. McClelland.
2015. Egg boons: central components of marine fatty acid food webs. Ecology 96:362–372.

Ganias, K.
2013. Determining the indeterminate: evolving concepts and methods on the assessment of the fecundity pattern of fishes. Fish. Res. 138:23–30.

Ganias, K., S. Somarakis, A. Machias, and A. Theodorou.
2004. Pattern of oocyte development and batch fecundity in the Mediterranean sardine. Fish. Res. 67:13–23.

Ganias, K., S. K. Lowerre-Barbieri, and W. Cooper.
2015. Understanding the determinate–indeterminate fecundity dichotomy in fish populations using a temperature dependent oocyte growth model. J. Sea Res. 96:1–10.

Ganias, K., F.-A. Mouchlianitis, C. Nunes, A.-M. Costa, and M.-M. Angélico.
2017. A reassessment of the fecundity type of Atlantic horse mackerel (*Trachurus trachurus*) in Atlantic Iberian waters (ICES division IXa) shows that indeterminate spawners can cease recruiting oocytes during the spawning season. ICES J. Mar. Sci. 74:31–40.

Govoni, J. J.
1997. The association of the population recruitment of gulf menhaden, *Brevoortia patronus*, with Mississippi River discharge. J. Mar. Syst. 12:101–108.

Grier, H. J. and M. C. Uribe Aranzábal.
2009. The testis and spermatogenesis in telosts. *In* Reproductive biology and Phylogeny of fishes (agnathans and bony fishes), vol. 8A (B. G. M. Jamieson, ed.), p. 119–142. Science Publishers, Enfield, NH.

Huntsman, G. R., and R. B. Chapoton.
1973. Biostatistical data acquisition in the menhaden fisheries. Trans. Am. Fish. Soc. 102:452–456.

Isaac-Nahum, V. J., R. de D. Cardoso, G. Servo, and C. L. del B. Rossi-Wongtschowski.
1988. Aspects of the spawning biology of the Brazilian sardine, *Sardinella brasiliensis* (Steindachner, 1879), (Clupeidae). J. Fish Biol. 32:383–396.

Klibansky, N., and F. S. Scharf.
2015. Success and failure assessing gonad maturity in sequentially hermaphroditic fishes: comparisons between macroscopic and microscopic methods. J. Fish Biol. 87:930–957.

Kruschke, J. K.
2014. Doing Bayesian data analysis: a tutorial with R, JAGS, and Stan, 2nd ed., 776 p. Academic Press, London.

Lajud, N.A., J. M. Díaz de Astarloa, and M. González-Castro.
2016. Reproduction of *Brevoortia aurea* (Spix & Agassiz, 1829) (Actinopterygii: Clupeidae) in the Mar Chiquita Coastal Lagoon, Buenos Aires, Argentina. Neotrop. Ichthyol. 14:e150064..

Lewis, R. M., and C. M. Roithmayr.
1981. Spawning and sexual maturity of Gulf menhaden, *Brevoortia patronus*. Fish. Bull. 78:947–951.

Lo, N. C. H., B. J. Macewicz, and D. A. Griffith.
2010. Spawning biomass of Pacific sardine (*Sardinops sagax*) off the U.S. in 2010. NOAA Tech. Memo. NMFS-SWFSC-463, 35 p.

Lowerre-Barbieri, S. K., K. Ganias, F. Saborido-Rey, H. Murua, and J. R. Hunter.
2011. Reproductive timing in marine fishes: variability, temporal scales, and methods. Mar. Coast. Fish. 3:71–91.

Macchi, G. J., and E. M. Acha.
2000. Spawning frequency and batch fecundity of Brazilian menhaden, *Brevoortia aurea*, in the Río de la Plata estuary off Argentina and Uruguay. Fish. Bull. 98:283–289.

McBride, R. S., R. Ferreri, E. K. Towle, J. M. Boucher, and G. Basilone.
2016. Yolked oocyte dynamics support agreement between determinate- and indeterminate-method estimates of annual fecundity for a northeastern United States population of American shad. PLoS ONE 11(10):e0164203.

Murua, H., and F. Saborido-Rey.
2003. Female reproductive strategies of marine fish species of the north Atlantic. J. Northwest Atl. Fish. Soc. 33:23–31.

Plummer, M.
2003. JAGS: a program for analysis of Bayesian graphical models using Gibbs sampling. *In* Proceedings of the 3rd International workshop on distributed statistical computing (DSC 2003); Vienna, Austria, 20–22 March 2003 (K. Hornik, F. Leisch, and A. Zeileis, eds.), 1–10 p. Technische Universität Wien, Vienna, Austria. [Available from website.]

R Core Team.
2015. R: a language and environment for statistical computing. R Foundation for Statistical Computing, Vienna, Austria. [Available from website, accessed March 2015.]

Sagarese, S. R., M. A. Nuttall, T. M. Geers, M. V. Lauretta, J. F. Walter III, and J. E. Serafy.
2016. Quantifying the trophic importance of Gulf Menhaden within the northern Gulf of Mexico ecosystem Mar. Coast. Fish. 8:23–45.

Schueller, A. M., D. S. Vaughan, and J. W. Smith.
2012. Length–length conversions and weight–length relationships for Gulf menhaden (*Brevoortia patronus*) in the Gulf of Mexico. Gulf Mex. Sci. 30:54–59.

Shaw, R. F., W. J. Wiseman Jr., R. E. Turner, L. J. Rouse Jr., R. E. Condrey, and F. J. Kelly Jr.
1985. Transport of larval gulf menhaden *Brevoortia patronus* in continental shelf waters of western Louisiana: a hypothesis. Trans. Am. Fish. Soc. 114:452–460.

Sogard, S. M., D. E. Hoss, and J. J. Govoni.
1987. Density and depth distribution of larval gulf menhaden, *Brevoortia patronus*, Atlantic croaker, *Micropogonias undulatus*, and spot, *Leiostomus xanthurus*, in the northern Gulf of Mexico. Fish. Bull. 85:601–609.

Stockley, P., M. J. G. Gage, G. A. Parker, and A. P. Møller.
1997. Sperm competition in fishes: the evolution of testis size and ejaculate characteristics. Am. Nat. 149:933–954.

Tsikliras, A. C., and E. Antonopoulou.
2006. Reproductive biology of round sardinella (*Sardi-*

nella aurita) in the north-eastern Mediterranean. Sci. Mar. 70:281–290.

Tsikliras, A. C., E. Antonopoulou, and K. I. Stergiou.
2010. Spawning period of Mediterranean marine fishes. Rev. Fish Biol. Fish. 20:499–538.

Vaughan, D. S., K. W. Shertzer, and J. W. Smith.
2007. Gulf menhaden (*Brevoortia patronus*) in the U.S. Gulf of Mexico: fishery characteristics and biological reference points for management. Fish. Res. 83:263–275.

West, G.
1990. Methods of assessing ovarian development in fishes: a review. Aust. J. Mar. Freshw. Res. 41:199–222.

Williams, E. H and K. W. Shertzer.
2015. Technical documentation of the Beaufort Assessment Model (BAM). NOAA Tech. Memo NMFS-SEFSC-671, 43 p.

Wootton, R. J.
1998. Ecology of teleost fishes, 2nd ed., 392 p. Kluwer Academic Publishers, Dordrecht, Netherlands.

National Marine Fisheries Service NOAA

Fishery Bulletin
established in 1881

Spencer F. Baird
First U.S. Commissioner of Fisheries and founder of *Fishery Bulletin*

Management strategy evaluation for the Atlantic surfclam (*Spisula solidissima*) using a spatially explicit, vessel-based fisheries model

Kelsey M. Kuykendall (contact author)[1]
Eric N. Powell[1]
John M. Klinck[2]
Paula T. Moreno[1]
Robert T. Leaf[1]

Email address for contact author: kelsey.kuykendall@usm.edu

[1] Gulf Coast Research Laboratory
The University of Southern Mississippi
703 East Beach Drive
Ocean Springs, Mississippi 39564

[2] Center for Coastal Physical Oceanography
Department of Ocean, Earth, and Atmospheric Sciences
4111 Monarch Way, 3rd Floor
Old Dominion University
Norfolk, Virginia 23529

Abstract—The commercially valuable Atlantic surfclam (*Spisula solidissima*) is harvested along the northeastern continental shelf of the United States. Its range has contracted and shifted north, driven by warmer bottom water temperatures. Declining landings per unit of effort (LPUE) in the Mid-Atlantic Bight (MAB) is one result. Declining stock abundance and LPUE suggest that overfishing may be occurring off New Jersey. A management strategy evaluation (MSE) for the Atlantic surfclam is implemented to evaluate rotating closures to enhance Atlantic surfclam productivity and increase fishery viability in the MAB. Active agents of the MSE model are individual fishing vessels with performance and quota constraints influenced by captains' behavior over a spatially varying population. Management alternatives include 2 rules regarding closure locations and 3 rules regarding closure durations. Simulations showed that stock biomass increased, up to 17%, under most alternative strategies in relation to estimated stock biomass under present-day management, and LPUE increased under most alternative strategies, by up to 21%. When incidental mortality caused by the fishery increased, the benefits seen under the alternative management were enhanced. These outcomes suggest that area management involving rotating closures could be valuable in insulating the stock and the commercial fishery from further declines as a northerly shift in range proceeds.

Manuscript submitted 28 June 2016.
Manuscript accepted 27 March 2017.
Fish. Bull. 115:300–325 (2017).
Online publication date: 4 May 2017.
doi: 10.7755/FB.115.3.3

The views and opinions expressed or implied in this article are those of the author (or authors) and do not necessarily reflect the position of the National Marine Fisheries Service, NOAA.

The Atlantic surfclam (*Spisula solidissima*) is an economically valuable bivalve common to the sandy bottoms off the northeastern coast of the United States and Canada (Weinberg, 2005). The range of the Atlantic surfclam before recent effects of global warming spanned the western North Atlantic Ocean continental shelf from Nova Scotia to northern South Carolina, at depths of 10 m to 50 m, and temperature determines the range boundaries (Goldberg and Walker, 1990; Weinberg, 1998; Jacobson and Weinberg[1]; NEFSC[2]). They are generally not found where average bottom temperatures exceed 25°C (Cargnelli et al., 1999). Atlantic surfclams are relatively sessile planktivorous filter feeders that rarely vacate their burrow unless resuspended by storms or they are escaping predators (Ropes and Merrill, 1973; Prior et al., 1979), after which they rapidly reburrow into the substrate (Weinberg, 2005). The life span of Atlantic surfclam is approximately 30 years and has a maximum-recorded shell length (SL) of 226 mm (Fay et al.[3]; Cargnelli et al., 1999; Munroe et al., 2016).

The range of Atlantic surfclam has been shifting north and offshore since approximately 1970, driven primarily by warming bottom water temperatures (Cargnelli et al., 1999;

[1] Jacobson, L., and J. Weinberg. 2006. Atlantic surfclam (*Spisula solidissima*). *In* Status of fishery resources of the Northeastern US (R. Mayo, F. Serchuk, and E. Holmes, eds.), 1–8 p. Northeast Fish. Sci. Cent., Woods Hole, MA. [Available from website.]

[2] NEFSC (Northeast Fisheries Science Center). 2013. 56th Northeast Regional Stock Assessment Workshop (56th SAW) assessment summary report. U.S. Dep. Commer, Northeast Fish. Sci. Cent. Ref. Doc. 13-04, 42 p. [Available from website.]

[3] Fay, C. W., R. J. Neves, and G. B. Pardue. 1983. Species profiles: life histories and environmental requirements of coastal fishes and invertebrates (mid-Atlantic) surf clam. U.S. Fish. Wildl. Serv., FWS/OBS-82/11.13, U.S. Army Corps Eng., TR EL-82-4, 23 p.

Weinberg, 2005; Munroe et al., 2013; Hofmann et al., in press). Early evidence of this trend is the disappearance of Atlantic surfclams in Virginia and Maryland state waters between the 1970s and the 1990s (Loesch and Ropes, 1977; Powell[4]; Hofmann et al., in press) and the shift of the southern fishery from the Delmarva Peninsula to ports north (Powell et al., 2015). From the 1997 to 1999 period, the Atlantic surfclam population was considered to be near carrying capacity (NEFSC[2]). Abundances were once high on the continental shelf off the Delmarva Peninsula, but declines in growth, maximum size, and tissue weight (Weinberg, 1998, 1999) were accompanied by increased mortality in this region (Weinberg, 2005; Weinberg et al.[5]). Separate fisheries-independent surveys conducted in 2002 by the Northeast Fisheries Science Center of the National Marine Fisheries Service (NMFS) and the New Jersey Department of Environmental Protection revealed that a large mortality event had occurred sometime after 1999 that extirpated Atlantic surfclams from the southern inshore region off Delmarva Peninsula, followed by stock declines in both state and inshore federal waters off New Jersey (Powell[4]; Kim and Powell, 2004). An additional survey conducted in 2004 (Weinberg et al.[5]) confirmed the northward and offshore shift in the Atlantic surfclam stock.

One result of these mortality events was the redistribution of the stock north: namely an increasing abundance off the coast of Long Island, New York; the expansion of the population on Georges Bank; and the movement of the seaward boundary of the southern portion of the stock offshore in response to increased bottom water temperatures (Weinberg, 2005; Munroe et al., 2013; NEFSC[2]). Simulations by Narváez et al. (2015) based on stock assessment data from the Northeast Fisheries Science Center and bottom temperature time series obtained through implementation of the Regional Ocean Modeling System for the northwestern Atlantic indicated that episodic warm years caused elevated mortality events in older and larger clams and that these events have occurred with increasing frequency over the last several decades of the 20th century. In the simulation study, Narváez et al. (2015) found that thermal stress decreased the Atlantic surfclam stock by 2–9% on the shelf regions that coincide with a majority of the regions used by the commercial fishery.

The Atlantic surfclam reaches marketable sizes of 120 to 150 mm SL within 6–7 years depending upon food availability and water temperature (Weinberg, 1998; Cargnelli et al., 1999; Weinberg et al., 2002; NEFSC[2]). Growth rates within the first 3 to 5 years have been reported to be similar across much of the range of the Atlantic surfclam before the 1999 mortality event (Cargnelli et al., 1999). Increased bottom water temperatures above approximately 20°C negatively affect Atlantic surfclam nutrition by reducing ingestion rate and leading to a reduction in growth rate, condition, and maximum size (Marzec et al., 2010; Munroe et al., 2013; Munroe et al., 2016). Munroe et al. (2016) found that the maximum size had, in fact, declined for much of the stock since 1980. Simulation modeling of Atlantic surfclam population dynamics shows that this outcome can be derived solely from rising bottom water temperatures (Munroe et al., 2013, 2016), although a change in food supply would result in the same outcome.

Along the Mid-Atlantic coast, the Atlantic surfclam has supported a fishery since the 1960s that reached total revenues of $29 million in 2011 (Weinberg, 1999; Weinberg et al.[5]; NEFSC[2]). The average rate of fishing-induced mortality (commonly termed "fishing mortality") in the stock south of Hudson Canyon has been higher than the fishing mortality rate over the whole stock and of the northern region since 2002; however, the fishing mortality rate, which historically has been less than 25% of the natural mortality rate (M=0.15/year), remains below the natural mortality rate (NEFSC[2]).

For the last 30 years, most of the commercial landings within the U.S. Exclusive Economic Zone have been harvested along the coast of New Jersey and the Delmarva Peninsula (Weinberg, 1999; NEFSC[2]). Landings in this region within the last decade have declined coincident with the latest phase of contraction in the distribution range of this species. According to the latest stock assessment, the Atlantic surfclam is not overfished, and overfishing is unlikely to occur in the next 5–7 years (NEFSC[2]). However, declining stock abundance has led to the termination of a once thriving clam fishery in the most southerly portions of its range since 2000. A decline in landings per unit of effort (LPUEs), coupled with rising fishing morality rates, has generated concern for the sustainability of the stock off New Jersey (Powell[4]; Weinberg et al.[5]; NEFSC[2]). The reopening of Georges Bank for harvesting of clams in 2010 (NOAA, 2012)—an area that was closed in 1990 owing to the risk of harvesting clams contaminated with paralytic shellfish poison (Jacobson and Weinberg[1]) —allowed some relief from fishing pressure in other regions, but landings over much of the remainder of the stock continue to produce the steady decline observed since 2008 (Fig. 1) (NEFSC[2]).

Declining abundance and LPUE south of Hudson Canyon have driven stakeholders' desire to enhance production in the New Jersey portion of the stock (Fig. 1), possibly through the implementation of area management, which has proven to be a useful tool for improving production in fisheries of sessile species (Powell et al., 2008; Cooley et al., 2015). Examples of fisheries where implementation of this strategy has been successful are the fisheries for sea scallop (*Placopecten magellanicus*) in the Mid-Atlantic Bight (MAB) and

[4] Powell, E. N. 2003. Maryland inshore surf clam, *Spisula solidissima*, survey August 2003 cruise report. Final report to J. H. Miles & Co. Inc., 19 p. Haskin Shellfish Research Laboratory, Port Norris, NJ.

[5] Weinberg, J. R., E. N. Powell, C. Pickett, V. A. Nordahl Jr, and L. D. Jacobson. 2005. Results from the 2004 cooperative survey of Atlantic surfclams. U.S. Dep. Commer., Northeast Fish. Sci. Cent. Ref. Doc. 05-01, 41 p. [Available from website.]

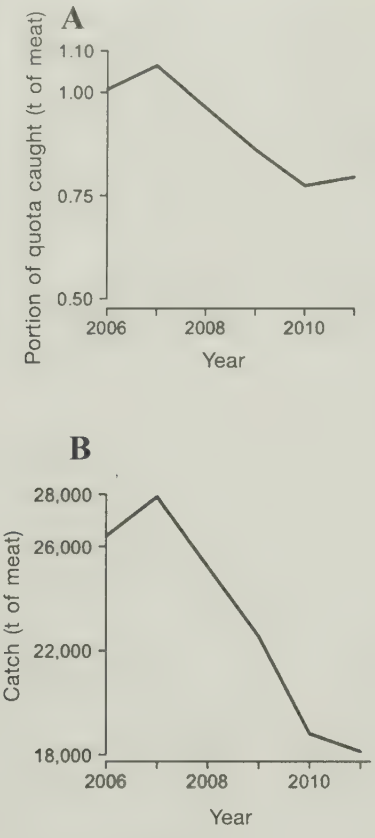

Figure 1

Landings of Atlantic surfclam (*Spisula solidissima*) during 2008–2013 in the Mid-Atlantic Bight determined from a stock assessment by the NOAA Northeast Fisheries Science Center (NEFSC[2]). (**A**) The portion of the quota harvested from the entire stock off the northeastern coast of the United States (shown in metric tons [t] of meat). The opening of Georges Bank is responsible for the slight improvement in the percentage of quota harvested in 2010. (**B**) The amount of catch that was reported from only the southern region of the fishing area along the northeastern coast of the United States, which excludes Georges Bank.

New England regions (Cooley et al., 2015), and the oyster fishery in Delaware Bay (Powell et al., 2008). One method for examining the risks and benefits associated with area management and management plans in general is to conduct a management strategy evaluation (Smith, 1994). An MSE is a quantitative tool used to evaluate a range of possible management procedures by comparing performance statistics or metrics (Butterworth and Punt, 1999; Martell et al.[6]; Punt et al., 2014). Butterworth et al. (1997) describe management procedures as "a set of rules which utilize prespecified data to provide recommendations for management actions." Performance metrics must be chosen carefully, preferably in collaboration with the stakeholders of the fishery, to ensure clear and easy interpretation of simulation results (Francis and Shotton, 1997). As examples, MSE has been used to contrast the performance of fishery alternative management strategies in the Pacific halibut (*Hippoglossus stenolepis*) (Martell et al.[6]), rock lobster (*Jasus edwardsii*) (Punt et al., 2013), and U.S. southeastern king mackerel (*Scomberomorus cavalla*) (Miller et al., 2010) fisheries (see Spillman et al., 2009; Baudron et al., 2010; Bastardie et al., 2010 for additional examples).

The objective of our study is to evaluate a range of area management options that may improve the Atlantic surfclam stock and the Atlantic surfclam fishery in the MAB. The Atlantic surfclam stock for this study is defined as the portion of the U.S. stock from approximately Shinnecock, New York, south to Chesapeake Bay. After specification of management options, the results of a series of simulations are presented and evaluated on the basis of performance metrics estimated with varying Atlantic surfclam population dynamics and a range of commercial procedures, including fishing behaviors. The inclusion of fishing behavior is critical because captains respond to new management measures, and this response will in part determine the degree of success of those management measures after implementation (Bockstael and Opaluch, 1983; Gillis et al., 1995; Mackinson et al., 1997; Dorn, 2001; Millischer and Gascuel, 2006). Subsequent statistical analyses of performance metrics pertinent to population productivity and fishery sustainability will be used to identify preferred management options that provide significant improvement in performance metrics in comparison with present-day management.

Materials and methods

Description of the model used for management strategy evaluation

The spatially explicit fishery economics simulator (SEFES) is an individual-based model of a temporally and spatially variable stock of Atlantic surfclam harvested by a fleet of individual commercial vessels (Fig. 2). The primary model is written in Fortran 90 and is then processed in MATLAB,[7] vers. R2015B (MathWorks, Natick,

[6] Martell, S., B. Leaman, and I. Stewart. 2014. Developments in the management strategy evaluation process, fisheries objectives, and implications for harvest policy and decision making. IPHC Rep. Assess. Res. Act. 2013:239–260. [Available from website.]

[7] Mention of trade names or commercial companies is for identification purposes only and does not imply endorsement by the National Marine Fisheries Service, NOAA.

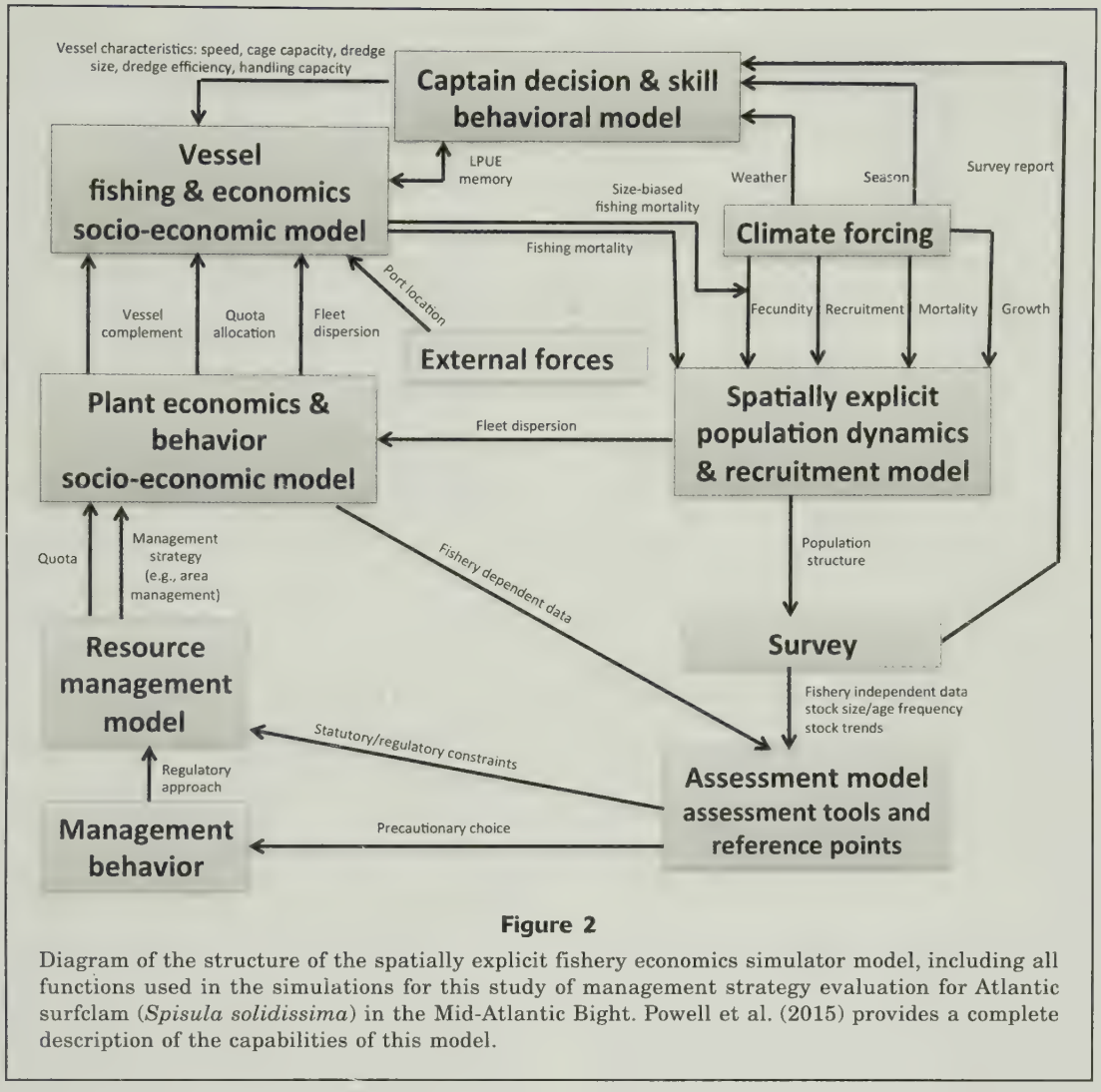

Figure 2

Diagram of the structure of the spatially explicit fishery economics simulator model, including all functions used in the simulations for this study of management strategy evaluation for Atlantic surfclam (*Spisula solidissima*) in the Mid-Atlantic Bight. Powell et al. (2015) provides a complete description of the capabilities of this model.

MA) and analyzed with SAS statistical software, vers. 9 (SAS Institute Inc., Cary, NC). Models that track fishing fleets spatially or seasonally are becoming increasingly important (Holland and Sutinen, 2000; Hutton et al., 2004; Mahévas and Pelletier, 2004; Monroy et al., 2010; van Putten et al., 2012). The SEFES model permits simulation of the entire fishing fleet and each vessel operating independently according to specified criteria. Powell et al. (2015) provide a detailed model description. Pertinent details for this study are summarized here.

The spatial domain of the model consists of a rectangular grid of cells with areas of 10′ of latitude by 10′ of longitude. The 10′-square resolution of these cells corresponds with the resolution of data reported in logbooks (NEFSC[2]). The grid, which is specified for the MAB, consists of 17 cells in the east–west dimension and 26 cells in the north–south dimension. Each cell, or 10′ square, is classified as land, fishable area, or unfishable area by a spatial mask. Three land cells specify the location of home ports located from north to south at 1) Oceanside, New York, 2) Atlantic City, New Jersey, and 3) Point Pleasant, New Jersey. Of the 400 ocean cells, 52 are fishable areas and the remaining cells are areas presently poorly inhabited or uninhabited by Atlantic surfclam (Fig. 3).

Active agents of the model are the 19 commercial vessels that harvest Atlantic surfclam under imposed operational constraints and decisions from the vessel captain. Operational constraints, which can vary among vessels, include vessel speed, maximum allowed time at sea, harvest capacities, and imposed harvest quotas. Each active vessel in the fleet is specified uniquely in the model and is committed to 1 of 3 home ports on the basis of location where that vessel usually offloads its catch. The commercial vessels travel within the spatial domain and harvests Atlantic surfclam based on decisions by the captains of where trip quotas can be met most efficiently (i.e., shortest time to fill the vessel with the lowest operational costs). The captains' decisions are based on "memories" that are built from information regarding LPUEs

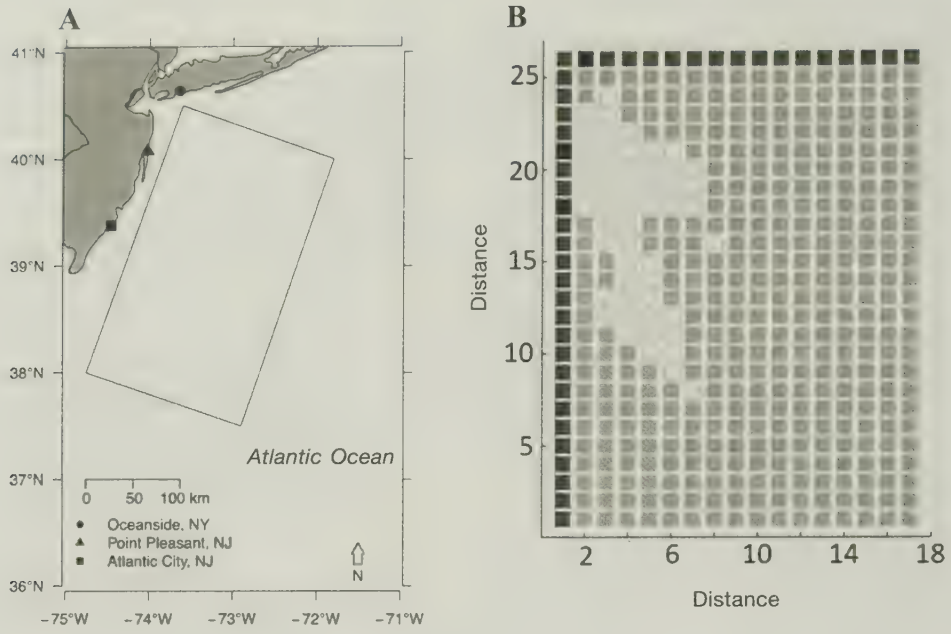

Figure 3

(**A**) Map showing the location of home ports and a representation of the model domain outlined for this study of management strategy evaluation for Atlantic surfclam (*Spisula solidissima*) in the Mid-Atlantic Bight. (**B**) Model domain with ports (black squares), fishable areas (white squares), unfishable areas (light gray squares), and land (dark gray squares). Each cell in the domain has a resolution of 10′×10′. The domain contains 52 10′ squares available to the fishery (white squares). Distance represents distances along the x and y axis of ten-minute squares in the grid.

for 10′ squares that were fished. The memory of LPUE for a 10′ square fished during a trip is updated after each trip. Over time a captain's memory of the entire domain degrades as the stock changes because the captain has up-to-date information only for recently fished 10′ squares. Each captain has a skill level that can range from 1 to 10 in the model—a level that determines the amount of time the dredge is actively fishing with 10 representing 100%. All captains in this study had a skill level of 10. See Powell et al. (2015) for a more detailed description of "captain memory development" and skill levels.

Each simulation spans a total of 201 years. The time step is given in days and certain fishing activities are time-stepped in hours, and data for evaluation of performance metrics are collected annually. Model days are converted to calendar dates to allow for seasonal variability in weather and fishing behaviors (e.g., fewer trips during winter months). No fishing occurs in the first 100 years of each simulation to allow the Atlantic surfclam population to reach equilibrium with specified characteristics, such as abundance and distribution of individuals that are based on larval survival. After this period of time, the population is near carrying capacity and is characterized by a locally patchy distribution with regional characteristics consistent with the latitudinal and cross-shelf temperature gradients. The next 25 years represents historical fishing. During this time, a captain's memories of stock distribution and LPUE develops and the stock is fished down to a desired specified level. Area management is imposed in year 126 and the final 76 years are used to evaluate the area management option (i.e. the combination of closure location rule and closure duration used) in relation to present-day management.

Three initial stock distributions ranging from dense to sparse levels of patchiness were specified to cover a range in stock patchiness. Patchiness was established by assigning new recruits to each 10′ square by using a negative binomial random distribution that produced distinctive variance in the abundance of clams in each 10′ square relative to the mean abundance for all 10′ squares. Variation in patchiness of the distribution is included in this study as a sensitivity analysis with a range that is typical of bivalve populations and consistent with Northeast Fisheries Science Center Atlantic surfclam and ocean quahog (*Arctica islandica*) survey data. An Allee effect was not included; population densities are assumed not to limit fertilization efficiency. Recruitment is an annual event. The recruitment rate is set by a broodstock–recruitment relationship (Powell et al., 2015) that results in levels of postsettlement abundance that are representative of present-day abundance that is based on data from the Northeast Fisheries Science Center 2011 Atlantic surfclam and ocean quahog survey.

Atlantic surfclams are distributed in length-based size classes. Average wet weights (W) are calculated with an allometric relationship of the form (Marzec et al., 2010):

$$W = aL^b, \quad (1)$$

where L = the length in millimeters.

Parameter values come from Marzec et al. (2010). Growth and mortality rates vary latitudinally and across-shelf for each 10′ square. The growth rate of Atlantic surfclam is calculated from a von Bertalanffy growth curve (with a growth rate (k) that increases in the northern and eastward direction) by using the following equation:

$$L_A = L_\infty(1 - e^{-kA}), \quad (2)$$

where L = length in millimeters; and
A = age in years.

Parameters are based on Munroe et al. (2016) and NEFSC[2]. Natural mortality is imposed by using a constant mortality rate across all size classes consistent with the presently accepted stock assessment model (NEFSC[2]) and the analysis of Weinberg (1999) and is specified to increase from northeast to southwest across the domain to reduce Atlantic surfclam abundance at the southern and inshore extremes of the range as observed.

A survey of the simulated clam population is conducted annually on 1 November and includes the most recent recruitment event. The true clam density for each 10′ square is used for this survey and samples are taken from every 10′ square in the domain. Results from the survey are then used to set the annual quota based on a quota cap established by the fishery management plan (FMP) for the Atlantic surfclam (MAFMC[8]), the presently accepted biological reference points (NEFSC[2]), and the allowable biological catch control rules. The annual quota biomass is then converted to bushels of clams. In practice, the Atlantic surfclam allowable biological catch has always been above the FMP quota cap. The stock has never been overfished and overfishing has never occurred. Consequently, in these simulations, the total allowable catch remained stable at the FMP quota cap of 3.5 million bushels. Thus, simulations address management options for a fishery in which overfishing does not occur and for which the stock is not overfished—simulations consistent with the conditions present throughout the 2000 to 2012 period as documented in the most recent federal assessment (NEFSC[2]).

For the current FMP for Atlantic surfclams, an individual transferable quota system is used that allocates a number of cage landings to each of the shareholders (McCay et al., 1995; MAFMC[9]; NEFSC[2]). In practice, these shares are amassed through direct ownership or lease by processing plants and quotas are issued to the vessels each of which fishes exclusively for specific processing plants. That is, the fishery is vertically integrated with processing plants holding quotas that they distribute to vessels that land catch only at designated ports. Within this model, the current FMP is implemented and area management is added to the management plan. Each processing plant distributes its fraction of the total quota to its vessels weekly. The weekly quota is limited to twice the vessel hold size serving to limit the number of trips per vessel to 2 trips/week, a number consistent with industry practice. During each simulation, a vessel harvests clams on the basis of the captain's decision and memory of fishing areas and according to imposed harvest quotas. The vessels fish to capacity if possible, given the constraint that time at sea is restricted during the warmer months to limit deterioration of the catch because Atlantic surfclam vessels have no or a limited capacity for refrigeration. Captains' memories are updated after each fishing trip. Harvest rates are calculated from tow speed, dredge width, dredge efficiency, the size selectivity of the dredge, and the skill of the captain. Tow speed, dredge width, dredge efficiency, and the size selectivity of the dredge are based on federal survey program data reported from 2011 (e.g., NEFSC[2]) and data received in 2013 from vessel owners and captains on standard operating conditions for harvesting Atlantic surfclam.

Simulation experiments

The essential elements of an MSE include management objectives, performance metrics, and management options (Smith, 1994). The primary management objective is to insulate both the Atlantic surfclam stock and the commercial LPUE from further decline. The evaluation of alternative management procedures for both the enhancement of the Atlantic surfclam stock and the economics of the industry is based on statistical analysis of performance metrics. The performance metrics are rooted in interviews with representatives from processing plants, industry trade organizations, and vessel captains to ensure appropriateness. The performance metrics chosen are important in that they provide metrics that allow commercial stakeholders to evaluate the results of each management procedure based on their business model. A total of 5 performance metrics were used. Two of these metrics are used to measure the population: clam whole-stock density, which is the number of clams ≥120 mm SL per square meter (the fishable stock is defined as clams ≥120 SL mm [NEFSC[2]]), and the number of clams per bushel. Three metrics were used to measure the effect of area management on the

[8] MAFMC (Mid-Atlantic Fishery Management Council). 1986. Amendment #6 to the fishery management plan for Atlantic surf clam and ocean quahog fisheries, rev. ed., 102 p. Mid-Atlantic Fishery Management Council, Dover, DE [Available from website.]

[9] MAFMC (Mid-Atlantic Fishery Management Council). 2013. Atlantic surfclam information document, 9 p. Mid-Atlantic Fishery Management Council, Dover, DE. [Available from website, accessed September 2014.]

commercial industry: 1) LPUE, which is the number of bushels fished per hour; 2) the number of 10′ squares fished; and 3) the total distance traveled per fishing trip (in kilometers). The location of ports and processing plants are invariable, consistent with present-day economic limitations that make the movement of processing capacity an implausible adaptation. The management options include a range of closure locations and durations discussed later in this section.

Alternative hypotheses about population dynamics, often termed "states of nature," such as dispersion and abundance of a stock, can cause marked differences in the density and disposition of a stock and influence the success of management alternatives (Punt and Hilborn, 1997; McAllister and Kirkwood, 1998; Hilborn, 2003). In this study, variations in stock distribution are simulated as differing degrees of patchiness obtained by increasing the ratio of the variance in recruitment among 10′ squares to the mean recruitment for the entire population, with each degree being a variance-to-mean ratio approximately twice the value of the previous one (e.g., medium patchiness has a variance-to-mean ratio that is approximately twice that of low patchiness). Stock abundance is representative of present-day abundance in 2011 (NEFSC[2]) based on abundance data from the Northeast Fisheries Science Center Atlantic surfclam and ocean quahog survey in 2011 (NEFSC[2]).

Incidental mortality of clams that remain on the sea floor after dredging is investigated by setting incidental mortality to 0% and 20% of the clams encountered by the dredge but not caught in the dredge. The assumption that is currently made by NMFS is that incidental mortality occurs at an intermediate value of approximately 12% (NEFSC[2]) based on Meyer et al. (1981). For each of the degrees of patchiness and for the 2 levels of incidental mortality, simulations were performed with present-day management (termed "base cases" hereafter) for a comparison with simulations of area management options.

Incorporation and manipulation of various commercial procedures allow an investigation of the fishery and the plausible options for enhancement of economic opportunities. Captain behavioral types, closure durations, closure locations, and years to harvest (i.e., the elapsed time for a small clam of specified size to reach a defined market size) have all been identified as pertinent commercial features when considering management strategies. Commercial procedures are based on interviews conducted with industry leaders, including representatives from processing plants and trade organizations, and vessel captains.

One of 3 captain behavioral types (standard, survey, confident) is included in each simulation. Captain behaviors are exclusive to each captain type (e.g., confident captains do not use survey data). Standard captains do not search for new fishing grounds and do not use survey data. Survey captains update their knowledge every 3 years with data from NMFS population surveys. The use of NMFS survey data by captains is common practice and has been found to improve performance in simulation studies (Powell et al., 2015). Confident captains spend 20% of fishing time searching for new fishing grounds. In simulations, searching behavior produces similar positive changes in performance because using survey data (Powell et al., 2015) and searching is reported as a desirable practice by captains. Each individual simulation has a defined degree of stock patchiness and captain type (Table 1). Nine simulations, 1 simulation for each combination of captain type and stock patchiness, constitute 1 set of cases, hereafter termed an ennead (Fig. 4).

Hypotheses of this study are that area management will be beneficial for the Atlantic surfclam stock and commercial fishery. A comparison of performance metrics between enneads under present-day and those under alternative management allowed us to test our hypotheses (Fig. 5). Management alternatives consist of closures of one 10′ square per year during the 76 simulated fishing years. The management alternatives simulate the addition of area closures to the current management plan. Area closure locations are based on 1 of 2 rules; a given rule remains in effect throughout the 76 simulated fishing years. If rule 1 is executed, the 10′ square with the highest ratio of the number of small clams to the number of market-size clams is closed each year. Rule 1 focuses on the importance of the proportional presence of small clams. If rule 2 is imposed, the 10′ square with the largest density of small clams (number of clams per square meter) is closed each year. Rule 2 considers the population of small clams as a whole over an area. Closure durations of 3, 5, and 7 years are compared with no closures. This results in 3, 5, or 7 10′ squares being closed during each of the simulated years once the initial span of time specified has elapsed. The closure durations would result in 6%, 10%, and 14%, respectively, of the fishable area being closed in any year after the maximum number of 10′ squares were closed (e.g., for the 5-year closure duration, five 10′ squares [10% of the fished area] would be closed at a given time).

Success of both of the area management rules for closure location varies depending on the definition of a small clam (i.e., a clam that is smaller than market size). The definition of a small clam implemented in the simulations is a value that depends on the time required for a clam to grow to market size (120 mm SL; NEFSC[2]). The specified size depends on growth rate, which is variable across the domain. This variation allows clams to grow faster in some regions than in others, depending on water temperature. A range of years (from 2 to 5 years) to reach harvest size is investigated in this study. The number of small clams is determined on the basis of the smallest SL that would reach market size (120 mm SL) in a defined period of time. All clams with SL that would reach market size, or larger, in the defined amount of time in a 10′ square, but <120 mm SL (i.e., less than market size), are counted to invoke closure location rule 1 or 2 depending on which rule is being used for a given set of simulations. For convenience, an average of the minimum sizes for all

Table 1

Varying characteristics of model simulations used in the management strategy evaluation for the Atlantic surfclam (*Spisula solidissima*) in the Mid-Atlantic Bight. The structure of each set of cases is shown in bold. Incidental mortality applies to clams that are not retained by the dredge. Nine individual simulations (in bold) represent one set of cases, an ennead (see also Fig. 4). An ennead was run for each level of incidental mortality, each management option, each closure duration, and each definition of a small clam for a total of 72 (2×3×3×4) enneads. Market-size clams are ≥120 mm shell length (SL). LPUE is measured as number of bushels fished per hour. Three initial stock distributions ranging from dense to sparse levels of patchiness were specified to cover a range in stock patchiness. Patchiness was established by assigning new recruits to each 10′ square by using a negative binomial random distribution that produced distinctive variance in the abundance of clams in each 10′ square relative to the mean abundance for all 10′ squares.

	Model configurations				Ennead complement	
Performance metrics	Levels of incidental mortality	Management options	Closure duration (yr)	Definitions of a small clam	Patchiness	Captain type
Stock density (number of clams ≥75 mm SL/m²)	0%	Present-day—no closures	3	104 mm SL	**High**	**Standard**
Number of clams per bushel	20%	Rule 1—close the 10′ square with the highest ratio of the number of small clams to the number of market-sized clams	5	93 mm SL	**Medium**	**Confident**
LPUE (bushels/h)		Rule 2—close the 10′ square with the highest number of small clams/m²	7	80 mm SL	**Low**	**Survey**
Number of 10′ squares fished				64 mm SL		
Distance traveled during fishing (km)						

10′ squares is used to identify groups of clams with the same maximal elapsed time to market size for our presentation of simulation results. These averages are 104, 93, 80, and 64 mm SL for 2, 3, 4, and 5 growth years, respectively, to reach 120 mm SL.

Statistical evaluation of alternative management strategies

Each comparison between present-day and alternative management is based on an ennead of simulations with varying captain behavior and patchiness of recruitment (Table 1) for each defined size of a small clam and each specified closure duration. This results in 4 enneads per closure duration (1 set of 9 for each definition of a small clam) and 12 enneads per closure location rule (Fig. 4). The structure of the base case is composed of the same states of nature and captain behaviors as the alternative management cases, excluding area closures. Each ennead is designed to evaluate the interaction of patchiness of distribution with captain behavior in order to evaluate the sensitivity of outcomes to this key interaction.

Management strategies were compared by using the nonparametric Wilcoxon signed-rank test (Conover, 1980). This test uses the difference in metric values between 2 outcomes—in this case the difference between the base case and the otherwise equivalent simulation under alternative management (e.g., closure location rules 1 and 2, closure durations, and small clam definitions (i.e., years to market size, Fig. 5). Each comparison was based on 76 years of simulated time, with 1 difference calculated for each of the 76 years; therefore, a single Wilcoxon test was based on n=76 (Fig. 6). Because each year was different from each succeeding or preceding year because a 10′ square was opened and closed each year and because each vessel and captain operated independently in each year with their own behaviors and differing memories, each year represented a unique pairwise comparison of the area management option and the otherwise equivalent base case. Therefore, 9 Wilcoxon tests were conducted for each ennead. The likelihood of the number of significant outcomes from these 9 tests exceeding chance was evaluated by an exact binomial test (Conover, 1980). Any comparison yielding more than 1 significant difference between the base case and area management option out of the 9 simulations performed exceeded the number expected by chance at α=0.05.

Performance metrics were evaluated by the proportion of simulations that resulted in an increased performance metric in comparison with the base case with the same composition and the amount of increase seen in those significant simulations. Management strate-

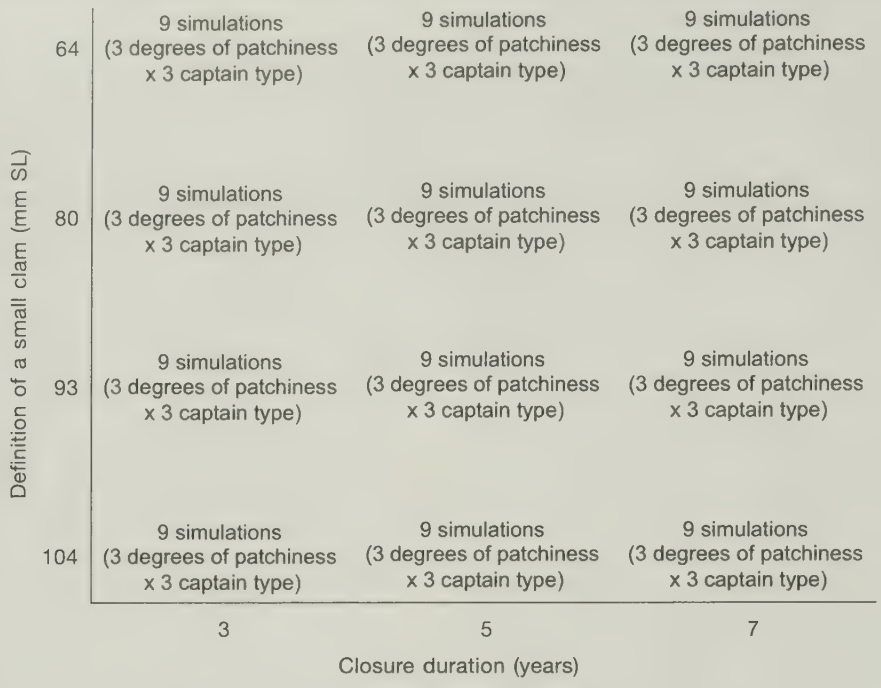

Figure 4

Matrix design for the sets of simulations used in pairwise comparisons of performance metrics for this study of the management strategy evaluation for the Atlantic surfclam (*Spisula solidissima*) in the Mid-Atlantic Bight. The matrix is repeated for each of the 2 closure location rules (rule 1: ratio of the number of small clams to the number of market-size clams; Rule 2: number of small clams per square meter). The increase in degree of patchiness approximately doubles between each level (i.e., the most patchy distribution is twice as patchy as the intermediate degree of patchiness). The 3 captain types are standard (does not search or use survey data), survey (uses survey data but does not search fishing grounds), and confident (searches but does not use survey data). Definitions of a small clam are given as of clams is given as shell length (SL) in millimeters.

gies that result in a large proportion of simulations that showed improvement in comparison with the base case (even if the proportional increase is small) are preferable because the scenario would be more likely to result in improvements if implemented than a scenario with few simulations showing improvement; that is, improvement can be expected over a wider range of contingencies influenced by differential recruitment patterns and captains' behaviors. It is possible that management decisions could be based on a large amount of increase even though the possibility of that outcome is low. For this reason, investigation of the possibility of the outcomes and the magnitude of the changes seen are included in this study. In addition to a comparison of the sets of alternative management and base cases, a second series of comparisons was conducted between alternative area management strategies; these offer additional insight as to which management options offer the most benefit.

In certain scenarios, a 4-year closure duration was examined in addition to the 3-, 5-, and 7-year closures. The performance metric values for the 4-year closure duration routinely fell between the 3- and 5-year closure durations performance metric values as seen in the number of clams per bushel and LPUE included in Table 2 as examples for comparison with simulation results discussed subsequently. For this reason, results of simulations with the use of the 4-year closure duration will not be presented subsequently.

Results

Closure location based on rule 1: the ratio of small clams to market-size clams

Stock density A greater proportion of simulations show a significant increase in stock density when the definition of a small clam was 93–120 mm SL or 80–120 mm SL (Table 3), which is representative of clams expected to reach market size (120 mm SL) in ≤3 and ≤4 years respectively. As the duration of the closure increased

Table 2

Summary statistics for average proportion differences for the number of clams per bushel and landings per unit of effort (LPUE), measured as the number of bushels fished per hour and given as examples of the results for the model that used the 4–year closure duration in an evaluation of management strategy for the Atlantic surfclam (*Spisula solidissima*) in the Mid–Atlantic Bight. Comparison can be made with data in Table 6. Size of clams is given as shell length (SL) in millimeters, and closure duration is measured in years. N is the number of simulations where a significant difference exists between the performance metric under present–day or alternative management at present–day abundance. The maximum N is 9.

		Definition of a small clam															
		104 mm SL				93 mm SL				80 mm SL				64 mm SL			
		Closure duration (yr)															
		3	4	5	7	3	4	5	7	3	4	5	7	3	4	5	7
Number of clams per bushel																	
Present management	N	5	9	9	9	2	9	9	9	2	5	9	9	2	3	9	9
	χ^2	0.01	0.02	0.03	0.04	0.01	0.02	0.03	0.04	0.01	0.01	0.02	0.04	0.01	0.01	0.01	0.03
Alternative management	N	0	0	0	0	0	0	0	0	0	0	0	0	0	0	0	0
	χ^2	–	–	–	–	–	–	–	–	–	–	–	–	–	–	–	–
LPUE																	
Present management	N	0	1	1	1	0	1	0	1	0	0	1	1	0	0	0	1
	χ^2	–	0.03	0.04	0.05	–	0.04	–	0.02	–	–	0.05	0.04	–	–	–	0.02
Alternative management	N	4	7	3	5	6	5	7	4	7	9	7	3	5	5	8	4
	χ^2	0.06	0.09	0.05	0.06	0.07	0.07	0.08	0.12	0.05	0.05	0.08	0.12	0.07	0.05	0.07	0.09

ing closed for some duration of years. A 10′ square that has been closed for a longer duration will result in the landing of larger clams and have a higher stock density, and therefore LPUE will be higher and lead to the vessels targeting these 10′ squares for a larger number of trips. Consequently, fewer 10′ squares will be visited to fill quotas. Increasing the incidental mortality imposed on clams that remain after dredging resulted in a larger percentage of simulations with significantly fewer 10′ squares fished during the year. Increased incidental mortality also caused larger percent decreases in the number of 10′ squares visited under alternative management.

Distance traveled per fishing trip In an average of 24% (range: 11–33%; Table 3) of 3-year closure simulations, the distance traveled to the fishing ground increased significantly, with an average increase in distance over all simulations of 3% (Fig. 7, Table 4). The 5-year closure duration also resulted in an average increase in distance traveled of 3% (Fig. 7, Table 4), but 47% (range: 44–56%; Table 3) of simulations showed significantly increased distance traveled under area management. The 7-year closure duration demonstrated the highest percentage of cases having significantly greater distances traveled (average: 58%; Table 3). Accordingly, the 7-year closure duration also resulted in the largest average percent increase in distance traveled (8%; Fig. 7, Table 4). As closure duration increases, some of the 10′ squares that are closed are close to the ports; the fishery would target these otherwise. Thus travel distance increases. A longer closure duration results in more 10′ squares close to the ports being closed: distance traveled must increase commensurately. The average percent increase in distance traveled was 4% (Fig. 7, Table 4) for all closure durations. When incidental mortality imposed on clams that remain after dredging was increased, the percentage of simulations that had significantly greater distances traveled under area management decreased (Table 5).

Closure location based on rule 2: the number of small clams per square meter

Stock density The 3-year closure duration resulted in an average increase of 4% in stock density (Fig. 8, Table 6), but an average of only 36% (range: 33–44%; Table 7 of simulations showed significantly increased stock density compared with that under present-day management. The 5-year closure duration resulted in an average increase in stock density of 4% (Fig. 8). The 5-year closure duration also had the highest average percentage of simulations that showed a significant stock density increase compared to present-day management (range: 33–67%; average: 50%; Table 7). The 7-year closure duration resulted in a 5% average increase in stock density (Fig. 8). On average, the 7-year closure duration showed significant increases in stock density in only 39% (range 0-56%; Table 7) of the simulations in comparison with present-day management. An increase in incidental mortality enhances the effect of alternative management (Table 8

Table 3

Evaluation of model simulations in which closure location rule 1 was used to examine the influence of area management on the stock and commercial fishery of Atlantic surfclam (*Spisula solidissima*) in the Mid-Atlantic Bight. Tabulated are the proportion of simulations where metrics used to evaluate the Atlantic surfclam population and commercial fishery were significantly greater under present-day management or alternative management under closure location rule 1 and with present-day abundance. Rule 1 mandates that the cell with the highest ratio of the number of small clams to the number of market-size clams be closed each year. There were 9 simulations per percentage. Any fraction over 0.11 (1 significant difference out of 9) is unlikely to occur by chance (exact binomial test: α=0.05; Conover, 1980). Size of clams is given as shell length (SL) in millimeters, closure duration is measured in years, and LPUE means landings per unit of effort.

	Definition of a small clam											
	104 mm SL			93 mm SL			80 mm SL			64 mm SL		
	Closure duration (yr)											
	3	5	7	3	5	7	3	5	7	3	5	7
Stock density												
Present management	0.44	0.44	0.11	0.11	0.11	0.00	0.22	0.11	0.11	0.33	0.22	0.56
Alternative management	0.44	0.33	0.56	0.44	0.67	0.44	0.56	0.56	0.44	0.22	0.33	0.33
Number of clams per bushel												
Present management	0.56	1.00	1.00	0.22	1.00	1.00	0.22	1.00	1.00	0.22	1.00	1.00
Alternative management	0.00	0.00	0.00	0.00	0.00	0.00	0.00	0.00	0.00	0.00	0.00	0.00
LPUE												
Present management	0.00	0.11	0.11	0.00	0.00	0.11	0.11	0.00	0.11	0.00	0.00	0.44
Alternative management	0.44	0.33	0.56	0.67	0.56	0.44	0.78	0.78	0.33	0.56	0.89	0.44
Number of 10′ squares fished												
Present management	0.44	0.56	0.67	0.33	0.44	0.56	0.44	0.56	0.44	0.44	0.44	0.56
Alternative management	0.22	0.00	0.11	0.11	0.00	0.00	0.11	0.00	0.00	0.33	0.00	0.00
Total distance traveled												
Present management	0.11	0.00	0.00	0.11	0.00	0.00	0.00	0.11	0.00	0.11	0.00	0.00
Alternative management	0.33	0.56	0.78	0.11	0.44	0.67	0.33	0.44	0.44	0.22	0.44	0.44

resulting in average stock density increases of 7–8% over the range of closure durations and definitions of a small clam.

Number of clams per bushel As the closure duration increased, the catch contained fewer clams per bushel; however, this effect did not vary significantly with a change in the definition of a small clam. The percentage of simulations that showed significantly more clams per bushel under present-day management reached the highest average of 97% (range: 89–100%; Table 7) for 7-year closure durations. With a 7-year closure duration, the number of clams per bushel was 3% higher under present-day management (Fig. 8, Table 6). The trend of fewer clams per bushel in area management options was muted by an increase in incidental mortality. Fewer simulations had significantly more clams per bushel under present-day management. The number of clams per bushel averaged 4% higher under present-day management than under the 7-year closure duration.

Landings per unit of effort All of the examined closure durations resulted in average increases of 8% in LPUE (Fig. 8, Table 6). The 3-year closure duration resulted in an increase in LPUE in an average of 64% of simulations (range: 56–89%; Table 7) when compared with LPUE under present-day management. The 5-year closure duration showed significantly enhanced LPUE in an average of 56% of simulations and resulted in significant increases in LPUE in an average of 64% of simulations (range: 44–78%; Table 7) when compared with LPUE under present-day management. The 7-year closure duration resulted in the least number of simulations having significantly increased LPUE (average: 42%; range: 22–67%; Table 7). The longest closure having the least amount of simulations with significantly improved LPUE might be attributed to the locations of closure. A closure based on the number of small clams per square meter might result in closure of some 10′ squares with the most total clams (i.e., small and market-size clams). As the closure duration increases, more 10′ squares are closed at a time. With the 7-year closure duration, more of the 10′ squares with high clam densities might be closed, thus causing a lower average LPUE.

Increased incidental mortality resulted in fewer simulations having significantly increased LPUE (Table 8). However, of the simulations where LPUE was significantly enhanced by alternative management, the

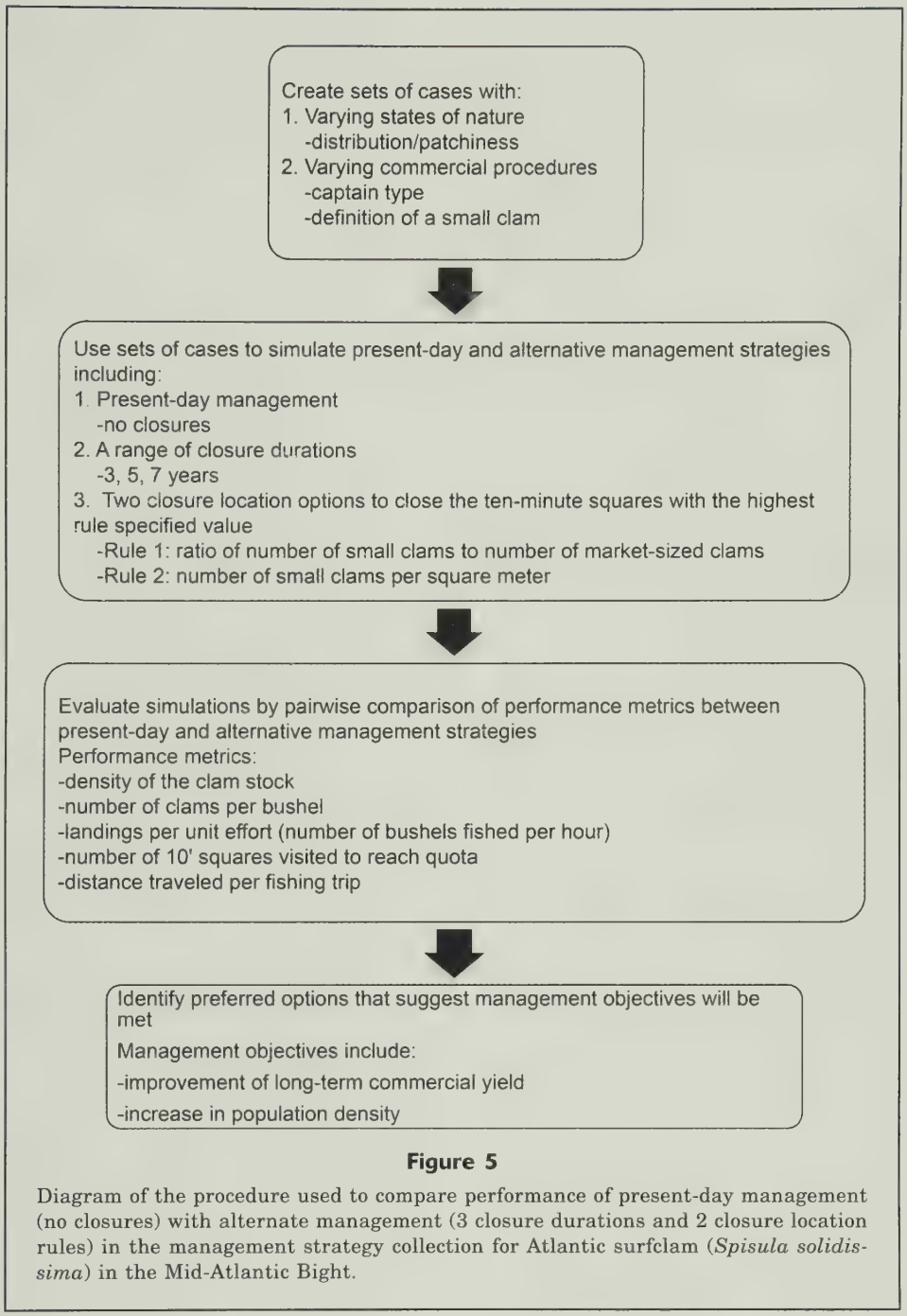
Create sets of cases with:
1. Varying states of nature
-distribution/patchiness
2. Varying commercial procedures
-captain type
-definition of a small clam
Use sets of cases to simulate present-day and alternative management strategies including:
1. Present-day management
-no closures
2. A range of closure durations
-3, 5, 7 years
3. Two closure location options to close the ten-minute squares with the highest rule specified value
-Rule 1: ratio of number of small clams to number of market-sized clams
-Rule 2: number of small clams per square meter
Evaluate simulations by pairwise comparison of performance metrics between present-day and alternative management strategies
Performance metrics:
-density of the clam stock
-number of clams per bushel
-landings per unit effort (number of bushels fished per hour)
-number of 10' squares visited to reach quota
-distance traveled per fishing trip
Identify preferred options that suggest management objectives will be met
Management objectives include:
-improvement of long-term commercial yield
-increase in population density

Figure 5

Diagram of the procedure used to compare performance of present-day management (no closures) with alternate management (3 closure durations and 2 closure location rules) in the management strategy collection for Atlantic surfclam (*Spisula solidissima*) in the Mid-Atlantic Bight.

from 3 to 7 years, the average percentage of simulations with significant increases in stock density under area management increased across all definitions of a small clam. The 3-year closure duration resulted in an average increase in stock density of 5% (Fig. 7, Table 4); 44% (Table 3) of simulations showed a significant increase in stock density compared to present-day management. The 5-year closure duration resulted in an average 4% increase in stock density over all definitions of a small clam (Fig. 7, Table 4). The greatest average percentage of simulations that showed a significant increase in stock density compared with that under present-day management is seen with the 5-year closure duration (range: 33–67%; average: 47%; Table 3). The 7-year closure duration resulted in a 7% average increase in stock density (Fig. 7, Table 4), the largest average stock density increase across all definitions of a small clam. The 7-year closure duration showed a significant increase in stock density in an average of 44% (range: 33–56%; Table 3) of the simulations in comparison with present-day management. When the imposed incidental mortality on clams not retained

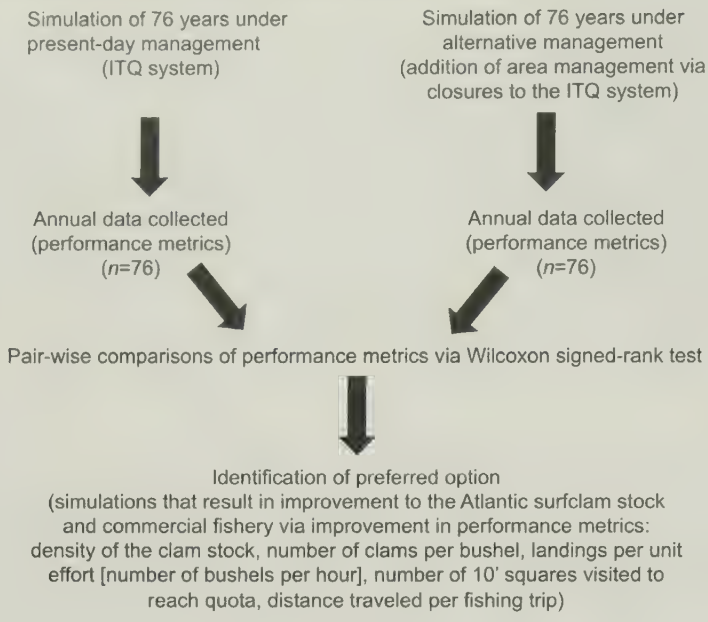
Simulation of 76 years under present-day management (ITQ system)
Simulation of 76 years under alternative management (addition of area management via closures to the ITQ system)
Annual data collected (performance metrics) (n=76)
Annual data collected (performance metrics) (n=76)
Pair-wise comparisons of performance metrics via Wilcoxon signed-rank test
Identification of preferred option
(simulations that result in improvement to the Atlantic surfclam stock and commercial fishery via improvement in performance metrics: density of the clam stock, number of clams per bushel, landings per unit effort [number of bushels per hour], number of 10′ squares visited to reach quota, distance traveled per fishing trip)

Figure 6

Diagram of the methods used to identify a preferred option to meet management objectives (i.e., improvement in the biomass of the Atlantic surfclam (*Spisula solidissima*) stock and economic opportunities of the commercial fishery in the Mid-Atlantic Bight). ITQ=individual transferrable quota.

by the dredge is increased from 0% to 20%, a higher percentage of simulations show significantly increased stock density and the degree of increase in stock density was also larger (Table 5). The increase in stock density with an increase in incidental mortality can be explained by the fact that without closures (i.e., under present-day management), small clams are subjected to additional mortality over the entire stock. Because of the closure rules, the fishery is shifted from regions where mortality on small clams would be most significant to areas of lesser impact because fewer small clams reside there. A closed 10′ square offers protection to the clams inside it until that 10′ square is reopened to the fishery, and these 10′ squares are characterized by a disproportionate number of small clams. As a consequence, the total mortality on small clams over the entire stock is reduced and stock density commensurately increases.

Number of clams per bushel As the closure duration increased from 3 to 7 years, fewer clams were required to fill a bushel. Having fewer clams per bushel suggests that larger clams are landed under alternative management and that as the duration of the closure increased, the size of landed clams increased. The percentage of simulations that showed significantly more clams per bushel under present-day management reached 100% (Table 3) for all 5-year and 7-year closure durations. The number of clams per bushel was on average 4% greater under present-day management than under the 7-year closure duration (Fig. 7, Table 4). The increased clam size as the duration of the closure increased was not affected by an increase in incidental mortality (Table 5).

Landings per unit of effort As the size defining a small clam decreased, a greater proportion of simulations had significant LPUE increases under the 5- and 7-year closure durations in comparison with LPUE under present-day management. The proportion of clams in the stock defined as small increased as the size defining a small clam decreased. For example, as the definition of a small clam changed from 93–120 mm SL to 80–120 mm SL, more clams in the population are defined as small because the clams between 92 and 80 mm SL are now added to the number of clams deemed to be small. The LPUE declines when the size definition increases from 80–120 mm SL to 93–120 mm SL. The 10′ squares with the highest clam density, which are now dominated by fewer small clams when the 93–120 mm SL definition is used, are being closed on the basis of the closure location rule (close 10′ square with largest ratio of the number of small clams to the number of market-size clams). Thus, more clams are protected when the definition of a small clam is smaller (i.e., 80–120 mm SL) which leads to a larger number of clams in the stock when the 10′ square reopens.

All of the examined closure durations resulted in average increases of 6% in LPUE (Fig. 7, Table 4). The 3-year closure duration resulted in 61% (Table 3) of simulations showing a significant increase in LPUE compared with that under present-day management. The 5-year closure duration had the highest average percentage of simulations that showed a significant increase in LPUE compared with LPUE under present-day management (range: 33–89%; average: 64%; Table 3). The 7-year closure duration had the lowest average percentage of simulations showing a significant increase in LPUE in comparison with that under present-day management (range: 33–56%; average: 44%; Table 3). When additional incidental mortality is imposed, the effect of alternative management in increasing the LPUE is enhanced (Table 5). The 5-year closure duration resulted in an average 15% increase in LPUE, and 75% of simulations had significantly increased LPUE in comparison with that under present-day management (Table 5).

Number of 10′ squares fished The number of 10′ squares fished during a year increased as the closure duration decreased (Fig. 7, Table 4) because captains are targeting 10′ squares that recently opened after be-

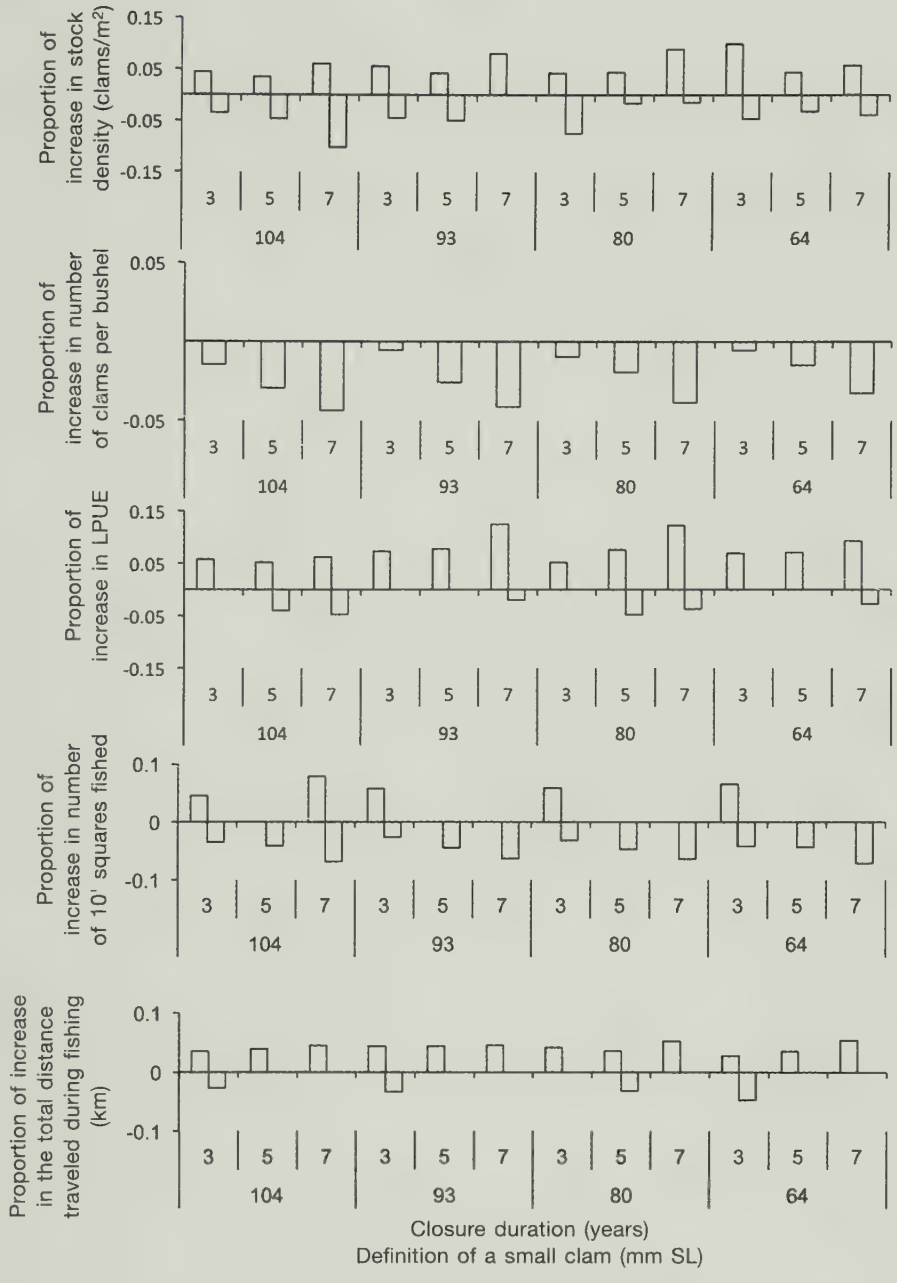

Figure 7

The proportion of change in performance metrics used to evaluate the effect of closure location rule 1 on the Atlantic surfclam (*Spisula solidissima*) population and commercial fishery in the Mid-Atlantic Bight. The effect is averaged for all simulations where a significant difference between present-day and alternative management exists (see Table 3 for the fraction of total simulations used to generate each bar value and Table 7 for summary statistics). Rule 1 mandates that the cell with the highest ratio of the number of small clams to the number of market-size clams be closed each year. Bars in the positive region represent proportional differences for simulations favoring alternative management. Proportional differences under present-day management represent simulations favoring present-day management and are represented as negative values for clarity. The metric of landings per unit of effort (LPUE) is the number of bushels per hour, and definitions of a small clam are given as shell length (SL) in millimeters.

Table 4

Summary statistics for the average proportion of change (shown in Fig. 7) in performance metrics used to evaluate the effect of closure location rule 1 on the Atlantic surfclam (*Spisula solidissima*) population and on the commercial fishery in the Mid-Atlantic Bight. Rule 1 mandates that the cell with the highest ratio of the number of small clams to the number of market-size clams be closed each year. Size of clams is given as shell length (SL) in millimeters, closure duration is measured in years, and LPUE means landings per unit effort. N is the number of simulations where a significant difference exists between the performance metric under present-day or alternative management at present-day abundance. The maximum N is 9.

		Definition of a small clam											
		104 mm SL			93 mm SL			80 mm SL			64 mm SL		
		Closure duration (yr)											
		3	5	7	3	5	7	3	5	7	3	5	7
Stock density													
Present management	N	4	4	1	2	1	0	2	1	1	3	2	5
	χ^2	0.04	0.05	0.10	0.04	0.05	–	0.08	0.02	0.01	0.05	0.03	0.04
	Min	0.01	0.02	–	0.04	–	–	0.07	–	–	0.04	0.03	0.02
	Max	0.08	0.08	–	0.05	–	–	0.08	–	–	0.05	0.04	0.06
Alternative management	N	4	3	6	3	6	4	5	5	4	2	3	3
	χ^2	0.04	0.03	0.06	0.06	0.04	0.08	0.04	0.04	0.09	0.10	0.04	0.06
	Min	0.02	0.02	0.04	0.03	0.02	0.03	0.02	0.02	0.04	0.03	0.03	0.05
	Max	0.07	0.05	0.09	0.08	0.10	0.12	0.08	0.10	0.14	0.17	0.05	0.06
Number of clams per bushel													
Present management	N	5	9	9	2	9	9	2	9	9	2	9	9
	χ^2	0.01	0.03	0.04	0.01	0.03	0.04	0.01	0.02	0.04	0.01	0.01	0.03
	Min	0.01	0.02	0.03	0.01	0.02	0.03	0.01	0.01	0.03	0.01	0.01	0.02
	Max	0.02	0.04	0.07	0.01	0.04	0.06	0.01	0.03	0.06	0.01	0.02	0.05
Alternative management	N	0	0	0	0	0	0	0	0	0	0	0	0
	χ^2	–	–	–	–	–	–	–	–	–	–	–	–
	Min	–	–	–	–	–	–	–	–	–	–	–	–
	Max	–	–	–	–	–	–	–	–	–	–	–	–
LPUE													
Present management	N	0	1	1	0	0	1	0	1	1	0	0	1
	χ^2	–	0.04	0.05	–	–	0.02	–	0.05	0.04	–	–	0.02
	Min	–	–	–	–	–	–	–	–	–	–	–	–
	Max	–	–	–	–	–	–	–	–	–	–	–	–
Alternative management	N	4	3	5	6	7	4	7	7	3	5	8	4
	χ^2	0.06	0.05	0.06	0.07	0.08	0.12	0.05	0.08	0.12	0.07	0.07	0.09
	Min	0.02	0.04	0.04	0.04	0.03	0.06	0.02	0.05	0.09	0.02	0.02	0.06
	Max	0.07	0.06	0.10	0.20	0.16	0.21	0.14	0.13	0.17	0.18	0.11	0.15
Number of 10′ squares fished													
Present management	N	4	5	6	3	4	5	4	5	4	4	4	5
	χ^2	0.03	0.04	0.07	0.03	0.04	0.06	0.03	0.05	0.06	0.04	0.04	0.07
	Min	0.02	0.02	0.05	0.02	0.04	0.05	0.02	0.02	0.03	0.02	0.04	0.05
	Max	0.05	0.06	0.09	0.03	0.05	0.08	0.04	0.08	0.09	0.10	0.05	0.10
Alternative management	N	2	0	1	1	0	0	1	0	0	3	0	0
	χ^2	0.04	–	0.08	0.06	–	–	0.06	–	–	0.07	–	–
	Min	0.04	–	–	–	–	–	–	–	–	0.05	–	–
	Max	0.06	–	–	–	–	–	–	–	–	0.09	–	–
Total distance traveled													
Present management	N	1	0	0	1	0	0	0	1	0	1	0	0
	χ^2	0.03	–	–	0.03	–	–	–	0.03	–	0.05	–	–
	Min	–	–	–	–	–	–	–	–	–	–	–	–
	Max	–	–	–	–	–	–	–	–	–	–	–	–
Alternative management	N	3	5	7	1	4	6	3	4	4	2	4	4
	χ^2	0.03	0.04	0.04	0.04	0.04	0.05	0.04	0.04	0.05	0.03	0.03	0.05
	Min	0.03	0.03	0.03	–	0.02	0.02	0.04	0.02	0.03	0.02	0.02	0.03
	Max	0.04	0.05	0.07	–	0.07	0.06	0.05	0.04	0.08	0.03	0.05	0.08

Table 5

Evaluation of the model simulations in which closure location rule 1 was used to examine the influence of increased incidental mortality on the stock and commercial fishery of Atlantic surfclam (*Spisula solidissima*) in the Mid-Atlantic Bight. Tabulated are the proportion of simulations where metrics used to evaluate the Atlantic surfclam population and the effect of area management on the commercial industry were significantly greater under alternative management with 0% or 20% incidental mortality with present-day abundance. Rule 1 mandates that the cell with the highest ratio of the number of small clams to the number of market-size clams is closed each year. Number of clams per bushel is not included because present-day management always has higher numbers of clams per bushel. There were 9 simulations per percentage. Any fraction over 0.11 (1 significant difference out of 9) is unlikely to occur by chance (exact binomial test: α=0.05; Conover, 1980). Size of clams is given as shell length (SL) in millimeters, closure duration is measured in years, and LPUE means landings per unit of effort.

	Definition of a small clam											
	104 mm SL			93 mm SL			80 mm SL			64 mm SL		
	Closure duration (yr)											
	3	5	7	3	5	7	3	5	7	3	5	7
Stock density												
0% incidental mortality	0.44	0.33	0.56	0.44	0.67	0.44	0.56	0.56	0.44	0 22	0.33	0.33
20% incidental mortality	0.56	0.78	0.78	0.44	0.78	0.78	0.22	0.56	0.67	0.22	0.56	0.56
LPUE												
0% incidental mortality	0.44	0.33	0.56	0.67	0.56	0.44	0.78	0.78	0.33	0.56	0.89	0.44
20% incidental mortality	0.67	0.78	0.56	0.67	0.89	0.78	0.44	0.67	0.56	0.22	0.67	0.78
Number of 10′ squares fished												
0% incidental mortality	0.22	0.00	0.11	0.11	0.00	0.00	0.11	0.00	0.00	0.33	0.00	0.00
20% incidental mortality	0.22	0.00	0.11	0.00	0.00	0.11	0.11	0.11	0.11	0.11	0.00	0.00
Total distance traveled												
0% incidental mortality	0.33	0.56	0.78	0.11	0.44	0.67	0.33	0.44	0.44	0.22	0.44	0.44
20% incidental mortality	0.11	0.33	0.56	0.56	0.22	0.44	0.33	0.44	0.44	0.33	0.22	0.44

average proportion of increase in LPUE was improved. The 5-year closure duration showed the most improvement with LPUE increased by an average of 12% (compared with 8% without additional mortality).

Number of 10′ squares fished As the duration of a closure increased, the percentage of simulations with significantly more 10′ squares fished during the year decreased. The average percentage of increase in 10′ squares fished under present-day management and over all alternative management strategies was only 3% and 4% respectively, however (Fig. 8, Table 6). The high percentage of simulations that showed no significant difference between present-day and any closure duration (66%, 75%, and 59% for the 3-, 5-, and 7-year closure durations; Table 7), accompanied by the small percent changes, indicate little effect of any alternative management strategy in changing the number of 10′ squares visited during fishing. As incidental mortality increased, slightly fewer 10′ are visited with increasing closure duration (Table 8). The percentage of cases where significantly fewer 10′ squares were visited under alternative management increased; however, the average percentage of increases of 10′ squares visited under present-day or alternative management were still 5% or less (Fig. 8, Table 6).

Distance traveled per fishing trip The distance traveled per fishing trip increased significantly in 94% of simulations for the 3-year closure duration and in 90% of simulations for the 5- and 7-year closure durations (Table 7). The average percent increase for each of the closure durations was only 5%, however (Fig. 8, Table 6). An increase in incidental mortality resulted in a lower percentage of simulations with increased distance traveled during fishing trips (averages of 41%, 61%, and 64% for the 3-, 5-, and 7-year closure durations; Table 8). The percentage of increase was less than 4% for all closure durations.

Discussion

Perspective

The goal of this study was to use an MSE to investigate possible options that could enhance productivity in the Atlantic surfclam stock without unjustifiably limiting the fishery through undesirable economic impacts. An MSE allows an evaluation of alternative management options on the basis of performance metrics that are understood by and valuable to both stakeholders and fishery managers. The range contraction of Atlantic

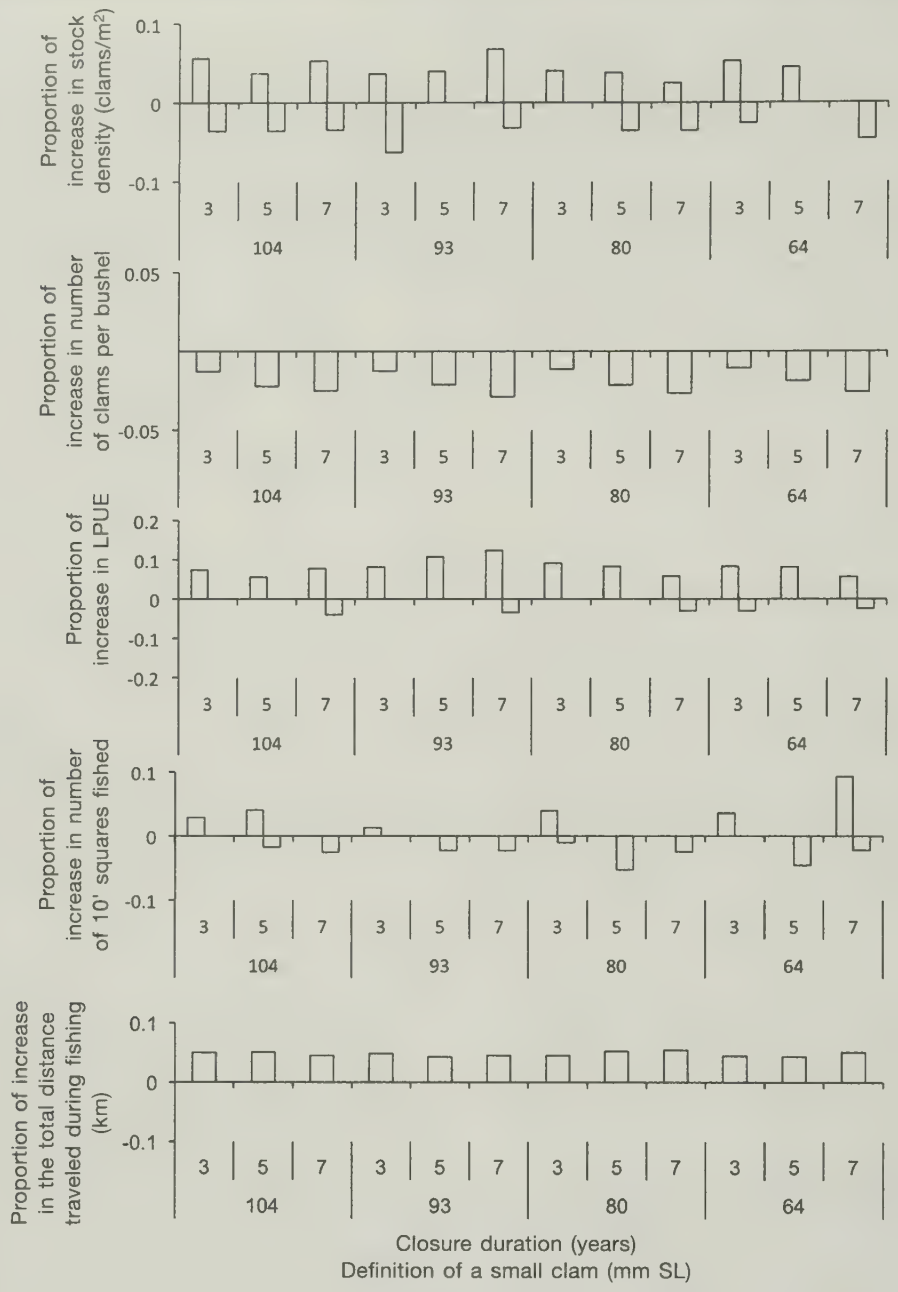

Figure 8

The proportion of change in performance metrics used to evaluate the effect of closure location rule 2 on the Atlantic surfclam (*Spisula solidissima*) population and commercial fishery in the Mid-Atlantic Bight averaged for all simulations where a significant difference between present-day and alternative management exists (see Table 6 for the fraction of total simulations used to generate each bar value and Table 8 for summary statistics). Rule 2 mandates that the cell with the highest density of small clams (number of clams per square meter) be closed each year. Bars in the positive region represent proportional differences under alternative management. Proportional differences under present-day management are represented in negative values for clarity. The metric of landings per unit of effort (LPUE) is the number of bushels per hour, and definitions of a small clam are given as shell length (SL) in millimeters.

Table 6

Summary statistics for average proportion of change (shown in Fig. 8) in performance metrics used to evaluate the effect of closure location rule 2 on the Atlantic surfclam (*Spisula solidissima*) population and commercial fishery. Size of clams is given as shell length (SL) in millimeters, closure duration is measured in years, and LPUE means landings per unit of effort. N is the number of simulations where a significant difference exists between the performance metric using present-day or alternative management at present-day abundance. The maximum N is 9.

		Definition of a small clam											
		104 mm SL			93 mm SL			80 mm SL			64 mm SL		
		Closure duration (yr)											
		3	5	7	3	5	7	3	5	7	3	5	7
Stock density													
Present management	N	3	1	1	2	0	2	0	1	1	3	0	1
	χ^2	0.04	0.04	0.03	0.06	–	0.03	–	0.04	0.04	0.03	–	0.05
	Min	0.03	–	–	0.05	–	0.02	–	–	–	0.01	–	–
	Max	0.04	–	–	0.08	–	0.05	–	–	–	0.04	–	–
Alternative management	N	3	4	5	4	3	4	4	6	5	2	5	0
	χ^2	0.06	0.04	0.05	0.04	0.04	0.07	0.04	0.04	0.02	0.05	0.04	–
	Min	0.04	0.02	0.02	0.02	0.02	0.04	0.01	0.01	0.01	0.02	0.03	–
	Max	0.07	0.05	0.11	0.08	0.07	0.11	0.06	0.07	0.04	0.09	0.09	–
Number of clams per bushel													
Present management	N	6	8	8	7	8	9	6	9	9	3	8	9
	χ^2	0.01	0.02	0.03	0.01	0.02	0.03	0.01	0.02	0.03	0.01	0.02	0.03
	Min	0.01	0.01	0.01	0.01	0.01	0.01	0.01	0.01	0.01	0.01	0.01	0.01
	Max	0.02	0.04	0.05	0.02	0.04	0.05	0.02	0.04	0.05	0.02	0.04	0.05
Alternative management	N	0	0	0	0	0	0	0	0	0	0	0	0
	χ^2	–	–	–	–	–	–	–	–	–	–	–	–
	Min	–	–	–	–	–	–	–	–	–	–	–	–
	Max	–	–	–	–	–	–	–	–	–	–	–	–
LPUE													
Present management	N	0	0	1	0	0	1	0	0	1	1	0	1
	χ^2	–	–	0.04	–	–	0.03	–	–	0.03	0.03	–	0.02
	Min	–	–	–	–	–	–	–	–	–	–	–	–
	Max	–	–	–	–	–	–	–	–	–	–	–	–
Alternative management	N	5	7	4	5	4	3	8	6	6	5	7	2
	χ^2	0.07	0.06	0.08	0.08	0.10	0.12	0.09	0.08	0.06	0.08	0.08	0.06
	Min	0.02	0.04	0.03	0.04	0.05	0.07	0.03	0.04	0.02	0.03	0.03	0.03
	Max	0.16	0.09	0.19	0.14	0.20	0.21	0.20	0.18	0.09	0.20	0.20	0.08
Number of 10′ squares fished													
Present management	N	0	1	4	0	1	2	1	2	4	0	3	4
	χ^2	–	0.02	0.03	–	0.02	0.02	0.01	0.05	0.02	–	0.05	0.02
	Min	–	–	0.01	–	–	0.01	–	0.02	0.01	–	0.02	0.01
	Max	–	–	0.08	–	–	0.04	–	0.08	0.04	–	0.07	0.04
Alternative management	N	3	2	0	1	0	0	2	0	0	2	0	0
	χ^2	0.03	0.04	–	0.01	–	–	0.04	–	–	0.04	–	–
	Min	0.01	0.01	–	–	–	–	0.01	–	–	0.01	–	–
	Max	0.06	0.08	–	–	–	–	0.07	–	–	0.06	–	–
Total distance traveled													
Present management	N	0	0	0	0	0	0	0	0	0	0	0	0
	χ^2	–	–	–	–	–	–	–	–	–	–	–	–
	Min	–	–	–	–	–	–	–	–	–	–	–	–
	Max	–	–	–	–	–	–	–	–	–	–	–	–
Alternative management	N	9	9	8	9	8	7	8	8	8	8	7	9
	χ^2	0.05	0.05	0.04	0.05	0.04	0.05	0.04	0.05	0.05	0.04	0.04	0.05
	Min	0.03	0.04	0.02	0.03	0.03	0.03	0.03	0.04	0.02	0.03	0.02	0.03
	Max	0.07	0.07	0.07	0.07	0.06	0.07	0.07	0.08	0.08	0.08	0.07	0.08

Table 7

Evaluation of model simulations in which closure location rule 2 was used to examine the influence of area management on the Atlantic surfclam (*Spisula solidissima*) stock and commercial fishery in the Mid-Atlantic Bight. Tabulated are the proportion of simulations where metrics used to evaluate the Atlantic surfclam population and commercial fishery were significantly greater under present-day or alternative management with closure location rule 2 with present-day abundance. Rule 2 mandates that the cell with the highest density of small clams (number of clams per square meter) be closed each year. There were 9 simulations per percentage. Any fraction over 0.11 (1 significant difference out of 9) is unlikely to occur by chance (exact binomial test: α=0.05; Conover, 1980). Size of clams is given as shell length (SL) in millimeters, closure duration is measured in years, and LPUE means landings per unit of effort.

	Definition of a small clam											
	104 mm SL			93 mm SL			80 mm SL			64 mm SL		
	Closure duration (yr)											
	3	5	7	3	5	7	3	5	7	3	5	7
Stock density												
Present management	0.33	0.11	0.11	0.22	0.00	0.22	0.00	0.11	0.11	0.33	0.00	0.11
Alternative management	0.33	0.44	0.56	0.44	0.33	0.44	0.44	0.67	0.56	0.22	0.56	0.00
Number of clams per bushel												
Present management	0.67	0.89	0.89	0.78	0.89	1.00	0.67	1.00	1.00	0.33	0.89	1.00
Alternative management	0.00	0.00	0.00	0.00	0.00	0.00	0.00	0.00	0.00	0.00	0.00	0.00
LPUE												
Present management	0.00	0.11	0.11	0.00	0.00	0.11	0.00	0.00	0.11	0.11	0.00	0.22
Alternative management	0.56	0.67	0.44	0.56	0.44	0.33	0.89	0.67	0.67	0.56	0.78	0.22
Number of 10′ squares fished												
Present management	0.00	0.11	0.44	0.00	0.11	0.22	0.11	0.22	0.44	0.00	0.33	0.44
Alternative management	0.67	0.22	0.00	0.11	0.00	0.00	0.22	0.00	0.00	0.22	0.00	0.11
Total distance traveled												
Present management	0.00	0.00	0.00	0.00	0.00	0.00	0.00	0.00	0.00	0.00	0.00	0.00
Alternative management	1.00	1.00	0.89	1.00	0.89	0.78	0.89	0.89	0.89	0.89	0.78	1.00

surfclam as a result of increasing bottom water temperatures in the MAB is understood by both groups and has implications not only for the Atlantic surfclam population itself but also for the commercial fishery supported by the clam stock in this area. The commercial fishery, which historically extended as far south as northern Virginia in the MAB, is now concentrated off the New Jersey shore (Cargnelli et al., 1999; Jacobson and Weinberg[1]; NEFSC[2]). The ongoing increase in fishing pressure in this region, as a consequence of the range contraction, is already manifesting itself as a reduced LPUE and an increasing inability to catch the allocated quota. Local overfishing is likely to occur as consolidation of fishing pressure in this area increases. Barring modifications to the present-day management plan or transfer of additional effort northeast to southern New England and Georges Bank, LPUE will likely continue to decline. Because of the location of processing plants, such a transfer of effort would be extremely expensive and therefore represents an economically implausible option. The present-day management plan offers no responsive option. The need to improve the condition of the stock while allowing continued support of the historical fishery is a major challenge.

Area management, such as temporary or permanent closures (Walters, 2000; Bloomfield et al., 2012; Córdova-Lepe et al., 2012), has proven to be a useful tool to improve shellfish fisheries. The inclusion of fishermen's behavior in area management is essential because the response of the fishery to management measures is critical in the evaluation of preferred and realistic options (Hilborn, 1992; Gillis et al., 1995; Millischer and Gascuel, 2006; Link et al., 2011). Although this MSE model (SEFES) captures the essential components of a highly variable system (i.e., the Atlantic surfclam population and fishery), some assumptions are required. The lack of knowledge about incidental Atlantic surfclam mortality as a result of dredging procedures requires an assumption concerning the degree of its importance. Fishing gear also can generate incidental shell damage (Witbaard and Klein, 1994; Gilkinson et al., 2005; Vasconcelos et al., 2011) that, in the case of bivalves, may not be easily repaired (Alexander and Dietl, 2001; Moschino et al., 2003). Consequently, simulations were conducted for 0% and 20% incidental mortality of the clams encountered but not retained by the dredge with the upper value chosen from limited a priori data. Another source of uncertainty is determining the annual number and distribution of recruits across the Atlantic surfclam population. In order to account for the mean annual number and distribution of recruits, simulations included a range of degrees of patchiness in re-

Table 8

Evaluation of model simulations in which closure location rule 2 was used to examine the influence of increased incidental mortality on the Atlantic surfclam (*Spisula solidissima*) stock and commercial fishery in the Mid-Atlantic Bight. Tabulated are the proportion of simulations where metrics used to evaluate the Atlantic surfclam population and the effect of area management on the commercial industry were significantly greater under alternative management with 0% or 20% incidental mortality using closure location rule 2 with present-day abundance. Rule 2 mandates that the cell with the highest density of small clams (number of clams per square meter) be closed each year. Number of clams per bushel is not included because present-day management always has higher numbers of clams per bushel. There were 9 simulations per percentage. Any fraction over 0.11 (1 significant difference out of 9) is unlikely to occur by chance (exact binomial test: α=0.05; Conover, 1980). Size of clams is given as shell length (SL) in millimeters, closure duration is measured in years, and LPUE means landings per unit of effort.

	Definition of a small clam											
	104 mm SL			93 mm SL			80 mm SL			64 mm SL		
	Closure duration (yr)											
	3	5	7	3	5	7	3	5	7	3	5	7
Stock density												
0% incidental mortality	0.33	0.44	0.56	0.44	0.33	0.44	0.44	0.67	0.56	0.22	0.56	0.00
20% incidental mortality	0.22	0.33	0.44	0.56	0.22	0.44	0.44	0.56	0.56	0.22	0.44	0.22
LPUE												
0% incidental mortality	0.56	0.67	0.44	0.56	0.44	0.33	0.89	0.67	0.67	0.56	0.78	0.22
20% incidental mortality	0.44	0.44	0.33	0.67	0.22	0.44	0.67	0.67	0.56	0.33	0.56	0.44
Number of 10′ squares fished												
0% incidental mortality	0.67	0.22	0.00	0.11	0.00	0.00	0.22	0.00	0.00	0.22	0.00	0.11
20% incidental mortality	0.22	0.00	0.00	0.11	0.00	0.00	0.22	0.00	0.00	0.11	0.11	0.00
Total distance traveled												
0% incidental mortality	1.00	1.00	0.89	1.00	0.89	0.78	0.89	0.89	0.89	0.89	0.78	1.00
20% incidental mortality	0.44	0.67	0.67	0.33	0.67	0.56	0.22	0.56	0.67	0.67	0.56	0.67

cruitment. A net downcoast drift of larvae previously identified in larval dispersion studies was not included because postsettlement mortality appears to have a much larger effect on patchiness (Zhang et al., 2015, 2016): postsettlement mortality was incorporated into the model as patchy recruitment. Additional assumptions were made regarding the influence of climate change on the stock and commercial fishery over the simulated timespan of fishing years used to compare performance metrics (76 years). Climate change will likely continue over the next 76 years (Scavia et al., 2002; Feely et al., 2009); it follows that changes in the population dynamics and range of the Atlantic surfclam also will occur (e.g., Munroe et al., 2016). The extent to which climate change will influence the Atlantic surfclam stock is impossible to assess; therefore, the set of simulations used in this study does not include anticipated future conditions. Even if the geographic range of clams was to change over the coming 76 years, the outcomes of area management discussed here rely primarily on a constant ambit of physiological responses by the Atlantic surfclam within its habitable range and on the recognition that the Atlantic surfclam fishery has a limited ambit to adapt to changes in Atlantic surfclam density, whether that density increases or declines (Powell et al., 2016). Additionally, realistically predicting the improvement in vessel technology and its influence on a captain's skill and vessel economics is totally speculative. It may be assumed that developments will occur that increase vessel and harvest efficiency (i.e., become more fuel efficient, provide improved onboard refrigeration); however, unlike the gear of many fisheries, the efficiency of hydraulic dredges is already near 80% on good fishing grounds, so that substantial improvements in catch efficiency are unlikely. The extent to which these developments will affect the stock and commercial industry over a 76-year time span is unquantifiable, but such changes are unlikely to drastically change the outcome of area management as simulated in this study, because these outcomes are primarily influenced by varying fishing pressure across the stock under a defined FMP quota cap. The area management options presented in this study could be implemented long before major changes in the fleet configuration could take place. For this reason, changes in boat characteristics and the skill of captains are held constant over the 76-year period of simulation.

Influence of area management on Atlantic surfclam stock

Performance metrics used to evaluate the influence of area management on the MAB Atlantic surfclam stock

Table 9

Summary of alternative management strategies for determining the management option that offers benefits to both the stock and commercial fishery of the Atlantic surfclam (*Spisula solidissima*) in the Mid-Atlantic Bight. Plus signs indicate the management strategy (either present-day or area management through closures) that resulted in the highest values of performance metrics. In situations where equivalent proportions of simulations resulted in increases, a plus sign is given to both strategies (i.e., landings per unit of effort).

Performance metric	Present-day management	Rule 1 (ratio of the number of small clams to market-size clams)	Rule 2 (number of small clams/m^2)
Stock density (number of clams/m2)		+	
Number of clams per bushel	+		
Landings per unit of effort (bushels/h)		+	+
Number of 10′ squares fished	+		
Total distance traveled (km)			+

are 1) the whole-stock density of clams recruited to the fishery (i.e., clams ≥120 mm SL), and the 2) number of clams per bushel. Simulations suggest that implementation of closure location rule 1 offers greater improvement to the stock, as measured by an increase in whole-stock density or a decrease in the number of clams per bushel due to an increase in clam size, in comparison with implementation of closure location rule 2 (Table 9). That is, closing a 10′ square on the basis of the proportional abundance of small clams offers improved outcomes in comparison with the same choice that is based on the density of small clams. The stock density showed a 4–7% increase under closure location rule 1. To put these values in perspective, the increase is more than double the fraction of the stock removed by the fishery in a given year over the entire stock and is very near the exploitation rate for the area of highest exploitation, offshore New Jersey.

Tracking the number of clams per bushel also is one way to evaluate the status of the stock. A thriving stock will have larger clams and consequently the fishery will require fewer clams to fill a bushel. That is, landing larger clams results in fewer individuals being removed from the population under a specified quota, thus conserving stock density. One of the critical characteristics of the Atlantic surfclam fishery is that fishing economics and fishery management are specified in terms of volume, whereas the stock itself is best defined in terms of number of individuals. The number of clams per bushel is significantly lower under area management in an average 31% of 3-year closure duration simulations and 100% of the 5- and 7-year closure duration simulations, regardless of the definition of a small clam. An increase of 4% in the number of clams required to fill a bushel under present-day management equates to an excess of about 3 clams per bushel when compared with alternative management. Three fewer clams per bushel translates to around 1 less bushel being required to fill a cage (32 bushels=1 cage). Annually, the equivalent of approximately 4557 cages would therefore remain in the fishable stock because these animals would not be needed to fill the quota during fishing trips. About 81 extra trips of a boat capable of carrying 56 cages would be supported. Alternatively, these clams increase whole-stock density.

Influence of area management on the commercial fishery

Performance metrics used to evaluate the influence of area management on the Atlantic surfclam fishery are LPUE, the number of 10′ squares visited yearly, and the total distance traveled by the fishing vessel. Closure location rule 1 results in greater opportunities for the commercial fishery (Table 9). LPUE is increased significantly over all definitions of a small clam in an average of 61%, 64%, and 44% of simulations for the 3-, 5-, and 7-year closures respectively (Table 3). The greatest percent increase in LPUE under closure location rule 1 produced enough time saved at sea to enable transit for an additional 16.7 km (9 nautical miles), or the addition of one 10′ square in any direction from the port, increasing the fishable area under the dock-to-dock time constraint imposed by the rate of spoilage of clams on deck. With an increase in incidental mortality, the extra time saved by an increase of 15% in LPUE would allow the boats to travel to 2 additional 10′ squares in the same amount of time (approximately 36 h from the start of fishing to the landing of the clams during the warmer months of the year). A 6% increase in LPUE would result in a boat that is capable of carrying 56 cages filling all cages about 2 h faster per trip, thus permitting more transit time to fish farther from home port—37.0 km (20 nautical miles) for most vessels steaming at 5 m/s (10 kn), under the 36-h time constraint. A 15% increase in LPUE would equate to a reduction of 5 h of fishing time per trip. As fuel use is highest while fishing (both the main engine and water pump are running), any increase in LPUE exerts an

important economic gain in reducing the cost of fuel relative to the value of the landed clams.

The number of 10′ squares visited during fishing increases significantly in an average of 7% of simulations over all closure durations and definitions of a small clam in comparison with an average of 49% of simulations under present-day management. A reduction in the number of 10′ squares visited suggests that captains (who choose a fishing location on the basis of highest catch rate, but who are limited in the summer by the 36-h time constraint) target the recently opened 10′ squares. The distance traveled during fishing also increases significantly in up to 58% of simulations. An increase in distance traveled occurs in some cases because the closed 10′ squares are close to the home ports and require that captains steam farther away from port to fish. In addition, some of the 10′ squares recently opened are farther from home port, but the higher LPUE makes travel to them economically advantageous. Reduced distance is often preferred because reduced steaming time reduces operational costs, thus increasing profit margins, unless the additional cost of steaming is compensated by a reduction in other trip costs. This would be the case if LPUE also increases, as it does in these simulations. If a vessel steams for 8 h at a speed of 5 m/s, a 4% increase in distance traveled would result in approximately an additional 7.4 km (4 nautical miles), which would allow fishing of 1 additional 10′ square away from home port without substantial additional costs if that 10′ square yielded a higher LPUE.

Influence of control rules

The criterion used to select a closure location is important for the success of management in offering enhanced stock densities and additional economic opportunity to the industry. Two closure location rules were investigated that represent end-members [extreme options] of a range of choices for a control rule; one places importance on the number of small clams in relation to the number of market-size clams (rule 1) and the other places importance on the density of small clams in an area (rule 2). Optimizing area management would require evaluation of the influence of combined rules, such as the 10′ square with the highest density of small clams among the 25% of 10′ squares with the highest proportion of small clams. A comparison of the end-member options, however, shows that stock density increased in a higher percentage of simulations under closure location rule 1, the proportional rule, in comparison with closure location rule 2 and present-day management. Average percent increases in stock density are also higher under closure location rule 1. Accordingly, an increase in stock density is seen when the 10′ square with the greatest number of small clams in comparison with the number of market-size clams is closed to fishing for some duration of years. Both closure location rules resulted in an average of 64% of simulations having increased LPUE when compared with present-day management (i.e., no closures). A higher average percentage of increase resulted with closure location rule 2. However, closure location rule 1 resulted in an increase in LPUE as the closure duration increased, as opposed to a gradual decline seen when using closure location rule 2. An increase in LPUE when high importance is placed on the presence of small clams suggests that protecting small clams is a key factor in offering more economic opportunity to the fishing industry.

When the choice of closure location is based on the ratio of the number of small clams to the number of market-size clams (rule 1), the percentage of simulations where fewer 10′ squares were fished was much higher. This result suggests that these 10′ squares retain high catch rates longer under closure location rule 1. When the closure location is based on rule 1, transit distance was increased in substantially fewer simulations in comparison with closure location based on closure location rule 2 or present-day management. A decrease in distance traveled in a comparison of closure location rules 1 and 2 suggests that when importance is placed on the ratio of the number of small clams to the number of market-size clams, even though the 10′ squares closed may be near home ports, once open they provide improved catch rates more often than if the location of the closed 10′ square was selected on the basis of abundance of small clams alone. This outcome is consistent with the more persistent targeting of these 10′ squares under closure location rule 1.

The average percent increase in the number of clams per bushel—a metric directly related to the size of landed clams—is essentially equal for both closure location rules. Because some of the performance metrics (e.g., number of clams per bushel) showed little difference between the 2 closure rules, a third option of combining the 2 rules might offer additional benefits for the commercial fishery. However, on the basis of the percentage of simulations that indicated improvement of the stock and the margins of increase, the 5-year closure duration under closure location rule 1, which relies on the proportion of small clams to identify a 10′ square to close, offers the most benefit for the stock and therefore is identified as the preferred option. Of greatest importance is the increase in whole-stock density that occurs while landings are retained near levels of the present day. In addition, based on the percentage of simulations that indicate additional economic opportunities offered to the commercial fishery, the 5-year closure duration under closure location rule 1 offers the most benefit to the stock and thus again is identified as the preferred option.

Influence of incidental mortality

Little information exists about the incidental mortality of clams encountered by the dredge but that remain on the seafloor. NEFSC[2] assumes 12% incidental mortality, but this assumption is based on very little data and primarily on the outcome for market-size clams (Meyer et al., 1981), few of which

remain uncaught with modern high-performance hydraulic dredges (Hennen et al., 2012; NEFSC[2]). The fate of small clams is effectively unknown. Therefore, we investigated the effect of area management under the assumption of 0% and 20% incidental mortality. Pairwise comparisons of the present-day management simulation under the assumption of increased incidental mortality with simulations implementing area management options, also with increased incidental mortality, produced performance metrics that were then compared with the performance metrics with 0% mortality. Additional mortality enhanced the positive effect of area management in most situations under closure location rule 1. The percentage of simulations with enhanced performance metrics under area management was greater with increased incidental mortality. Also, the average percent increase across all metrics was enhanced. In most simulations with the use of closure location rule 2, increased incidental mortality had little effect on the percentage of simulations with improved performance metrics. The most notable difference in the percentage of simulations with improved performance metrics in comparisons of the 2 levels of incidental mortality is seen in the total distance traveled. A larger percentage of simulations with increased distance traveled is seen with 0% incidental mortality in contrast with simulations with 20% incidental mortality. A large effect of incidental mortality with the use of closure location rule 1 and a small effect with closure location rule 2 suggests that a combination of the 2 closure location rules could offer some clarity for determining the real effect of increased incidental mortality.

The enhancement of the effect of area management at increased levels of incidental mortality can be attributed to the protection of clams in closed areas. The effect of area management is enhanced because 10′ squares with high clam abundances (regardless of the closure rule) are protected, and thus fewer are removed from the stock as a result of incidental mortality. When incidental mortality is increased from 0% to 20%, mortality is increased in areas that are fished; however, in the closed areas, this mortality is not occurring and these regions have the highest number of clams that would be subject to this source of mortality.

Preferred management options

The importance of the presence and abundance of small clams becomes apparent upon examining the performance metrics that suggest improvement over present-day management. Of the 2 closure location rules, the rule that places importance on a population dominated by small clams (rule 1) produces a greater increase in simulated stock abundance and LPUE over time in comparison with a a location closed on the basis of the density of small clams (rule 2). An increase in the percentage of simulations where fewer 10′ squares are fished occurs because the closed 10′ squares produce higher catch rates once open than the 10′ squares that are not closed. An increase in the distance traveled during fishing trips is also seen, some of which results from closed 10′ squares being close to home ports and some of which stems from the favorable (i.e., higher) LPUEs in recently opened 10′ squares farther from port. No obvious difference is seen between the 2 closure location rules for the size of landed clams (i.e., the number of clams per bushel). This difference between area management and present-day management in the size of clams landed is nonetheless of great importance because the lower fishing mortality rate increases survivorship of large clams and contributes to the increase in whole-stock density routinely observed in area management simulations, directly and through an increase in spawning stock biomass.

Simulations indicate that the 5-year closure duration derives the largest benefits for the stock and also the commercial fishing industry. Although average percent increases in stock density and LPUE are greater when closure duration is longer, the percentage of simulations showing improvement over present-day management is greatest with the 5-year closure duration. Based on the overall improvements in performance metrics seen with closure location rule 1 and the 5-year closure duration simulations, the preferred option that simultaneously offers additional opportunities for growth of the stock and improvements to the commercial fishery is to close areas specified by closure location rule 1 for 5 years. Future research into area management options should include an investigation of an intermediate closure rule or a combination of closure rules. Nonetheless, the results of these analyses strongly suggest that both the Atlantic surfclam stock and fishery would experience a positive change by the inclusion of an area management program in the MAB region.

Acknowledgments

This research was supported by the National Science Foundation (NSF) Science Center for Marine Fisheries (SCeMFiS) under NSF award 1266057 and through membership fees provided by the SCeMFiS Industry Advisory Board. This article is based, in part, on a thesis submitted by the senior author for fulfillment of the Master of Science degree at The University of Southern Mississippi. The authors thank the SCeMFiS member organizations for providing detailed information on vessel characteristics for all vessels targeting Atlantic surfclams, which allowed realistic simulations of the industry to be performed.

Literature cited

Alexander, R. R., and G. P. Dietl.
2001. Shell repair frequencies in New Jersey bivalves: a recent baseline for tests of escalation with tertiary, mid-Atlantic congeners. Palaios 16:354–371.

Bastardie, F., M. Vinther, J. R. Nielsen, C. Ulrich, and M. S. Paulsen.
2010. Stock-based vs. fleet-based evaluation of the multi-annual management plan for the cod stocks in the Baltic Sea. Fish. Res. 101:188–202.

Baudron, A., C. Ulrich, J. R. Nielsen, and J. Boje.
2010. Comparative evaluation of a mixed-fisheries effort-management system based on the Faroe Islands example. ICES J. Mar. Sci. 67:1036–1050.

Bloomfield, H. J., C. J. Sweeting, A. C. Mill, S. M. Stead, and N. V. C. Polunin.
2012. No-trawl area impacts: perceptions, compliance and fish abundances. Environ. Conserv. 39:237–247.

Bockstael, N. E., and J. J. Opaluch.
1983. Discrete modelling of supply response under uncertainty: the case of the fishery. J. Environ. Econ. Manage. 10:125–137.

Butterworth, D. S., and A. E. Punt.
1999. Experiences in the evaluation and implementation of management procedures. ICES J. Mar. Sci. 56:985–998.

Butterworth, D. S., K. L. Cochrane, and J. A. A. De Oliveira.
1997. Management procedures: a better way to manage fisheries? The South African experience. *In* Global trends: fisheries management; (E. K. Pikitch, D. D. Huppert, and M. P. Sissenwine, eds.), p. 83–90. Am. Fish. Soc., Bethesda, MD.

Cargnelli, L. M., S. J. Griesbach, D. B. Packer, and E. Weissberger.
1999. Essential fish habitat source document: Atlantic surfclam, *Spisula solidissima*, life history and habitat characteristics. NOAA Tech. Memo. NMFS-NE-142, 13 p.

Conover, W. J.
1980. Practical nonparametric statistics, 2 ed., 493 p. John Wiley and Sons Inc., New York.

Cooley, S. R., J. E. Rheuban, D. R. Hart, V. Luu, D. M. Glover, J. A. Hare, and S. C. Doney.
2015. An integrated assessment model for helping the United States sea scallop (*Placopecten magellanicus*) fishery plan ahead for ocean acidification and warming. PLoS ONE 10(5):e0124145.

Córdova-Lepe, F., R. Del Valle, and G. Robeldo.
2012. A pulse fishery model with closures as function of the catch: conditions for sustainability. Math. Biosci. 239:169–177.

Dorn, M. W.
2001. Fishing behavior of factory trawlers: a hierarchical model of information processing and decision-making. ICES J. Mar. Sci. 58:238–252.

Feely, R. A., S. C. Doney, and S. R. Cooley.
2009. Ocean acidification: present conditions and future changes in a high-CO_2 world. Oceanography 22:36–47.

Francis, R. I. I. C., and R. Shotton.
1997. "Risk" in fisheries management: a review. Can. J. Fish. Aquat. Sci. 54:1699–1715.

Gilkinson, K. D., D. C. Gordon Jr., K. G. MacIsaac, D. L. McKeown, E. L. R. Kenchington, C. Bourbonnais, and W. P. Vass.
2005. Immediate impacts and recovery trajectories of macrofaunal communities following hydraulic clam dredging on Banquereau, eastern Canada. ICES J. Mar. Sci. 62:925–947.

Gillis, D. M., R. M. Peterman, and E. K. Pikitch.
1995. Implications of trip regulations for high-grading; a model of the behavior of fishermen. Can. J. Fish. Aquat. Sci. 52:402–415.

Goldberg, R., and R. L. Walker.
1990. Cage culture of yearling surf clams, *Spisula solidissima* (Dillwyn, 1817), in coastal Georgia. J. Shellfish Res. 9:187–193.

Hennen, D. R., L. D. Jacobson, and J. Tang.
2012. Accuracy of the Patch model used to estimate density and capture efficiency in depletion experiments for sessile invertebrates and fish. ICES J. Mar. Sci. 69:240–249.

Hilborn, R.
1992. Current and future trends in fisheries stock assessment and management. S. Afr. J. Mar. Sci. 12:975–988.
2003. The state of the art in stock assessment: where we are and where we are going. Sci. Mar. 67:15–20.

Hofmann, E. E., E. N. Powell, J. M. Klinck, D. M. Munroe, R. Mann, D. B. Haidvogel, D. A. Narváez, X. Zhang, and K. M. Kuykendall.
In press. Factors affecting distribution of the Atlantic surfclam (*Spisula solidissima*), a continental shelf biomass dominant, during a period of climate change. J. Shellfish Res.

Holland, D. S., and J. G. Sutinen.
2000. Location choice in New England trawl fisheries: old habits die hard. Land Econ. 76:133–149.

Hutton, T., S. Mardle, S. Pascoe, and R. A. Clark.
2004. Modelling fishing location choice within mixed fisheries: English North Sea beam trawlers in 2000 and 2001. ICES J. Mar. Sci. 61:1443–1452.

Kim, Y., and E. N. Powell.
2004. Surfclam histopathology survey along the Delmarva mortality line. J. Shellfish Res. 23:429–441.

Link, P. M., U. A. Schneider, and R. S. J. Tol.
2011. Economic impacts of changes in fish population dynamics: the role of the fishermen's harvesting strategies. Environ. Model. Assess. 16:413–429.

Loesch, J. G., and J. W. Ropes.
1977. Assessment of the surfclam stocks in near shore waters along the Delmarva Peninsula and in the fishery south of Cape Henry. Proc. Natl. Shellfish. Assoc. 67:29–34.

Mackinson, S., U. R. Sumaila, and T. J. Pitcher.
1997. Bioeconomics and catchability: fish and fishers behaviour during stock collapse. Fish. Res. 31:11–17.

Mahévas, S., and D. Pelletier.
2004. ISIS-Fish, a generic and spatially explicit simulation tool for evaluating the impact of management measures on fisheries dynamics. Ecol. Model. 171:65–84.

Marzec, R. J., Y. Kim, and E. N. Powell.
2010. Geographical trends in weight and condition index of surfclams (*Spisula solidissima*) in the mid-Atlantic Bight. J. Shellfish Res. 29:117–128.

McAllister, M. K., and G. P. Kirkwood.
1998. Bayesian stock assessment: a review and example application using the logistic model. ICES J. Mar. Sci. 55:1031–1060.

McCay, B. J., C. F. Creed, A. C. Finlayson, R. Apostle, and K. Mikalsen.
1995. Individual transferrable quotas (ITQs) in Canadian and US fisheries. Ocean Coast. Manage. 28:85–115.

Meyer, T. L., R. A. Cooper, and K. J. Pecci.
1981. The performance and environmental effects of a hydraulic clam dredge. Mar. Fish. Rev. 43(9):14–22.

Miller, T. J., J. A. Blair, T. F. Ihde, R. M. Jones, D. H. Secor, and M. J. Wilberg.
2010. FishSmart: an innovative role for science in stakeholder-centered approaches to fisheries management. Fisheries 35:424–433.

Millischer, L., and D. Gascuel.
2006. Information transfer, behavior of vessels and fishing efficiency: an individual-based simulation approach. Aquat. Living Resour. 19:1–13.

Monroy, C., S. Salas, and J. Bello-Pineda.
2010. Dynamics of fishing gear and spatial allocation of fishing effort in a multispecies fleet. N. Am. J. Fish. Manage. 30:1187–1202.

Moschino, V., M. Deppieri, and M. G. Marin.
2003. Evaluation of shell damage to the clam *Chlamelea gallina* captured by hydraulic dredging in the northern Adriatic Sea. ICES J. Mar. Sci. 60:393–401.

Munroe, D. M., E. N. Powell, R. Mann, J. M. Klinck, and E. E. Hofmann.
2013. Underestimation of primary productivity on continental shelves: evidence from maximum size of extant surfclam populations. Fish. Oceanogr. 22:220–233.

Munroe, D. M., D. A. Narváez, D. Hennen, L. Jacobson, R. Mann, E. E. Hofmann, E. N. Powell, and J. M. Klinck.
2016. Fishing and bottom water temperature as drivers of change in maximum shell length in Atlantic surfclams (*Spisula solidissima*). Estuar. Coast. Shelf Sci. 170:112–122.

NOAA (National Oceanic and Atmospheric Administration).
2012. Magnuson-Stevens Fishery Conservation and Management Act provisions; fisheries of the northeastern United States; Atlantic surfclam and ocean quahog fishery. Fed. Reg. 77(244):75057–75064.

Narváez, D. A., D. M. Munroe, E. E. Hofmann, J. M. Klinck, E. N. Powell, R. Mann, and E. Curchitser.
2015. Long-term dynamics in Atlantic surfclam (*Spisula solidissima*) populations: the role of bottom water temperature. J. Mar. Syst. 141:136–148.

Powell, E. N., K. A. Ashton-Alcox, J. N. Kraeuter, S. E. Ford, and D. Bushek.
2008. Long-term trends in oyster population dynamics in Delaware Bay: regime shifts and response to disease. J. Shellfish Res. 27:729–755.

Powell, E. N., J. M. Klinck, D. M. Munroe, E. E. Hofmann, P. Moreno, and R. Mann.
2015. The value of captains' behavioral choices in the success of the surfclam (*Spisula solidissima*) fishery on the U.S. Mid-Atlantic coast: a model evaluation. J. Northwest Atl. Fish. Sci. 47:1–27.

Powell, E. N., J. M. Klinck, E. E. Hofmann, P. Moreno, K. M. Kuykendall, D.M. Munroe, and R. Mann.
2016. Captains' response to a declining stock as anticipated in the surfclam (*Spisula solidissima*) fishery on the U.S. Mid-Atlantic coast by model evaluation. Ocean Coast. Manage. 134:52–68.

Prior, D. J., A. M. Schneiderman, and S. I. Greene.
1979. Size-dependent variation in the evasive behaviour of the bivalve mollusc *Spisula solidissima*. J. Exp. Biol. 78:59–75.

Punt, A. E., and R. Hilborn.
1997. Fisheries stock assessment and decision analysis: the Bayesian approach. Rev. Fish Biol. Fish. 7:35–63.

Punt, A. E., F. Trinnie, T. I. Walker, E. McGarvey, J. Feenstra, A. Linnane, and K. Hartmann.
2013. The performance of a management procedure for rock lobsters, *Jasus edwardsii*, off western Victoria, Australia in the face of non-stationary dynamics. Fish. Res. 137:116–128.

Punt, A. E., T. A'mar, N. A. Bond, D. S. Butterworth, C. L. de Moor, J. A. A. De Oliveira, M. A. Haltuch, A. B. Hollowed, and C. Szuwalski.
2014. Fisheries management under climate and environmental uncertainty: control rules and performance simulation. ICES J. Mar. Sci. 71:2208–2220.

Ropes, J. W., and A. S. Merrill.
1973. To what extent do surf clams move. Nautilus 87:19–21.

Scavia, D., J. C. Field, D. F. Boesch, R. W. Buddemeier, V. Burkett, D. R. Cayan, M. Fogarty, M. A. Harwell, R. W. Howarth, C. Mason, et al.
2002. Climate change impacts on U.S. coastal and marine ecosystems. Estuaries 25:149–164.

Smith, A. D. M.
1994. Management strategy evaluation—the light on the hill. *In* Population dynamics for fisheries management. Australian Society for Fish Biology workshop proceedings; Perth, Australia, 24–25 August 1993 (D. A. Hancock, ed.), p. 249–253. Australian Society for Fish Biology, North Beach, Australia.

Spillman, C. M., D. P. Hamilton, and J. Imberger.
2009. Management strategies to optimise sustainable clam (*Tapes philippinarum*) harvests in Barbamarco Lagoon, Italy. Estuar. Coast. Shelf Sci. 81:267–278.

van Putten, I. E., S. Kulmala, O. Thébaud, N. Dowling, K. G. Hamon, T. Hutton, and S. Pascoe.
2012. Theories and behavioural drivers underlying fleet dynamics models. Fish Fish. 13:216–235.

Vasconcelos, P., A. Morgado-André, D. Morgado-André, and M. B. Gaspar.
2011. Shell strength and fishing damage to the smooth clam (*Callista chione*): simulating impacts caused by bivalve dredging. ICES J. Mar. Sci. 68:32–42.

Walters, C.
2000. Impacts of dispersal, ecological interactions, and fishing effort dynamics on efficacy of marine protected areas: how large should protected areas be? Bull. Mar. Sci. 66:745–757.

Weinberg, J. R.
1998. Density-dependent growth in the Atlantic surfclam, *Spisula solidissima*, off the coast of the Delmarva Peninsula, USA. Mar. Biol. 130:621–630.

1999. Age-structure, recruitment, and adult mortality in populations of the Atlantic surfclam, *Spisula solidissima*, from 1978 to 1997. Mar. Biol. 134:113–125.

2005. Bathymetric shift in the distribution of Atlantic surfclams: response to warmer ocean temperature. ICES J. Mar. Sci. 62:1444–1453.

Weinberg, J. R., T. G. Dahlgren, and K. M. Halanych.
2002. Influence of rising sea temperature on commercial bivalve species of the U.S. Atlantic coast. Am. Fish. Soc. Symp. 32:131–140.

Witbaard, R., and R. Klein.
1994. Long-term trends on the effects of the southern North Sea beamtrawl fishery on the bivalve mollusc *Arctica islandica* L. (Mollusca, Bivalvia). ICES J. Mar. Sci. 51:99–105.

Zhang, X., D. Haidvogel, D. Munroe, E. N. Powell, J. Klinck, R. Mann, and F. S. Castruccio.
2015. Modeling larval connectivity of the Atlantic surfclams within the Middle Atlantic Bight: model development, larval dispersal and metapopulation connectivity. Estuar. Coast. Shelf Sci. 153:38–53.

Zhang, X., D. Munroe, D. Haidvogel, and E. N. Powell.
2016. Atlantic surfclam connectivity within the Middle Atlantic Bight: mechanisms underlying variation in larval transport and settlement. Estuar. Coast. Shelf Sci. 173:65–78.

National Marine
Fisheries Service
NOAA

Fishery Bulletin
established in 1881

Spencer F. Baird
First U.S. Commissioner
of Fisheries and founder
of *Fishery Bulletin*

Investigations into the distribution of sample sizes for determining age composition of multiple species

Peter-John F. Hulson (contact author)
Dana H. Hanselman
S. Kalei Shotwell

Email address for contact author: pete.hulson@noaa.gov

Auke Bay Laboratories
Alaska Fisheries Science Center
National Marine Fisheries Service, NOAA
17109 Point Lena Loop Road
Juneau, Alaska 99801

Abstract—Collecting age-composition data is a critical aspect of stock assessment; however, there are no biological or statistical investigations that support optimization of the distribution of sample size across species. Sample sizes for both collection and age-reading are often set by using ad hoc or historical values. Investigations into quantifying the trade-offs when allocating sample sizes across species are needed because resources for age determination are always limited. In this study we performed analyses to investigate the distribution of sample sizes to determine ages across multiple species by using methods derived from sampling theory and simulation testing of stock assessment models. We found that, in terms of methods based on sampling theory, distribution of sample size under 2-stage sampling could be significantly related to the life-history characteristics of the species. Results from simulation analysis illustrated that the influence of sample sizes required to determine age composition of fish on uncertainty in stock assessment models was related to uncertainty in a survey index and recruitment variability of the species being assessed. The simulation analysis highlighted cases in which larger age-composition sample size did not appreciably decrease uncertainty in the stock assessment model, in particular, for species with lower recruitment variability and larger survey index uncertainty.

Manuscript submitted 6 April 2016.
Manuscript accepted 4 April 2017.
Fish. Bull. 115:326–342 (2017)
Online publication date: 16 May 2017.
doi: 10.7755/FB.115.3.4

The views and opinions expressed or implied in this article are those of the author (or authors) and do not necessarily reflect the position of the National Marine Fisheries Service, NOAA.

Age-composition data sets provide the fundamental information necessary for application of statistical catch-at-age assessment (SCAA) models used to estimate population dynamics and to manage commercial fisheries (Quinn and Deriso, 1999; Maunder and Punt, 2013). Age composition data allow the tracking of year classes through time, providing an improved understanding of population dynamics compared with that gained from analyzing fishery catch per unit of effort or survey biomass indices alone. Although theoretically the uncertainty in age composition can be reduced by increasing sample size, agencies have limited age-reading capacity (because of budgetary constraints on the number of hours age-reading scientists can spend reading ages from otoliths, as well as the number of age-reading scientists that a science center can employ.

A formal method for determining the most efficient distribution of sample size across species would be useful for the allotment of limited time, personnel, and funding; however, there is little to no existing guidance in the literature. The lack of scientific rigor used in choosing sample sizes for determining age composition at the NOAA Alaska Fisheries Science Center (AFSC) was noted in the 2013 NOAA Office of Science and Technology program review (AFSC[1]) of data collection and management. The reviewers noted that in light of potentially shrinking budgets, the current level of age-reading capabilities at AFSC may not be sustainable. Even though this conclusion was specific to the AFSC review, this topic is applicable globally, whenever agencies are balancing age-reading priorities with other data collection or assessment priorities in their stock assessment programs.

If a method were to be adopted that based age-composition sampling across species on a statistical or biological basis, the distribution of sample size would be different from that of the current method, and some species would experience an increase in the samples sizes used to determine age composition of fish [hereafter "the age-composition sample size"], while others would result in a decrease. A resulting important issue when discussing these changes in sample sizes for determining age composition is the subsequent influence of increasing or decreasing sample size

[1] AFSC (Alaska Fisheries Science Center). 2013. Summary report: Alaska Fisheries Science Center science data collection review, 40 p. [Available from website.]

on the uncertainty of estimates determined from SCAA models. This is, however, a different investigation than the application of sample size within an SCAA model, or, the idea of effective sample size. The topic of effective sample size and the use of age or length composition data within stock assessments has received extensive attention in recent years (Francis, 2011; Maunder, 2011). This study is also a different investigation from that of optimizing the number of hauls from which age-composition samples are obtained (Pennington et al., 2002; Hulson et al., 2011). While effective sample size is certainly related to the precision and accuracy that results from an SCAA model (Hulson et al., 2012) and determining the number of tows to sample is an important practical consideration (Pennington and Vølstad, 1994), here we are interested in *how* to distribute age-composition sample sizes across species before the data are input in a stock assessment model and after decisions have been made on the number of samples within a tow.

We followed a 2-step procedure to address the 2 topics presented in the preceding paragraphs: 1) how to distribute age-composition sample sizes across species on a statistical or biological basis, and 2) what is the effect on SCAA model uncertainty for species with different life histories by increasing or decreasing age-composition sample size. In the first step we used methods derived from sampling theory to determine the minimum sample sizes necessary to achieve certain sampling goals for multiple species (Quinn and Deriso, 1999). Using this statistical procedure, we then attempted to relate these sample sizes to life-history characteristics of the species investigated to explore whether there exists a biological basis for distribution of sample size across multiple species. In the second step we used simulation to isolate and evaluate the influence of sample sizes that determine age composition from fishery-independent sources on resulting uncertainty in estimates from SCAA models. The simulation analysis was applied to 3 species types with different life-history and survey characteristics to evaluate how age-composition sample size, in combination with survey index uncertainty, influenced SCAA model results and if this influence is disproportionate among different species type life histories. In addition to exploring these 2 topics the underlying goal of the research of this study is to provide preliminary guidance for prioritizing the distribution of sample size for age composition across multiple species, which has not been previously attempted or provided in fisheries research.

Materials and method

Step 1: distribution of sample sizes to determine age composition across multiple species

Age and length observations from fishery-independent bottom trawl surveys conducted by the AFSC in the Gulf of Alaska (GOA), Aleutian Islands (AI), and Bering Sea (BS) were used to evaluate the distribution of sample sizes needed to determine age composition (henceforth, the term "age sample sizes"). These surveys provided an excellent opportunity to evaluate sample sizes for age composition because of the longevity of the surveys and the number of different species sampled for ages. Data (AFSC bottom trawl surveys, website) were used from trawl surveys conducted in the GOA from 1984 to 2011 (triennially from 1984 to 1999 then biennially from 2001 to 2011, e.g., Raring et al., 2011), in the AI from 1980 to 2010 (triennially from 1980 to 1986 and from 1991 to 1997, then biennially from 2000 to 2006 and 2010 on, e.g., von Szalay et al., 2011), and in the BS from 1982 to 2011 (annually; e.g., Lauth and Conner, 2014). In the interest of brevity we refer to von Szalay et al. (2011) for a detailed description of how the survey index and age–length compositions are estimated from the surveys. Our interest was the distribution of age-composition sample sizes across species before indices are estimated; therefore the details concerning the indices are not provided here.

Species included were those for which the number of aged otoliths were greater than 3000 across the time series of the trawl surveys. Within a given haul, the majority of species are sampled for ages with 2-stage sampling: 1) with a fixed allocation method, and 2) the remainder of species sampled with simple random sampling (SRS). Species were categorized into 3 types that included 'flatfish,' 'rockfish,' and 'roundfish' (Table 1). Including rougheye (*Sebastes aleutianus*) and blackspotted (*Sebastes melanostictus*) rockfish, which are assessed as a complex and considered a 'single species' in the context of this study (Spencer and Rooper[2]; Shotwell et al.[3]), there were 15 species and 23 stocks investigated across all areas, including 10 flatfish, 7 rockfish, and 6 roundfish stocks. Otoliths that were read by both a 'reader' and a 'tester' were also collected for each of these species to evaluate the influence of aging error on estimates of age-composition sample size.

We estimated sample sizes for age composition following the method for 2-stage sampling outlined in Quinn and Deriso (1999, chapter 8). In the first stage of sampling a subsample of fish from the total catch is taken to obtain lengths (either total or fork length depending on the species) and in the second stage of sampling a subset of these fish are then sampled for age determination within each predetermined length bin. There are several methods proposed to obtain the

[2] Spencer, P. D., and C. N. Rooper. 2014. Assessment of the blackspotted and rougheye rockfish stock complex in the Bering Sea/Aleutian Islands. *In* Stock assessment and fishery evaluation report for the groundfish resources of the Bering Sea/Aleutian Islands regions. North Pacific Management Council, Anchorage, AK. [Available from website.]

[3] Shotwell, S. K., D. H. Hanselman, J. Heifetz, and P.-J. F. Hulson. 2015. Assessment of the rougheye and blackspotted rockfish stock complex in the Gulf of Alaska. *In* Stock Assessment and fishery evaluation report for the groundfish resources of the Gulf of Alaska. North Pacific Management Council, Anchorage, AK. [Available from website.]

Table 1

Total mean length and age-composition sample sizes per survey and total number of ages sampled combined across years from the NOAA Alaska Fisheries Science Center bottom trawl surveys for the Gulf of Alaska (GOA, 1984–2011), Aleutian Islands (AI, 1980–2010), and Bering Sea (BS, 1982–2011) for the species investigated for this study. The "/" used between Rougheye and blackspotted rockfish denotes that these species are assessed as a complex rather than individual species.

Species: common name (scientific name, acronym)	Region	Mean sample size for length	Mean sample size M for ages	Total sample size for ages
Flatfish				
Alaska plaice (*Pleuronectes quadrituberculatus*, AP)	BS	11,934	347	5800
Flathead sole (*Hippoglossoides elassodon*, FS)	BS	17,354	458	7997
Northern rock sole (*Lepidopsetta polyxystra*, NRS)	BS	34,045	441	6751
Yellowfin sole (*Limanda aspera*, YS)	BS	32,025	707	20,539
Arrowtooth flounder (*Atheresthes stomias*, AF)	GOA	61,142	924	9244
Dover sole (*Microstomus pacificus*, DS)	GOA	7064	404	4642
Flathead sole (*H. elassodon*, FS)	GOA	21,364	572	5723
Northern rock sole (*Lepidopsetta polyxystra*, NRS)	GOA	8337	434	3474
Rex sole (*Glyptocephalus zachirus*, RS)	GOA	15,687	423	4563
Rock sole (*L. bilineata*, SRS)	GOA	10,136	455	3638
Rockfish				
Northern rockfish (*Sebastes polyspinis*, NR)	AI	7405	483	4990
Pacific ocean perch (*S. alutus*, POP)	AI	19,878	1068	10,876
Rougheye/blackspotted rockfish (*S. aleutianus/melanostictus*, RB)	AI	1701	428	3611
Light dusky rockfish (*S. variabilis*, LDR)	GOA	1883	385	4191
Northern rockfish (*S. polyspinis*, NR)	GOA	4195	413	4521
Pacific ocean perch (*S. alutus*, POP)	GOA	19,658	1119	11,511
Rougheye/blackspotted rockfish (*S. aleutianus/melanostictus*, RB)	GOA	3950	516	5279
Roundfish				
Atka mackerel (*Pleurogrammus monopterygius*, AM)	AI	9187	598	6068
Walleye pollock (*Gadus chalcogrammus*, WP)	AI	16,087	1280	12,498
Pacific cod (*Gadus macrocephalus*, PC)	BS	12,241	883	21,731
Walleye pollock (*G. chalcogrammus*, WP)	BS	106,317	1455	42,078
Pacific cod (*G. macrocephalus*, PC)	GOA	12,138	607	6676
Walleye pollock (*G.s chalcogrammus*, WP)	GOA	31,387	1428	17,139

second stage sample and 2 are investigated here: proportional allocation (selecting samples proportional to the length distribution) and fixed allocation (a fixed number of samples from each length class). The method outlined in Quinn and Deriso (1999) allows estimation of minimum sample sizes necessary to achieve a target level of precision (on the basis of a specified coefficient of variation [CV]) for all ages in the age composition data. The primary components used to estimate sample size is the estimated proportion-at-age ($\hat{\theta}_a$), the within-length interval variance component of the estimated proportion-at-age (F_a for fixed allocation, V_a for proportional allocation) and the between-length interval variance component of the estimated proportion-at-age (B_a). In simple terms, one can think of within-length interval variance as the variability of ages within a given length bin (or, the number of ages represented for a given length) and between-length interval variance as the variability in length bins within a given age (or, the number of lengths represented for a given age). From Quinn and Deriso (1999) an unbiased estimator under 2-stage random sampling is represented by the following equation:

$$\hat{\theta}_{a,y} = \sum_{l=1,..,J} \hat{\alpha}_{l,y} \hat{\theta}_{l,a,y}, \quad (1)$$

where $\hat{\alpha}_{l,y}$ = the observed proportion of fish at length l in year y (the number of observations at length l divided by the total number of length observations); and

$\hat{\theta}_{l,a,y}$ = the observed proportion of fish of length l and age a in year y (the number of age observations at length l and age a divided by the number of age observations at length l).

The within-length interval variance for fixed allocation sampling ($F_{a,y}$) is defined as

$$F_{a,y} = J \sum_{l=1,..,J} \hat{\alpha}^2_{l,y} \hat{\theta}_{l,a,y} (1 - \hat{\theta}_{l,a,y}), \quad (2)$$

where J = the total number of length intervals; and $\hat{\alpha}_{l,y}$ and $\hat{\theta}_{l,a,y}$ are as defined above.

For proportional allocation, the within-length interval variance ($V_{a,y}$) is defined by Quinn and Deriso (1999) as:

$$V_{a,y} = \sum_{l=1,..,J} \hat{\alpha}_{l,y} \hat{\theta}_{l,a,y} (1 - \hat{\theta}_{l,a,y}). \quad (3)$$

Finally, the between-length interval variance ($B_{a,y}$) is given as

$$B_{a,y} = \sum_{l=1,..,J} \hat{\alpha}_{l,y}(\hat{\theta}_{l,a,y} - \hat{\theta}_{a,y})^2. \quad (4)$$

For fixed allocation, the formula to estimate the age-composition sample size in year y (A_y) is given by

$$A_y = \frac{F_{a,y}}{\hat{\theta}^2_{a,y} CV^2 - B_{a,y}/L_y} + J, \quad (5)$$

where $F_{a,y}$ = the within-length interval variance (Eq. 2);
$\hat{\theta}_{a,y}$ = the proportion of fish at age a (Eq. 1);
CV refers to the target CV in the age composition;
$B_{a,y}$ = the between-length interval variance (Eq. 4);
L_y = the number of length observations in year y; and
J = the number of length intervals.

Age-composition sample size at some level of precision given proportional allocation was estimated with

$$A_y = \frac{V_{a,y}}{\hat{\theta}^2_{a,y} CV^2 - B_{a,y}/L_y}, \quad (6)$$

where $V_{a,y}$= the within-length interval variance (Eq. 3) and the other terms are the same as in Equation 5.

For consistency across species, the length classes were set at 1-cm bins and were not grouped.

We also estimated the sample size necessary to obtain some target CV under SRS. Under SRS, the age-composition sample size at some level of precision was estimated with

$$A_y = \frac{(1 - \hat{\theta}_{a,y})}{\hat{\theta}_{a,y} CV^2}, \quad (7)$$

which is derived from the variance of a multinomial distribution.

Four sampling goals to achieve some target level of precision in age composition were investigated that represented 2 general categories based on 1) a single age class, or 2) a group of age classes that were related to the total number of ages in the population. The overall point of each of these sampling goals was to investigate standardized sampling goals across species that achieved the same level of uncertainty in the age-composition data. The first sampling goal was to achieve the target CV for the most frequently caught age (i.e., the age class with the largest annual proportion-at-age). The second sampling goal was to achieve the target CV for the age class with the maximum within-length interval variance (i.e., the age class with the least information on age from the length data). The third sampling goal was to achieve the target CV for the top 25% of age classes caught (i.e., proportionally the same number of age classes across species). Finally, the fourth sampling goal was to achieve the target CV for age classes with proportions-at-age that were on average (across time) greater than the inverse of half of the maximum age (i.e., greater than some proportion that is related to the longevity of the species investigated). As an example of this final sampling goal, for a maximum age of 84 years for Pacific ocean perch (*Sebastes alutus*), we would try to achieve a CV for all ages with proportions that were on average greater than 1/42 or 2.4%. It should be noted that it is often difficult to set a sampling goal without prior sampling having been completed.

The CVs ranging from 10 to 25% were initially evaluated (by 5% intervals) to estimate age-composition sample sizes under fixed and proportional allocation across the species investigated. We investigated estimated sample sizes with the same age-composition CV across species to form a basis for comparison. The trends and patterns in distribution of sample size across species, which was our focus, were extremely similar across the different CVs and we present only the results of a target CV of 15%. The overall estimated sample sizes and proportions of the total sample size presented for each species were the median across the years of the bottom trawl surveys needed to obtain the target CV in the age composition. To show the distribution of sample size across species we calculated the species-specific proportion of the total sample size within each sampling goal (dividing the species-specific estimated sample size for some sampling goal by the sum of the estimated sample sizes across species for that sampling goal).

We also investigated the use of species-specific aging error in the estimation of sample sizes. Reader-tester agreement data was compiled for all the species and stocks investigated from the AFSC Age and Growth Laboratory. Two aging error cases were investigated: the first was when aging error was not incorporated, the second was when aging error was incorporated. The amount of aging error (i.e., the age-reading error standard deviation [SD] by age) was investigated for each species and stock according to the methods of Richards et al. (1992) and Hiefetz et al. (1998). In order to construct and implement a generalized aging error method for all species and stocks, a constant CV was used across ages for each species and stock. Aging error was implemented into the estimates of sample size by multiplying the species-specific aging error matrix by the observed proportion of fish of length l and age a in year y ($\hat{\theta}_{l,a,y}$).

We evaluated the relationships between the distribution of age-composition sample size across species and life-history characteristics of species by comparing the proportion of total sample size estimates with 4 statistics. The 4 statistics were focused on instantaneous growth rates (i.e., the slope of the tangent of the growth curve at some age), calculated as the derivative of the von Bertalanffy growth curve (von Bertalanffy, 1938). The life-history statistics investigated included the natural log of 1) the instantaneous growth rate at 20% of the maximum age observed; 2) the instantaneous growth rate of the age at 50% of the asymptotic length (L_∞); 3) the mean population instantaneous growth rate (the instantaneous growth rate at age weighted by the observed proportions at age); and 4) the minimum life-

time growth rate (simply calculated as L_∞ divided by the maximum age observed). Growth for each species was estimated by using the von Bertalanffy growth curve fitted to the mean age and length observations by using AD Model Builder (Fournier et al., 2012). Estimates of the von Bertalanffy growth curve parameters for each of the species investigated when aging error is not included and when it is included (along with the maximum age observed in the bottom trawl surveys) are provided in Supplementary Table 1 (online only). Relationships between the distribution of age sample size and other life-history characteristics were also investigated (including the von Bertalanffy estimated growth coefficient, κ), but for brevity we show these 4 statistics because they resulted in the strongest relationship with the distribution of age-composition sample sizes.

Step 2: sample size for determining age composition and SCAA model uncertainty

A simulation approach was used to evaluate the influence of the magnitude of fishery-independent survey uncertainty (including both age composition and biomass) on resulting SCAA model uncertainty across species types. Operating models for the species types were constructed with simplified versions of the stock assessments for 3 species: GOA arrowtooth flounder (*Atheresthes stomias* [Turnock and Wilderbuer[4]]) as an example for the flatfish species type, Pacific ocean perch ([Hanselman et al.[5]]) as an example for the rockfish species type, and walleye pollock (*Gadus chalcogrammus* [Dorn et al.[6]]) as an example for the roundfish species type.

The operating models for the 3 species types were constructed by fitting standard SCAA models to similar data sources for each example species. Catch-at-age in year y ($C_{a,y}$) was modeled with the Baranov (1918) catch equation and numbers-at-age in year y ($N_{a,y}$) were estimated by following the theory of survival presented by Ricker (1975), which are given by

$$C_{a,y} = N_{a,y}\frac{F_{a,y}}{Z_{a,y}}(1-e^{-Z_{a,y}}) \text{ and} \quad (8)$$

$$N_{a+1,y+1} = N_{a,y}e^{-Z_{a,y}}, \quad (9)$$

where $Z_{a,y}$ = the instantaneous total mortality, composed of natural mortality, $M_{a,y}$, and fishing mortality, $F_{a,y}$.

Fishing mortality was modeled as year-specific and age-specific factors (Doubleday, 1976),

$$F_{a,y} = s_a f_y, \quad (10)$$

where s_a = age-specific selectivity (asymptotic); and
f_y = the annual fishing mortality rate for fully selected fish.

Data that were fitted in the objective function to construct the operating models included total catch biomass (lognormal), commercial fishery age and length compositions (multinomial, effective sample size set at the square root of sample size), bottom trawl survey biomass (lognormal), and bottom trawl survey age composition (multinomial, effective sample size set at square root of sample sizes). The primary differences between the actual stock assessment models and the simplified SCAA models used here included combined-sex rather than sex-specific models, time-invariant survey catchability and selectivity, time-invariant fishing selectivity, and effective sample sizes used. The point of constructing the operating models was not to replicate the exact results of each assessment but to obtain reasonable parameter estimates indicative of the 3 species type life histories. Parameter estimates from the final 30 years of the time series of the operating models for each species type were treated as 'true' values from which process error in recruitment and observation error in survey age compositions and biomass were generated. The parameter estimates used in the operating models for each of the 3 species types investigated are provided in Supplementary Table 2 (online only). The same time scale and amount of data (annually) were used for each species type so that resulting uncertainty in the estimation models was not sensitive to the length or quantity of the data time series.

Process error in recruitment was generated from the operating models with the lognormal distribution. Recruitment deviation parameters were generated independently following the estimation method used in the stock assessment SCAA models (as opposed to using autocorrelation or a stock-recruitment model). The mean recruitment on the log-scale was 6.3 (SD 0.32) for arrowtooth flounder, which was comparable to the 2011 assessment values with a log-scale mean of 6.3 (SD 0.29) from 1980 to 2011 (Turnock and Wilderbuer[4]). For Pacific ocean perch the log-scale mean recruitment used was 3.9 (SD 0.45), which was similar to the 2011 assessment mean from 1980 to 2011 of 3.9 (SD 0.49) (Hanselman et al.[5]). The log-scale mean recruitment was 6.23 (SD 0.70) for walleye pollock, the mean was slightly larger than the assessment mean of 6.0, and the SD was smaller from the assessment value of 0.92 from 1980 to 2011 (Dorn et al.[6]).

For each process error replicate of recruitment, observation error was then generated in age composition

[4] Turnock, B. J., and T. K. Wilderbuer. 2011. Assessment of the arrowtooth flounder stock in the Gulf of Alaska. *In* Stock assessment and fishery evaluation report for the groundfish resources of the Gulf of Alaska. North Pacific Management Council, Anchorage, AK. [Available from website.]

[5] Hanselman, D., S. K. Shotwell, P. J. F. Hulson, J. Heifetz, and J. N. Ianelli. 2011. Assessment of the Pacific ocean perch stock in the Gulf of Alaska. *In* Stock assessment and fishery evaluation report for the groundfish resources of the Gulf of Alaska. North Pacific Management Council, Anchorage, AK. [Available from website.]

[6] Dorn, M., K. Aydin, S. Barbeaux, M. Guttormsen, K. Spalinger, and W. Palsson. 2011. Assessment of the walleye pollock stock in the Gulf of Alaska. *In* Stock assessment and fishery evaluation report for the groundfish resources of the Gulf of Alaska, p. 51–146. North Pacific Management Council, Anchorage, AK. [Available from website.]

Table 2

Minimum and maximum estimated age sample sizes across sampling goals under simple random sampling (SRS), proportional allocation (PA), and fixed allocation (FA) from the NOAA Alaska Fisheries Science Center bottom trawl surveys for the Gulf of Alaska (GOA, 1984–2011), Aleutian Islands (AI, 1980–2010), and Bering Sea (BS, 1982–2011). Estimated sample sizes without aging error are shown on the left of the "|" symbol and sample sizes including aging error are shown on the right (species acronyms are provided in Table 1). The top row for each species type contains the average of the minimum and maximum. Species acronyms are explained in Table 1.

Species	Region	SRS	PA	FA
Flatfish				
Avg.	Min–Max	269–730 | 301–737	205–659 | 244–706	447–1354 | 523–1374
AP	BS	286–687 | 300–716	224–666 | 259–676	530–1330 | 616–1298
FS	BS	278–640 | 318–604	197–565 | 236–574	356–1079 | 389–1066
NRS	BS	192–570 | 208–727	136–380 | 152–406	370–882 | 446–890
YS	BS	232–662 | 249–676	150–614 | 178–630	314–1358 | 338–1365
AF	GOA	240–458 | 254–615	151–410 | 190–548	369–836 | 445–941
DS	GOA	460–1686 | 560–1515	377–1614 | 492–1785	646–3058 | 820–3124
FS	GOA	268–616 | 297–594	222–556 | 258–570	600–1416 | 718–1432
NRS	GOA	210–579 | 226–564	174–526 | 188–530	400–1028 | 430–1025
RS	GOA	217–888 | 257–852	187–801 | 224–843	478–1699 | 576–1700
SRS	GOA	310–516 | 342–504	236–462 | 265–498	410–853 | 447–898
Rockfish				
Avg.	Min–Max	406–1823 | 516–2967	348–1977 | 467–3002	805–4805 | 1072–6494
NR	AI	360–1433 | 427–1533	335–1400 | 402–1516	566–3082 | 1024–3386
POP	AI	319–2000 | 416–6319	261–2702 | 366–6218	650–4882 | 782–12224
RB	AI	678–2522 | 989–2523	661–2822 | 980–2662	1928–8584 | 2871–7710
LDR	GOA	258–1030 | 290–1172	210–1044 | 206–1146	524–2726 | 516–3040
NR	GOA	406–1423 | 464–1456	342–1371 | 421–1433	660–4139 | 860–3918
POP	GOA	346–1670 | 370–5015	231–1718 | 249–5300	473–3886 | 338–9380
RB	GOA	477–2684 | 655–2751	396–2781 | 642–2740	837–6333 | 1116–5801
Roundfish				
Avg.	Min–Max	126–350 | 133–329	55–255 | 62–256	147–509 | 200–576
AM	AI	110–174 | 112–180	72–150 | 75–155	155–342 | 178–379
WP	AI	170–499 | 191–427	110–446 | 135–374	238–849 | 334–876
PC	BS	109–262 | 117–254	20–137 | 40–188	134–299 | 187–389
WP	BS	108–490 | 109–510	50–404 | 8–412	92–827 | 105–942
PC	GOA	138–294 | 143–242	69–133 | 105–157	191–323 | 318–427
WP	GOA	118–383 | 125–359	6–260 | 8–250	70–413 | 75–440

and biomass from survey data. Observation error in survey age-composition data from the operating model was generated with the multinomial distribution. To evaluate the influence of age-composition sample size in a fishery-independent survey on SCAA model results, 13 sample sizes were used to generate trawl survey age composition data that ranged from 10 to 100,000 (by multiples of 2.5 and 2, e.g., 10, 25, 50, 100, 250, 500...).

The influence of survey biomass uncertainty was evaluated concurrent with age composition uncertainty with 4 index uncertainty cases. These cases focused on the CV used to generate observation error in the log-normal survey biomass time series. Index case E0 generated log-normal survey biomass data with a CV set at the average obtained by the AFSC bottom trawl survey in the GOA (CV≈9% for arrowtooth flounder, 25% for Pacific ocean perch, and 18% for walleye pollock). Index case E1 multiplied the CV in case E0 by 2. Index case E2 set the CV at 10% for all species types, and E3 set the CV at 25% for all species types. Although some of the index cases may not occur in reality (for example, setting the CVs equal across species), our goal was to investigate the relationship with survey index CV as well as age composition based on survey data and a range of values is needed. Unlike the actual AFSC bottom trawl survey time series in the GOA (which is triennial from 1984 to1999 and biannual from 1999 to 2011) this simulation analysis generated annual trawl survey biomass and age-composition data, so that variability in model estimation results was not sensitive to gaps in the time series based on data from the trawl surveys.

In the estimation models, the same number of parameters was estimated for each species type so that resulting uncertainty was more directly comparable and was not sensitive to parameter differences. Estima-

tion models had 35 parameters that included log-scale mean recruitment (1), recruitment deviations (30), natural mortality (1), survey catchability (1), and logistic parameters for survey selectivity (2). The models fitted age-composition data from the trawl survey with the multinomial distribution and biomass data from the trawl survey with the log-normal distribution. The sample sizes and CVs used to generate the age composition and biomass data, respectively, from the trawl data were treated as known and used in the estimation models so that uncertainty was not misspecified.

For each of the 100 replicates of recruitment that were generated, 100 replicates of survey age composition and index were generated and fitted by the estimation models. For presentation we focus on the CV of the total biomass of the final year estimated by the SCAA model because this particular quantity allows consideration of the uncertainty in potential quantities of interest to management.

Results

Step 1: distribution of sample sizes to determine age composition across multiple species

Overall, the results of the distribution of sample size for age-composition among the species types investigated with the AFSC bottom trawl survey data were consistently similar across sampling goals (Fig. 1), sampling methods (Fig. 2), and whether or not aging error was included (Fig. 3, A–D). Proportionally speaking, the distribution of age samples was in general the smallest for roundfish, intermediate for flatfish, and largest for rockfish (Figs. 1–3). Upon combining sample sizes across species types, we found that the distribution of sample size for the collection of otoliths for age reading was around 10% for roundfish, 30–40% for flatfish, and 50–60% for rockfish (left panels, Figs. 1–3). An interesting species that was a counter-example to the general results was Dover sole (*Microstomus pacificus*) in the GOA, which is the longest lived flatfish species investigated. In some sampling goals Dover sole resulted in a larger proportion of the total sample size than some rockfish species. Consistent patterns or large differences in the distribution of sample sizes in relation to location (e.g., among the GOA, AI, or BS) were not apparent across sampling goals, sampling methods, or cases of aging error for species that resided in more than one region investigated.

A few minor differences resulted in the distributions of sample size for individual species across sampling goals (Fig. 1) and sampling methods (Fig. 2); however, the overall pattern of distribution by species type dominated the results of the distribution of sample size for collecting age samples. When aging error was included in the distribution of sample size, there were some differences in total sample size proportions among some of the roundfish and flatfish species but there were no differences when aging error was not included (for example, AI Atka mackerel (*Pleurogrammus monopterygius*) or GOA Arrowtooth flounder), although, the overall distribution by species type was again consistent (Fig. 3, A and C). When directly comparing across species, sampling goals, and sampling methods, we found that the sample sizes required when aging error was included were predominantly larger than when aging error was not included (Table 2). The slope parameter from a linear regression between estimated sample sizes that did and did not include aging error was significantly greater than 1 and the intercept parameter was significantly greater than 0, indicating that estimated sample sizes when aging error was included are larger than when aging error was not included (Fig. 3E). On average, when aging error was included, the sample size needed to increase by around 10% for flatfish and roundfish, and over 40% for rockfish to achieve the same level of uncertainty as when aging error was not included.

Upon investigating the within- and between-length interval variance components across species there were patterns that emerged that could explain the resulting distribution of sample size across species (Fig. 4). In general, the between-length interval variance was smallest for rockfish, intermediate for flatfish, and largest for roundfish. Alternatively, the within-length interval variance (under both proportional and fixed allocation) was, in general, smallest for roundfish, intermediate for flatfish, and largest for rockfish. Significant relationships resulted among all 4 life-history statistics investigated and the proportion of total sample size across sampling goals (Fig. 5, including aging error, shown as an example). The weakest relationship was between the log of estimated sample size and the log of the growth rate at 50% of L_∞ with coefficient of multiple determination (R^2) values of 0.61 (Fig. 5B). The strongest relationship was found between the log of median sample size and the log of the minimum lifetime growth rate with R^2 values of 0.88 (Fig. 5D).

Estimated sample sizes were comparable to AFSC bottom trawl survey sample sizes. Across the flatfish species investigated, the range between the average minimum and maximum sample sizes to achieve the sampling goals investigated was between 205 and 1374 samples (Table 2), which contains the actual average sample size taken by the AFSC bottom trawl surveys and is approximately 500 samples per year (Table 1). For the rockfish species investigated, the range of average minimum and maximum sample sizes to achieve our sampling goals was from 348 to 6494 samples (Table 2), which also contains the actual average yearly sample size of 630 samples taken by the AFSC bottom trawl surveys (Table 1). The range of the average minimum and maximum sample sizes to achieve the sampling goals for the roundfish investigated was between 55 and 576 samples (Table 2), the average annual sample size taken by the AFSC bottom trawl surveys of around 1040 samples (Table 1) was larger than this range. The estimated sample sizes were, in

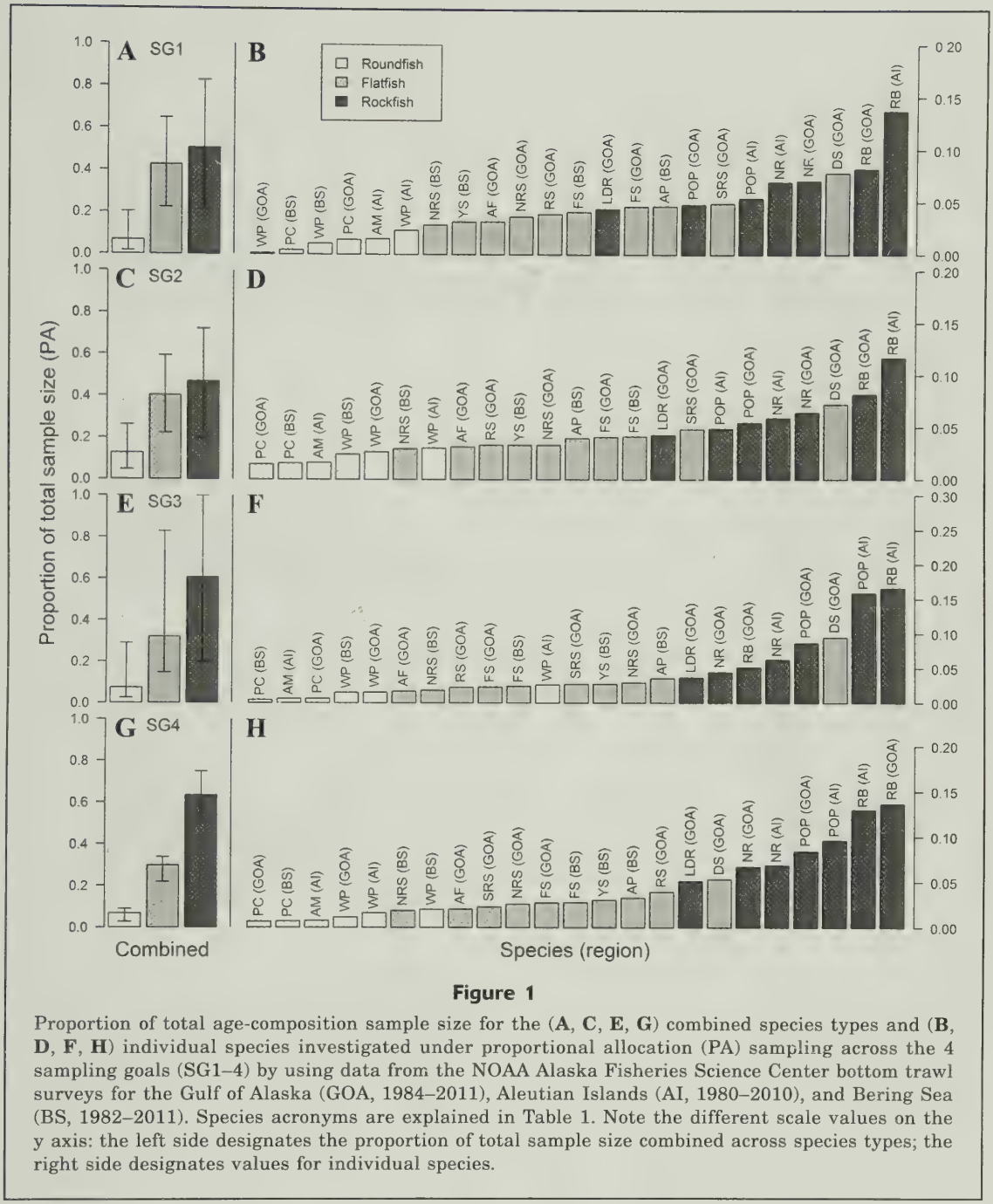

Figure 1

Proportion of total age-composition sample size for the (**A**, **C**, **E**, **G**) combined species types and (**B**, **D**, **F**, **H**) individual species investigated under proportional allocation (PA) sampling across the 4 sampling goals (SG1–4) by using data from the NOAA Alaska Fisheries Science Center bottom trawl surveys for the Gulf of Alaska (GOA, 1984–2011), Aleutian Islands (AI, 1980–2010), and Bering Sea (BS, 1982–2011). Species acronyms are explained in Table 1. Note the different scale values on the y axis: the left side designates the proportion of total sample size combined across species types; the right side designates values for individual species.

general, of similar magnitude between SRS and proportional allocation sampling across the sampling goals. Both SRS and proportion sampling required almost half the number of age samples to achieve the same amount of uncertainty as that obtained with fixed allocation, which is the current method for the majority of species sampled by the AFSC bottom trawl survey. Compiled results of the estimated sample sizes sampling goals investigated are shown in Table 2 to reduce the number of results presented; the estimated sample sizes for each species investigated across the sampling goals, sampling methods, and whether or not aging error was included are provided in Supplementary Tables 3–5 (online only).

Step 2: sample size for determining age composition and SCAA model uncertainty

The CV of total biomass in the final year of the estimation models for flatfish, rockfish, and roundfish decreased at different rates with increasing age-composition sample size from survey data and eventually

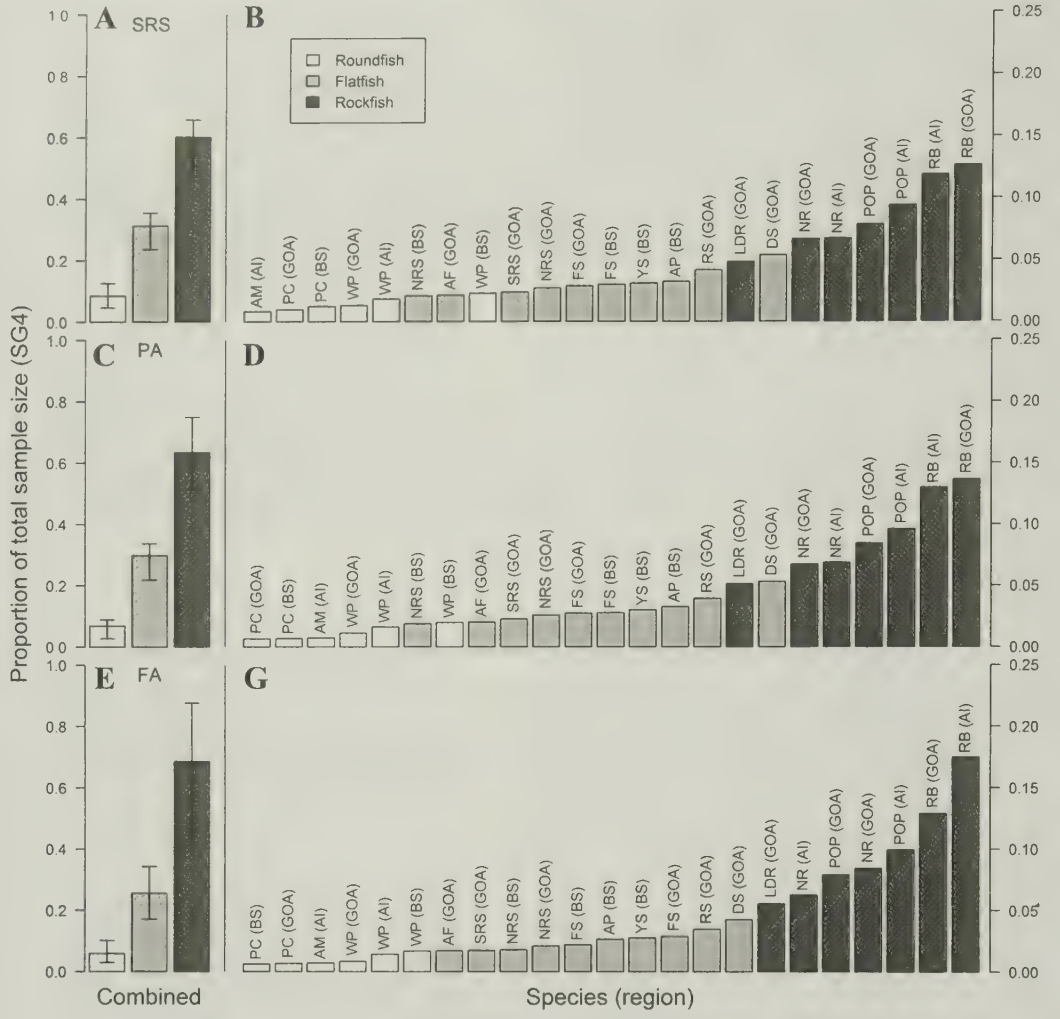

Figure 2

Proportion of total age-composition sample size for the (**A**, **C**, **E**) combined species types and (**B**, **D**, **G**) individual species investigated under simple random sampling (SRS), proportional allocation (PA), and fixed allocation (FA) sampling by using data from the NOAA Alaska Fisheries Science Center bottom trawl surveys for the Gulf of Alaska (GOA, 1984–2011), Aleutian Islands (AI, 1980–2010), and Bering Sea (BS, 1982–2011). Sampling goal 4 (SG4) is used for illustration. Species acronyms are explained in Table 1. Note the different scale values on the y axis: the left side designates the proportion of total sample size combined across species types; the right side designates values for individual species.

approached a minimum value for the index uncertainty cases E0–E3 (Fig. 6). For each of the index uncertainty cases the minimum CV obtained, or baseline, was related to the underlying magnitude of the CV in survey biomass. In uncertainty cases E0 and E1 (Fig. 6, A and B), the baseline CV of the final year's total biomass was smallest for flatfish, intermediate for roundfish, and largest for rockfish, which followed the relative magnitude of the underlying uncertainty in the survey index data for these 3 species types. In all index uncertainty cases, CV reduction resulting from increased age-composition sample size (the maximum CV obtained compared to the baseline) was greatest for the roundfish group (text in top right corner of each plot in Fig. 6) and the smallest for the flatfish group, with rockfish intermediate.

The sample size for which the CV in the total biomass of final year changed by less than 2.5% for all species types, which we define as the point of diminishing returns, and was larger in cases with smaller survey index uncertainty than in cases with larger survey index uncertainty (vertical lines with arrows in Fig. 6). For example, the sample size at the point of diminishing returns for case E0 of 2500 samples was larger

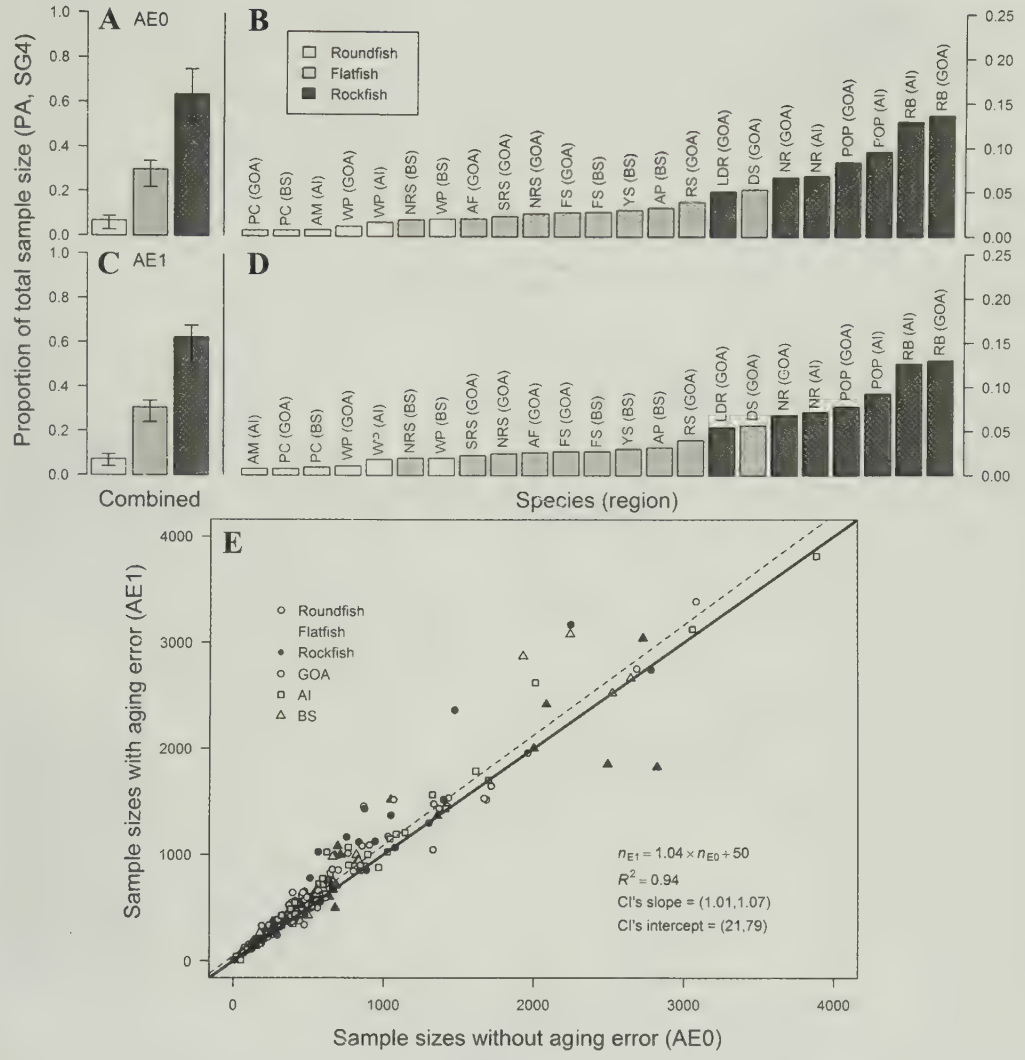

Figure 3

Proportion of total age-composition sample size for the (**A**, **C**) combined species types and (**B**, **D**) individual species investigated without aging error (AE0) and with aging error (AE1) and (**E**) direct comparison of estimated age-composition sample sizes with and without aging error by using data from the NOAA Alaska Fisheries Science Center bottom trawl surveys for the Gulf of Alaska (GOA, 1984–2011), Aleutian Islands (AI, 1980–2010), and Bering Sea (BS, 1982–2011). Proportional sampling and sampling goal 4 (SG4) are used for illustration. Species acronyms are explained in Table 1. n_{E1}=age-composition sample size with aging error; n_{E0}=age-composition sample size without aging error; R^2=coefficient of multiple determination; CI=confidence interval. Note the different scale values on the y axis: the left side designates the proportion of total sample size combined across species types; the right side designates values for individual species.

than the sample size of 500 samples for case E1 (vertical lines with arrows in each plot in Fig. 6). Likewise, the sample sizes at the point of diminishing returns were greater for E2 (5000) compared with E3 (500).

Correlation analysis between changes in the estimates of the CV in the biomass of the final year, recruitment variability, and survey index uncertainty from the estimation model emphasized the relationship between these quantities and sample size. The percent change in the CV of the total biomass of the final year (relative difference between largest CV compared with baseline CV, or, the minimum CV obtained) was positively correlated with recruitment variability (0.54; Fig. 7A). Conversely, the uncertainty in the survey index was negatively correlated with the percent change in the CV of biomass in the final year (–0.57; Fig. 7B). Taken alone, however, neither of these correlations was as strong as when the percent change in the CV of to-

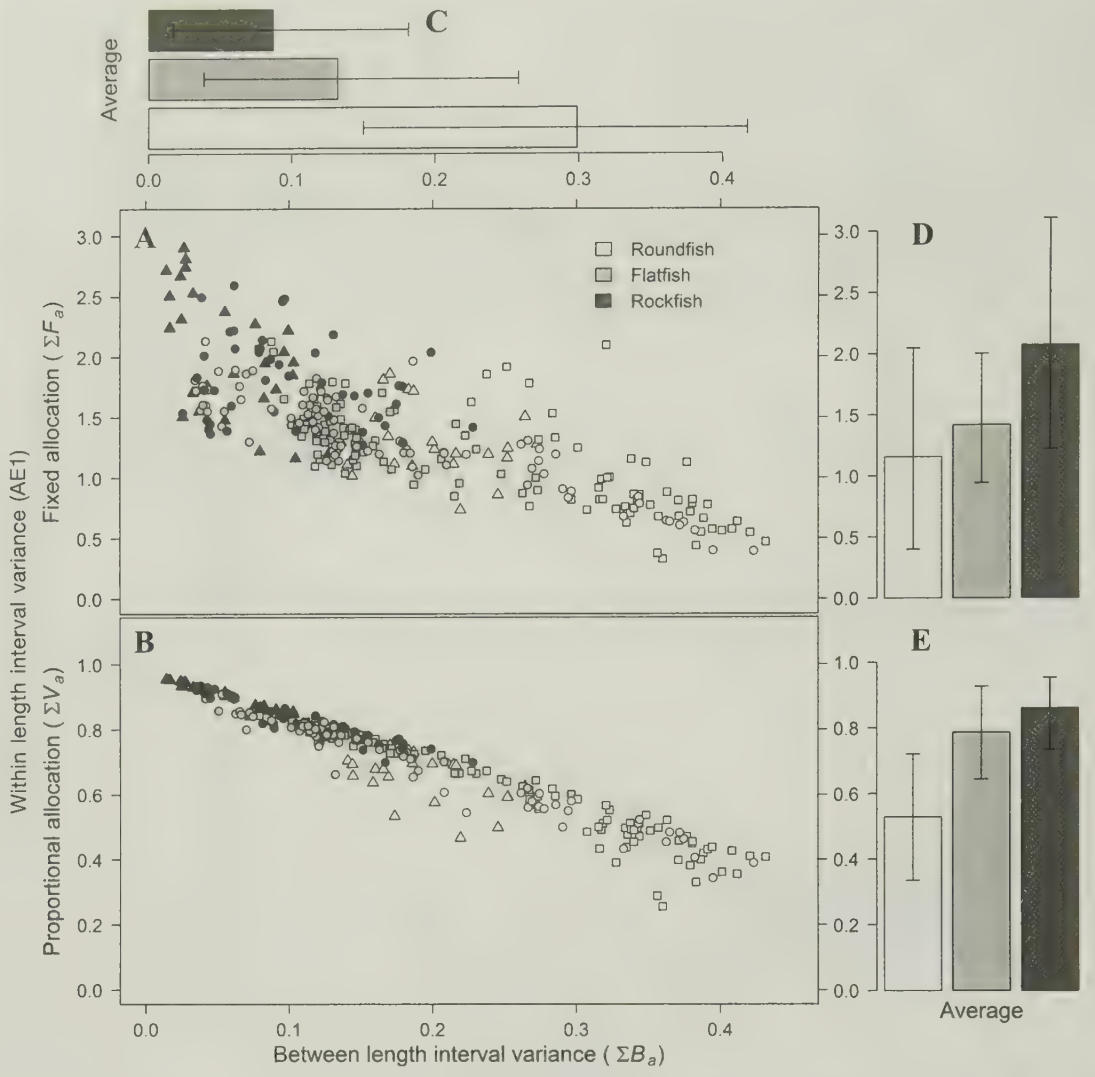

Figure 4

Comparison for fixed allocation and proportional allocation of the within-length interval variance, (**A**) for fixed allocation and (**B**) for proportional allocation, and of the between-length interval variance for the species investigated (estimated with aging error [AE1] by using data from the NOAA Alaska Fisheries Science Center bottom trawl surveys for the Gulf of Alaska [GOA, 1984–2011], Aleutian Islands [AI, 1980–2010], and Bering Sea [BS, 1982–2011]). Barplots indicate the averages of **(C)** the between-length variance and within-length interval variance, (**D**) for fixed allocation and (**E**) for proportional allocation for species types.

tal biomass in the final year was correlated with the ratio of recruitment variability divided to the survey index uncertainty, which was 0.96 (Fig. 7C).

Discussion

When thinking about the most efficient and appropriate manner to distribute sample sizes for age across multiple species, whether in a fishery-independent survey or from a commercial or recreational fishery, there are a number of factors to consider. All of these can be reduced to answering a single question: What is the relative value of each additional otolith to stock assessment? Although this can be posed as a simple question, it is not simple to answer. It is an optimization problem that requires balance among biology and life-history, statistics and stock assessment, and the commercial value and importance of the fisheries to user groups. Although this study is the first attempt in the fisheries literature to directly address this question, we recognize that many more factors than those con-

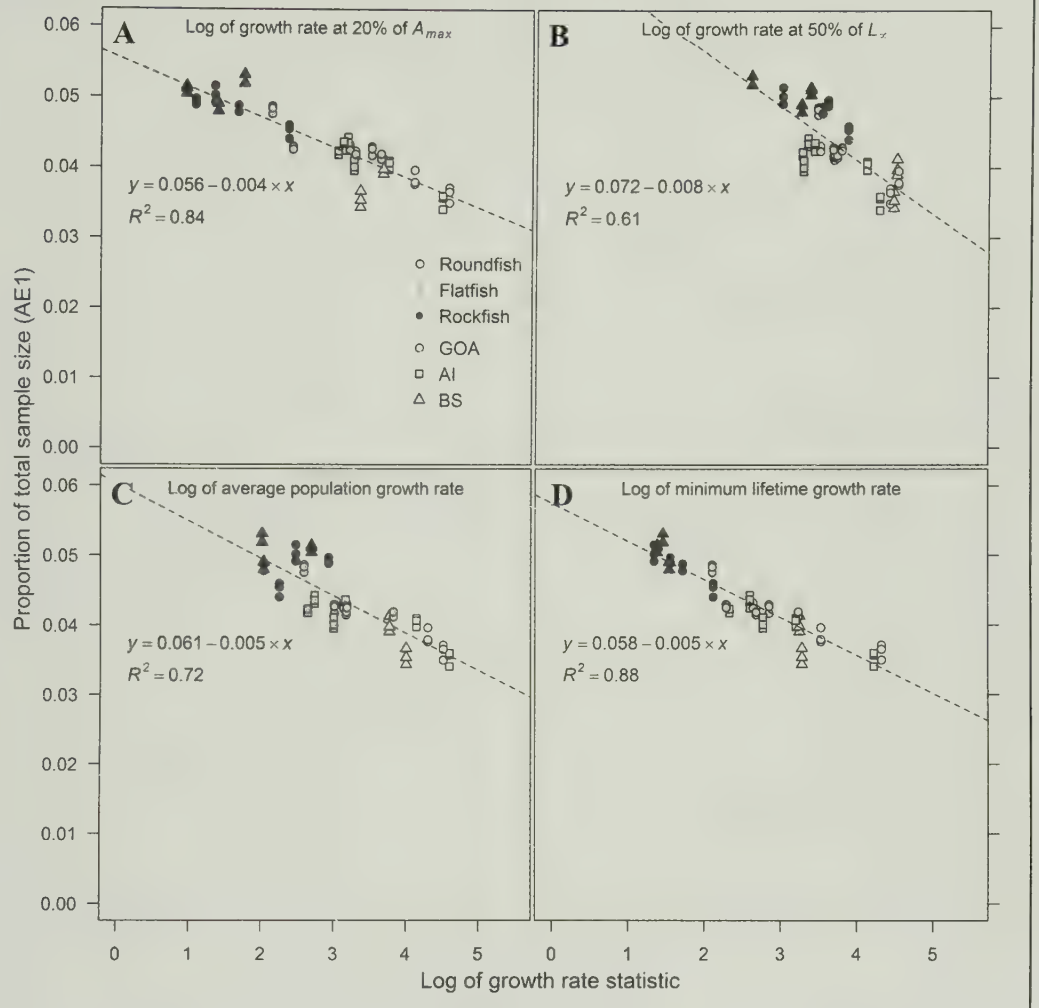

Figure 5

Linear relationships among the life-history statistics evaluated—(**A**) log of growth rate at 20% of the maximum age observed (A_{max}); (**B**) log of growth rate at 50% of asymptotic length (L_∞); (**C**) log of average population growth rate; and (**D**) log of minimum lifetime growth rate—and the estimated proportion of total sample size by species across the sampling goals and sampling methods evaluated when including aging error (AE1) in analyses with data from the NOAA Alaska Fisheries Science Center bottom trawl surveys for the Gulf of Alaska (GOA, 1984–2011), Aleutian Islands (AI, 1980–2010), and Bering Sea (BS, 1982–2011). R^2=coefficient of multiple determination.

sidered here should be investigated to obtain a more definitive answer to this question. Although, at some point it must be recognized that the uncertainty inherent in collecting and analyzing fisheries data, and the simplifications that are unavoidable in simulation analyses, make a comprehensive answer to this question unobtainable. In this study we have, however, provided several useful and interesting results that can be considered when approaching the issue of age sample size distribution and its subsequent influence on stock assessment.

The use of sampling theory, to estimate age sample sizes for each species, resulted in surprisingly consistent patterns in comparisons of the resulting sample sizes across species in a distributional sense rather than by restricting the results to only species-specific evaluation. Upon viewing the species-specific sample sizes as a proportion of total sample size, regardless of the sampling goal, sampling method, or whether aging error was applied, the same pattern emerged. The rockfish species type required the largest proportion of total sample size, flatfish were intermediate, and roundfish required the lowest proportion of total sample size. Potentially the most interesting results of this study were the relationships between the distributions of sample size and life-history characteris-

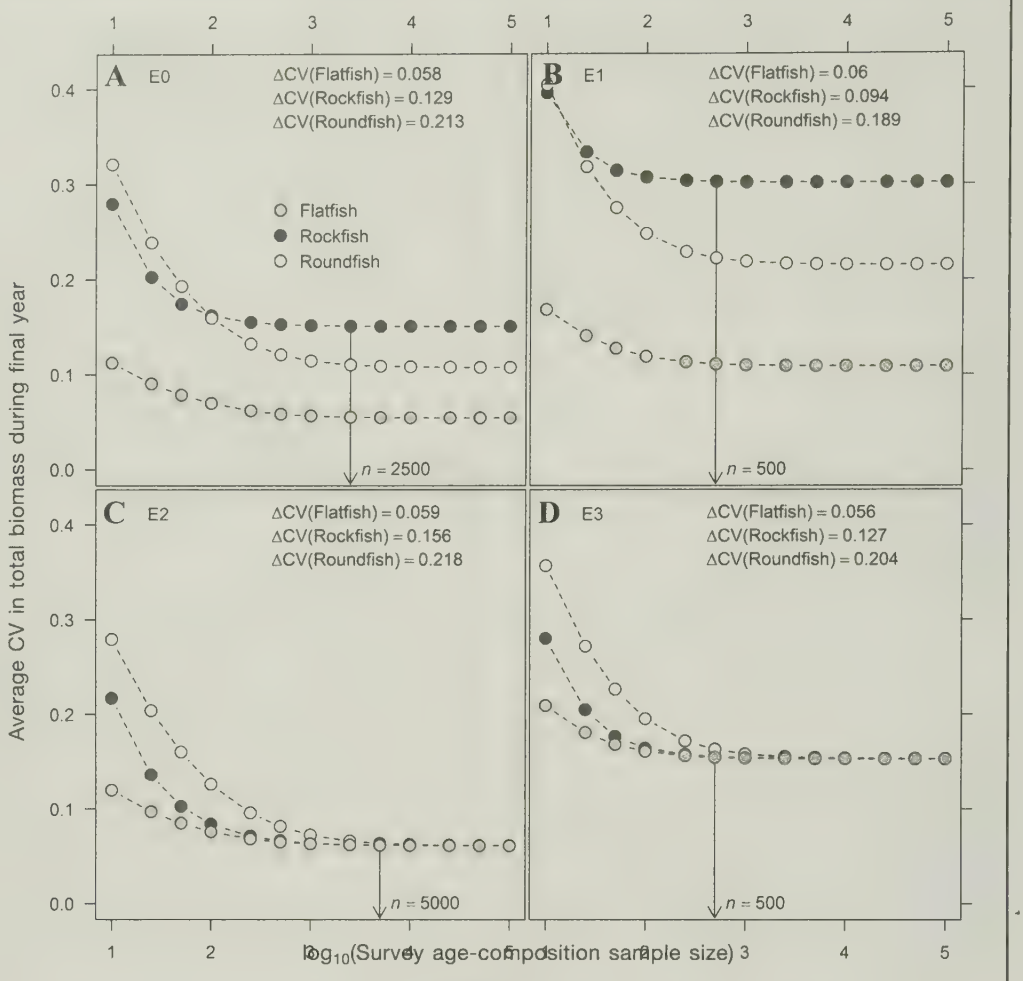

Figure 6

Coefficient of variation (CV) for biomass during the final year from the estimation models for the species types (flatfish, rockfish, and roundfish) evaluated across survey age-composition sample sizes (per species) and survey index uncertainty cases (**A**) E0, (**B**) E1, (**C**) E2, and (**D**) E3. Text in the top right corners of each graph denotes the absolute change in CV for each species type, and the vertical lines with arrows indicate the age sample size beyond which the CV in the biomass during the final year changed less than 2.5% for all 3 species types.

tics, in particular growth. It was shown that the relative proportion of sample size could be related to the growth rates of the species considered. The significant relationships between the proportion of age-composition sample sizes by species and life-history statistics could be due partially to the patterns in the variance between- and within-length intervals that resulted with species types.

On the basis of our results of this study, species that are relatively slower growing require more samples to determine age composition than those that are relatively faster growing. The overall idea being that for relatively faster growing species, there is more distinction between the lengths at a given age; thus, the length composition is relatively more informative regarding age than it is for slower growing species, and fewer age samples are need to determine the age composition when performing 2-stage sampling. These results are also generalizable beyond just the species sampled by the AFSC bottom trawl surveys. Any fisheries science organization around the world will be constrained by the total number of otoliths it can process in a given year when considering how to distribute age sample size in a fishery-independent survey or fishery. The guidance that this study provides is that the growth characteristics of the species being sampled can help determine the relative magnitude of the sample size that should be used for each species. However, the results of this study should be taken in light of the caveats inherent to the method used to determine the dis-

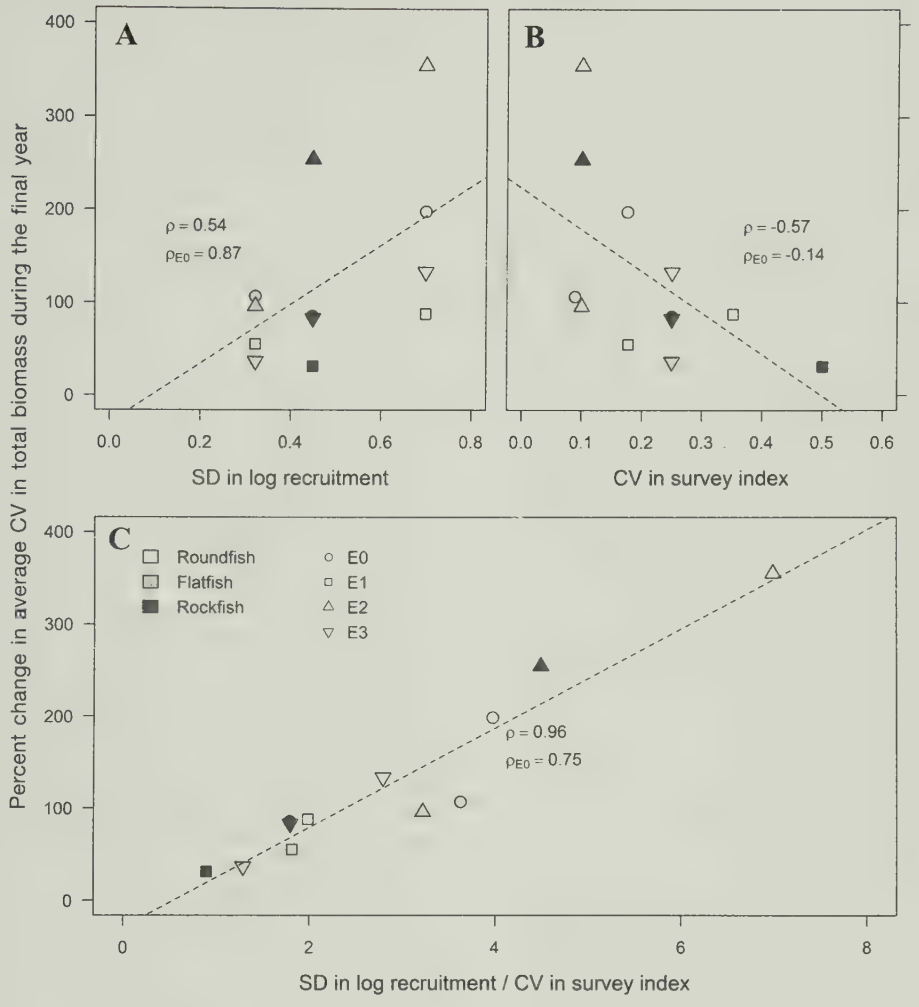

Figure 7

Correlations of (**A**) standard deviation (SD) in log-scale recruitment, (**B**) the coefficient of variation (CV) of the survey index, and (**C**) SD in log-scale recruitment divided by the CV of the survey index with the resulting percent change in the CV in biomass during the final year from the estimation models across survey age-composition sample sizes for each survey index uncertainty case (E0–E3) evaluated (correlation in text shown for case E0). ρ=Pearson's correlation coefficient for all survey index uncertainty cases; ρ_{E0}=Pearson's correlation coefficient for survey index uncertainty case E0 only.

tribution of sample size. We will discuss 3 of these: 1) cost, 2) intrahaul correlation, and 3) commercial value of the species.

Cost, in terms of collecting age samples, would be defined as the cost in time (which is proportional to labor costs) required to both collect and read any given otolith. For example, when otoliths are collected, it is somewhat more difficult to obtain an otolith from a rockfish than from a roundfish or flatfish. There could also be differences in the amount of time it takes to obtain lengths of certain species. In terms of reading otoliths, more time is required to read a rockfish otolith than a flatfish or roundfish otolith, if for no other reason than that rockfish are longer-lived and have more annuli to count than flatfish or roundfish. Additionally, we found that aging error had a relatively larger influence on rockfish species than on roundfish or flatfish. This finding would increase the cost in time because more otoliths would need to be read to obtain the same amount of information in the age-composition data. Cost could also be a function of sampling method, with the highest cost associated with fixed-allocation 2-stage sampling and lower costs associated with proportional allocation 2-stage sampling or SRS (in terms of the sample size necessary to achieve the same amount of uncertainty). Methods have been developed to include

cost in estimating sample sizes required for age composition (Schweigert and Sibert, 1983; Lai, 1987), however, the data on cost for the species sampled by the AFSC was not available at the time of this study.

Intrahaul correlation arises owing to the similarity of fish ages within a given haul or the spatial distribution of these ages in comparison with the spatial distribution of sampling, which then leads to over-dispersion of uncertainty when compared with what would be determined from multinomial sampling (McAllister and Ianelli, 1997). Intrahaul correlation in sampling for ages has recently been the subject of several studies (Pennington et al., 2002; Hulson et al., 2011), as well as investigations of how to account for intrahaul correlations in SCAA models (Francis, 2011; Maunder, 2011; Hulson et al., 2012). Although intrahaul correlation has received attention in the literature in terms of integration into stock assessment models, it is not clear at this point in time how intrahaul correlation could be incorporated in estimating optimal distribution of age-composition sample sizes across species before a stock assessment. The magnitude of the difference between effective sample size and the actual sample size collected is influenced by the age aggregations within schools or the spatial distribution of the species sampled, which may not be consistent across species. This should be a topic for future consideration but is beyond the scope of the current study.

Value in this case would be defined as the value of the fishery, the sampling efforts of which are supporting stock assessment. Using fisheries assessed by the AFSC as an example, the walleye pollock fishery in the eastern BS supports one of the largest and most valuable groundfish fisheries in the world (Ianelli et al.[7]). The stock would require a decrease in age-composition sample size if the results of the current study were implemented in the AFSC bottom trawl age-sampling design. Including value into the sampling theory method has not been previously explored but, mathematically speaking, it could be implemented in a similar manner to that of cost. It is more challenging, however, to determine how age sample size affects the potential value of a fishery. The results of the simulation analysis show that changing sample size in age composition affects the resulting uncertainty in an SCAA model. Methods have been proposed that would take into account uncertainty when setting management quantities such that when uncertainty in SCAA model results increase, the harvest target rate decreases to account for this uncertainty (Prager and Shertzer, 2010). The eastern BS pollock assessment employs a buffer based on the uncertainty of the estimation of the harvest target. Therefore, if sample sizes were decreased and SCAA model uncertainty increased substantially, the potential value of the fishery could decrease. A more rigorous analysis of value would have to include the numerous other factors that are a part of the overall value of a fishery (e.g., a decrease in quota could increase the price per kilogram or increase long-term value). Age-composition sample size may indeed be a very small factor in terms of value, but value is unquestionably one of the main factors influencing how age-composition sample sizes are currently allocated by the AFSC.

The simulation analyses with the SCAA model provide guidance on the factors to consider when adjusting age-composition sample sizes in a multispecies data collection program. The results suggest that life-history and survey index uncertainty play key roles in determining the magnitude of influence that changing age-composition sample size has on SCAA model uncertainty. The results of the simulation analysis indicated that age-composition sample size has a greater impact on the resulting uncertainty in SCAA models for species with high recruitment variability or low survey index uncertainty, or both. In contrast, for species with low recruitment variability or high survey index uncertainty, or both, changes in age-composition sample size have a smaller influence on the resulting uncertainty from a SCAA model. Returning to the eastern BS walleye pollock example, the recruitment variability of this stock is higher than that of most species, and it has intermediate survey index uncertainty (intermediate between rockfish and flatfish species); therefore, decreasing age-composition sample size would potentially have a larger impact than decreasing sample size for a flatfish species, for example, that has lower recruitment variability and low survey index uncertainty.

To isolate the effect of the fishery-independent survey data sources (index and age composition) we made several simplifying assumptions in our simulation. These involved including process and observation error in the fishery data sources (e.g., different catch histories and different levels of uncertainty in the catch data) which would also influence the uncertainty resulting from an SCAA model and could decrease the relative influence of the fishery-independent survey data sources. An additional consideration that was not made in our simulation is the potential for gaps in the fishery-independent survey data (which is the case for the AI and GOA bottom trawl survey data) and how that influences age-composition sample size in the resulting SCAA model uncertainty. The strength of the relationships between increasing or decreasing age-composition sample size and recruitment variability and survey index uncertainty is possibly due to the simplifying assumptions made in the simulation analysis. Although, magnitudes in changes to the SCAA model uncertainty could be different with the use of more sophisticated simulations, we hypothesize that these correlations may be qualitatively the same regardless of the complexity of the simulation analysis. We recommend that future research into investigating the influence of age-composition sample size on SCAA model results, and how that relates to optimal distri-

[7] Ianelli, J. N., T. Honkalehto, S. Barbeaux, and S. Kotwicki. 2015. Assessment of the walleye pollock stock in the Eastern Bering Sea. *In* Stock assessment and fishery evaluation report for the groundfish resources of the Bering Sea/Aleutian Islands regions. North Pacific Management Council, Anchorage, AK. [Available from website.]

bution of sample size across species, should be undertaken with more complex simulation analyses than the scope of this article allows.

We have attempted to synthesize the use of sampling theory with SCAA model simulation analyses to address 2 primary questions: 1) how to distribute age-composition sample sizes across species, and 2) what is the effect on SCAA model uncertainty by increasing or decreasing age-composition sample size for species with different life histories. In addressing the first question, if a goal of sampling is to obtain age compositions with a similar degree of uncertainty across species, the sample sizes should be distributed on the basis of life-history characteristics, in particular growth rates. In addressing question 2, at the same time one should keep in mind that the relationship between age-composition sample size and resulting SCAA model uncertainty can be disproportionate because of species-specific characteristics, and is related to the recruitment variability and survey index uncertainty of the species modeled. We had to make several simplifying assumptions because of the breadth of the topic of optimal distribution of age-composition sample size across species. It is due to these simplifying assumptions that we are reluctant to suggest absolute ranges of age sample sizes for each species, but we do contend that there are life-history characteristics, in particular growth, that can be considered when discussing the distribution of sample size. Optimal allocation of sample size has historically been an extremely important topic, although not one that has received attention in the literature. As fisheries research resources appear to be shifting away from traditional survey and stock assessments toward process studies, government agencies will continue to seek guidance for current allocation strategies. We suggest that future developments be focused on developing both sampling theory to take into account various aspects of sampling that currently are not considered and more sophisticated simulation analyses with SCAA models to place the discussion of sample size distribution across species in terms of risk of overfishing, accuracy of results, and value to managers and stakeholders.

Acknowledgments

We would like to thank P. Malecha, J. Heifetz, and P. Spencer for helpful comments and advice. We also thank J. Short for providing the reader-tester data to determine aging error. Three anonymous reviews also helped make substantial improvements to this manuscript.

Literature cited

Baranov, F. I.
1918. On the question of the biological basis of fisheries. Nauchn. Issled. Ikhtiol. Inst. Izv. 1:81–128. [In Russian.]

Doubleday, W. G.
1976. A least-squares approach to analyzing catch at age data. Int. Comm. Northw. Atl. Fish., Res. Bull. 12:69–81.

Fournier, D. A., H. J. Skaug, J. Ancheta, J. Ianelli, A. Magnusson, M. N. Maunder, A. Nielsen, and J. Sibert.
2012. AD Model Builder: using automatic differentiation for statistical inference of highly parameterized complex nonlinear models. Optim. Methods Softw. 27:233–249.

Francis, R. I. C. C.
2011. Data weighting in statistical fisheries stock assessment models. Can. J. Fish. Aquat. Sci. 68:1124–1138.

Heifetz, J., D. Anderi, N. E. Maloney, and T. L. Rutecki.
1998. Age validation and analysis of aging error from marked and recaptured sablefish, *Anoplopoma fimbria*. Fish. Bull. 97:256–263.

Hulson, P.-J. F., D. H. Hanselman, and T. J. Quinn II.
2011. Effects of process and observation errors on effective sample size of fishery and survey age and length composition using variance ratio and likelihood methods. ICES J. Mar. Sci. 68:1548–1557.
2012. Determining effective sample size in integrated age-structured assessment models. ICES J. Mar. Sci. 69:281–292.

Lai, H.-L.
1987. Optimum allocation for estimating age composition using age-length key. Fish. Bull. 85:179–185.

Lauth, R. R., and J. Conner.
2014. Results of the 2011 eastern Bering Sea continental shelf bottom trawl survey of groundfish and invertebrate cauna. NOAA Tech. Memo. NMFS-AFSC-266, 176 p.

Maunder, M. N.,
2011. Review and evaluation of likelihood functions for composition data in stock-assessment models: estimating the effective sample size. Fish. Res. 109:311–319.

Maunder, M. N., and A. E. Punt.
2013. A review of integrated analysis in fisheries stock assessment. Fish. Res. 142:61–74.

McAllister, M. K., and J. N. Ianelli.
1997. Bayesian stock assessment using catch-age data and the sampling-importance resampling algorithm. Can. J. Fish. Aquat. Sci. 54:284–300.

Pennington, M., and J. H. Vølstad.
1994. Assessing the effect of intra-haul correlation and variable density on estimates of population characteristics from marine surveys. Biometrics 50:725–732.

Pennington, M., L.-M. Burmeister, and V. Hjellvik.
2002. Assessing the precision of frequency distributions estimated from trawl-survey samples. Fish. Bull. 100:74–80.

Prager, M.H., and K. W. Shertzer.
2010. Deriving acceptable biological catch from the overfishing limit: implications for assessment models. North Am. J. Fish. Manage. 30:289–294.

Quinn, T. J., II, and R. B. Deriso.
1999. Quantitative fish dynamics, 542 p. Oxford Univ. Press, New York.

Raring, N. W., P. G. von Szalay, F. R. Shaw, M. E. Wilkins, and M. H. Matrin.
2011. Data report: 2001 Gulf of Alaska bottom trawl survey. NOAA Tech. Memo. NMFS-AFSC-225, 179 p.

Richards, L. J., J. T. Schnute, A. R. Kronlund, and R. J. Beamish.
1992. Statistical models for the analysis of aging error. Can. J. Fish. Aquat. Sci. 49:1801–1815.
Ricker, W. E.
1975. Computation and interpretation of biological statistics of fish populations. Bull. Fish. Res. Board Can. 191, 382 p.
Schweigert, J. F., and J. R. Sibert.
1983. Optimizing survey design for determining age structure of fish stocks: an example from British Columbia Pacific herring (*Clupea harengus pallasi*). Can. J. Fish. Aquat. Sci. 40:588–597.
von Bertalanffy, L.
1938. A quantitative theory of organic growth (inquiries on growth laws. II). Human Biol. 10:181–213.
von Szalay, P. G., C. N. Rooper, N. W. Raring, and M. H. Martin.
2011. Data report: 2010 Aleutian Islands bottom trawl survey. NOAA Tech. Memo. NMFS-AFSC-215, 153 p.

National Marine Fisheries Service
NOAA

Fishery Bulletin
established in 1881

Spencer F. Baird
First U.S. Commissioner of Fisheries and founder of *Fishery Bulletin*

Quantifying the behavior of fish in response to a moving camera vehicle by using benthic stereo cameras and target tracking

David A. Somerton (contact author)[1]
Kresimir Williams[1]
Matthew D. Campbell[2]

Email address for contact author: dsomerton4@gmail.com

[1] Resource Assessment and Conservation Engineering Division
Alaska Fisheries Science Center
National Marine Fisheries Service, NOAA
7600 Sand Point Way NE
Seattle, Washington 98115

[2] Mississippi Laboratories
Southeast Fisheries Science Center
National Marine Fisheries Service, NOAA
3209 Frederic Street
Pascagoula, Mississippi 39567

Abstract—Underwater cameras increasingly are being used on remotely operated, autonomous, or towed vehicles to provide fishery-independent survey data in areas unsuitable for bottom trawls. To observe and quantify avoidance and attraction behaviors of fish to these vehicles, we developed an observational test bed consisting of 3 benthic stereo cameras, set in a straight line, on a coral reef in the Gulf of Mexico. During one pass of a towed camera vehicle, one of the benthic cameras viewed a school of vermilion snapper (*Rhomboplites aurorubens*) that exhibited a variety of avoidance behaviors. Stereo analysis was used to position some these fish, and target tracking was used to estimate their swimming performance and schooling characteristics for each second from the time the research vessel had passed the benthic cameras to the time of arrival of the towed underwater vehicle. The fish showed little reaction to the tow vessel but responded to the tow cable by swimming laterally and downward, then rapidly increased their swimming speed and avoidance behavior when the towed vehicle came into view. The use of observational test beds, stereo photography, and target tracking allows quantification of the avoidance response and provides a means to determine which stimuli produced by the sampling process elicit fish avoidance behaviors.

Manuscript submitted 20 July 2016.
Manuscript accepted 24 April 2017.
Fish. Bull. 115:343–354 (2017)
Online publication date: 16 May (2017).
doi: 10.7755/FB.115.3.5

The views and opinions expressed or implied in this article are those of the author (or authors) and do not necessarily reflect the position of the National Marine Fisheries Service, NOAA.

For most commercial and recreational marine fish species in the United States, bottom trawl surveys provide fishery-independent indices of abundance needed for stock assessment modeling. However, bottom trawl surveys cannot be used in areas that are too steep or rocky, have fragile epibenthos, such as coral, or are legally closed to trawling. As an alternative to bottom trawling in such areas, optical assessment increasingly is being used, especially with the use of camera systems on stationary platforms (Campbell et al., 2015) or mobile platforms, such as remotely operated vehicles (Adams et al., 1995), autonomous underwater vehicles (Clarke et al., 2009), towed vehicles (Lembke et al., 2013), and manned submersibles (Yoklavich et al., 2007).

One concern that has been raised about fish density or abundance estimates produced by such camera systems is that they could be biased as a result of attraction, avoidance, and incomplete detection of fish (Trenkel et al., 2004; Stoner et al., 2008; Ryer et al., 2009; McIntyre et al., 2015). Studies have addressed such sampling bias by quantifying fish behavior as seen from the camera vehicles themselves. (Lorance and Trenkel, 2006; Yoklavich et al., 2007) or by estimating the relative sampling efficiency of different camera vehicles (Laidig et al., 2013). However, there have been few attempts to obtain independent estimates of sampling efficiency of camera vehicles or to conduct in situ observational studies of fish behavior in response to camera vehicles by using an independent observational method that is unlikely to elicit behavioral responses.

Similar concerns about sampling efficiency have been raised concerning survey bottom trawls. However, bottom trawls have been in use much longer than camera vehicles, and a variety of techniques have been developed to estimate components of trawl sampling bias, such as herding (Engås and Godø, 1989a) and escapement under the footrope (Engås and Godø, 1989b). In some cases, these

techniques have been applied to estimate the size selectivity of a survey trawl (Somerton et al., 2007) and even of the absolute catchability of a trawl survey (Somerton et al., 2013). Estimating the sampling efficiency of a survey method or the catchability of a survey can be important for stock assessments because estimates of these quantities can be incorporated into stock assessment models (Maunder and Punt, 2013) as Bayesian priors to improve model reliability. Inclusion of such priors in stock assessment models is especially important for developing surveys, like those envisioned for camera vehicles, because the survey time series will initially be too short to adequately inform the model (Somerton et al., 1999).

To help develop methods for estimating the sampling efficacy of camera vehicles and to understand better the stimuli produced by these vehicles that may influence sampling efficiency, the U.S. National Marine Fisheries Service initiated the Untrawlable Habitat Strategic Initiative, which conducts experiments to observe and quantify the reactions of fish to remotely operated vehicles, autonomous underwater vehicles, and towed camera vehicles. For the first experiment, which is considered here, an observational test bed was developed that consisted of unlit, bottom-mounted stereo cameras set in shallow, clear water to unobtrusively observe the responses of fish to various types of camera vehicles. The study site was a sponge and soft coral reef that is situated in the northeastern Gulf of Mexico and is inhabited by a variety of tropical fishes, including several species of snappers and groupers important to commercial and recreational fisheries (Coleman et al.[1]).

Several independent strategies were used to quantify the responses of fish. One of these was to measure changes in the relative density of fish in the area viewed by single cameras (Campbell[2]) and by DIDSON[3] imaging sonars (Sound Metrics, Bellevue, WA) (Wakefield[4]) as the benthic cameras were approached by camera vehicles. Another strategy, described here, was to quantitatively assess fish behavior in response to the camera vehicles by using stereo images to repeatedly measure the 3-dimensional positions of individual fish over time (i.e., target tracking). This type of information, in turn, allowed measurement of changes in swimming speed and direction of individual fish as well as attributes of school structure indicative of their behavioral state.

Target tracking methods have been used previously to quantify changes in fish behavior in several settings. For laboratory studies, stereo photography has been used, with both target tracking and other analytical techniques, to quantify the movement of individual fish and the coordinated movement of fish schools (Tien et al., 2004; Viscido et al., 2004). For in situ studies, several acoustic methods have been used for target tracking. These methods include the use of buoy-mounted, split-beam sonars to track the avoidance of fishing vessels or bottom trawls by individual cod (Handegard and Tjøstheim, 2005) and the use of DIDSON imaging sonars to track the escapement of individual walleye pollock (*Gadus chalcogrammus*) from a pelagic trawl (Williams et al., 2013). Optical methods are rarely used for aquatic in situ experiments because 1) water clarity typically limits the feasible range that cameras can image objects and 2) artificial lighting, which can itself alter fish behavior, is needed in other than very shallow water.

Our initial intention was to use optical target tracking on several species of snappers and groupers that are relatively solitary, benthic-oriented, and commonly seen in the study area. However, at one location, a school of vermilion snapper (*Rhomboplites aurorubens*) was viewed repeatedly by the benthic stereo cameras, and, during one pass of the towed camera vehicle (Lembke et al., 2013), the school was viewed during the entire period between the transits of the tow vessel and the camera vehicle. Here we focus on this single observation of a schooling species rather than on our more numerous observations on solitary species because our intent is to demonstrate that in situ optical target tracking with stereo cameras can be used to quantify changes in individual and group behaviors that are often associated with predator avoidance (Parrish et al., 2002; Viscido et al., 2004) are also displayed in response to a camera vehicle. To aid the development of stealthier camera vehicles, we consider the linkages between these behavioral changes and the stimuli produced by the camera vehicle and its tow vessel that could have triggered the changes. In addition, we provide an example of how target tracking can be used to estimate sampling efficiency of camera vehicles.

Materials and methods

Description of the study

The experiment was conducted from 17 through 19 July 2014 on the Florida Middle Grounds, which is a reef of calcareous sponges and soft corals situated in the northeast Gulf of Mexico (Coleman et al.[1]; Wakefield[4]). This reef has a relatively flat top, at a depth range of 23–32 m, and steep slopes. The highest fish abundance and diversity concentrated near the junction of the reef top and slope. The target species, vermilion snapper, is

[1] Coleman, F., G. Dennis, W. Jaap, G. P. Schmahl, C. Koenig, S. Reed, and C. Beaver. 2004. Part I: Status and trends in habitat characterization of the Florida Middle Grounds. Final report to the National Oceanic and Atmospheric Administration Coral Reef Conservation Grant Program, 135 p. [Available from website.

[2] Campbell, M. D, 2016. Unpubl. data. Mississippi Laboratories, Southeast Fish. Sci. Cent., Natl. Mar. Fish. Serv., 3209 Frederic St. Pascagoula, MS 39567.

[3] Mention of trade names or commercial companies is for identification purposes only and does not imply endorsement by the National Marine Fisheries Service, NOAA.

[4] Wakefield, W. W., II. 2015. Unpubl. data. Newport Facility, Northwest Fish. Sci. Cent., Natl. Mar. Fish. Serv., 2032 SE OSU Dr., Newport, OR 97365-5275.

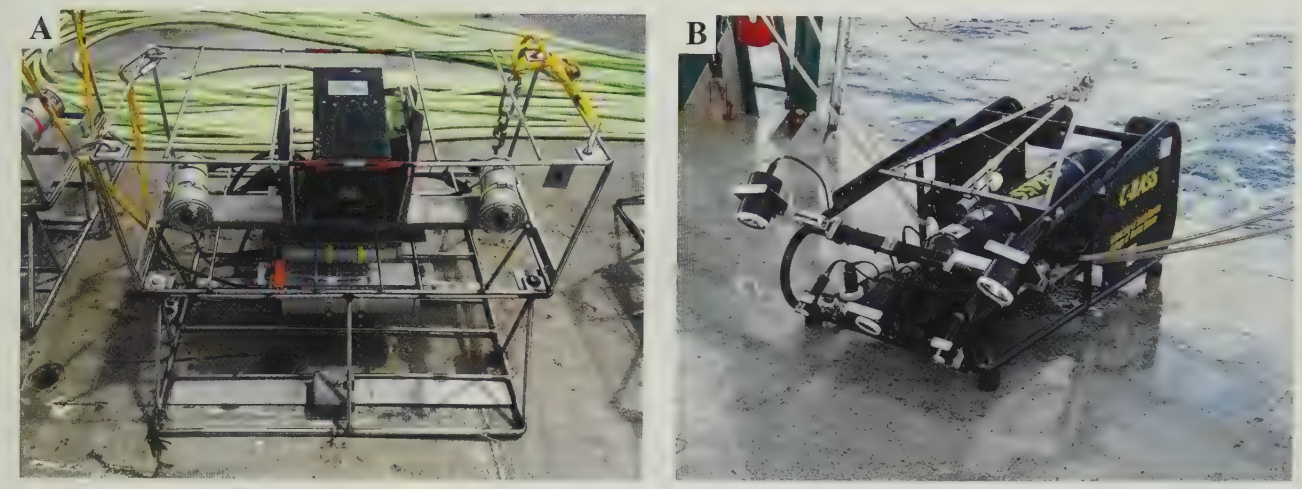

Figure 1

Photographs of (**A**) an observation cage, containing the Modular Optical Underwater Survey System, a DIDSON imaging sonar (black rectangular box), and the bridles used to attach the cage to the longline (yellow lines at the top), and (**B**) the camera-based assessment survey system (C-BASS) towed camera vehicle shown before being launched from the stern of the RV *Pelican*. The cage and camera vehicle were used in an experiment conducted in July 2014 in the northeast Gulf of Mexico.

an important commercial and recreational species and is a dominant component of the reef fish assemblage in the southeastern United States. During the night, vermilion snapper forage on planktonic and benthic prey on both reefs and their adjacent sand flats. However, during the day, they are reported to form resting schools on the tops of reefs (Grimes, 1979; Sedberry and Cuellar, 1993). Viewed from our cameras, the behavior of the school of vermilion snapper in the study area was consistent with this notion.

To quantify changes in fish behavior, an observational test bed was set up at select locations on a daily basis. The test bed consisted of 3 observation cages (Fig. 1) measuring 94 cm wide, 94 cm long, and 67 cm high. The cages were attached at 61 m intervals along a groundline with anchors and buoy lines at each end of the groundline separated by 61 m from the nearest cage (Wakefield[4]). The groundline was set off the stern of the tow vessel (RV *Pelican*) under tension, from anchor to anchor, so that the line was straight and all camera cages had the same general geographic orientation. Each of the cages had an unlit, monochrome stereo camera system, known as the Modular Optical Underwater Survey System, equipped with 2 Prosilica GT 1920 cameras with 2.82-MP resolution (Allied Vision Technologies, Stadtroda, Germany) that were rigidly attached to an aluminum frame with a baseline separation of approximately 75 cm. Once filming was initiated, synchronized stereo photos were taken at 5 Hz continuously for up to 8 h. In addition, each cage contained a dual-frequency acoustic imaging system (DIDSON; Belcher, 2002), and the 2 end cages also contained a long baseline acoustic beacon to obtain information on cage position and to aid navigation of the vehicles to within visual range of the camera cages.

The towed camera vehicle used in the experiment collected both video and still optical imagery with forward- and side-mounted cameras that were angled downward approximately 45° from level and illuminated with 4 continuous 85-W LED lights. The camera vehicle frame measured 1.2 m wide by 0.7 m tall by 1.7 m long and was designed to be towed at approximately 1.8 m/s with a target off-bottom distance of 2.5 m (Fig. 1; Lembke et al., 2013). The towing cable was standard 10.8-mm hydrographic wire that passed over an A-frame along the centerline of the vessel. At the depths in the experimental area and at a towing speed of 1.5–2.0 m/s, the camera vehicle trailed behind the vessel by ~40–50 m.

At each sampling site, the observation cages were deployed, then the positions of the end cages were estimated by using a long-baseline system after circling the entire array with the vessel. Approximately 1–2 h after cage deployment, depending on the time required to obtain quality positions, the camera vehicle was launched and towed near the cages with a target horizontal distance of 3–5 m at closest approach to each camera. Towing always occurred in the same direction when the camera vehicle passed by the cages, and replicate passes were separated in time by ~20–25 min.

Stereo camera calibration

Accuracy of estimates of fish position depend on the quality and precision of the calibration of the stereo camera. Calibration of the Modular Optical Underwa-

ter Survey System cameras proceeded according to the methods described in Williams et al. (2010, 2013) with the Camera Calibration Toolbox for Matlab (Bouguet, 2014). Calibration images of a submerged (freshwater) checkerboard test pattern (9 by 7 matrix of 108-mm squares) were captured by each camera of the Modular Optical Underwater Survey System at a distance of about 3 m. The checkerboard was tilted and rotated along all 3 axes into 25 poses, which were held stationary for ~5 s. Paired stereo images were later viewed and 1 paired image from ~25 paired images in each pose was selected for analysis on the basis of image clarity and the required presence of all 4 corners of the checkerboard in both images. By using the camera calibration software, each of the paired images was sequentially displayed, and the 4 external corners of each checkerboard image were manually identified. This information was then used to estimate the optical distortion of each camera and the translation and relative rotation of the camera pair to define a measurement coordinate system.

Once calibrated, the 3-dimensional position within this coordinate system can be determined for any object in the joint (i.e. overlapping) field of view of the stereo cameras. The axes of this coordinate system are the y-axis, increasing monotonically with distance from the lens of the left camera (optical axis), and the x-axis and z-axis, which are measured perpendicular to the y-axis in the horizontal (positive to the left, as seen by the camera) and the vertical planes (positive upwards).

Measuring fish positions

Fish positions were measured from images recorded during 2 time periods. The first time period (disturbed case) consisted of a 22-s period between the time when the tow vessel was at its shortest distance to the benthic camera (i.e., passage time) and the time when the camera vehicle just entered the field of view of the benthic camera and the last tracked vermilion snapper completely exited the field of view. The second time period (undisturbed case) consisted of a 10-s period taken 20 min after the previous vessel passage time (an interval which was assumed to be sufficiently long to allow disturbed fish to return to their undisturbed state) and 5 min before the passage time of the disturbed case. During the 2 cases, the same school was viewed with the same camera under nearly identical viewing conditions; consequently the cases were essentially one sequence with a 5-min break to reduce video processing time.

For each of these 2 periods, paired stereo images were processed as follows. During each second, 5 stereo paired frames were collected, but only frames 2–4 were used to estimate fish position (although fish position in each second can be estimated with only a single frame, estimation of swimming velocity required 3 successive frames). Starting with the first of these frames, 25 fish were selected at progressively increasing distances from the camera. Each fish was then followed and positioned (i.e., x, y, z coordinates) sequentially through the 3 frames by using the Stereo Tracker stereo measurement software (Fig. 2; Williams et al.[5]) and techniques described in Williams et al. (2010, 2013). In all cases, the fish snout was used as the reference feature for measurement because it was the easiest feature to consistently locate. Therefore, for each second, in both the disturbed and the undisturbed cases, the data available for target tracking were the x, y, and z coordinate positions of 25 fish individually followed through 3 successive frames. To reduce the influence of possible random measurement errors, these data were smoothed by fitting a straight line to the 3 positions of each fish on each coordinate axis as a function of time (function lm in R statistical software, vers. 3.3.1; [R Core Team, 2016]), then by using the fitted model to predict the positions at the 3 times. The position of each fish during each second was subsequently based on its smoothed position during the second frame.

Distance off the bottom

Because the benthic cameras imaged the bottom, as well as the fish, from a fixed position, it was possible to construct a topographical map of the bottom expressed in the same coordinate system as that used to view the fish and then to use this map to determine the distance of each fish from the bottom. First, the coordinates of 30 locations on the bottom were measured with the software, and then a topographic map of the bottom was estimated by fitting the z coordinates of these positions as a smooth function of the x and y coordinates by using generalized additive modeling (function gam in the mgcv package for R). The fitted function was then used to predict the z coordinate of the bottom at the x and y coordinates of every fish position, and that z coordinate, when negated and added to the z coordinate of the fish itself, produced the distance off bottom (d) in each frame for every fish. The group distance off bottom (D) during each second was then calculated as the mean of the d values for all the fish in the group.

Tracking the camera vehicle to determine its sampling path

The stereo cameras were used to position the forward, right-hand corner of the camera vehicle frame at 3 times during its passage through the field of view of the benthic camera to calculate its trajectory on the horizontal plane. The trajectory, which was assumed to follow a straight line, was estimated by fitting straight lines to the x and y coordinates individually as a function of time. Because the trajectory was nearly parallel to the x-axis, the trajectory of the camera vehicle center line was estimated by adding the half width of

[5] Williams, K., R. Towler, P. Goddard, R. Wilborn, and C. Rooper. 2016. *Sebastes* stereo image analysis software. AFSC Processed Rep. 2016-03, 42 p. Alaska Fish. Sci. Cent., Natl. Mar. Fish. Serv., 7600 Sand Point Way NE, Seattle, WA 98115. Report

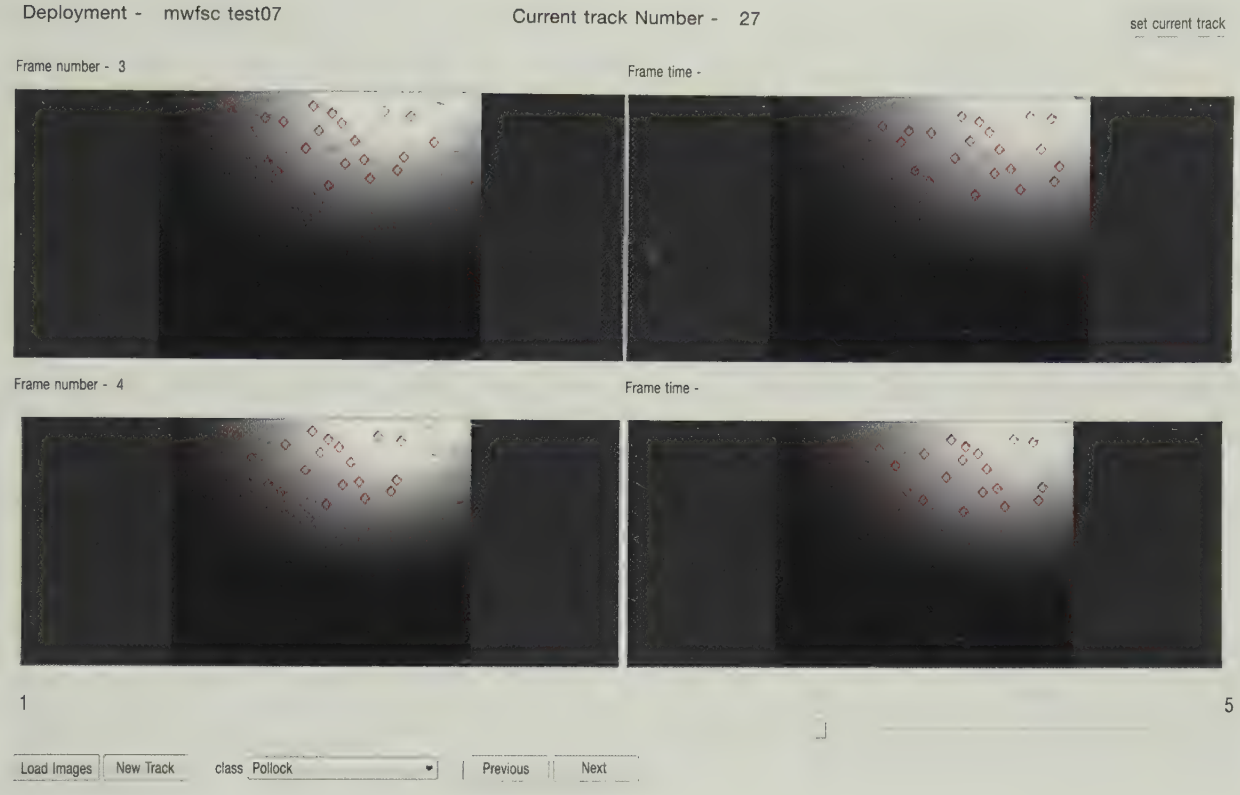

Figure 2

Screen shot of a session in Stereo Tracker (Williams et al.[5]), the software used for tracking a school of vermilion snapper (*Rhomboplites aurorubens*) in 2014 in the northeast Gulf of Mexico. The upper 2 frames show the paired images from the previous time interval; the lower frames show the paired images for the current time interval. All previously measured fish are indicated with red diamonds, and the fish being tracked is indicated with a green circle to ease identification of the same fish across time intervals.

the vehicle frame (0.6 m) to the y coordinates. The distal and proximal edges of the vehicle sampling path, spanning the width of the area for counting fish, were then calculated as the center line path (± the approximate half width of the estimated field of view of the vehicle [~3.7 m]). The sampling path was used, in conjunction with the measured fish positions on the horizontal plane, to determine whether vermilion snapper occupied the sampling path prior to the arrival of the camera vehicle and, if so, when they left the path.

Individual velocity, mean speed, and direction of swimming Individual swimming velocity (V_j) in each coordinate direction ($V_{x,j}$, $V_{y,j}$, $V_{z,j}$) was calculated for each fish (indexed by j) during each second as the difference in the smoothed beginning and ending positions divided by the elapsed time (0.4 s). Mean individual speed and direction were calculated from the velocity vectors both in 3 dimensions, as well as from projections on the x–y plane and the z-axis separately to better visualize the lateral and vertical movements associated with avoidance behavior. Mean swimming speed (S) during each second was calculated first by determining the individual speeds from the estimated velocity vectors and then by determining the means of these values; that is,

$$S = \overline{sqrt(V_{x,j}^2 + V_{y,j}^2 + V_{z,j}^2}, \quad (1)$$

where V_z was omitted in this equation for horizontal speed, and V_x and V_y were omitted for vertical speed. Mean swimming heading, on the x–y plane, was calculated as the mean of the individual swimming headings, expressed in degrees counter clockwise from the direction of vehicle travel, after correcting for the slight misalignment between the direction of travel and the x-axis of the camera coordinate system.

Group velocity, speed, and swimming polarity Group velocity (U) on each coordinate axis (U_x, U_y, U_z) was calculated each second from the difference in the mean positions of the 25 fish between the second and fourth frames, divided by the elapsed time. Group speed (S_g)

was then calculated from the 3 coordinate velocity vectors as

$$S_g = sqrt(U_x^2 + U_y^2 + U_z^2). \quad (2)$$

Swimming polarity, which is a measure of the alignment in swimming direction of individuals relative to that of the group, was calculated as the mean of the angular deviations (θ_i) between the individual velocities (V_j) and the group velocity (U) (Viscido et al., 2005):

$$\theta_j = \cos^{-1}\left[\frac{V_j \cdot U}{|V|_j |U|}\right], \quad (3)$$

where "·" is the vector dot product; and "| |" is the absolute value.

The individual swimming polarities were then converted to a nondimensional mean value to simplify interpretation (Viscido et al., 2004) as:

$$\Phi = \frac{\overline{(90° - \theta_j)}}{90°}. \quad (4)$$

In this notation, fish swimming directions become increasingly parallel as Φ approaches 1.0.

Nearest neighbor distance Nearest neighbor distance of each individual fish to other group members is defined in the following manner (Viscido et al., 2005):

$$NND_j = \min^{f0}(d_{j,1}, d_{j,2} \ldots d_{j,p}), \quad (5)$$

where $d_{j,k}$ = the distance between the j^{th} fish and each of the p remaining fish.

Nearest neighbor distance of the group is the mean over the p+1 members of the group.

The above metrics of group behavior were calculated identically for both the disturbed and undisturbed periods, but the use of those descriptors differed between these periods. For the disturbed period, we were interested in the temporal change of the metrics in response to the tow vessel and camera vehicle. In contrast, for the undisturbed case, we used the metrics to set a reference level to use as a baseline for comparison with the disturbed case. We assumed that the values of each metric were relatively constant over the 10-s interval and that they characterized the undisturbed state of each metric as its mean and standard deviation.

Results

The response of the vermilion snapper to the vessel, tow cable, and camera vehicle can be considered from the perspective of individual behavior, but, because this is a schooling species, response can also be considered from the perspective of the group behavior of the school. First, we considered the movement attributes of individual fish. These attributes are best seen as a time series of mean swimming vectors, which, in Figure 3, are represented by the mean speed and direction and were projected separately on the horizontal plane (x- and y-axes) and vertical direction (z-axis). At the moment that the tow vessel passed the camera (t=0), the mean horizontal swimming direction was aligned with and almost directly away (180°) from the tow direction; however, the swimming direction abruptly changed to 270° at 11 s, so that the fish were swimming perpendicular to the tow path, and again at 20 s to approximately 315°, so that they were swimming obliquely away from the towed camera. Horizontal swimming speed, indicated by the lengths of the movement vectors in Figure 3, increased at 11 s and again at 20 s in accordance with the directional changes. Therefore, as expressed on the horizontal plane, there were 2 changes in swimming speed and direction that essentially partitioned the time series into 3 distinct periods.

Vertical swimming speed and direction changed in a similar pattern. The vertical swimming direction is initially slightly upward until 10 s, when it shifts abruptly downward for 1 s before a horizontal shift in direction (Fig. 3). The downward shift in vertical swimming direction was also accompanied by an increase in swimming speed.

These changes in vertical swimming speed led to changes in the mean distance of the fish from the bottom (Fig. 4). The initial upward speed of the fish resulted in a gradual increase in distance off bottom. However, synchronously with the changes in horizontal and vertical swimming direction, the distance off bottom rapidly decreased from a maximum of ~4 m at 8 s after vessel passage to ~1 m at 22 s. Perhaps the reduction in vertical swimming speed seen in the last 2 s of the series (Fig. 3) is the result of the school reaching this close proximity to the bottom.

Next, we considered the descriptors of group behavior: group speed; individual speed; and swimming polarity. These descriptors also displayed a temporal pattern with 3 distinct periods. Group speed (i.e., movement of the school itself), over the entire period after vessel passage, was elevated considerably above its value during the undisturbed case, and 2 distinct increases were observed, one starting at ~11 s and another starting at ~18 s (Fig. 5A). These changes in group speed are related to changes in individual speed and swimming polarity, but the relative influence of each factor changes over time. Mean individual swimming speed (now expressed in 3 dimensions) was barely elevated above its value in the undisturbed case and increased only gradually during the first 17 s after vessel passage, but the rate of increase distinctly accelerated starting at ~18 s (Fig. 5B). In contrast, swimming polarity (i.e., the alignment of individuals) was elevated greatly above its value in the undisturbed case over the entire record and a distinct rate of increase was observed at ~11 s (Fig. 5C). Therefore, changes in group speed (i.e., movement of the school) were primarily determined by changes in swimming polarity until the last few seconds when individual swimming speed greatly increased.

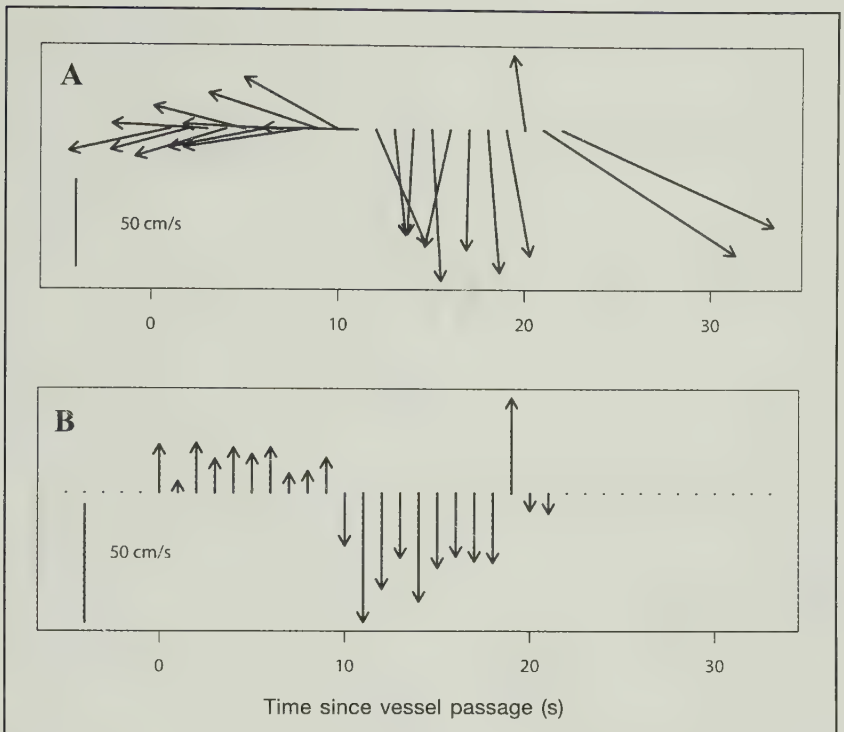

Figure 3

Mean individual swimming speed and direction of vermilion snapper (*Rhomboplites aurorubens*) in the northeast Gulf of Mexico in 2014, expressed as either (**A**) degrees counter clockwise relative to the camera vehicle tow path (toward the right) on the horizontal plane and as (**B**) degrees up and down in the vertical plane. Time is in seconds since the passage of the tow vessel was recorded by the benthic camera. On the horizontal plane, the direction of travel is from left to right; therefore, a left arrow is directed away from the tow vessel and toward the approaching camera vehicle. On the vertical plane, the horizontal line represents zero speed. The closest approach of the vehicle was at 23 s after the passage of the vessel, and the velocity of the camera vehicle was 1.5 m/s. Hence, the approximate distance in meters from the vehicle to the fish school can be calculated as $(23-t)\times 1.5$, where t is the time in seconds after vessel passage.

The nearest neighbor distance followed an almost inverse pattern, with a distinct, strong, decrease starting at about 11 s (Fig. 5D). Therefore, over the entire encounter with the camera vehicle and its tow vessel, the school increased its swimming speed initially by the individual fish aligning with each other and finally by increasing the individual swimming rate. In addition, as the alignment of individuals was increasing, their spacing became progressively tighter.

One important effect of these changes in behavior was a decrease in the abundance of vermilion snapper within the area that was subsequently transited by the camera vehicle during its survey (i.e., count path; Fig. 6). At the time of vessel passage (t=0) all 25 measured fish were within the count path of the camera vehicle, but later, in response to the various stimuli produced, the fish moved closer to the fixed camera and ultimately out of the count path. When the camera vehicle actually occupied the count path, at t=23 s, no vermilion snapper remained in the count path and none were seen in the forward cameras used for counting (although some fish were seen by the laterally pointed cameras not used for counting). Therefore, in this particular case, the vermilion snapper avoided sampling by the camera vehicle.

Discussion

The school of vermilion snapper observed in this study experienced a variety of visual and auditory stimuli between their undisturbed state (5 min before passage of the tow vessel) and the arrival of the camera vehicle. These stimuli triggered responses both at an individual level (i.e., swimming speed and direction), as well as at a group level (i.e., alignment of and spacing

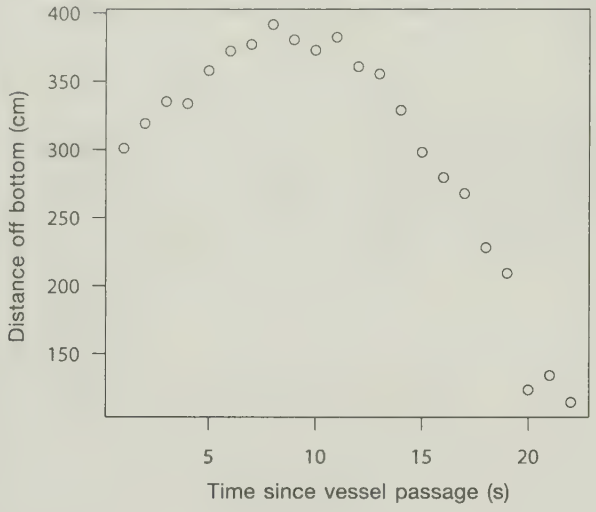

Figure 4

Mean distance of the vermilion snapper (*Rhomboplites aurorubens*) off bottom, measured in the northeast Gulf of Mexico in 2014, as a function of the time since passage of the tow vessel was recorded by the benthic camera. The closest approach of the vehicle was at 23 s, and the vehicle velocity was 1.5 m/s; therefore, the approximate distance in meters of the vehicle to the fish school can be calculated as $(23–t)\times1.5$, where t is the time in seconds after vessel passage.

between individuals within the school). The responses, especially swimming direction, changed abruptly twice, separating the period into 3 phases that can be considered sequentially increasing states: arousal, awareness, and flight.

During the first phase (arousal), up to 11 s after vessel passage, the fish were in a heightened state of arousal, presumably in response to the sound or sight of the passing tow vessel, because their group swimming speed and polarity were distinctly greater than the levels observed during the undisturbed period. Although this behavior was clearly a response, it had not progressed to active avoidance of the vessel because the individual swimming direction was still aligned with the path of the vessel and had a slight upward component of movement. Previously documented fish reactions to an overhead or recently passed vessel usually involved lateral motion or diving (Handegard and Tjøstheim, 2005; De Robertis and Handegard, 2013).

In the second phase (awareness), from about 12 s to 19 s after vessel passage, the fish displayed increasing signs of arousal, including an increase in group speed and polarity and a steady decline in nearest neighbor distance, all of which both theoretical and laboratory studies typically have shown are correlated and change with the arousal state of the school (Magurran and Pitcher, 1987; Parrish et al., 2002). During this phase, the fish started to display distinct avoidance behavior characterized by abrupt changes in horizontal direction from nearly parallel to nearly perpendicular to the path of the camera vehicle. In addition, vertical swimming switched from slightly upward to strongly downward. We interpret these behavioral changes as responses to the tow cable, which, by midway in the transit interval, would appear to the fish as a silhouetted object, approximately 10 m above the school (assuming no hysteresis in the tow cable), and approaching the fish at a downward velocity of ~0.9 m/s. Presumably, the tow cable also would produce vibrational stimuli along with the visual stimuli, but we were unable to distinguish the relative importance of the 2 stimuli in eliciting the observed response. Such downward and lateral avoidance behavior has been described previously for cod in response to the towing warps of bottom trawlers (Handegard and Tjøstheim, 2005).

During the third phase (flight), from 20 s to 22 s, individual fish direction on the horizontal plane abruptly changed from perpendicular to about 45° away from the line of vehicle travel and swimming speed began to increase at an accelerating rate. During this period, nearest neighbor distance rapidly declined and polarity increased. Group speed rapidly increased, primarily because the individual rate of swimming increased in addition to the polarity (group speed equals mean individual speed when polarity equals 1.0). We suspect that the these changes were reactions to the sight or sound of the camera vehicle, which was approximately 8 m from the center of the field of view of the benthic camera when the strong change in direction occurred 19 s after vessel passage. Although not silhouetted against the sky, the camera vehicle must have been conspicuous to the fish at this distance because it has 4 continuously illuminated lights and has a looming movement that has been shown to elicit reactions in some Pacific groundfishes (Ryer et al., 2009).

These behavioral changes in response to the passage of the vessel, tow cable, and camera vehicle are consistent with the notion of threat-sensitive predator avoidance (Helfman, 1989; Domenici, 2010; Rieucau et al., 2014) where, because of energetic costs (Ydenberg and Dill, 1986), fish balance timing and strength of escape behaviors against the risk of predation. This tradeoff often results in a graded response, starting with an increase in awareness of the threat and progressing to flight when the predatory attack is initiated. Therefore, for example, in the first phase, fish displayed indications of increased awareness but no obvious avoidance. In the second phase, fish initiated avoidance behavior; however, they did not greatly increase their individual swimming speed, presumably because the perceived threat was relatively small and approaching slowly. In the third phase, fish encountered the camera vehicle, changed their swimming direction so that it was directly away from the threat, and rapidly accelerated their individual swimming speed, presumably because the camera vehicle was large and moving rapidly and, therefore, presented a more serious threat.

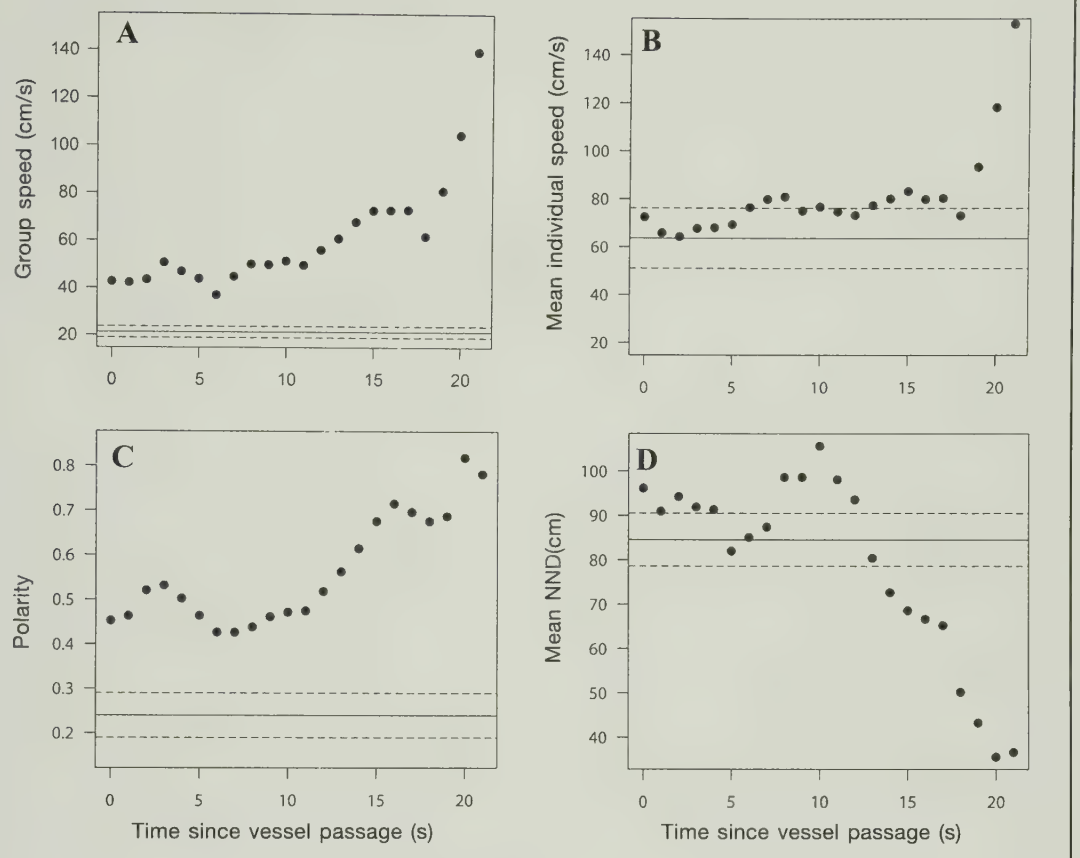

Figure 5

Variation in (**A**) group speed, (**B**) mean individual speed, (**C**) swimming polarity, and (**D**) nearest neighbor distance (NND) for a school of vermilion snapper (*Rhomboplites aurorubens*) in the northeast Gulf of Mexico in 2014 is shown for the disturbed time period, the 22-s period from passage of the tow vessel to 1 s before entry of the camera vehicle into the benthic camera field of view. The horizontal lines represent the mean (solid) and 95% confidence intervals (dashed) of each school descriptor during the undisturbed period, the 10-s period taken 20 min after the previous vessel passage. The closest approach of the vehicle was at 23 s, and the vehicle velocity was 1.5 m/s; therefore, the approximate distance in meters of the vehicle to the fish school can be calculated as $(23-t)\times 1.5$, where t is the time in seconds after vessel passage.

We emphasize that the fish response to a camera vehicle during a single pass should not necessarily be considered typical because there are a variety of factors that could have been influential. First, stimulus detection by individual fish or the school may vary with environmental conditions. For example, detection of visual stimuli will be diminished in turbid or low-light conditions. Second, the behavioral response to a given level of stimulus may vary with previous experience of such stimuli. A response to vessel noise, for example, may be less in areas with high vessel traffic because of acclimatization to stimuli. Third, the behavioral response to a given level of stimulus may vary with the perceived level of predatory threat. For example, an avoidance response may be inhibited in complex habitats that provide nearby refuge. Consequently, we expect behavioral responses to be varied and recognize that considerable additional field studies will be needed to provide realistic predictions of behavioral responses to stimuli produced by moving camera vehicles.

We deemed the 10-s interval that occurred 5 min before passage of the tow vessel to be indicative of the values of the school and individual fish descriptors during an undisturbed state. However, the school had previously experienced the disturbance created by the setting of the benthic cameras and 2 prior passes of the towed camera system; therefore, an *undisturbed* state should be considered in a relative sense. Our qualitative observations of the behavior of vermilion snapper toward the benthic cameras indicate that the school returned to fairly calm behavior within a few minutes

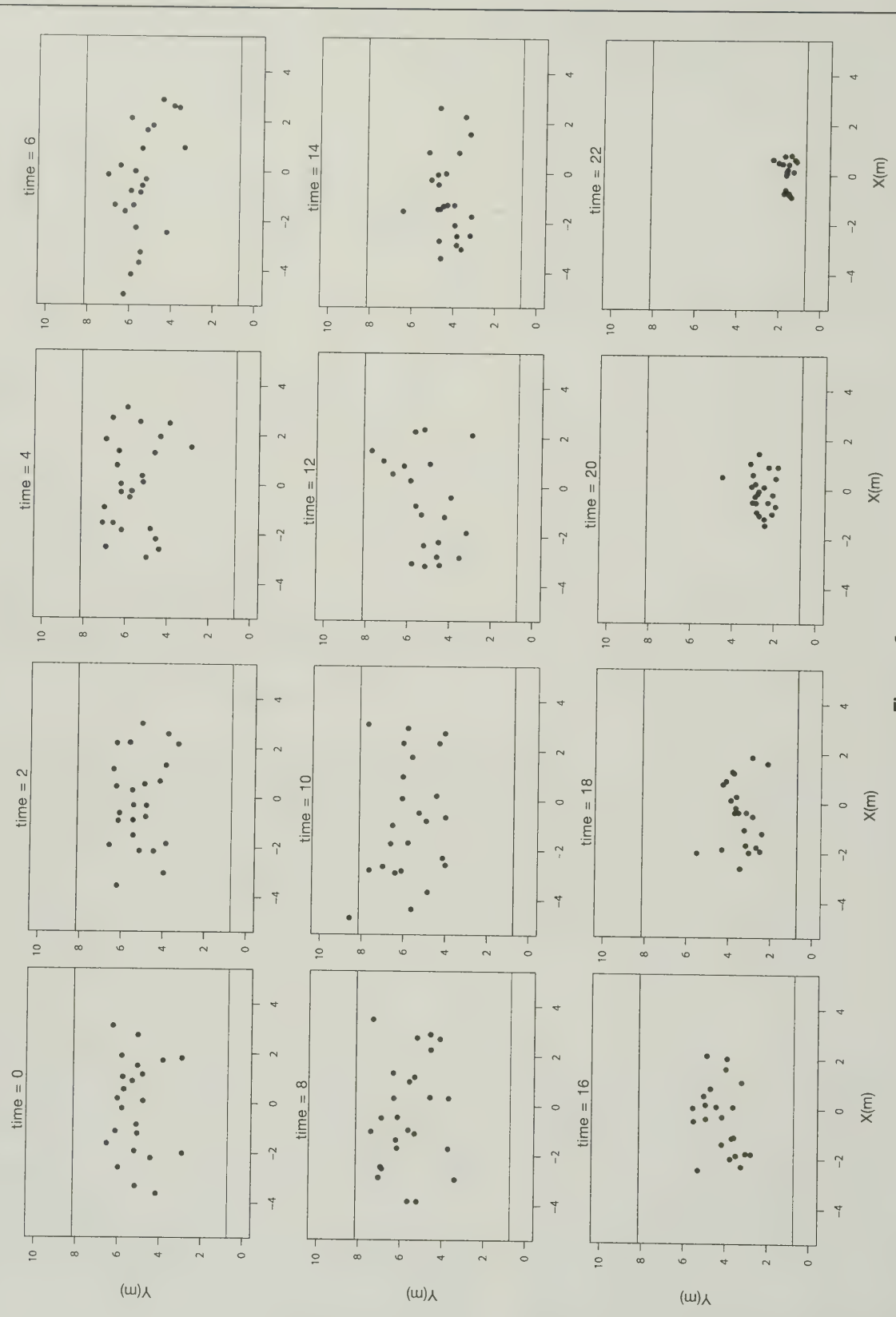

Figure 6

For alternate 1-s periods, from vessel passage to camera vehicle passage, plots of the positions (dots) of vermilion snapper (*Rhomboplites aurorubens*) in the northeast Gulf of Mexico in 2014, along with the count path (between the lines) of the camera vehicle when it passed the stationary camera at 23 s. After 11 s, the fish increasingly grouped together and moved toward the camera (X=0, Y=0). By 22 s, just before the camera vehicle entered the benthic camera field of view, the few fish remaining within the count path were positioned along its edge, and, in the next second, all had exited the count path.

after passage of the towed vehicle. Consequently, we felt that the passage of ~20 min after the last disturbance would approximate undisturbed conditions. Unfortunately, schools of vermilion snapper were not observed before the first passage of the camera vehicle to confirm this notion.

The design of our experiment (i.e., placing fixed cameras on the bottom to observe fish behavior in response to moving camera systems) provided a unique perspective on how these systems actually sample the fish community. During the one pass of the camera vehicle, for example, no vermilion snapper were counted by the moving camera vehicle, but the alternate view provided by a benthic camera (Fig. 6) showed that vermilion snapper were indeed within the tow path of the camera vehicle but had vacated it immediately before they would have been imaged by the forward directed cameras on the vehicle.

Besides confirming that fish avoidance had occurred during the pass of the camera vehicle, the use of the fixed cameras, especially the use of stereo and optical target tracking, allowed quantification of the timing and strength of the avoidance behaviors, which in turn, provided an indication of the possible stimuli that may have elicited these behaviors. For example, vessel noise has been implicated repeatedly as a stimulus sufficient to trigger fish avoidance behavior (De Robertis and Handegard, 2013), but, in this particular pass of the camera vehicle, vessel noise did not trigger any overt avoidance behavior. The sight or sound of the tow cable likely triggered the initial overt avoidance behaviors but was insufficient to drive the fish out of the path of the camera vehicle. However, the sight or sound of the camera vehicle seemed to increase the avoidance behavior sufficiently to cause the fish to vacate the count path before they could be seen and counted by the camera vehicle. These metrics of the timing and strength of the fish response could be used to help redesign the camera vehicle so that it could be stealthier and produce stimuli below the thresholds required to trigger avoidance behaviors.

The purpose for this article is to demonstrate the utility of fixed benthic cameras and stereo photography to measure the positions of a moving camera system, the target fish species, and the bottom topography, as well as how these measurements can be used to better understand how moving camera vehicles sample fish communities. The example we provide was based on one fortuitous pass of the camera vehicle in view of a single benthic camera while a school of vermilion snapper were present; consequently, our observations could be quite different had the sampling been at greater depths or in more turbid water (Abrahams and Kattenfeld, 1997) and certainly would have been different for other target species. However, when the use of stereo photography from fixed benthic cameras is appropriate, it can allow quantification of fish behaviors and help define the effect of this behavior on density estimates derived from images obtained with moving camera vehicles.

Acknowledgments

Financial support for this research was provided by the National Marine Fisheries Service, Office of Science and Technology, through the Untrawlable Habitat Strategic Initiative. We thank the captain and crew of the RV *Pelican* for their efforts during the field experiment. In addition, we thank S. Stienessen, S. Grasty, and S. Murawski for reviewing the manuscript and providing helpful suggestions.

Literature cited

Abrahams, M. V., and M. G. Kattenfeld.
1997. The role of turbidity as a constraint on predator–prey interactions in aquatic environments. Behav. Ecol. Sociobiol. 40:169–174.

Adams, P. B., J. L. Butler, C. H. Baxter, T. E. Laidig, K. A. Dahin, and W.W. Wakefield.
1995. Population estimates of Pacific coast groundfishes from video transects and swept-area trawls. Fish. Bull. 93:446–455.

Belcher, E.
2002. Dual-frequency identification sonar. DIDSON operation manual, 4.47.15, 44 p. Sound Metrics, Seattle, WA.

Bouguet, J.-Y.
2014. Camera Calibration Toolbox for Matlab. [Available from website, accessed November 2014.]

Campbell, M. D., A. G. Pollack, C. T. Gledhill, T. S. Switzer, and D. A. DeVries.
2015. Comparison of relative abundance indices calculated from two methods of generating video count data. Fish. Res. 170:125–133.

Clarke, M. E., N. Tolimieri, and H. Singh.
2009. Using the Seabed AUV to assess populations of groundfish in untrawlable areas. *In* The future of fisheries science in North America. Fish and Fisheries Series, vol. 31 (R. J. Beamish and B. J. Rothschild, eds.), p. 357–372. Springer Science + Business Media B.V., Dordrecht, Netherlands.

De Robertis, A., and N. O. Handegard.
2013. Fish avoidance of research vessels and the efficacy of noise-reduced vessels: a review. ICES J Mar. Sci. 70: 34–45.

Domenici, P.
2010. Context-dependent variability in the components of fish escape response: integrating locomotor performance and behavior. J. Exp. Zool. 313A:59–79.

Engås, A., and O. R. Godø.
1989a. The effect of different sweep lengths on the length composition of bottom-sampling trawl catches. J. Cons. 45:263–268.
1989b. Escape of fish under the fishing line of a Norwegian sampling trawl and its influence on survey results. J. Cons. Int. Explor. Mer. 45:269–276.

Grimes, C. B.
1979. Diet and feeding ecology of the vermilion snapper, *Rhomboplites aurorubens* (Cuvier), from North Carolina and South Carolina waters. Bull. Mar. Sci. 29:53–61.

Handegard, N. O., and D. Tjøstheim.
2005. When fish meet a trawling vessel: examining the behavior of gadoids using a free-floating buoy and acoustic split-beam tracking. Can. J. Fish. Aquat. Sci. 62:2409–2422.

Helfman, G. S.
1989. Threat-sensitive predator avoidance in damselfish-trumpetfish interactions. Behav. Ecol. Sociobiol. 24:47–58.

Laidig, T. E., L. M. Krigsman, and M. M. Yoklavich.
2013. Reactions of fishes to two underwater survey tools, a manned submersible and a remotely operated vehicle. Fish. Bull. 111:54–67.

Lembke, C., S. Murawski, X. Shi, S. Butcher, A. Silverman, and S. Grasty.
2013. Development and sea trials of a new camera-based assessment survey system for reef fish stocks assessment. *In* Proceedings of MTS/IEEE 2013 OCEANS; San Diego, CA, 23–27 September. [Available from Marine Technology Society, 1100 H St. NW, Suite LL-100, Washington, DC 20005.]

Lorance, P., and V. M. Trenkel.
2006. Variability in natural behaviour, and observed reactions to an ROV, by mid-slope fish species. J. Exp. Mar. Biol. Ecol. 332:106–119.

Magurran, A. E., and T. J. Pitcher.
1987. Provenance, shoal size and the sociobiology of predator-evasion behavior in minnow shoals. Proc. R. Soc. Lond., B 229:439–465.

Maunder, M. N., and A. E. Punt.
2013. A review of integrated analysis in fisheries stock assessment. Fish. Res. 142:61–74.

McIntyre, F. D., F. Neat, N. Collie, M. Stewart, and P. G. Fernandes.
2015. Visual surveys can reveal rather different 'pictures' of fish densities: comparison of trawl and video camera surveys in the Rockfall Bank, NE Atlantic Ocean. Deep-Sea Res., I 95:67–74.

Parrish, J. K., S. V. Viscido, and D. Grünbaum.
2002. Self-organized fish schools: an examination of emergent properties. Biol. Bull. 202:296–305.

Rieucau, G., K. M. Boswell, A. De Robertis, G. J. Macaulay, and N.O. Handegard.
2014. Experimental evidence of threat-sensitive collective avoidance responses in a large wild-caught herring school. PLoS ONE 9(1):e86726.

Ryer, C. H., A. W. Stoner, P. J. Iseri, and M. L. Spenser.
2009. Effects of simulated underwater vehicle lighting on fish behavior. Mar. Ecol. Prog. Ser. 391:97–106.

R Core Team.
2016. R: a language and environment for statistical computing. R Foundation for Statistical Computing, Vienna, Austria. [Available from website, accessed June 2016.]

Sedberry, G. R., and N. Cuellar.
1993. Planktonic and benthic feeding by the reef-associated vermilion snapper, *Rhomboplites aurorubens*. Fish. Bull. 91:699–709.

Somerton, D., J. Ianelli, S. Walsh, S. Smith, O. R. Godø, and D. Ramm.
1999. Incorporating experimentally derived estimates of survey trawl efficiency into the stock assessment process: a discussion. ICES J. Mar. Sci. 56:299–302.

Somerton, D. A., P. T. Munro, and K. L. Weinberg.
2007. Whole-gear efficiency of a benthic survey trawl for flatfish. Fish. Bull. 105:278–291.

Somerton, D. A., K. L. Weinberg, and S. E. Goodman.
2013. Catchability of snow crab (*Chionoecetes opilio*) by the eastern Bering Sea bottom trawl survey estimated using a catch comparison experiment. Can. J. Fish. Aquat. Sci. 70:1699–1708.

Stoner, A. W., C. H. Ryer, S. J. Parker, P. J. Auster, and W. W. Wakefield.
2008. Evaluating the role of fish behavior in surveys conducted with underwater vehicles. Can. J. Fish. Aquat. Sci. 65:1230–1243.

Tien, J. H., S. A. Levin, and D. I. Rubenstein.
2004. Dynamics of fish shoals: identifying key decision rules. Evol. Ecol. Res. 6:555–565.

Trenkel, V. M., P. Lorance, and S. Mahevés.
2004. Do visual transects provide true population density estimates for deepwater fish? ICES J. Mar. Sci. 61:1050–1056.

Viscido, S. V., J. K. Parrish, and D. Grünbaum.
2004. Individual behavior and emergent properties of fish schools: a comparison of observation and theory. Mar. Ecol. Prog. Ser. 273:239–249.
2005. The effect of population size and number of influential neighbors on the emergent properties of fish schools. Ecol. Model. 183:347–363.

Williams, K., C. N. Rooper, and R. Towler.
2010. Use of stereo camera systems for assessment of rockfish abundance in untrawlable areas and for recording pollock behavior during midwater trawls. Fish. Bull. 108:352–362.

Williams, K., C. D. Wilson, and J. K. Horne.
2013. Walleye pollock (*Theragra chalcogramma*) behavior in midwater trawls. Fish. Res.143:109–118.

Ydenberg, R. C., and L. M. Dill.
1986. The economics of fleeing from predators. Adv. Stud. Behav. 16:229–249.

Yoklavich, M. M., M. S. Love, and K. A. Forney.
2007. A fishery-independent assessment of an overfished rockfish stock, cowcod (*Sebastes levis*), using direct observations from an occupied submersible. Can. J. Fish. Aquat. Sci. 64:1795–1804.

National Marine Fisheries Service
NOAA

Fishery Bulletin
established in 1881

Spencer F. Baird
First U.S. Commissioner of Fisheries and founder of *Fishery Bulletin*

Incorporating uncertainty into a length-based estimator of natural mortality in fish populations

Freddy O. López Quintero[1]
Javier E. Contreras-Reyes (contact author)[2,3]
Rodrigo Wiff[4]

Email address for contact author: javier.contreras@ifop.cl

[1] Departamento de Matemática
Instituto Venezolano de Investigaciones Científicas
Carretera Panamericana, Km 11, Altos de Pipe
Estado Miranda 1020-A, Venezuela

[2] División de Investigación Pesquera
Instituto de Fomento Pesquero
Avenida Almirante Blanco Encalada 839
Valparaíso 2361827, Chile

[3] Instituto de Estadística
Universidad de Valparaíso
Avenida Gran Bretaña 1111
Valparaíso 2360102, Chile

[4] Center of Applied Ecology and Sustainability
Pontificia Universidad Católica de Chile
Avenida Libertador Bernardo O'Higgins 328
Santiago 8331150, Chile

Abstract—Natural mortality (M) is one of the most important life history attributes of functioning fish populations. The most common methods to estimate M in fish populations provide point estimates which are usually constant across sizes and ages. In this article, we propose a framework for incorporating uncertainty into the length-based estimator of mortality that is based on von Bertalanffy growth function (VBGF) parameters determined with Bayesian analysis and asymmetric error distributions. Two methods to incorporate uncertainty in M estimates are evaluated. First, we use Markov chains of the estimated VBGF parameters directly when computing M and second, we simulate the posterior distribution of VBGF parameters with the copula method. These 2 approaches were applied and compared by using the extensive database available on age and growth for southern blue whiting (*Micromesistius australis*) harvested in the southeast Pacific. The copula approach provides advantages over Markov chains and requires far less computational time, while conserving the underlying dependence structure in the posterior distribution of the VBGF parameters. The incorporation of uncertainty into length-based estimates of mortality provides a promising way for modeling fish population dynamics.

Manuscript submitted 30 August 2016.
Manuscript accepted 11 April 2017.
Fish. Bull. 115:355–364 (2017).
Online publication date: 18 May 2017.
doi: 10.7755/FB.115.3.6

The views and opinions expressed or implied in this article are those of the author (or authors) and do not necessarily reflect the position of the National Marine Fisheries Service, NOAA.

Natural mortality (M) rate is one of the most important parameters shaping the population dynamics of fish populations (Siegfried and Sansó[1]; Brodziak et al., 2011). It is defined as the death rate of fish due to causes other than fishing, such as predation, senescence, cannibalism, starvation, and other natural factors. Despite the key importance of M in fish and fisheries modeling, this parameter is extraordinarily difficult to estimate accurately. Methods for determining M in fish populations generally entail one of 2 approaches: 1) direct methods which estimate M from observations on survival, with methods derived from tagging or telemetry experiments, 2) indirect methods that estimate mortality from other, more easily obtained parameters, often from life history traits, such as age and growth, and maturity. Direct methods provide the most precise estimates of M, but those approaches are data intensive and usually cost prohibitive and therefore preclude their application to a large number of fish stocks. Indirect methods are therefore commonly applied because they are easy, fast, and cheap to implement for most harvested fish populations.

Indirect estimators are based on correlations of M in well-studied stocks with other life history attributes, such as individual growth, longevity and maturity. The underlying assumption in all indirect methods is that the relationship between M and other life history parameters is the same for thoroughly studied stocks and lesser-studied ones where this method is usually applied. For most indirect methods, an estimate of M is computed, which is invariant across age and size classes, although this parameter is dependent on age and size (Gislason et al., 2010). The relationship between M and age and size is usually defined as a negative exponential function in which early life stages include much greater mortality than later ones, especially after reaching sexual maturity. Nevertheless, M estimators, whether they

[1] Siegfried, K. I., and B. Sansó. 2009. A review for estimating natural mortality in fish populations. Southeast Data, Assessment, and Review SEDAR 19-RD29, 31 p. [Available from website.]

are size dependent or not, provide only point estimates of mortality. Uncertainty in M estimates from indirect methods have not been investigated in detail and have usually been based on ad-hoc approaches (Cubillos et al., 1999; Quiroz et al., 2010; Wiff et al., 2011). These methods incorporate uncertainty in M by taking growth parameters from the literature and their associated uncertainty (e.g. standard deviation, covariance, confidence interval), and then by drawing empirical distributions of these parameters to propagate uncertainty in M estimates, usually assuming Gaussian error.

A promising method for estimating M-at-length based on life history theory, has recently been proposed by Gislason et al. (2010) and Charnov et al. (2013), and depends entirely on von Bertalanffy growth function (VBGF) parameters. For these researchers, appropriate uncertainty in growth estimates become a key issue in assessing uncertainty in M estimates. Most ad-hoc approaches to incorporate statistical variability in M are based on a 2-step model that keeps estimations of growth parameters and M separated. Therefore, in this article, we consider the inclusion of 2 different sources of uncertainty in the modeling, one over the growth parameters and another from the proposed structural M-at-length mortality estimator.

Uncertainty in M estimates derived from indirect methods come from 2 main sources. First, uncertainty depends on the variability among species or stocks for which the empirical relationship has been proposed. This source of uncertainty is usually referred to as "method error" because it represents how "accurate" the empirical model is (Quiroz et al., 2012). The second source of uncertainty is related to the error within the species-specific parameters that feeds into the indirect method (e.g., growth parameters). This source of uncertainty is called "trait error" because it represents the uncertainty in life history parameters of the stock or population for which M is being estimated.

The trait-error of estimated growth parameters can be converted into M estimates as the iterative parameter updates of a Bayesian estimation with a non-Gaussian distribution. In particular, Gaussian error distribution for estimating growth parameters can resolve some even nonsensical shortcomings, for instance negative length values. Distributions based on age–length fishing selectivity are usually skewed as a result of a size-selective sampling process (Contreras-Reyes et al., 2014; Montenegro and Branco, 2016). In addition, in harvested fish populations, an accumulative effect of fishing on size-at-age exists. Growth rates vary among individuals (Sainsbury, 1980) and fishing selectivity removes faster growing individuals from each particular age class. Moreover, in some studies, in which VBGF parameters are estimated, the assumption of Gaussian error distribution sometimes lacks adequacy, especially with the presence of outliers, which could lead to questionable estimates (see Contreras-Reyes and Arellano-Valle, 2013; Contreras-Reyes et al., 2014, and references therein).

In our analysis we used 2 methods to incorporate uncertainties in the M-at-length estimates. Both depend on information that can be drawn from a Bayesian estimation derived from VBGF parameters. The first method takes advantage of the Markov chains and, after convergence, those chains are directly incorporated into the M calculation. In particular, we used the Bayesian results generated by López Quintero et al. (2017) as a baseline. For the second method, we propose taking the dependent structure, which is concentrated in the posterior distribution of parameters, and using this structure for simulating a distribution with the same dependent features based on the copula method (Nelsen, 2006). This last approach has the advantage that, even without the precision in the joint distribution of parameters, we can obtain samples that preserve the dependence between the observed variables by only approximating its marginal distributions, at a much lower computational cost. We apply the length-based M estimators, using a data set corresponding to 24,942 individuals of southern blue whiting (*Micromesistius australis*) collected from Chilean continental waters over the period 1997–2010 (J. Contreras-Reyes, unpubl. data). Their total lengths and ages were recorded and assigned by studying their otoliths. Further information about this data set can be found in Contreras-Reyes et al. (2014) and references therein.

Material and methods

Growth model and M-at-length

Let $L(x)$ be the theoretical expected value of the length related to an individual at age x. The (specialized) VBGF function is defined as

$$L(x) = L_\infty(1 - e^{-K(x-t_0)}). \quad (1)$$

This equation represents the simplest formulation of the VBGF (Essington et al., 2001), which is described by 3 parameters: L_∞ represents asymptotic length (in length units e.g. centimeters): K represents the growth rate coefficient usually expressed in inverse time units: and t_0 is the theoretical age (usually in years) at length zero. Parameters of the VBGF are estimated from observed length-at-age pairs such as (x, y), where y is the length at age x.

Equation 1 can also be modeled in terms of a multiplicative structure for random errors

$$y_i = L(x_i)\varepsilon_i, \quad (2)$$

where y_i = the length at age x_i of the ith sampled subject, $i = 1,...,n$; $L_\infty>0$, $K>0$, $t<\min\{x_1,...,x_n\}$; and ε_i are independent (not necessarily identical) non-negative random errors (Contreras-Reyes et al., 2014).

With this assumption, the VBGF in Equation 2 corresponds to the multiplicative nonlinear regression with logarithmic random errors. The additive structure of the original model in Equation 2 is easily recovered by applying logarithmic properties, such as $y'_i = L'(x_i) + \varepsilon'_i$,

with $y'_i = \log y_i$, $L'(x_i) = \log L(x_i)$, and $\varepsilon_i' = \log \varepsilon_i$ which are independent random errors. The estimated parameters can be used to compute a M-at-length estimator.

Gislason et al. (2010) proposed an indirect method for estimating M-at-length, using previous estimations of M, habitat temperature and the VBGF parameters. Their proposed M-at-length estimator is only a function of the VBGF parameters and habitat temperature. Charnov et al. (2013) re-analyzed the data set assembled by Gislason et al. (2010) and concluded that coefficients of growth parameters of the previous M-at-length estimator did not differ from the general life history theory described in Charnov (1993). The analysis in Charnov et al. (2013) also provides a theoretical basis for estimating indirectly M-at-length from life history theory. In this reductionist approach, the M-at-length in fish populations is based entirely on the VBGF parameters and can be estimated by the expression

$$M(L) = K\left(\frac{L_\infty}{L}\right)^{3/2}, \quad (3)$$

where M = the natural mortality rate at length L; and the other parameters are estimated from the VGBF.

Natural mortality model

Method error was incorporated in this model by following a log-normal regression model of the form

$$\log M(L) = \beta_0 + \beta_1 \log \frac{L_\infty}{L} + \beta_2 \log K + \log \eta, \quad (4)$$

where $\log \eta$ = an independent additive Gaussian error, $\log \eta \sim N(0,\sigma_\eta^2)$.

Parameter σ_η^2 corresponds to the uncertainty given by the mortality expression (Eq. 3), which came from the Gislason et al. (2010) database and comprises 168 more or less independent estimates for marine and brackish water fish. In order to have an approximation of σ_η^2, as well as β_0, β_1, and β_2, we estimate the log-normal regression model with normal prior distributions with mean 0 and large variance for β_i, $N(0,\sigma_\eta^2)$, i = 0, 1, 2, and an inverse gamma distribution, Inv-$\Gamma(\alpha,\beta)$, for with small values for the scale and rate hyperparameters, (α, β) on a Bayesian framework.

In the Results section, the estimated parameters are presented with this approach for the same data set used by Charnov et al. (2013).

Life history parameters

Bayesian approach Assuming the multiplicative structure of Equation 3, Contreras-Reyes et al. (2014) considered a skew-t distribution for the errors ε_i', denoted by $\varepsilon_i' = \log \varepsilon_i \sim ST(\mu_i,\sigma_i^2,\lambda,\nu), i = 1,\ldots,n$. More specifically, we assumed that the original multiplicative errors ε_i, i = 1,..., n, are independently distributed random variables following a log-skew-t distribution (Azzalini et al., 2002; Marchenko and Genton, 2010) with parameters of location, dispersion, shape and degrees of freedom given by μ_i, σ_η^2, λ, and ν>2, respectively. Then, the log-transformed lengths are $y_i' = \log y_i \sim ST(\mu_i + L_i,\sigma_i^2,\lambda,\nu)$, i = 1,..., n, with $L_i' = \log L(x_i)$. Thus, the density of $y_i' = \log y_i$ is

$$f(y_i' \mid x_i,\mu_i,\sigma_i^2,\lambda,\nu) = \frac{2}{\sigma_i} t(z_i;\nu) T\left(\lambda z_i \sqrt{\frac{\nu+1}{\nu+z_i^2}};\nu+1\right), y_i' \in R, \quad (5)$$

where $z_i = (y_i' - \mu_i - L_i') / \sigma_i$ is a standardized version of y_i', and $t(z;\nu)$ and $T(z;\nu)$ represent the usual symmetric Student's t density and cumulative distribution function, respectively. In this case, we assume that the original lengths follow a log-skew-t distribution, denoted by $y_i \sim LST\left(\mu_i + L_i,\sigma_i^2,\lambda,\nu\right)$, i = 1,..., n. The power function $m(\rho; x_i) = x_i^{2\rho}$ introduces heteroscedasticity into the dispersion parameter $\sigma_i^2 = \sigma^2 m(\rho; x_i)$ (Contreras-Reyes and Arellano-Valle, 2013).

A Bayesian analysis for the log-skew-t VBGF is proposed. If independence is assumed, the likelihood function $f(y' \mid x, \theta)$ of the unknown parameter vector $\theta = (L_\infty, K, t_0, \sigma^2, \rho, \lambda, \nu)^\top = (\beta^\top, \sigma^2, \rho, \lambda, \nu)^\top$ is considered with Equation 5. The Bayesian model specification involves a prior distribution for each parameter of θ to be inserted into Equation 3 in the case of L_∞ and K, respectively and inference on θ rests on posterior distribution $\pi(\theta \mid x, y') \propto f(y' \mid x, \theta)\, \pi(\theta)$.

In the specific case of southern blue whiting (López Quintero et al., 2017), the prior distributions were the following: $L_\infty \sim TN_{(0,\infty)}$ (0,100); $K \sim \Gamma(15,100)$; $-t_0 \sim \Gamma(14,4)$; $\pi(\rho) \propto 1$ (a non-informative prior density); $\sigma^{-2} \sim \Gamma(0.1,0.1)$; $\lambda \sim N(0,100)$; and $\nu \sim TE_{[2,\infty)}$ (0.5), where $TN_{(0,\infty)}$ $(0,\sigma^2)$ denotes the truncated normal density at interval $(0,\infty)$ with zero mean and variance σ^2, $TE_{[c,\infty)}$ (λ) denotes the truncated exponential density at interval $[c,\infty)$ with parameter λ, and $\Gamma(\alpha, \beta)$ represents the gamma distribution whose shape and rate parameter are α and β, respectively.

Copula approach The copula method is used when considering 2 random variables represented by their joint (cumulative) distribution function, $H(u,v) = H(F(x), G(y))$, where u and v denote the values of $F(x)$, and $G(y)$, respectively. Our main objective is to simulate random variables from $H(u,v)$.

Most of the sampling methods are based on the assumption that $F(x)$ and $G(y)$ are known but the joint distribution $H(F(x), G(y))$ is not. A naive framework would be that in which samples are drawn independently from each marginal distribution, yet this approach is would be misleading because underlying dependent structures in H will be lost. Alternatively, a copula C between F and G can be used as a function such that $C(F(x), G(x)) = H(u,v)$. This function can be recognized as a distribution function on $[0,1]^d$ (for a dimension d) whose arguments are the marginal distribution of the joint distribution. Thus, as in any statistical distribution, C depends on some parameters, say θ.

A copula can be simulated by using different approaches depending on the family they belong to, e.g., Gaussian, Archimedean, Extreme-value, and others.

Each of these families have their own set of parameters (dos Santos Silva and Lopes, 2008). Owing to an important result from copula theory, we are able to simulate from H, even if unknown, only requiring the marginal distributions, F and G, and the copula C_θ (see Sklar's Theorem in Nelsen, 2006).

In order to imitate the joint distribution H, the copula C_θ and the marginal distributions F and G need to be estimated. Doing so could create various situations, namely: if F and G belong to known families, we could use a parametric framework to obtain $\hat{C}_\theta$, by either estimating all parameters associated with both marginal and copula inside a single routine in a procedure known as *full maximum-likelihood*, or by estimating the parameters in 2 stages. The first stage includes estimating parameters of marginal distributions and afterwards the parameters in copula. This approach is commonly known as *inference functions for margins* (Cherubini et al., 2004). There are also intermediate procedures where the marginal distributions are estimated nonparametrically. Results are then plugged into the copula parameters obtained by the maximum likelihood estimation. This latter approach is called "canonical maximum likelihood"or "maximum pseudo-likelihood" and is based on the empirical estimation of the distribution functions F and G. This strategy is applied when the families of marginal distributions are unknown (McNeil et al., 2005). In all these cases, to estimate the copula C we need approximations for F and G, denoted by $\hat{F}$ and $\hat{G}$, respectively. These quantities are known as "pseudo-samples" or "pseudo-observations" and provide valuable information for the type of dependency between the original variables (see Fig. 2 and McNeil et al., 2005).

We obtained the empirical posterior distributions for K and L_∞, where the exact marginal and joint family distributions are unknown. We consider the Gaussian copula with parameter ρ, $|\rho|<1$, which is the usual correlation coefficient that measures the linear association between 2 variables.

The Gaussian copula has a nonclosed form,

$$C_\rho(u,v)=\frac{1}{2\pi\sqrt{1-\rho^2}}\int_{-\infty}^{\Phi^{-1}(u)}\int_{-\infty}^{\Phi^{-1}(v)} e^{\frac{w^2-2\rho wz+z^2}{2(1-\rho^2)}}\,dwdz, \quad (6)$$

and to estimate it, the likelihood function,

$$\ell(\rho)=\sum_{i=1}^{n}\log\left[c_\rho\left\{F(\hat{x}_i),G(\hat{y}_i)\right\}\right], \quad (7)$$

needs to be maximized, where $c_\rho(a,b)=\frac{\partial^2}{\partial u\,\partial v}C_\rho(u,v)$ and $\Phi_{(\cdot)}$ represents the cumulative normal distribution. We are following the maximum pseudolikelihood approach where the marginal distributions $F(x)$ and $G(y)$ are estimated nonparametrically as follows:

$$F(\hat{x}_i)=\frac{1}{n+1}\sum_{i=1}^{n}I\{K\le x_i\} \text{ and} \quad (8)$$

$$G(\hat{x}_i)=\frac{1}{n+1}\sum_{i=1}^{n}I\{L_\infty\le y_i\}. \quad (9)$$

Using the copula estimate parameters, we draw samples from $C_\theta = C_\rho$, as suggested in Nelsen (2006). Furthermore, to obtain samples on the same scale of K and L_∞, instead of the (0,1) interval, we apply the appropriate quantile functions to the simulated marginal copula. These quantile functions depend on the original marginal distributions.

M-at-length estimation

To obtain an estimator of Equation 3, we take N estimated values of parameters L_∞ and K, represented as $L_\infty^{(j)}$ and $K^{(j)}$, respectively, $j = 1,...,N$. All these values are used for each of the values of fish lengths, y_i, $i = 1,...,J$, where the value of J is one of the distinct values of the age. The estimated values $K^{(j)}$ and $L_\infty^{(j)}$ are obtained from either the Bayesian chains values after convergence or from the copula simulation. To complete the estimator, it is then perturbed with the uncertainty η_i (method error) of Equation 4, recovered from the M modeling,

$$M_{y_i}^{(j)}=K^{(j)}\left(\frac{L_\infty^{(j)}}{y_i}\right)^{3/2}\eta_i, \quad (10)$$

with $j = 1,...,N$, $i = 1,...,J$.

In order to emphasize that the mortality estimator depends on individual i through the length variable, y, the subscript y_i is added to the notation. Using the Equation 10, we draw samples at each length i. Uncertainty in the VBGF parameters (trait error) is guaranteed by using Markov chains or copula iterations, the incorporation of η_i, whereas M estimators have their own uncertainty abridged σ_η parameter.

Furthermore, to include the dependence structure between age and length in the mortality estimation, we use the predicted value $\hat{L}(x_i)$ instead of y_i. Using Equation 1, we obtain the mortality estimator with the following equation:

$$M_{y_i}^{(j)}=K^{(j)}\left(\frac{L_\infty^{(j)}}{\hat{L}(x_i|\tilde{\beta})}\right)^{3/2}\eta_i, \quad (11)$$

where j = 1,...,N;
i = 1,...,J; and
$\tilde{\beta}$ = $(\tilde{L}_\infty,\tilde{K},\tilde{t}_0)^\top$ are point estimates, such as median values from posterior distribution for (L_∞, K, t_0) which can be taken from previous studies.

Results from both approaches, with Bayesian chains or copula simulation, are then compared.

All statistical methods used in this study were developed with the software R[2] (vers. 3.1.0 or higher; R Core Team, 2014). Bayesian estimations were carried out with the program JAGS, vers. 3.4 or higher (Plummer, 2003). Copula estimation was conducted with the R package copula, vers. 0.999-12 or higher, developed by Hofert et al. (2015). The length and the

[2] Mention of trade names or commercial companies is for identification purposes only and does not imply endorsement by the National Marine Fisheries Service, NOAA.

Table 1

Mean estimates, with standard deviations (SDs) and 95% highest posterior density (HPD) intervals, of Bayesian log-normal model parameters from fitting the regression of natural mortality (M) to the von Bertalanffy growth function parameters, the asymptotic length, the growth rate coefficient, and the theoretical age at length zero by using the Equation 4 and data in Charnov et al. (2013).

Parameter	Estimates	SD	95% HPD interval
β_0	−0.050	0.110	−0.267, 0.163
β_1	−1.467	0.125	−1.714, −1.226
β_2	1.007	0.075	0.860, 1.153
σ_η	0.749	0.041	0.666, 0.825

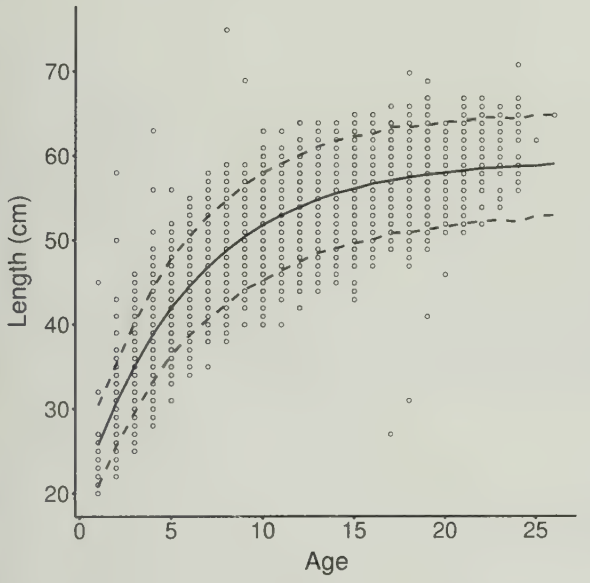

Figure 1

Length-at-age composition for southern blue whiting (*Micromesistius australis*) collected from Chilean continental waters during 1997–2010 (open circles), fitted with the von Bertalanffy growth function: the solid line corresponds to the fit of the log-skew-t model with a heteroscedastic power variance function (Table 2). Dashed lines correspond to the 95% highest posterior density for the fitted log-skew-t model. Fish length was measured as total length in centimeters.

burn-in period of the considered chains is 20,000 iterations and 10,000, respectively. Last, a machine running on Linux (kernel 4.6), with an Intel Core i5 processor (Intel Corp., Santa Clara, CA) and 7.7 GB of random-access memory, processed all these computations.

Table 2

Mean estimates, with standard deviations (SDs) and 95% highest posterior density (HPD) intervals, of the von Bertalanffy growth function parameters from the power log-skew-t model. The parameters are asymptotic length (L_∞), growth rate coefficient (K), negative theoretical age at length zero ($-t_0$), heteroscedasticity (ρ), dispersion (σ^2), skewness (λ), and degrees of freedom (ν).

Parameter	Estimates	SD	95% HPD interval
L_∞	59.573	0.090	59.386, 59.755
K	0.162	0.001	0.159, 0.165
$-t_0$	2.454	0.042	2.367, 2.541
ρ	−0.180	0.009	−0.197, −0.161
σ^2	0.011	0.001	0.010, 0.013
λ	−1.096	0.053	−1.200, −0.997
ν	14.322	1.047	12.457, 16.586

Results

Table 1 shows the estimates from the M model with Bayesian inference. Differences between these results and those reported in Charnov et al. (2013) were caused by the method used to incorporate uncertainty. However, the actual values of the estimated parameters were very similar. The standard deviation, σ_η, is then a key parameter underpinning the method error, which is assumed to be a log-normal random variable η in Equations 10 and 11.

Figure 1 shows the application of the power log-skew-t model fitted to the observed length-at-age data (for southern blue whiting) by using the VBGF parameters summarized in Table 2 and estimated with Bayesian inference. This curve was created by simulating 10,000 log-skew-t random values from each age and then by taking the 95% highest posterior density interval. Further details regarding the Bayesian estimation, such as residual diagnostic and sensitivity analysis, can be found in López Quintero et al. (2017). Those authors also showed that the heteroscedastic parameter allows a better model with small variance across observed ages in southern blue whiting. In addition, extreme values for younger and older fish (i.e., <9 and >16 years) were accounted for by the estimated degree of freedom parameter. Moreover, the credibility intervals showed that observations were affected by the negative heteroscedastic parameter, $\hat{\rho}$.

The marginal distributions estimated empirically with Equations 8 and 9 and the pseudosamples $\hat{F}$ and $\hat{G}$ from copula are shown in Figure 2. We first observed that points concentrate around the diagonal of unit square. The relationship between pseudosamples is linear and negative. Particularly, the Bayesian Markov chain simulation, shown in Figure 2A, which was obtained directly from the estimated VBGF parameters.

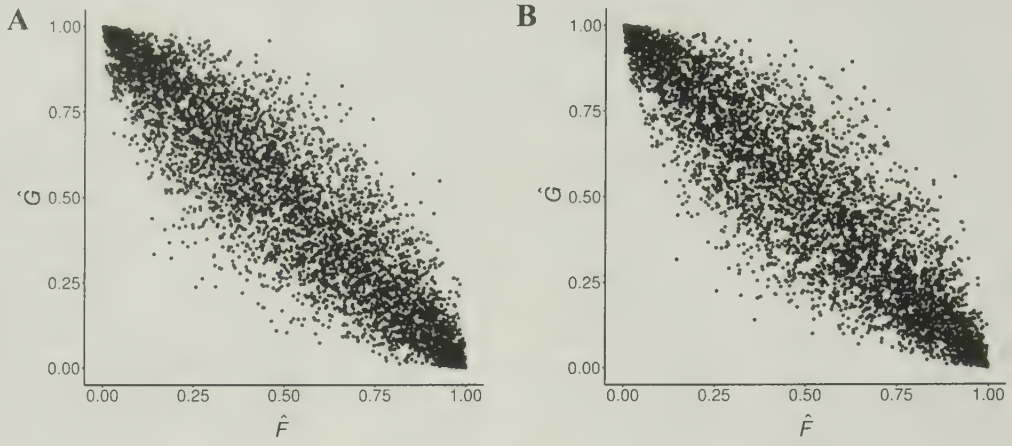

Figure 2

Scatter plots of pseudo-observations, or approximations of distribution functions ($\hat{F}$ and $\hat{G}$), from simulations (**A**) where Markov chains of estimated von Bertalanffy growth function (VBGF) parameters were used directly and (**B**) where copulas were applied to the posterior distribution of VBGF parameters.

In Figure 2B, the relationship between both parameters was recovered by using a Gaussian copula drawing from the empirical posterior distribution. Both plots corresponded with a graphical representation of the intrinsic dependence of the pseudosamples.

Figures 3A and 3B show the estimated parameters from chains and their marginal histograms are displayed in Figures 4A and 4B. The histograms in Figure 4C and 4B were built by assigning a roughly heuristic normal distribution to each marginal, but other alternatives are still possible. These plots ensure the dependence and shape between K and L_∞ parameters. We can also include the related quantile functions in the sample generation if the exact distributions for K and L_∞ are known. In our study, we particularly considered the Gaussian copula in Figure 3B because of the dependence between pseudosamples generated for both marginal posterior distributions of K and L_∞ which looked linear and strongly negative (Fig. 3A; coefficient of correlation [r]= −0.912 (standard error 0.006; t-value= −157.14; P-value <0.001).

Additionally, both methods showed a strong correla-

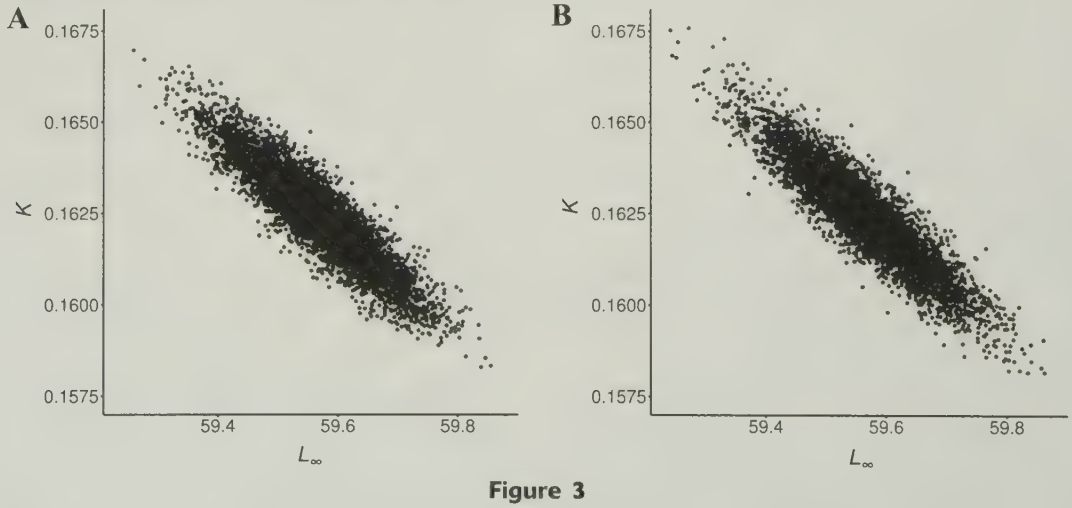

Figure 3

Scatter plots of asymptotic length (L_∞) and growth rate coefficient (K) of the von Bertalanffy growth function showing results (**A**) from simulations based on posterior distribution and (**B**) from the copula approach.

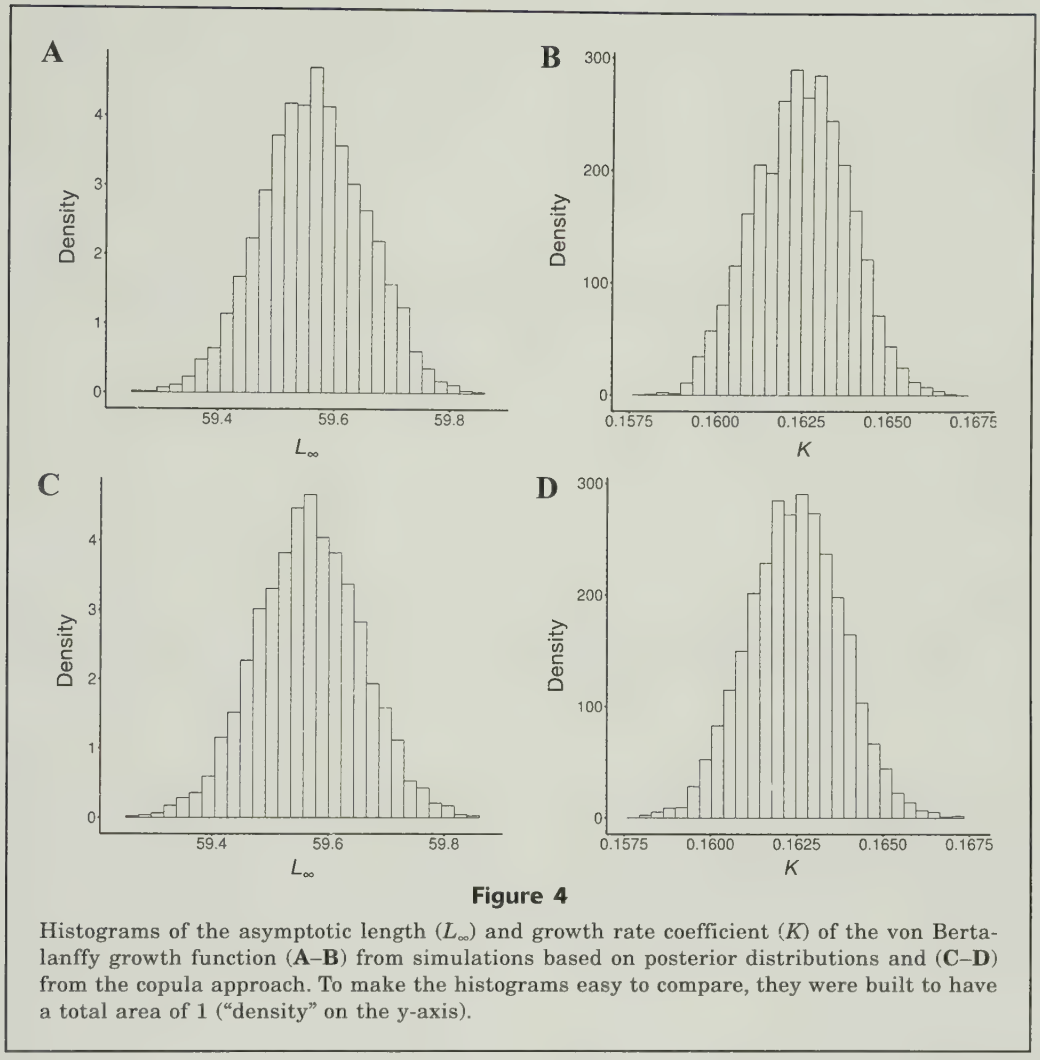

Figure 4

Histograms of the asymptotic length (L_∞) and growth rate coefficient (K) of the von Bertalanffy growth function (**A–B**) from simulations based on posterior distributions and (**C–D**) from the copula approach. To make the histograms easy to compare, they were built to have a total area of 1 ("density" on the y-axis).

tion between K and L_∞. Note the copula method keeps the correlation structure reported in Siegfried and Sansó (2006) and López Quintero et al. (2017). These simulated values of $K^{(j)}$ and $L_\infty{}^{(j)}$, from both, Markov chain or from copula, will be used in the expression M-at-length estimation.

Figure 5 shows the simulated M derived from Equations 10 and 11, by using both the Markov chains and copula approaches. Uncertainty at each age was incorporated by simulating the posterior distributions of each VBGF parameter. The uncertainty for the method error was incorporated through the random variable η (as explained in the *Materials and methods* section). The empirical distributions related to the copula method showed a similar shape to that with the Markov chains method because we have assumed marginals of the Gaussian family. The empirical distributions behavior can change depending on the class of copula used and the available information for marginals (dos Santos Silva and Lopes, 2008). Moreover, it has been assumed that M follows a slow exponential decay with length (Gedamke and Hoenig, 2006). On the other hand, recent empirical and theoretical work has shown that M represents a decreasing exponential function of length in fish populations (Gislason et al., 2010; Charnov et al., 2013). Specifically, for both methods, the percent change in the median values from the first to the sixth year is around 57%. It is important to note that the most of the methods used to estimate M consider this parameter as constant across ages and lengths within species (e.g. Pauly, 1980; Hewitt and Hoenig, 2005). These indirect methods are based on the assumption that M remains relatively constant in fish after they reach sexual maturity.

Discussion

We presented a mortality estimator that incorporates 2 sources of variability or uncertainty. One of them is associated with the VBGF parameters (trait error) and the other is related to the mortality model (model error) which is related to uncertainty in the original method described in Charnov et al. (2013). In relation

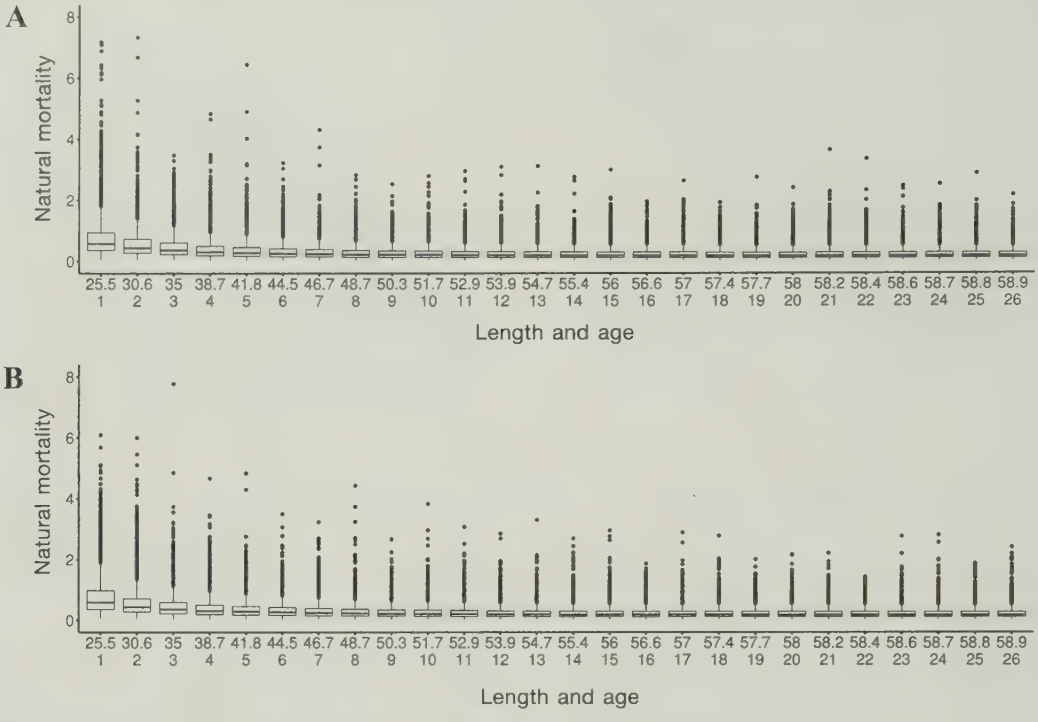

Figure 5

Boxplots of estimates of natural mortality in relation to total length (in centimeters) age in years (**A**) from direct simulation with Markov chains and (**B**) with the use of the copula method. The vertical black lines correspond to the observed median, the boxes represent the observed interval from the 25% residual quartile to the 75% residual quartile, the error bars are the observed interval from minimum to maximum residual value, and the dots are atypical residual values.

to the trait error, we presented 2 ways to incorporate uncertainty in length-based M estimators, drawing on an empirical distribution of VBGF parameters. First, the applied Bayesian methods simulate the M estimator directly with the posterior distribution of the VBGF parameters, with the method of López Quintero et al. (2017). This particular approach was preferred over that for traditional distributions (Siegfried and Sansó, 2006; Hamel, 2015), because this type of data usually contains a degree of asymmetry and extreme values. Additionally, an inadequate distribution may underestimate the real variance contained in the data. The model used gives great flexibility in modeling heteroscedasticity by adding a function dependent on the scale σ^2 and a heteroscedastic parameter, ρ (Contreras-Reyes et al., 2014). In addition, a copula method was usedd to approximate the posterior distribution and calculate the M estimator. The method proposed in this study provides a way to incorporate uncertainty in the length-based M estimator proposed by Charnov et al. (2013), while acknowledging both method and traits errors. Furthermore, our scheme can easily be extended to generate values of uncertainty in indirect methods used to estimate mortality, and therefore has the potential to improve actual ad-hoc methods for incorporating uncertainty, such as in Cubillos et al. (1999); Quiroz et al. (2010) and Wiff et al. (2011). Furthermore, we recommend the copula method instead of the Bayesian Markov chain approach to incorporate uncertainty in the M-at-length estimates for 2 reasons: 1) the copula method conserves the underlying dependence in the posterior distribution (see Figs. 3 and 4) and 2) it uses less computing time than the Bayesian Markov chain approach. For example, in our case the copula method required 1 s to compute each length class, whereas the same procedure takes at least 20 h with the Bayesian Markov chain approach. These differences in computational time result in part from the Metropolis–Hastings algorithm that is derived from the kernel of likelihood function and discards, by construction, many proposed values of parameters. Other algorithms, such as the Gibbs sampler, can take the advantage of the known conditional distributions, making the sampling process faster.

Additionally, it is important to note that the proposed M-at-length estimators are not conceptually limited to use a Bayesian estimation. Researchers can simulate the entire M-at-length structure just by knowing the dependence between parameters L_∞ and K. This can be achieved by reviewing specialized litera-

ture about the species under study and incorporating this information in the copula method. In addition, the method proposed is not limited to the use of Charnov et al. (2013) estimator as the underpinning model to relate M and growth parameters. A method for estimating M addressing uncertainty and considering environmental factors such temperature (e.g., Hewitt and Hoenig, 2005) can also be used.

As pointed out in the introduction, M is a key parameter in modeling any animal population but, it is crucial for harvested fish populations. Natural mortality affects these populations concurrently and continuously with fishing mortality to yield the total mortality rate, which determines the decay in the abundance of a population over time and therefore the size of the stock. Estimation of M within stock assessment models is difficult, and resultant estimates are usually imprecise (Vetter, 1988; Gavaris and Ianelli, 2002). Standard practice is therefore to use a constant value for M across sizes or ages—a value that is derived from indirect methods when fitting a population model. Most of the current stock assessment models are age or size based, and therefore the incorporation of an age or size constant value for M is misleading and may introduce a critical source of bias in abundance estimates. Recent stock assessment models recognize the importance of incorporating size-dependent mortality, and thus incorporating uncertainty in size-based models has become highly recommended (e.g., Clark, 1999; Fu and Quinn, 2000; Siegfried and Sansó[1]; Gislason et al., 2010; Lee and Chang[3]). We agree with Quiroz et al. (2010) in the sense that uncertainty, as reported here for size-based M estimates, can then be integrated into stock assessment models and used for management analysis through methods such as: 1) sensitivity analysis, where an assessment is conducted repeatedly for several values of size-based M (see McAllister et al., 1994; Patterson, 1999) drawn from the empirical distributions using copula methods; 2) Bayesian framework, by setting the empirical distributions as prior distributions of size-based M; and 3) state-space models, where uncertainty in M is incorporated as one of the random components regulating the stochasticity in the population dynamics (i.e. the model process error; see Millar and Meyer, 2000).

Acknowledgments

The authors are grateful to the Instituto de Fomento Pesquero for providing access to the data used in this work. J. Contreras-Reyes was supported partially beginning in 2016 by Comisión Nacional de Investigación Científica y Tecnológica (CONICYT) doctoral scholarship number 21160618. R. Wiff was funded beginning in 2014 by the Centro de Ecología Aplicada y Sustentabilidad (CAPES) project CONICYT FB 0002. We are sincerely grateful to the 3 anonymous reviewers for their comments and suggestions that greatly improved an early version of this manuscript.

[3] Lee, H.-H., and Y. J. Chang. 2013. Age-structured natural mortality for Pacific blue marlin based on meta-analysis and an ad hoc model. Working document ISC/13/BILLWG-1/07. Submitted to the International Scientific Committee for Tuna and Tuna-like Species in the North Pacific Ocean. [Available from website.]

Literature cited

Azzalini, A., T. Del Cappello, and S. Kotz.
2002. Log-skew-normal and log-skew-t distributions as models for family income data. J. Income Distrib. 11(3–4):12–20.

Brodziak, J., J. Ianelli, K. Lorenzen, and R. D. Methot Jr. (eds).
2011. Estimating natural mortality in stock assessment applications. NOAA Tech. Memo. NMFS-F/SPO-119, 38 p.

Charnov, E. L.
1993. Life history invariants: some explorations of symmetry in evolutionary ecology, 184 p. Oxford Univ. Press, Oxford, UK.

Charnov, E. L., H. Gislason, and J. G. Pope.
2013. Evolutionary assembly rules for fish life histories. Fish Fish. 14:213–224.

Cherubini, U., E. Luciano. and W. Vecchiato.
2004. Copula methods in finance, 310 p. John Wiley & Sons, West Sussex, UK.

Clark, W. G.
1999. Effects of an erroneous natural mortality rate on a simple age-structured stock assessment. Can. J. Fish. Aquat. Sci. 56:1721–1731.

Contreras-Reyes, J. E., and R. B. Arellano-Valle.
2013. Growth estimates of cardinalfish (*Epigonus crassicaudus*) based on scale mixtures of skew-normal distributions. Fish. Res. 147:137–144.

Contreras-Reyes, J. E., R. B. Arellano-Valle, and T. M. Canales.
2014. Comparing growth curves with asymmetric heavy-tailed errors: application to the southern blue whiting (*Micromesistius australis*). Fish. Res. 159:88–94.

Cubillos, L. A., R. Alarcón, and A. Brante.
1999. Empirical estimates of natural mortality for the Chilean hake (*Merluccius gayi*): evaluation of precision. Fish. Res. 42:147–153.

dos Santos Silva, R., and H. F. Lopes.
2008. Copula, marginal distributions and model selection: a Bayesian note. Stat. Computing 18:313–320.

Essington, T. E., J. F. Kitchell, and C. J. Walters.
2001. The von Bertalanffy growth function, bioenergetics, and the consumption rates of fish. Can. J. Fish. Aquat. Sci. 58:2129–2138.

Fu, C., and T. J. Quinn II.
2000. Estimability of natural mortality and other population parameters in a length-based model: *Pandalus borealis* in Kachemak Bay, Alaska. Can. J. Fish. Aquat. Sci. 57:2420–2432.

Gavaris, S., and J. N. Ianelli.
2002. Statistical issues in fisheries' stock assessments. Scand. J. Stat. 29:245–267.

Gedamke, T., and J. M. Hoenig.
2006. Estimating mortality from mean length data in nonequilibrium situations, with application to the assessment of goosefish. Trans. Am. Fish. Soc. 135:476–487.

Gislason, H., N. Daan, J. C. Rice, and J. G. Pope.
2010. Size, growth, temperature and the natural mortality of marine fish. Fish Fish. 11:149–158.

Hamel, O. S.
2015. A method for calculating a meta-analytical prior for the natural mortality rate using multiple life history correlates. ICES J. Mar. Sci. 72:62–69.

Hewitt, D. A., and J. M. Hoenig.
2005. Comparison of two approaches for estimating natural mortality based on longevity. Fish. Bull. 103:433–437.

Hofert, M., I. Kojadinovic, M. Maechler, and J. Yan.
2015. Copula: multivariate dependence with copulas. R package vers. 0.999-13. [Available from website.]

López Quintero, F. O., J. E. Contreras-Reyes., R. Wiff, and R. B. Arellano-Valle.
2017. Flexible Bayesian analysis of the von Bertalanffy growth function with the use of a log-skew-*t* distribution. Fish. Bull. 115:13–26.

Marchenko, Y. V., and M. G. Genton.
2010. Multivariate log-skew-elliptical distributions with applications to precipitation data. Environmetrics 21:318–340.

McAllister, M. K., E. K. Pikitch, A. E. Punt, and R. Hilborn.
1994. A Bayesian approach to stock assessment and harvest decisions using the sampling/importance resampling algorithm. Can. J. Fish. Aquat. Sci. 51:2673–2687.

McNeil, A. J., R. Frey, and P. Embrechts.
2005. Quantitative risk management: concepts, techniques and tools, 538 p. Princeton Univ. Press, Princeton, NJ.

Millar, R. B., and R. Meyer.
2000. Bayesian state-space modeling of age-structured data: fitting a model is just the beginning. Can. J. Fish. Aquat. Sci. 57:43–50.

Montenegro, C., and M. Branco.
2016. Bayesian state-space approach to biomass dynamic models with skewed and heavy-tailed error distributions. Fish. Res. 181:48–62.

Nelsen, R. B.
2006. An introduction to copulas, 2nd ed., 272 p. Springer-Verlag, New York.

Patterson, K. R.
1999. Evaluating uncertainty in harvest control law catches using Bayesian Markov chain Monte Carlo virtual population analysis with adaptive rejection sampling and including structural uncertainty. Can. J. Fish. Aquat. Sci. 56:208–221.

Pauly, D.
1980. On the interrelationships between natural mortality, growth parameters, and mean environmental temperature in 175 fish stocks. ICES J. Mar. Sci.39:175–192.

Plummer, M.
2003. JAGS: a program for analysis of Bayesian graphical models using Gibbs sampling. *In* Proceedings of the 3rd international workshop on distributed statistical computing (DSC 2003); Vienna, Austria, 20–22 March (K. Hornik, F. Leisch, and A. Zeileis, eds.), 10 p. [Available from website.]

Quiroz, J. C., R. Wiff, and B. Caneco.
2010. Incorporating uncertainty into estimation of natural mortality for two species of Rajidae fished in Chile. Fish. Res. 102:297–304.

R Core Team.
2014. *R:* a language and environment for statistical computing. R Foundation for Statistical Computing, Vienna, Austria. [Available from website. accessed April 2014.]

Sainsbury, K. J.
1980. Effect of individual variability on the von Bertalanffy growth equation. Can. J. Fish. Aquat. Sci. 37:241–247.

Siegfried, K. I., and B. Sansó.
2006. Two Bayesian methods for estimating parameters of the von Bertalanffy growth equation. Environ. Biol. Fish. **77**:301–308.

Vetter, E. F.
1988. Estimation of natural mortality in fish stocks: a review. Fish. Bull. 86:25–43.

Wiff, R., J. C. Quiroz, V. Ojeda., and M. A. Barrientos.
2011. Estimation of natural mortality and uncertainty in pink cusk-eel (*Genypterus blacodes* Schneider, 1801) in southern Chile. Lat. Am. J. Aquat. Res. 39:316–326.

National Marine
Fisheries Service
NOAA

Fishery Bulletin
established in 1881

Spencer F. Baird
First U.S. Commissioner
of Fisheries and founder
of *Fishery Bulletin*

Age and growth of the highly exploited narrownose smooth-hound (*Mustelus schmitti*) (Pisces: Elasmobranchii)

Juan M. Molina (contact author)[1]
Gabriela E. Blasina[2]
Andrea C. Lopez Cazorla[1,2]

Email address for contact author: jmmolina@criba.edu.ar

[1] Departamento de Biología, Bioquímica y Farmacia
Universidad Nacional del Sur
San Juan 670, Primer Piso
8000 Bahía Blanca, Buenos Aires, Argentina

[2] Instituto Argentino de Oceanografía
Consejo Nacional de Investigaciones Científicas y Técnicas
Florida 8000 (Camino La Carrindanga km 7,5)
8000 Bahía Blanca, Buenos Aires, Argentina

Abstract—The narrownose smooth-hound (*Mustelus schmitti*) is the most exploited elasmobranch of Argentina, Brazil, and Uruguay and is considered endangered (IUCN Red List of Threatened Species). Providing information on age and growth can improve efforts for conservation of this species. Therefore, our objective was to provide accurate estimates of the age structure and growth parameters for narrownose smooth-hound from Anegada Bay, an important shark nursery area in Argentina. In vertebrae of narrownose smooth-hound, we observed a pattern of alternating opaque and translucent bands and a yearly periodicity in the deposition of this pattern. Ages determined from vertebral band counts ranged from 0 to 11 years. Calculated longevity and total natural mortality rates were 20.87 years and 0.19/year for females and 12.24 years and 0.26/year for males, respectively. This species reached a size of approximately 400 mm in total length in the initial year of growth, and the age at first maturity was 7.61 years for females and 6.79 years for males. The slow growth and late age at maturity of the narrownose smoothhound indicate a need for additional conservation measures to rebuild the population and achieve a sustainable fishery in the 3 countries in which it is distributed.

Manuscript submitted 19 June 2016.
Manuscript accepted 9 May 2017.
Fish. Bull. 115:365–379 (2017).
Online publication date: 8 June 2017.
doi: 10.7755/FB.115.3.7

The views and opinions expressed or implied in this article are those of the author (or authors) and do not necessarily reflect the position of the National Marine Fisheries Service, NOAA.

The Chondrichthyes make up a class of vertebrates that are usually described as late-maturing fish with a moderate-to-long life span and an extended gestation period that produces a low number of developed offspring (Dulvy et al., 2008). Most chondrichthyans have limited geographic distributions and gather in schools by age, sex, and reproductive states (Barker and Schluessel, 2005). The characteristic slow population growth of these elsasmobranchs renders them highly vulnerable to fishing pressure (Dulvy et al., 2008; Cortés et al., 2010). Globally, chondrichthyan fish populations are declining (Camhi et al.[1])—a fact aggravated by a lack of knowledge of the biology for many species. This lack of information makes identifying threats to conservation challenging, and designing appropriate management measures almost impossible (Molina and Cooke, 2012).

The narrownose smooth-hound (*Mustelus schmitti*) is a small shark in the family Triakidae that attains a maximum total length (TL) of 110 cm (Menni, 1985). Endemic to the southwest Atlantic Ocean, this shark occurs in waters over the continental shelf, from coastal waters of less than 50 m to depths up to 120 m, throughout its range from southeastern Brazil to the Argentinean Patagonia (from 22°S to 47°S) (Menni, 1985). This shark is known to migrate seasonally, in large numbers, between wintering grounds in southern Brazil and summering grounds in Argentina (Figueiredo, 1977; Vooren, 1997). Seasonally, it also frequents estuaries, protected bays, and gulfs (Lopez Cazorla, 1987; Chiaramonte and Pettovello, 2000; Colautti et al., 2010; Molina, 2013).

The narrownose smooth-hound is the most exploited elasmobranch species (by both industrial and artisanal

[1] Camhi, M. D., S. V. Valenti, S. V. Fordham, S. L. Fowler, and C. Gibson (eds.). 2007. The conservation status of pelagic sharks and rays. Report of the IUCN Shark Specialist Group Pelagic Shark Red List Workshop, 78 p. IUCN Species Survival Commission Shark Specialist Group, Newbury, UK.

fishing fleets) found on the continental shelf in Argentina, Brazil, and Uruguay (Massa and Lasta[2]). The exploitation of this species throughout its range has led to declines in its population (Massa et al.[3]), and it has a global classification of endangered (IUCN Red List of Threatened Species), with a designation of vulnerable in Argentina and Uruguay (Massa et al., 2006). Narrownose smooth-hound caught off the coast of Brazil are part of the southern stock that migrates north every year. Therefore, the exploitation in nursery areas, in particular, has led to recruitment overfishing and a decline of ~85% in the total biomass from 1975 to 1995 (Haimovici, 1997). In Brazil, this species is categorized as critically endangered in the IUCN Red List of Threatened Species (Massa et al., 2006). Given its migratory behavior, there is great concern for the conservation of this shark over its entire range of distribution (Massa et al., 2006; Molina and Lopez Cazorla, 2011).

Sustainable fishing of small coastal sharks, which have a greater recovery potential (Stevens et al., 2000) than their larger counterparts, is theoretically possible to achieve if the key biological aspects are taken into consideration when designing management policy. The narrownose smooth-hound is one of the most studied sharks of Argentina: several scientific publications describe its reproduction, food habits, and other aspects of its biology (Menni, 1985; Menni et al., 1986; Cousseau et al.[4]; Chiaramonte and Pettovello, 2000; Sidders et al., 2005; Cortés and Massa[5]; Segura and Milessi, 2009; Colautti et al., 2010; Molina and Lopez Cazorla, 2011). However, little attention has been paid to age and growth of this species. To date, there are 2 documents, a M.S, thesis from Brazil (Batista, 1988) and a technical report from Argentina (Hozbor et al.[6]) that deal with this aspect. Science-based studies on age and growth are crucially important for research of population dynamics because, without accurate age and growth estimations, it is impossible to perform adequate fisheries stock assessments, make accurate forecasts, and provide effective management (Chugunova, 1963; Reeves, 2003; Methot and Wetzel, 2013). Therefore, the aim of this work was to provide accurate estimates of the age structure and growth parameters for the population of narrownose smooth-hound from Anegada Bay, an important shark breeding area in Argentina.

Materials and methods

Study area

Anegada Bay, located in the south of Buenos Aires Province in Argentina, has a wide variety of habitats, including wide, muddy intertidal areas, sandy bottom substrates, and sand and gravel beaches. In Anegada Bay, a multi-use protected area, the Reserva Natural de Uso Múltiple Bahía San Blas, was designated in 2001 (Provincial Law 12788; available from website), as a means of preserving not only fish species but also a wide variety of vertebrate species, such as several migratory birds, sea lions, and terrestrial mammals, that use the bay as nesting and feeding grounds. This bay is also considered a potential nursery area for narrownose smooth-hound (Molina and Lopez Cazorla, 2011). Artisanal and recreational fisheries were the main human activities in Anegada Bay. Whereas the latter still continues, in recent years, artisanal fishing has been prohibited within the boundaries of the reserve.

This study was conducted in the southern part of Anegada Bay, where 3 sampling stations were established: San Blas, Ría, and Los Pocitos (Fig. 1).

Sampling methods and data collection

Specimens of narrownose smooth-hound were collected seasonally in 2008: in February (summer), May (autumn), August (winter), and November (spring). The fishing gear consisted of 2 batteries of 7 bottom gill nets. Each net was 25 m long, 2 m high, and had different mesh sizes (64, 70, 80, 105, 135, 150, and 170 mm stretched) so that a wide range of fish sizes could be captured. Nets were placed parallel to the coast of the sampling stations at dusk, and collected 12 hours later at dawn.

All fish were first measured in situ to the nearest centimeter in TL and subsequently grouped into 1-cm size classes. A subsample composed of 10 randomly selected specimens of each size class was then used for further analysis. These 10 individuals were measured to the nearest millimeter in TL, their sex was determined, and the portion of vertebral column from below the first dorsal fin was removed. Vertebrae portions were

[2] Massa, A., and C. A. Lasta. 2000. Recursos a mantener: Gatuzo (*Mustelus schmitti*). *In* Síntesis del estado de las pesquerías marítimas argentinas y de la Cuenca del Plata. Años 1997–1998, con una actualizacion de 1999. Publicaciones Especiales INIDEP (S. I. Bezzi, R. Akselman, and E. E. Boschi, eds.), p. 129–137. [Available from Instituto Nacional de Investigación y Desarrollo Pesquero, Paseo Victoria Ocampo N°1, Escollera Norte, B7602HSA Mar del Plata, Provincia de Buenos Aires, Argentina.]

[3] Massa, A., C. A. Lasta, and C. R. Carozza. 2004. Estado actual y explotación del gatuzo (*Mustelus schmitti*). *In* Los peces marinos de interés pesquero. Caracterización biológica y evaluación del estado de explotación. Publicaciones Especiales INIDEP (R. P. Sánchez and S. I. Bezzi, eds.), p. 67–83. [Available from Instituto Nacional de Investigación y Desarrollo Pesquero, Paseo Victoria Ocampo N°1, Escollera Norte, B7602HSA Mar del Plata, Provincia de Buenos Aires, Argentina.]

[4] Cousseau, M. B., C. R. Carozza, and G. J. Macchi. 1998. Abundancia, reproducción y distribucion de tallas del gatuzo (*Mustelus schmitti*) en la Zona Común de Pesca Argentino-Uruguaya y en El Rincón. Noviembre, 1994. INIDEP Inf. Tec. 21:103–115. [Available from website.]

[5] Cortés, F., and A. Massa. 2006. Aspectos reproductivos del gatuzo (*Mustelus schmitti*). Inf. Téc. INIDEP, 10 p. [Available from website.]

[6] Hozbor, N. M., M. Sáez, and A. M. Massa. 2010. Edad y crecimiento de *Mustelus schmitti* (gatuzo), en la región costera bonaerense y uruguaya. INIDEP Inf. Invest. 49, 15 p. [Available from website.]

stripped of soft tissue with a scalpel and frozen for transportation and storage.

Preparation and sectioning of vertebrae

Vertebrae were prepared by following the methods described in Cailliet et al. (1990), Moulton et al. (1992), Natanson et al. (1995), Campana (2001), Conrath et al. (2002), and Lessa et al. (2016). Samples were cleaned of excess tissue and separated into individual centra so that they could be submerged in a solution of 2.5% sodium hypochlorite to remove connective tissue, without compromising the interpretability of growth bands. Bath duration varied between 5 and 30 min, depending on the size of the centra. Afterward, vertebrae were rinsed with tap water, air dried, and mounted on transparent epoxy resin. One section (approximately 0.2 mm thick) was then cut transversely through the focus with a diamond-bladed IsoMet Low Speed Saw[7] (Bueheler, Lake Bluff, IL).

Age determination

Vertebral sections were examined under a binocular microscope with transmitted light to identify opaque (hypomineralized, wide) and translucent (hypermineralized, narrow) bands. All counts were made with no knowledge of size, sex, or date of capture of the individual. The birth mark was identified by the angle change in growth bands and by the banding patterns on neonates and embryos. Bands consisting of opaque and translucent areas were identified along the corpus calcareum (Goldman et al., 2012) (Fig. 2) in each vertebra. Variation in the nature of the border of the vertebra was used to verify the temporal periodicity of the formation of each band type (Campana, 2001). The age of each individual fish was determined by the number of translucent bands, the date of capture, and the date of birth, which was assumed to be 1 January. This assumption is supported by the fact that a high proportion of gravid females were captured in a previous sampling campaign in December 2007 and by the high number of young of the year captured in February 2008 (Colautti et al., 2010). For example, a fish that was captured on 12 February 2008 and had 2 bands was calculated to have an age of 408 d (1.12 years).

Bias and precision of age estimations were assessed according to the methods proposed by Goldman et al. (2012). The thin sections of vertebrae from the same specimen were read twice by 2 different readers, and the analysis of bias in age determination was carried out with a bias plot (Campana et al., 1995; Officer et al., 1996). The indices of average percent error (Beamish and Fournier, 1981) and the average coefficient of variation (Chang, 1982) were calculated to assess the precision of the age determination between the 2 readers as well as between both readings of each reader (Ogle, 2015). Differences in readings between readers were reconciled by both readers reading a third time the samples for which they had different band counts. If agreement on a band count was not reached with the additional readings, the sample was eliminated from further analysis.

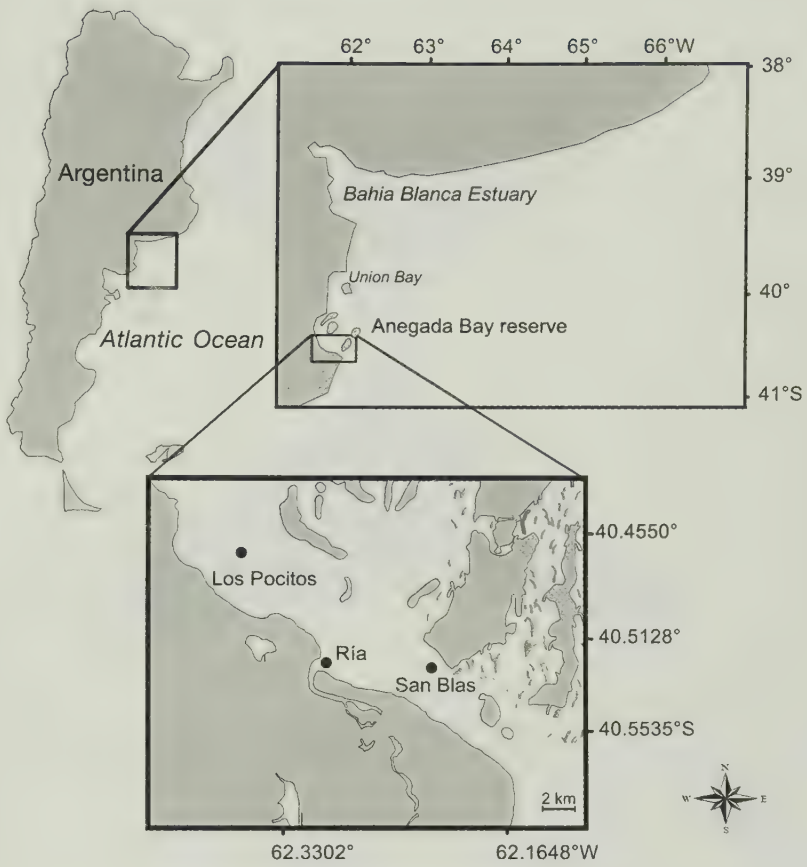

Figure 1

Map of the study area showing the 3 sampling stations, Los Pocitos, Ría, and San Blas, where narrownose smooth-hound (*Mustelus schmitti*) were captured in 2008 in a protected area, the Reserva Natural de Uso Múltiple Bahía San Blas, located in Anegada Bay, Buenos Aires Province, Argentina.

Estimates of somatic growth

To model growth, we used partial ages because they have been shown to be more accurate than rounded ages (Smart et al., 2013). To calculate the partial ages, we used the fraction of the year that had elapsed from the time of birth to the time each individual was collected. Partial ages were then grouped in 0.5-year bins.

[7] Mention of trade names or commercial companies is for identification purposes only and does not imply endorsement by the National Marine Fisheries Service, NOAA.

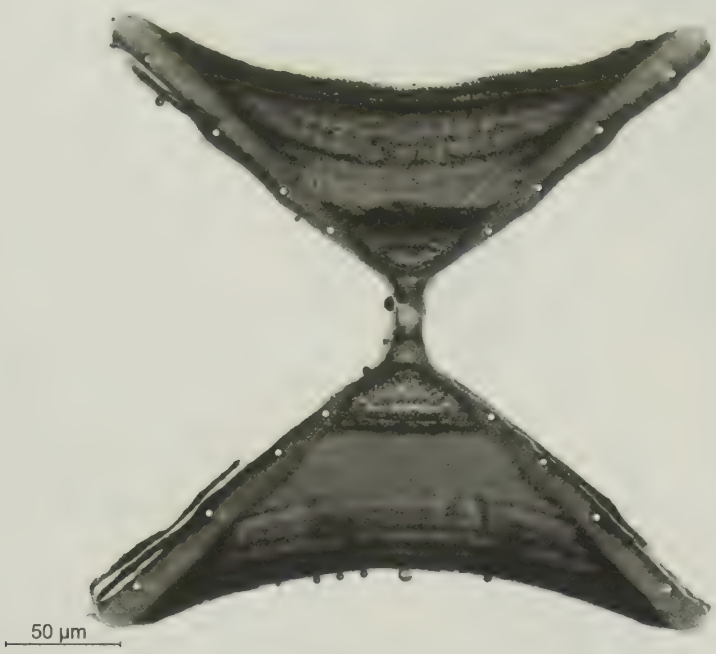

Figure 2

Image of a transverse section of the centrum of a vertebra of a narrownose smooth-hound (*Mustelus schmitti*) caught in Anegada Bay, Argentina, in 2008. The white dots indicate growth bands (narrow and hypermineralized). The first dot from the centrum is the birth mark.

We modeled growth by using a multimodel approach, a method recommended over the use of a single-model approach (Cailliet et al., 2006; Katsanevakis and Maravelias, 2008; Ogle, 2015). To fit the age data, 7 candidate growth models were chosen a priori: 3 variants of the von Bertalanffy growth function (VBGF) (von Bertalanffy, 1938), plus Francis and Mooij parameterizations of the VBGF model (Table 1; Francis, 1988; Mooij et al., 1999); the logistic function (Ricker, 1976); and the Gompertz function (Gompertz, 1825) with the parameterization of Ricker (1976). The 3 variants of the VBGF model used the original, traditional, and fixed length-at-birth parameter (L_0), respectively. The advantage of the model with the Francis parameterization lies in the noncorrelation between the growth coefficient (K) and the asymptotic length (L_∞) parameters (Francis, 1988). The model with the Mooij parameterization estimates the (G_{init}) parameter, which has a clear biological interpretation as the initial growth rate in length per year; in contrast, the VBGF growth parameter K cannot be interpreted biologically (Mooij et al., 1999).

For the fixed-L_0 variant model and the model with the Mooij parameterization, L_0 was calculated by following Conrath (2005) and using a value that represents a compromise between the largest embryo and the smallest free-living individual captured. For the original VBGF and logistic models, L_0 was estimated by the nonlinear least-squares routine. The use of L_0 is biologically meaningful for chondrichtyan fishes (Cailliet et al., 2006). The parameter L_∞ can be compared directly between models (the Francis parameterization of the VBGF allows for calculation of L_∞ and K; Ogle, 2015). In contrast, the parameters of growth completion of each model, K (VBGF), G (Gompertz), g (logistic), and G_{init} (Mooij), cannot be compared because they are measures of different processes.

For each model, the parameter estimates that were best fitted to the data were calculated by using the nls function in the statistical software R, vers. 3.2.4 (R Core Team, 2016) and specific functions from the FSA package, vers. 0.8.1, in R (Ogle, 2015).

Back-calculation methods are used to describe the growth history (lengths at previous ages) of each individual fish, and currently there are many approaches in use: Francis (1988) provides a thorough revision of back-calculation methods, and Goldman et al. (2012) and Cailliet et al. (2006) provide a review of these methods applied to chondrichthyan fishes. We employed a Fraser–Lee approach to back calculate the length-at-age data, with which we fitted our models to estimate the growth parameters, and compared length at ages calculated from our observational data.

To assess the fit of each model, we used a bias-corrected Akaike information criterion (AICc) and the Bayesian information criterion (BIC) (Burnham and Anderson, 2002; Katsanevakis, 2006; Zhu et al., 2009; Lopez Cazorla et al., 2014). The model with the lowest AICc and BIC values was chosen as the most appropriate to describe the growth of narrownose smooth-hound.

Differences, by sex, in estimates of growth parameters from the selected model were assessed with likelihood ratio tests (Kimura, 1980) and extra sum-of-squares tests (Ritz and Streibig, 2008). To identify which growth parameter differ between sexes, we fitted iterative models: the most complex model represents the case where all 3 growth parameters differ among sexes. The simplest model represents the case where none of the parameters differ between females and males. Between these 2 extremes, we built 3 models where 2 parameters differ and 3 models where only 1 parameter differs between sexes (Ogle, 2015). Protocols for selection of AICc and BIC were used to select the most appropriate model, as described previously.

To test the overall growth performance, the growth performance index (ϕ) was calculated (Pauly, 1984) by employing the parameters from the selected model:

$$\phi = \log_{10}K + 2\log_{10}L_\infty. \quad (1)$$

This index is useful because it reduces the correlation between L_∞ and K, and that reduction is desirable for comparisons of growth among studies of different species.

Table 1

Equations of the 7 growth models fitted to the length-at-age data of narrownose smooth-hound (*Mustelus schmitti*) collected in 2008 in Anegada Bay, Argentina, where VBGF=the von Bertalanffy growth function; L_t=length at age t; L_0= length at age 0; L_0*=the fixed length at age 0; t_1=age 1; t_3=the maximum age recorded;, t_2=an age between t_1 and t_3; L_1=length at age t_1; L_2=length at age t_1; L_3=length at age t_3; L_∞=asymptotic length; and K, g, G, and G_{init}=the growth coefficients of the different models. In the Francis model, $r=(L_3-L_2)\ /\ (L_2-L_1)$. In the Gompertz model, a=the instantaneous growth rate at the inflection point of the curve.

Model	Growth function
Original VBGF	$L_t = L_0 + (L_\infty - L_0) \times (1 - \exp^{[-K \times t]})$
Traditional VBGF	$L_t = L_\infty \times (1 - \exp^{[-K(t - t0)]})$
Fixed-L_0 VBGF	$L_t = L_0{}^* + (L_\infty - L_0{}^*) \times (1 - \exp^{(-K \times t)})$
Francis	$L_t = L_1 + (L_3 - L_1) \times ([1 - r^{2([t - t1] / [t3 - t1])}] / [1 - r^2])$
Mooij	$L_t = (G_{init} \times [L_\infty - L_0{}^*] / L_\infty) \exp^{(Ginit/L\infty)t}$
Logistic	$L_t = (L_0 \times L_\infty) / (L_0 + [L_\infty - L_0]) \exp^{(-g \times t)}$
Gompertz	$L_t = L_0 \times (\exp^{G[1 - \exp(-g \times t)]})$

The longevity was assumed to be the age at 95% of L_∞ by using Fabens (1965) equation. Natural mortality (M) was calculated, by following Booth et al. (2011), as the median of the empirical model of Pauly (1980), Hoenig (1983), and Jensen (1996):

$$M_{(Pauly)} = \exp(-0.0152 - 0.279\ln L_\infty + 0.6543\ln K + 0.463\ln T), \quad (2)$$

$$M_{(Hoenig)} = \exp(1.44 - 0.982\ln t_{max})), \text{ and} \quad (3)$$

$$M_{(Jensen)} = 1.6K, \quad (4)$$

where L_∞ and K = the VGBF model parameters;
T = the mean water temperature (12.7°C); and
t_{max} = the age of the oldest fish sampled (Hoenig, 1983).

Results

A total of 1577 narrownose smooth-hound, with sizes ranging from 300 to 810 mm TL (mean: 460 mm TL [standard error (SE) 90 mm]; mode: 390 mm TL), were collected. Of these sharks, 245 were subsampled. Sizes of subsampled fish ranged from 320 to 810 mm TL (mean: 490 mm [SE 90 mm TL]; mode: 400 mm TL) (Fig. 3). Of the fish examined, 52.46% were females, ranging in size between 331 and 810 mm TL, and 47.54% were males, with a size range of 320–791 mm TL.

In the vertebrae of narrownose smooth-hound, we observed a pattern of alternating opaque and translucent bands and an annual cycle in the seasonal evolution of the proportion of translucent edges (Fig. 4). Vertebrae with translucent margins increased in February (summer), reached a 76% peak in May (autumn), and decreased to a value of approximately 11% from August (winter) to November (spring).These data indicate a yearly periodicity in translucent band formation. The total number of individuals used for this analysis was slightly smaller than the total subsample number because of illegibility of the edge of the vertebra of 23 individuals. This illegibility was the result of an error in the concentration of hypochlorite used for cleaning. The outer layer of these 23 vertebrae was corroded by hypochlorite and, therefore, was illegible.

The ages determined for the total population ranged from 0 to 11 years. A pattern of increase in length with age was observed (Table 2); however, this pattern was not consistent at some ages, particularly at ages of 0–1 years and above 6–7 years, where the number of individuals was proportionally low. Results for back-calculated length at age indicated a more consistent pattern of increase in length with age but also abrupt leaps in length at older ages. The age bias plot shows no systematic bias between the 2 readers (Fig. 5), with a range of error from −2 to 1 band, and a percentage of agreement of 82.45%. Estimation of ages was highly precise, according to the average percent error and average coefficient of variation (4.54% and 3.23%, respectively). Band counts by reader 1 had a range of error of −3 to 3 bands and a percentage of agreement of 87.82%. Obtained values of average percent error and average coefficient of variation for reader 1 indicate a precise age estimation (3.94% and 2.79%, respectively). Band counts by reader 2 had a range of error from −4 to 3 bands and a percentage of agreement of 82.88%. Average percent error and average coefficient of variation for reader 2 indicate precise age estimation (3.05% and 2.15%, respectively).

Age 1 was the most predominant age for both sexes, representing 19.54% of all females and 19.64% of all males, followed by age 2 for females with 18.04% and age 3 for males with 17.85% (see Table 2).

Our back calculation of length-at-age data produced 2162 observations. Back-calculated mean and SE values are presented in Table 2. Although within the SE

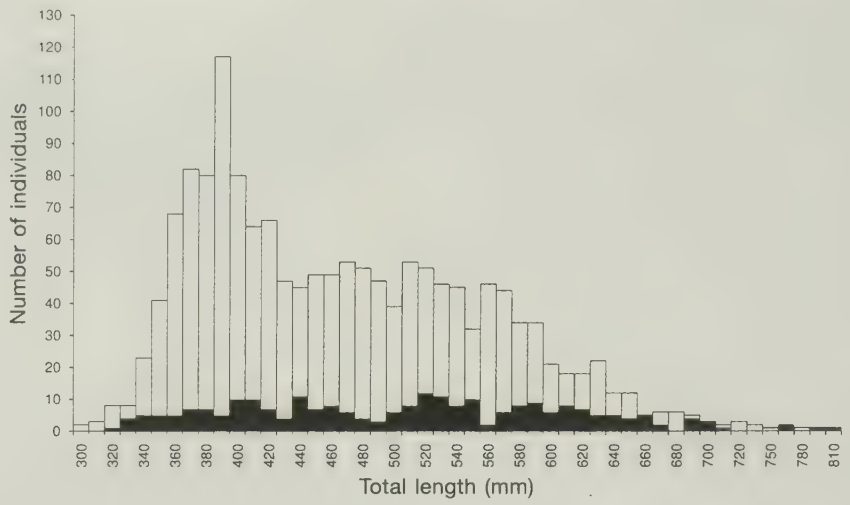

Figure 3

Size distribution of the narrownose smooth-hound (*Mustelus schmitti*) caught in Anegada Bay, Argentina, in 2008. The white bars represent the total sample (n=1547) at a given total length, and the black bars represent the subsample composed of 10 randomly selected specimens of each size (n=245). Samplings were conducted in February (summer), May (autumn), August (winter) and November (spring).

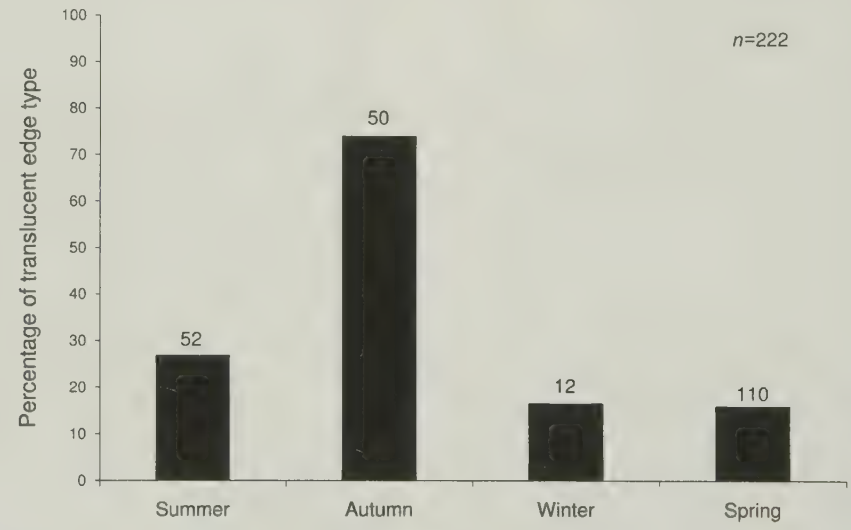

Figure 4

Seasonal change in the percentage of translucent bands at the edge of the vertebrae of narrownose smooth-hound (*Mustelus schmitti*) caught in Anegada Bay, Argentina, in 2008. The numbers above the bars indicate the number of individuals sampled in each season. Sampling was conducted seasonally in February (summer), May (autumn), August (winter), and November (spring). Note that the vertebrae of 222 individuals were used for age determination—a number slightly smaller than the the size of the subsample (n=245) because 23 individuals were not used as a result of the ilegibility of the edge of their vertebrae.

Table 2

Mean length at age of male and female narrownose smooth-hound (*Mustelus schmitti*) collected in 2008 in Anegada Bay, Argentina, according to vertebral readings. Fish lengths are given as total lengths (TLs) in centimeters, with standard errors (SEs). Back-calculation methods are used to describe the growth history (lengths at previous ages) of each individual fish sampled, providing a much larger sample size to perform modeling of growth to compare with growth from the observed data.

	Observed data						Back-calculated data					
	Females			Males			Females			Males		
Age	*n*	Mean TL	SE	*n*	Mean TL	SE	*n*	Mean TL	SE	*n*	Mean TL	SE
0	2	364.5	44.6	7	348.3	50.2	247	372.0	35.7	237	369.4	37.2
1	26	396.7	38.4	22	390.8	43.1	223	437.3	48.4	187	440.2	46.5
2	24	451.2	54.9	17	451.1	39.5	175	498.1	50.9	145	495.4	47.0
3	13	489.7	63.4	20	504.5	40.3	142	540.9	52.6	110	530.2	46.8
4	10	522.4	49.0	14	551.9	40.2	126	572.3	48.8	75	559.1	45.3
5	10	553.1	62.6	9	570.3	39.3	100	591.9	49.6	66	582.1	46.3
6	11	584.0	43.4	8	576.1	51.5	87	616.6	55.1	39	596.9	45.9
7	10	587.3	50.2	5	601.6	47.2	63	639.5	51.4	24	625.2	43.7
8	6	618.3	45.0	5	615.8	27.2	41	654.6	46.2	19	658.9	64.0
9	9	634.7	38.9	3	661.0	48.5	24	692.4	51.5	12	681.6	50.9
10	9	687.8	35.0	1	669.0		14	733.7	45.8	2	718.7	86.9
11	3	755.7	61.2	1	791.0		2	761.0	0.0	2	791.0	0.0

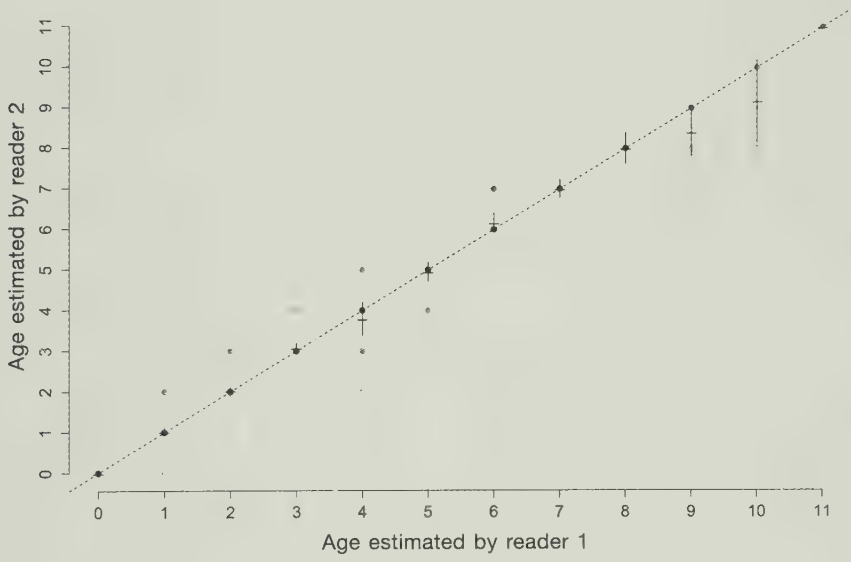

Figure 5

Differences in estimated ages (in years) for 2 readers of vertebrae of narrownose smooth-hound (*Mustelus schmitti*) caught in Anegada Bay, Argentina, in 2008. The dashed line represents total agreement of the readers, and the dots indicate differences between readers for individuals of each age, with darker shading representing a greater number of individuals. The short, black horizontal dashes represent the mean ages of individuals in each age class, and the vertical lines represent the standard deviations of the means.

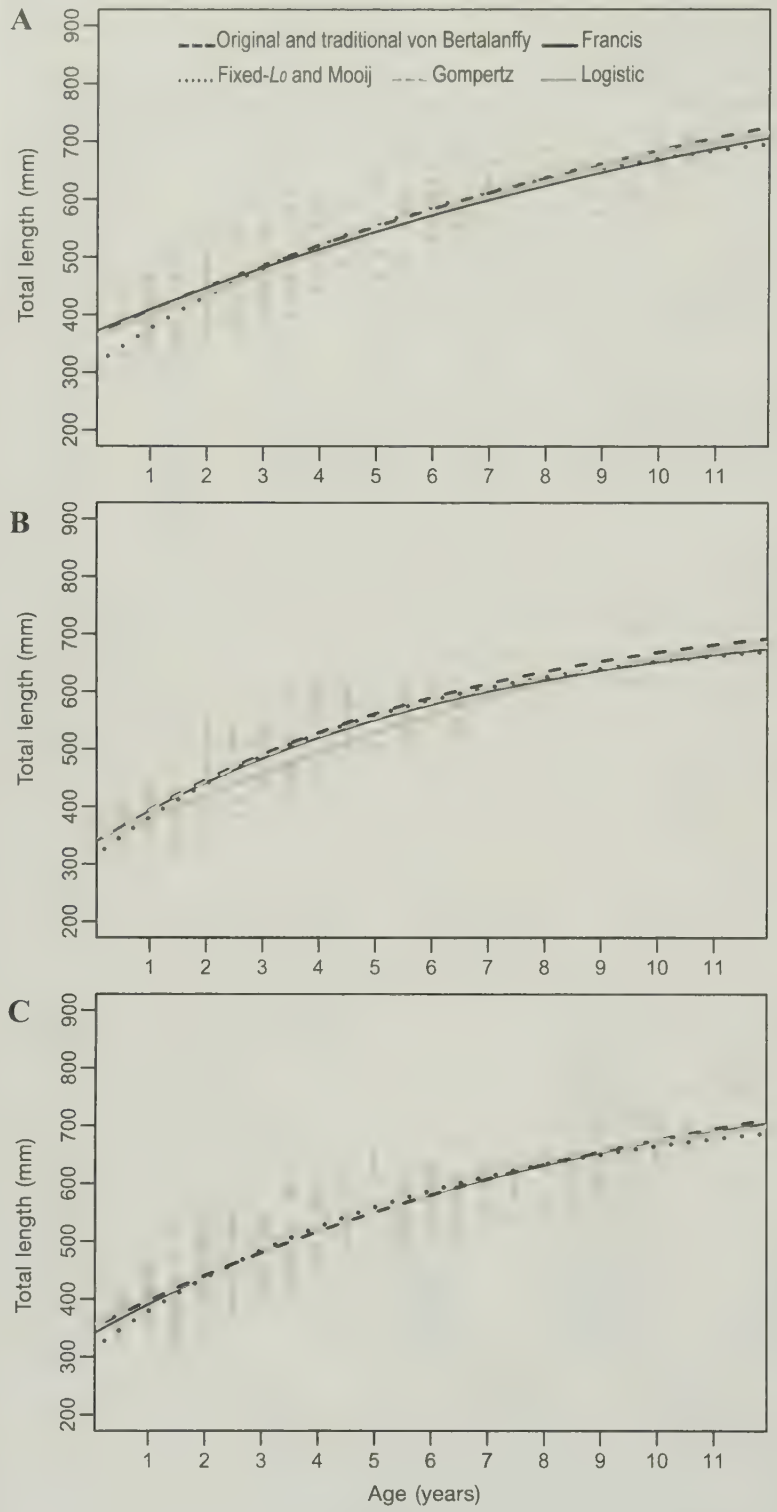

Figure 6

Growth curves for (**A**) females, (**B**) males, and (**C**) the entire sample of narrownose smooth-hound (*Mustelus schmitti*) captured in Anegada Bay, Argentina, in 2008. Black dots indicate data points for females and males. Note that curves for the original and traditional VBGF models and for the fixed-L_0 variant and the model with the Mooij parameterization are identical; therefore, each pair has only one type of line.

values of the means from the observational data, back-calculated lengths were higher than the observed lengths (i.e., a slight positive Lee phenomenon occurred in the data). This trend was more evident for females than for males.

The 7 growth models used to determine the growth parameters of narrownose smooth-hound fitted the age data adequately (Fig. 6, A and B). For females, the original and traditional VBGF, Francis parameterization (L_∞=888.93, calculated from L_1, L_2, and L_3), and Gompertz models provided somewhat similar estimates for L_∞. In comparison with results from those models, L_∞ from the fixed-L_0 variant and the model with the Mooij function were lower, and the logistic model provided an intermediate estimate of L_∞. For males, the situation was analogous; however, L_∞ from the logistic model was similar to the values of L_∞ estimated by the original and traditional VBGF, Francis parameterization (L_∞=748.05, calculated from L_1, L_2, and L_3), and Gompertz models. These parameter estimates are shown in Table 3. Back-calculated data fitted to the growth functions that were employed produced results similar to those obtained from the observational data. It is worth noting that, for females, the estimates for L_∞ were lower than those obtained from the observational data, but, for males, this pattern was not observed (Table 3).

For females, the original and traditional VBGF variants and the model with the Francis parameterization of the VBGF produced the smallest AIC and BIC values and the highest Akaike weight of evidence (w, the conditional probability of each model); when combined, these 3 growth models represented more than 65% of the weight of evidence (Table 4). The Gompertz model ranked second with a w of 0.17 for females. The fixed-L_0 VBGF variant and the model with the Mooij parameterization of the VBGF produced higher values of AIC and BIC and a low w for females. For males, the fixed-L_0 variant and the model with the Mooij parameterization had the lowest AIC and BIC values and high w. Although the original and traditional variants and the model with the Francis parameterization ranked second, they account for much of the combined w. All model

Table 3

Mean estimates, observed and back calculated (BC) with standard errors (SEs), of growth parameters for the narrownose smooth-hound (*Mustelus schmitti*) ca`ptured in Anegada Bay, Argentina, in 2008, determined with the 7 growth models. VBGF=the von Bertalanfy growth function; L_1=length at age 1; L_2=the length at an age between 1 and the maximum age recorded; L_3=length at maximum age recorded, L_∞=the asymptotic length; and K, g, G, and G_{init}=the growth coefficients of the different models. Lengths are given as total lengths in centimeters.

		Females				Males				Sexes combined			
Growth model		Observed estimate	SE	BC estimate	BC SE	Observed estimate	SE	BC estimate	BC SE	Observed estimate	SE	BC estimate	BC SE
Original VBGF	L_∞	893.71	109.23	864.89	33.01	762.56	72.15	786.43	62.55	855.14	77.52	878.81	13.80
	L_0	365.96	13.34	387.78	9.14	334.58	16.21	390.35	9.53	342.89	10.53	370.63	2.97
	K	0.061	0.036	0.166	0.028	0.151	0.047	0.137	0.036	0.104	0.026	0.150	0.014
Traditional VBGF	L_∞	893.73	109.23	864.88	33.01	762.56	72.16	786.43	62.55	855.14	77.52	878.81	13.80
	K	0.061	0.036	0.166	0.028	0.151	0.047	0.137	0.036	0.104	0.026	0.150	0.014
	t_0	−6.95	1.93	−4.26	0.60	−3.82	0.92	−5.02	0.92	−4.93	0.83	−4.60	0.19
Fixed-L_0 VBGF	L_∞	765.81	34.80	718.31	13.51	710.39	33.45	702.44	18.66	745.20	24.04	758.38	6.36
	K	0.160	0.024	0.217	0.019	0.190	0.030	0.340	0.025	0.169	0.016	0.174	0.016
Francis	L_1	365.96	13.34	387.78	9.14	334.58	16.21	390.35	9.53	342.89	10.53	373.36	6.58
	L_2	564.92	7.17	613.59	3.28	578.09	6.89	599.62	4.06	573.34	4.70	608.32	2.55
	L_3	706.33	15.43	704.18	10.79	683.05	21.78	698.32	16.49	700.12	12.12	704.26	9.09
Mooij	L_∞	765.81	34.80	718.31	13.51	710.39	33.45	702.44	18.66	745.20	24.04	758.38	6.36
	G_{init}	119.31	10.72	162.80	8.47	137.22	13.65	155.10	10.48	125.62	8.16	146.45	7.70
Gompertz	L_∞	862.53	102.37	840.93	24.81	742.70	43.51	751.05	44.11	788.81	47.01	749.33	22.76
	G	−0.13	0.11	−0.46	0.04	−0.28	0.06	−0.44	0.07	−0.20	0.06	−0.44	0.04
	t	0.13	0.04	0.22	0.03	0.22	0.05	0.19	0.04	0.16	0.03	0.21	0.02
Logistic	L_∞	815.52	51.93	777.30	8.38	758.68	51.94	757.36	11.37	753.75	34.22	730.46	18.14
	L_0	362.80	11.73	382.14	8.86	340.32	13.24	398.74	7.87	354.13	8.64	398.88	5.36
	g	0.182	0.020	0.406	0.018	0.208	0.027	0.402	0.023	0.223	0.028	0.260	0.023

curves fitted to the growth data can be observed in Figure 6A for females and 6B for males. Note that the original and traditional VBGF variants and the model with the Francis parameterization of the VBGF have the exact same AIC and BIC values because they are algorithmic modifications of the same model; hence, AIC and BIC values will not change. The same is true for the fixed-L_0 variant and the model with the Mooij parameterization of the VBGF.

We chose to use the original VBGF model in our comparisons of growth between sexes for narrownose smooth-hound. The likelihood ratio test for the original VBGF model revealed no significant differences in growth between sexes for each parameter (mean χ^2: 1.94 [SE 0.22]; P>0.15). Extra sum-of-squares tests produced a similar result, failing to identify any differences in the growth parameters between sexes (mean F=1.28 [SE 0.51]; P>0.15). The AIC, BIC, and w values presented in Table 5 also indicate that there were no differences between sexes in growth parameters. For females and males combined, estimates of the growth parameters from the 7 growth models are shown in Table 3, with the corresponding fitted growth curve shown in Figure 6C.

The overall ϕ, calculated by using the parameters of the original VBGF model, was 4.69 for females and 4.94 for males.

Longevity was 20.87 years and 12.24 years for females and males, respectively. Total natural mortality rates were 0.19/year and 0.26/year for females and males, respectively.

Discussion

Age and growth estimates for fish have been shown to be highly dependent on the size range of collected samples (Campana, 2001). For example, Lessa et al. (2016) in their study of the crocodile shark (*Pseudocarcharias kamoharai*) did not capture small individuals, and the lack of small fish introduced a bias in their estimates of the growth parameters. This bias makes their results applicable to only the study area or appropriate for extrapolation only for populations with a similar size composition. In long-lived species >30 years, e.g. Lamniformes like the white shark (*Carcharodon carcharias*), or the shortfin mako (*Isurus oxyrinchus*), the lack of larger individuals in a sample can result in an underestimation of maximum age (Ardizzone et al., 2006; Natanson et al., 2006; Hamady et al., 2014; Andrews and Kerr, 2015). In our study of narrownose smooth-hound, the size of individuals captured ranged from 300 mm TL up to 810 mm TL; in other studies, individuals >850 mm TL, when present, have not been

Table 4

Akaike and Bayesian information criterion (AIC and BIC) values and Akaike weight of evidence (w) for the 7 growth models applied to the age data of the narrownose smooth-hound (*Mustelus schmitti*) captured in 2008 in Anegada Bay, Argentina. VBGF=von Bertalanfy growth function.

	Females			Males		
Growth model	AIC	BIC	w	AIC	BIC	w
Original VBGF	1396.4	1407.9	0.22	1213.5	1224.4	0.14
Traditional VBGF	1396.4	1407.9	0.22	1213.5	1224.4	0.14
Fixed-L_0 VBGF	1401.6	1410.3	0.02	1212.4	1220.6	0.24
Francis	1396.4	1407.9	0.22	1213.5	1224.4	0.14
Mooij	1401.6	1410.3	0.02	1212.4	1220.6	0.24
Gompertz	1396.9	1408.4	0.17	1214.9	1225.8	0.07
Logistic	1397.5	1409.0	0.13	1216.3	1227.2	0.03

abundant (Menni, 1985; López Cazorla, 1987; Batista, 1988; Massa and Lasta[2]; Hozbor et. al.[6]). Some authors have reported maximum sizes for this species of up to 1020 mm TL, but fish in their studies were found in populations that inhabited open waters (Hozbor et al.[6]); all published studies conducted on populations inhabiting the coastal areas of Argentina have reported size ranges similar to those of our study (Chiaramonte and Pettovello, 2000; Sidders et al., 2005; Segura and Milessi, 2009). It is because of this similarity in size ranges that we consider our findings representative of and applicable to other coastal populations of narrownose smooth-hound.

Table 5

Akaike and Bayesian information criterion (AIC and BIC) values and Akaike weight of evidence (w) for 8 different versions of the original von Bertalanffy growth function model used for the comparison of growth between sexes: L_∞, L_0, K, the growth model where L_∞, L_0, and K are different between sexes; L_∞, K, the growth model where both L_∞ and K are different between sexes; L_∞, L_0, the growth model where both L_∞ and L_0 are different between sexes; L_0, K, the growth model where both L_0 and K are different between sexes; only L_∞, the growth model where only L_∞ is different among sexes; only K, the growth model where only K is different among sexes; only L_0, the growth model where only L_0 is different among sexes; and none, the growth model where all parameters are equal for both females and males.

Models	AIC	BIC	w
L_∞, L_0, K	2607.85	2632.36	<0.001
L_∞, K	2607.29	2628.30	0.005
L_∞, L_0	2607.89	2628.89	0.003
L_0, K	2607.83	2628.84	0.004
Only L_∞	2605.89	2623.40	0.053
Only K	2605.88	2623.39	0.053
Only L_0	2605.89	2623.39	0.053
None	2603.89	2617.90	0.829

Another important aspect of any age and growth study on fish is verification of the estimated parameters (Goldman et al., 2012). Verification of estimated age and growth parameters have been undertaken for several species of the *Mustelus* genus (i.e., Cailliet et al., 1990; Yudin and Cailliet, 1990; Moulton et al., 1992; Goosen and Smale, 1997; Farrell et al., 2010). This genus deposits growth bands annually, and the deposition of translucent bands occurs during summer–autumn (Cailliet et al., 1990; Yudin and Cailliet, 1990; Moulton et al., 1992; Goosen and Smale, 1997; Farrell et al., 2010); our results on narrownose smooth-hound correspond with this finding. Moreover, the associated notching pattern observed in our study was similar to patterns reported for other species of *Mustelus* (i.e., Moulton et al., 1992; Conrath et al., 2002; Farrell et al., 2010). The precision in interpreting these growth bands was also high between readers and within readers, providing confidence in the reproducibility of our results. The lack of an adequate number of older sharks in our sample might have led to an underestimation of L_∞; however, the similarity of estimates between our observational data and the back-calculated data fortunately indicates that our sample size was adequate. The lower SE values for the back calculations, compared with the SE values for the observational data, indicate that these calculations may accurately reflect the growth parameters for narrownose smooth-hound. Nevertheless, it is important to note that for back-calculated results, it is assumed that growth is constant and does not change over time (Goldman et al., 2012).

The maximum age determined for narrownose smooth-hound in our study is similar to ages reported for some species of *Mustelus* (Cailliet et al., 1990; Yudin and Cailliet, 1990; Farrell et al., 2010) and is lower than age ranges determined for larger *Mustelus* species (Yudin and Cailliet, 1990; Moulton et al., 1992; Goosen and Smale, 1997; Conrath et al., 2002; Farrell et al.,

Table 6

Size range (total lengths in millimeters), maximum age measured (t_{max}), asymptotic length (L_∞), and growth coefficient (K) of the von Bertalanffy growth function and growth performance index (ϕ) for 9 species of the *Mustelus* genus from this study and other studies.

Species	Size range (mm TL)	t_{max}	L_∞	K	ϕ	Main reference
Mustelus schmitti	300–810	11	894	0.06	4.69	This study
Mustelus schmitti	390–950	16	1000	0.10	5.00	Hozbor et al.[6]
Mustelus schmitti	250–960	14	1028	0.08	4.92	Batista, 1988
Mustelus antarcticus	600–1700	16	2000	0.12	5.68	Moulton et al., 1992
Mustelus californicus	235–1250	9	1500	0.17	5.58	Yudin and Cailliet, 1990
Mustelus henlei	257–1000	13	1000	0.22	5.34	Yudin and Cailliet, 1990
Mustelus manazo	680–800	10	2000	0.10	5.60	Cailliet et al., 1990
Mustelus mustelus	360–1640	24	2000	0.07	5.44	Goosen and Smale, 1997
Mustelus walkeri	410–1050	16	2000	0.07	5.44	Rigby et al., 2016
Mustelus asterias	440–1120	13	1000	0.19	5.27	Farrell et al., 2010
Mustelus canis	330–1320	16	1200	0.29	5.62	Conrath et al., 2002

2010; Rigby et al., 2016) (Table 6). To date, only one technical report and a M.S. thesis have described the age of narrownose smooth-hound (Batista, 1988; Hozbor et al.[6]), and both of these publications report on studies that included in their sampling fish older than the fish that we captured (Table 6). It is likely that the larger and older fish in the Hozbor et al.[6] and Batista (1988) studies account for the differences in range of ages between our study and theirs. The results of Hozbor et al.[6] are consistent with our results for the mean lengths at age for ages below 5 years, but, for animals >5 years, they report larger sizes at age. Batista's (1988) mean lengths at age, however, are greater than our estimations for almost all ages, but he did not provide length at age for age 0 and 1 and did not capture males older than 7 years, which makes throughout comparisons difficult.

In the population of narrownose smooth-hound in Anegada Bay, the rate of growth reflected in the increments in the mean length at age was not consistent for some ages. A similar phenomenon was reported by Hozbor et al.[6] and Batista (1988), as well as in studies of other shark species (Cailliet et al., 1990, Goldman et al., 2006, Farrel et al., 2010, Fernandez-Carvalho et al., 2015). In a number of other studies on the age and growth of elasmobranches, tables of length at age are not presented (e.g., Kusher et al., 1992; Goosen and Smale, 1997; Smith et al., 2003, 2007; McFarlane and King, 2006; Booth et al., 2011; Joung et al., 2016; Lessa et al., 2016); therefore, it is difficult to determine whether this phenomenon is more or less universal for elasmobranchs or restricted to certain species.

The narrownose smooth-hound attains an appreciably smaller L_∞ and K than other representatives of the *Mustelus* genus, with the exception of the starspotted smooth-hound (*M. manazo*) (Yudin and Cailliet, 1990; Table 6). In comparison with values reported by Batista (1988) and Hozbor et al.[6], who also worked with narrownose smooth-hound, values of L_∞ and K from our study were also much lower. A possible explanation for this result is that the overall size distribution of the samples used by Batista (1988) and Hozbor et al.[6] included many large individuals (>850 mm TL), which were not present in our study, and only a low number of small individuals (<400 mm TL) both of which had a consequent effect on the asymptotic behavior of the VBGF. In these 2 studies, more than 60% of the individuals were larger than 600 mm TL, but samples in our study only 20% of individuals were above that TL. As Campana (2001) points out, skewed size distributions can introduce bias in age estimates, and differences in size distributions between studies can accentuate such differences.

Differences in the estimations of L_∞ and K can also arise from differences in the aging techniques employed. Whereas Batista (1988) used whole vertebra and Hozbor et al.[6] employed sectioned vertebra, we used thinly sectioned slices. Despite their use of theoretically more imprecise vertebra preparations, these authors could identify ages >than 11 years with their methods, indicating that the use of whole vertebrae by Batista (1988) or sectioned vertebrae by Hozbor et al.[6] could be useful enough to study age for this species.

Another possible explanation is the difference in the period of sampling. Hozbor et al.[6] sampled during 2003–2004, almost 5 years before our research. Given the high level of fishing effort exerted on this species between 2004 and 2010 (Massa et al., 2006; Fernández Aráoz et al.[8]), it is possible that natural populations experienced a reduction in their maximum length be-

[8] Fernández Aráoz, N. C., A. N. Lagos, and C. R. Carozza. 2009. Asociación íctica costera bonaerense 'variado costero' capturas declaradas por la flota comercial Argentina durante el año 2008. INIDEP Inf. Tec. Of. 31, 26 p. [Available from website.]

cause larger fish are most likely to be captured first (Beverton and Holt, 1957; Hilborn, 1992). In the case of Batista (1988), sampling was conducted almost 30 years ago, before the considerable increase in fishing effort and capture that took place in Brazil that ultimately produced a decline in populations of narrownose smooth-hound as predicted by Haimovici (1997).

The explanation outlined in the previous paragraph is also supported by the difference observed in the mean length at age calculated in each study. In Hozbor et al.[6], fish with ages above 5 years had lengths that were larger by a mean of 68.8 mm and 64.1 mm TL for males and females, respectively, than the lengths in our study. Batista (1988) presents even greater differences, with fish up to 80 mm TL larger than the fish in our study. It is likely that the largest and oldest specimens present in the populations sampled by Hozbor et al.[6] and Batista (1988) were not present in the population we sampled because they would have been removed by fishing, and their absence from our sample, therefore, potentially influenced the estimate of L_∞ that we calculated. Reduction in the length by age is a serious consequence of overfishing in all fish populations (Beverton and Holt, 1957; Murawski, 2000; Froese, 2004); therefore, if this is the case, special attention should be paid to the possibility of stock depletion by fishing in the coastal populations of narrownose smooth-hound.

Lastly, geographic location may have played a role in the differences in parameter estimates between Hozbor et al.[6] and Batista (1988) and our study. The sampling area for Hozbor et al.[6] extended from the Uruguayan–Argentinean common fishing zone to the open sea region of El Rincón (39 – 41° S) in Argentina, and Batista (1988) performed his sampling on the Brazilian shelf near Rio Grande do Sul. Unfortunately, to our knowledge, biological differences between the stocks of narrownose smooth-hound of Argentina and Brazil have not been studied yet, or if they have, results remain unpublished.

Values of ϕ calculated for narrownose smooth-hound in our study indicate a slower rate than that of other representatives of the *Mustelus* genus. Results from Batista (1988) and Hozbor et al.[6] indicate growth rates similar to those in our study, albeit slightly greater (Table 6). It is important to point out that despite the differences in the estimations of L_∞ and K between our study and those of Batista (1988) and Hozbor et al.[6], the values of ϕ for this species were closer for those studies and ours than for studies of the other *Mustelus* species examined.

Differences in growth parameters, by sex, are commonplace with sharks, especially for viviparous species (Cortés et al., 2010), like the night shark (*Carcharhinus signatus*; Lessa et al., 2000), the crocodile shark (Lessa et al., 2016), and the bigeye thresher (*Alopias superciliosus*; Fernandez-Carvalho et al., 2015). However, there are also examples for which no differences exist between sexes , as with the sandbar shark (*C. plumbeus*; Casey et al., 1985), the oceanic whitetip shark (*C. longimanus*; Seki et al., 1998), the sharptooth houndshark (*Triakis megalopterus*; Booth et al., 2011), the bull shark (*C. leucas*; Neer et al., 2005), and the blue shark (*Prionace glauca*; Skomal and Natanson, 2003).The differences in estimated growth parameters for male and female narrownose smooth-hound, that are observed with other species, were not statistically significant in our study. Despite this lack of significant difference, males appear to grow faster in their first year (G_{init}: 137.22 mm TL of growth in the first year) than females (G_{init}: 119.31 mm TL of growth in the first year), and males also reach a higher TL at half t_{max} (L_2: 578.09 mm TL) than that of females (L_2: 564.92 mm TL), and females attain a larger L_∞. These types of differences have been reported recently for the closely related species, the eastern spotted gummy shark (*M. walkeri*; Rigby et al., 2016).

Successful and sustainable management of any fishery is based on robust and accurate estimates of growth, which in turn are dependent on quality age and growth studies (Fernandez-Carvalho et al., 2015). Therefore, it is essential to improve science-based fishery data. The narrownose smooth-hound of Anegada Bay has a relatively fast growth in its initial year of life, reaching a length of approximately 400 mm TL. Growth slows down in subsequent years, and, according to our results, length at first maturity (546 and 563 mm TL for males and females respectively; Colautti et al., 2010) is reached at an age of 7.61 years for females and 6.79 years for males. These values represent a maturation rate comparable to that of other species of *Mustelus*; for example, the eastern spotted gummy shark matures at an age around 7–9 years and at a length of 670 to 800 mm TL (Rigby et al., 2016).

This late age at first maturity of the narrownose smooth-hound is indicative of a high susceptibility to fishery-induced mortality and highlights the importance of conservation for the slow-maturing species in this genus. Consequently, narrownose smooth-hound individuals of 600 mm TL or less should be excluded from catches of commercial fisheries, an approach that would mean excluding sharks younger than, approximately, 7 years. Despite the relatively high rate of estimated natural mortality, modeling results indicate that protection of old adults is more appropriate than protection of juveniles in the case of shark fisheries (Prince, 2005). Whether this importance of protecting old adults applies to narrownose smooth-hound (or any other small triakid sharks) has yet to be evaluated and warrants further research.

The slow growth and late age at maturity (for fishing purposes) of the narrownose smooth-hound reported here indicate that this species is vulnerable to overexploitation and that the population studied may have signs of having been deeply affected. Ensuring both a sustainable population and fishery of this species requires management coordinated with a strong foundation on science-based studies for the entire distribution range of this species.

Acknowledgments

The financial support provided by Consejo Nacional de Investigaciones Científicas y Técnicas, Agencia Nacional de Promoción Científica y Tecnológica (project PAE 22666/0), and Universidad Nacional del Sur (project PGI 24/191) is gratefully acknowledged. We also thank N. Hozbor (Instituto Nacional de Investigación y Desarrollo Pesquero), who showed us preparation and observation techniques, and staff at the Laboratorio de Petrotomia (Universidad Nacional del Sur) for their generous assistance in vertebral inclusion.

Literature cited

Andrews, A. H., and L. A. Kerr.
2015. Validated age estimates for large white sharks of the northeastern Pacific Ocean: altered perceptions of vertebral growth shed light on complicated bomb $\Delta^{14}C$ results. Environ. Biol. Fish. 98:971–978.

Ardizzone, D., G. M. Cailliet, L. J. Natanson, A. H. Andrews, L. A. Kerr, and T. A. Brown.
2006. Application of bomb radiocarbon chronologies to shortfin mako (*Isurus oxyrinchus*) age validation. Environ. Biol. Fish. 77:355–366.

Barker, M. J., and V. Schluessel.
2005. Managing global shark fisheries: suggestions for prioritizing management strategies. Aquat. Conserv. 15:325–347.

Batista, V. S.
1988. Determinação de idade e análise do crescimento do cação *Mustelus schmitti* Springer 1939 (Elasmobranchii, Triakidae) da plataforma continental do Rio Grande do Sul. M.S. thesis, 99 p. Universidade Federal do Rio Grande, Rio Grande, Brazil.

Beamish, R. J., and D. A. Fournier.
1981. A method for comparing the precision of a set of age determinations. Can. J. Fish. Aquat. Sci. 38:982–983.

Beverton, R. J. H., and S. J. Holt.
1957. On the dynamics of exploited fish populations. Fish. Invest. Ser. II, vol. 19, 533 p. Her Majesty's Stationery Office, London.

Booth, A. J., A. J. Foulis, and M. J. Smale.
2011. Age validation, growth, mortality, and demographic modeling of spotted gully shark (*Triakis megalopterus*) from the southeast coast of South Africa. Fish. Bull. 109:101–112.

Burnham, K. P., and D. R. Anderson.
2002. Model selection and multimodel inference: a practical information-theoretic approach, 2nd ed., 488 p. Springer-Verlag, New York.

Cailliet, G. M.
1990. Elasmobranch age determination and verification: an updated review. *In* Elasmobranchs as living resources: advances in the biology, ecology, systematics, and the status of the fisheries (H. L. Pratt Jr., S. H. Gruber, and T. Taniuchi, eds.), p. 157–165. NOAA Tech. Rep. NMFS 90.

Cailliet, G. M., K. G. Yudin, S. Tanaka, and T. Taniuchi.
1990. Growth characteristics of two populations of *Mustelus manazo* from Japan based upon cross-readings of vertebral bands. *In* Elasmobranchs as living resources: advances in the biology, ecology, systematics, and the status of the fisheries (H. L. Pratt Jr., S. H. Gruber, and T. Taniuchi, eds.), p. 167–176. NOAA Tech. Rep. NMFS 90.

Cailliet, G. M., W. D. Smith, H. F. Mollet, and K. J. Goldman.
2006. Age and growth studies of chondrichthyan fishes: the need for consistency in terminology, verification, validation, and growth function fitting. Environ. Biol. Fish. 77:211–228.

Campana, S. E.
2001. Accuracy, precision and quality control in age determination, including a review of the use and abuse of age validation methods. J. Fish Biol. 59:197–242.

Campana, S. E., M. C. Annand, and J. I. McMillan.
1995. Graphical and statistical methods for determining the consistency of age determinations. Trans. Am. Fish. Soc. 124:131–138.

Casey, J. G., H. L. Pratt Jr, and C. E Stillwell.
1985. Age and growth of the sandbar shark (*Carcharhinus plumbeus*) from the western North Atlantic. Can. J. Fish. Aquat. Sci. 42:963–975.

Chang, W. Y. B.
1982. A statistical method for evaluating the reproducibility of age-determination. Can. J. Fish. Aquat. Sci. 39:1208–1210.

Chiaramonte, G. E., and A. D. Pettovello.
2000. The biology of *Mustelus schmitti* in southern Patagonia, Argentina. J. Fish Biol. 57:930–942.

Chugunova, N. I.
1963. Age and growth studies in fish; a systematic guide for ichthyologists, 132 p. Israel Program for Scientific Translations, Jerusalem, Israel. [Translated from Russian.]

Colautti, D., C. Baigun, A. Lopez Cazorla, F. Llompart, J. M. Molina, P. Suquele, and S. Calvo.
2010. Population biology and fishery characteristics of the smooth-hound *Mustelus schmitti* in Anegada Bay, Argentina. Fish. Res. 106:351–357.

Conrath, C. L.
2005. Reproductive biology. *In* Management techniques for elasmobranch fisheries (J. A. Musick and R. Bonfil, eds.), p. 103–126. FAO Fish. Tech. Pap. 474. FAO, Rome.

Conrath, C. L., J. Gelsleichter, and J. A. Musick.
2002. Age and growth of the smooth dogfish (*Mustelus canis*) in the northwest Atlantic Ocean. Fish. Bull. 100:674–682.

Cortés, E., F. Arocha, L. Beerkircher, F. Carvalho, A. Domingo, M. Heupel, H. Holtzhausen, M. N. Santos, M. Ribera, and C. Simpfendorfer.
2010. Ecological risk assessment of pelagic sharks caught in Atlantic pelagic longline fisheries. Aquat. Living Resour. 23:25–34.

Dulvy, K. N., J. K. Baum, S. Clarke, L. J. V. Compagno, E. Cortés, A. Domingo, S. Fordham, S. Fowler, M. P. Francis, C. Gibson, et al.
2008. You can swim but you can't hide: the global status and conservation of oceanic pelagic sharks and rays. Aquat. Conserv. 482:459–482.

Fabens, A. J.
1965. Properties and fitting of the von Bertalanffy growth curve. Growth 29:265–289.

Farrell, E. D., S. Mariani, and M. W. Clarke.
2010. Age and growth estimates for the starry smoothhound (*Mustelus asterias*) in the Northeast Atlantic Ocean. ICES J. Mar. Sci. 67:931–939.

Fernandez-Carvalho, J., R. Coelho, J. Mejuto, E. Cortés, A. Domingo, K. Yokawa, K.-M. Liu, B. García-Cortés, R. Forselledo, S. Ohshimo, et al.
2015. Pan-Atlantic distribution patterns and reproductive biology of the bigeye thresher, *Alopias superciliosus*. Rev. Fish Biol. Fish. 25:551–568.

Figueiredo, J. L.
1977. Manual de peixes marinhos do sudeste do Brasil. I. Introdução. Cações, raias e quimeras, 104 p. Museu de Zoologia, Univ. São Paulo, São Paulo, Brazil.

Francis, R. I. C. C.
1988. Are growth parameters estimated from tagging and age–length data comparable? Can. J. Fish. Aquat. Sci. 45:936–942.

Froese, R.
2004. Keep it simple: three indicators to deal with overfishing. Fish Fish. 5:86–91.

Gompertz, B.
1825. On the nature of the function expressive of the law of human mortality, and on a new mode of determining the value of life contingencies. Philos. Trans. R. Soc. Lond. 115:513–583.

Goldman, K. J., S. Branstetter, and J. A. Musick.
2006. A re-examination of the age and growth of sand tiger sharks, *Carcharias taurus*, in the western North Atlantic: the importance of ageing protocols and use of multiple back-calculation techniques. *In* Age and growth of chondrichthyan fishes: new methods, techniques and analysis (J. K. Carlson and K. J. Goldman, eds.), p. 241–252. Springer, Dordrecht, Netherlands.

Goldman, K. J., G. M. Cailliet, A. H. Andrews, and L. J. Natanson.
2012. Assessing the age and growth of chondrichthyan fishes. *In* Biology of sharks and their relatives, 2nd ed. (J. C. Carrier, J. A. Musick, and M. R. Heithaus, eds.), p. 423–452. CRC Press, Boca Raton, FL.

Goosen, A. J. J., and M. J. Smale.
1997. A preliminary study of age and growth of the smoothhound shark *Mustelus mustelus* (Triakidae). S. Afr. J. Mar. Sci. 18:85–92.

Haimovici, M.
1997. Recursos pesqueiros demersais da regiao sul, 80 p. Fundação dos Estudos do Mar, Rio de Janeiro, Brazil.

Hamady, L. L., L. J. Natanson, G. B. Skomal, and S. R. Thorrold.
2014. Vertebral bomb radiocarbon suggests extreme longevity in white sharks. PLoS ONE 9: e84006.

Hilborn, R.
1992. Can fisheries agencies learn from experience? Fisheries 17:6–14.

Hoenig, J. M.
1983. Empirical use of longevity data to estimate mortality rates. Fish. Bull. 82:898–903.

Jensen, A. L.
1996. Beverton and Holt life history invariants result from optimal trade-off of reproduction and survival. Can. J. Fish. Aquat. Sci. 53:820–822.

Joung, S.-J., C.-C. Chen, K.-M. Liu and T.-C. Hsieh.
2016. Age and growth estimates of the Kwangtung skate *Dipturus kwangtungensis* in the waters of northern Taiwan. J. Mar. Biol. Assoc. U.K. 96:1–8.

Katsanevakis, S.
2006. Modelling fish growth: model selection, multi-model inference and model selection uncertainty. Fish. Res. 81:229–235.

Katsanevakis, S., and C. D. Maravelias.
2008. Modelling fish growth: multi-model inference as a better alternative to *a priori* using von Bertalanffy equation. Fish Fish. 9:178–187.

Kimura, D. K.
1980. Likelihood methods for the von Bertalanffy growth curve. Fish. Bull. 77:765–776.

Kusher, D. I., S. E. Smith, and G. M. Cailliet.
1992. Validated age and growth of the leopard shark, *Triakis semifasciata*, with comments on reproduction. Environ. Biol. Fish. 35:187–203.

Lessa, R., F. M. Santana, V. Batista, and Z. Almeida.
2000. Age and growth of the daggernose shark *Isogomphodon oxyrhynchus*, from northern Brazil. Mar. Freshw. Res. 51:339–347.

Lessa, R., H. A. Andrade, K. L. De Lima, and F. M. Santana.
2016. Age and growth of the midwater crocodile shark *Pseudocarcharias kamoharai*. J. Fish Biol.

Lopez Cazorla, A. C.
1987. Contribución al conocimiento de la ictiofauna marina del área de Bahía Blanca. Ph.D. diss., 247 p. Univ. Nac. La Plata, La Plata, Argentina.

Lopez Cazorla, A., J. M. Molina, and C. Ruarte.
2014. The artisanal fishery of *Cynoscion guatucupa* in Argentina: exploring the possible causes of the collapse in Bahía Blanca estuary. J. Sea Res. 88:29–35.

Massa, A., N. Hozbor, G. E. Chiaramonte, A. D. Balestra, and C. M. Vooren.
2006. *Mustelus schmitti*. The IUCN Red List of Threatened Species 2006: e.T60203A12318268.

McFarlane, G. A., and J. R. King.
2006. Age and growth of big skate (*Raja binoculata*) and longnose skate (*Raja rhina*) in British Columbia waters. Fish. Res. 78:169–178.

Menni, R. C.
1985. Distribución y biología de *Squalus acanthias*, *Mustelus schmitti* y *Galeorhinus vitaminicus* en el Mar Argentino en agosto-setiembre de 1978 (Chondrichthyes). Rev. Mus. La Plata Nueva Ser. Secc. Zool. 13:151–182.

Menni, R. C., M. B. Cousseau, and A. R. Gosztonyi.
1986. Sobre la biología de los tiburones costeros de la Provincia de Buenos Aires. An. Soc. Cient. Argent. 213:3–27.

Methot, R. D., Jr., and C. R. Wetzel.
2013. Stock synthesis: a biological and statistical framework for fish stock assessment and fishery management. Fish. Res. 142:86–99.

Molina, J. M.
2013. La comunidad íctica de Bahía Anegada: estructura, composición, dinámica estacional y aspectos biológicos. Ph.D. diss., 234 p. Univ. Nac. Sur, Bahía Blanca, Argentina.

Molina, J. M., and A. Lopez Cazorla.
2011. Trophic ecology of *Mustelus schmitti* (Springer, 1939) in a nursery area of northern Patagonia. J. Sea Res. 65:381–389.

Molina, J. M., and S. J. Cooke.
2012. Trends in shark bycatch research: current status and research needs. Rev. Fish Biol. Fish. 22:719–737.

Mooij, W. M., J. M. Van Rooij, and S. Wijnhoven.
1999. Analysis and comparison of fish growth from small samples of length-at-age data: detection of sexual dimorphism in Eurasian perch as an example. Trans. Am. Fish. Soc. 128:483–490.

Moulton, P. L., T. I. Walker, and S. R. Saddlier.
1992. Age and growth studies of gummy shark, *Mustelus antarcticus* Günther, and school shark, *Galeorhinus galeus* (Linnaeus), from southern Australian waters. Aust. J. Mar. Freshw. Res. 43:1241–1267.

Murawski, S.
2000. Definitions of overfishing from an ecosystem perspective. ICES J. Mar. Sci. 57:649–658.

Natanson, L. J., J. G. Casey, and N. E. Kohler.
1995. Age and growth estimates for the dusky shark, *Carcharhinus obscurus*, in the western North Atlantic Ocean. Fish. Bull. 93:116–126.

Natanson, L. J., N. E. Kholer, D. Ardizzone, G. M. Cailliet, S. Wintner, and H. F. Mollet.
2006. Validated age and growth estimates for the shortfin mako, *Isurus oxyrinchus*, in the North Atlantic Ocean. Environ. Biol. Fish. 77:367–383.

Neer, J. A., B. A. Thompson, and J. K. Carlson.
2005. Age and growth of *Carcharhinus leucas* in the northern Gulf of Mexico: incorporating variability in size at birth. J. Fish Biol. 67:370–383.

Officer, R. A., A. S. Gason, T. I. Walker, and J. G. Clement.
1996. Sources of variation in counts of growth increments in vertebrae from gummy shark, *Mustelus antarcticus*, and school shark, *Galeorhinus galeus*: implications for age determination. Can. J. Fish. Aquat. Sci. 53:1765–1777.

Ogle, D. H.
2015. Introductory fisheries analyses with R, 317 p. Chapman and Hall/CRC, Boca Raton, FL.

Pauly, D.
1980. On the interrelationships between natural mortality, growth parameters, and mean environmental temperature in 175 fish stocks. ICES J. Mar. Sci. 39:175–192.
1984. Recent developments in the methodology available for the assessment of exploited fish stocks of reservoirs. *In* Status of African reservoir fisheries. CIFA Tech. Pap. 10 (J. M. Kapetsky and T. Petr, eds.), p. 321–326. FAO, Rome.

Prince, J. D.
2005. Gauntlet fisheries for elasmobranchs—the secret of sustainable shark fisheries. J. Northwest Atl. Fish. Sci. 35:407–416.

R Core Team.
2016. R: a language and environment for statistical computing. R Foundation for Statistical Computing, Vienna, Austria. [Available from website, accessed March 2016.]

Reeves, S. A.
2003. A simulation study of the implications of age-reading errors for stock assessment and management advice. ICES J. Mar. Sci. 60:314–328.

Ricker, W. E.
1976. Review of the rate of growth and mortality of Pacific salmon in salt water, and noncatch mortality caused by fishing. J. Fish. Board Can. 33:1483–1524.

Rigby, C. L., W. T. White, J. J. Smart, and C. A. Simpfendorfer.
2016. Life histories of two deep-water Australian endemic elasmobranchs: Argus skate *Dipturus polyommata* and eastern spotted gummy shark *Mustelus walkeri*. J. Fish Biol. 88:1149–1174.

Ritz, C., and J. C. Streibig.
2008. Nonlinear regression with R, 148 p. Springer-Verlag, New York.

Segura, A. M., and A. C. Milessi.
2009. Biological and reproductive characteristics of the Patagonian smoothhound *Mustelus schmitti* (Chondrichthyes, Triakidae) as documented from an artisanal fishery in Uruguay. J. Appl. Ichthyol. 25:78–82.

Seki, T., T. Taniuchi, H. Nakano, and M. Shimizu.
1998. Age, growth, and reproduction of the oceanic whitetip shark from the Pacific Ocean. Fish. Sci. 64:14–20.

Sidders, M. A., L. L. Tamini, J. E. Perez, and G. E. Chiaramonte.
2005. Biología reproductive del gatuzo *Mustelus schmitti* Springer, 1939 (Condrichtyes, Triakidae) en el area de Puerto Quequén, Provincia de Buenos Aires. Rev. Mus. Argent. Cienc. Nat., Nueva Ser. 7:89–101.

Skomal, G. B., and L. J. Natanson.
2003. Age and growth of the blue shark (*Prionace glauca*) in the North Atlantic Ocean. Fish. Bull. 101:627–639.

Smart, J. J., A. V. Harry, A. J. Tobin, and C. A. Simpfendorfer.
2013. Overcoming the constraints of low sample sizes to produce age and growth data for rare or threatened sharks. Aquat. Conserv. 23:124–134.

Smith, S. E., R. A. Mitchell, and D. Fuller.
2003. Age-validation of a leopard shark (*Triakis semifasciata*) recaptured after 20 years. Fish. Bull. 101:194–198.

Smith, W. D., G. M. Cailliet, and E. M. Melendez.
2007. Maturity and growth characteristics of a commercially exploited stingray, *Dasyatis dipterura*. Mar. Freshw. Res. 58:54–66.

Stevens, J. D., R. Bonfil, N. K. Dulvy, and P. A. Walker.
2000. The effects of fishing on sharks, rays, and chimaeras (chondrichthyans), and the implications for marine ecosystems. ICES J. Mar. Sci. 57:476–494.

Vooren, C. M.
1997. Demersal elasmobranchs. *In* Subtropical convergence environments: the coast and sea in the southwestern Atlantic (U. Seeliger, C. Odebrecht, and J. P. Castello, eds.), p. 141–146. Springer-Verlag, Berlin, Germany.

von Bertalanffy, L.
1938. A quantitative theory of organic growth (inquiries on growth laws. II). Human Biol. 10:181–213.

Yudin, K. G., and G. M. Cailliet.
1990. Age and growth of the gray smoothhound, *Mustelus californicus*, and the brown smoothhound, *M. henlei*, sharks from central California. Copeia 1990:191–204. Article

Zhu, L., L. Li, and Z. Liang.
2009. Comparison of six statistical approaches in the selection of appropriate fish growth models. Chin. J. Oceanol. Limnol. 27:457–467.

National Marine
Fisheries Service
NOAA

Fishery Bulletin
established in 1881

Spencer F. Baird
First U.S. Commissioner
of Fisheries and founder
of *Fishery Bulletin*

Fine-scale vertical movements of oceanic whitetip sharks (*Carcharhinus longimanus*)

Mariana Tolotti (contact author)[1,2]
Robert Bauer[1]
Fabien Forget[1]
Pascal Bach[1]
Laurent Dagorn[1]
Paulo Travassos[3]

Email address for contact author: mariana.travassos@ird.fr

[1] Unité Mixte de Recherche (UMR) Marine Biodiversity, Exploitation, and Conservation (MARBEC)
Institut de Recherche pour le Développement
Avenue Jean Monnet CS 30171
34203 Sète Cedex, France

[2] Departamento de Oceanografia
Universidade Federal de Pernambuco
Avenida Professor Moraes Rego, 1235–Cidade Universitária
50670-901 Recife, Brazil

[3] Departamento de Pesca e Aquicultura
Universidade Federal Rural de Pernambuco
Rua Dom Manoel de Medeiros s/n–Dois Irmãos
52171-900 Recife, Brazil

Abstract—Time series of depth data, obtained for 6 oceanic whitetip sharks (*Carcharhinus longimanus*) tagged with pop-up satellite archival tags, were analyzed in detail. The aim was to improve our knowledge of the vertical behavior of this species. Individuals were tagged in the Atlantic Ocean (n=5) and Indian Ocean (n=1) between 2011 and 2012. Deployment periods for these tags varied from 100 to 178 d. The sharks spent most of their time in the mixed layer, displaying the typical behavior of an epipelagic species. However, analyses revealed complex vertical movement patterns, including marked diel changes that reflect 3 different types of behavior. Results of the generalized additive models indicate that vertical movements were strongly correlated with variations in the depth of the mixed layer. A correlation between vertical movements and sea-surface temperature (SST) was also observed. When SST was above average, oceanic whitetip sharks increased their vertical amplitude, disregarding the reduction of the mixed layer. Thermoregulation likely allows this type of vertical movement.

Manuscript submitted 7 September 2016.
Manuscript accepted 15 May 2017.
Fish. Bull. 115:380–395 (2017).
Online publication date: 14 June 2017.
doi: 10.7755/FB.115.3.8

The views and opinions expressed or implied in this article are those of the author (or authors) and do not necessarily reflect the position of the National Marine Fisheries Service, NOAA.

The oceanic whitetip shark (*Carcharhinus longimanus*) is a pelagic predator threatened across the tropical oceans of the world (Bonfil et al., 2008). This species is a common bycatch of pelagic fisheries that target tuna (*Thunnus* spp.), swordfish (*Xiphias gladius*), and other tuna-like species (Beerkircher et al., 2002; Hall and Roman, 2013; Gallagher et al., 2014; Frédou et al., 2015; Oliver et al., 2015). The oceanic whitetip shark acquired its status of vulnerable globally and critically endangered in the northwest and western central Atlantic Ocean on the IUCN Red List of Threatened Species because of the increasing fishing pressure throughout its range and because of a lack of information regarding its biology and ecology (Baum et al., 2015). As a precautionary approach, a series of management measures that banned the landing, storing, and selling of oceanic whitetip sharks were implemented recently by management organizations of all regional tuna fisheries (Tolotti et al., 2015a). To date, this species is the only pelagic shark protected in the Atlantic, Pacific, and Indian oceans. The Convention on International Trade in Endangered Species of Wild Fauna and Flora has also included the oceanic whitetip shark in its Appendix II (CoP16 Prop. 42), which includes species for which trade must be closely controlled.

The lack of information regarding the biology and ecology of the oceanic whitetip shark is partly due to it being captured as bycatch—a situation that has historically resulted in few incentives for research and conservation (Barker and Schluessel, 2005). In light of the ocean-wide population declines observed for this species and because of the increasing interest in the conservation of bycatch species,

the scientific community recently has undertaken significant research to fill these wide gaps in scientific information. These studies include work on age, growth, and reproductive biology (Tambourgi et al., 2013; Joung et al., 2016), feeding (Madigan et al., 2015), genetics (Camargo et al., 2016; Li et al., 2016), fisheries (Rice and Harley[1]; Tolotti et al., 2013; Piovano and Gilman, 2016), and movement patterns and behavior (Musyl et al., 2011; Howey-Jordan et al., 2013; Tolotti et al., 2015b; Howey et al., 2016).

Data from satellite archival tags, together with fishery-dependent data, revealed valuable information concerning horizontal movements, depth preferences, and temperature ranges of the oceanic whitetip shark. Previous studies have shown that this wide-ranging species has a high degree of site fidelity and exhibits philopatric behavior (Howey-Jordan et al., 2013; Madigan et al., 2015; Tolotti et al., 2015b). They also have documented the epipelagic nature of this species and its high degree of vulnerability to open-ocean fisheries. These findings are new and have conservation applications, but several aspects of the behavior of this shark still need to be addressed. Detailed information on vertical movements within the epipelagic environment still need to be studied; most of the published research concerning this species has not explored vertical movements, and only general summaries have been provided.

Within the general framework of ecosystem-based fisheries management, it is essential to improve our knowledge of bycatch species (particularly for threatened species), including our knowledge of their behavior and vertical movement patterns (Pikitch et al., 2004; Garcia and Cochrane, 2005). The aim of this study was to analyze the vertical movements of the oceanic whitetip shark in order to extend our knowledge beyond the existing knowledge that this is an epipelagic species. The main objectives were 1) to investigate diel patterns and behavior types and 2) to analyze the influence of environmental factors on the vertical behavior of this shark.

Materials and methods

Time series of depth data for 6 oceanic whitetip sharks were analyzed. All data were obtained from pop-up satellite archival tags deployed in the Atlantic Ocean (n=5) and Indian Ocean (n=1) in 2011 and 2012 (Table 1). Deployment periods varied from 100 to 178 d. Summarized results, based on the data from the 5 tags deployed in the Atlantic Ocean, were previously presented in Tolotti et al. (2015b). The sharks in the Atlantic Ocean were tagged close to the equator on the western side of the Atlantic Ocean during commercial longline operations. The sharks were brought onboard for the tagging procedure, and tags were attached at the base of the first dorsal fin with a loop of polyamide monofilament. In addition to the vertical movements reported here, horizontal movements were observed for the sharks. After tagging, all individuals made extensive horizontal movements but remained mostly in the equatorial zone (Tolotti et al., 2015b). Only 1 shark migrated south. The shark tagged in the Indian Ocean was caught with a hand line during a research cruise in the Mozambique Channel. For the tagging procedure, this shark was brought on board and placed in a tagging cradle. The tag was attached intramuscularly under the first dorsal fin with a stainless steel tether and large Wilton anchors (Wildlife Computers Inc.,[2] Redmond, WA). From its tagging location in the Mozambique Channel, this individual migrated north, following the African coast to Somalia. The estimated tracks of all 6 tagged individuals are provided in Supplementary Figure 1 (online only).

Data description

Pop-up satellite archival tags typically record the ambient depth (pressure), water temperature, and light level at a high temporal resolution (for our study, the resolution was 10 s). This information is then used to generate different data products that are transmitted by satellite after the tags detach from the animal. Transmitted data products will depend on tag model and user-defined settings. Two models of pop-up satellite archival tags, manufactured by Wildlife Computers Inc., were used in this study, 5 MiniPATs and 1 PAT-Mk10. The MiniPATs were programmed to transmit depth data with a resolution of 5 min. The PAT-Mk10 does not transmit data as a time series, only as an aggregated summary of its records. However, this latter tag was physically recovered from Crystal Beach, Texas, after drifting at sea for about 1 year after its release from the shark. The recovery of this tag allowed the download of the complete depth and temperature time series with a 10-s resolution. The MiniPATs were not recovered. Although MiniPATs were not programmed to transmit temperature time-series data, other data produced and transmitted by the tags provided information on the surrounding environment. These products included a daily analysis of the surface mixed layer and sea-surface temperature (SST), as well as a summary of temperature at depth profiles. These data were also available from the recovered PAT-Mk10.

Data analysis

Vertical movement patterns The periods of the day were classified according to local times of sunrise and sunset, by following the procedure described in Tolotti et al. (2015b). In summary, the local times were based

[1] Rice, J., and S. Harley. 2012. Stock assessment of oceanic whitetip sharks in the western and central Pacific Ocean. West. Cent. Pacific Fish. Comm. WCPFC-SC8-2012/SA-WP-06, rev. 1, 53 p. [Available from website.]

[2] Mention of trade names or commercial companies is for identification purposes only and does not imply endorsement by the National Marine Fisheries Service, NOAA.

Table 1

Details from the electronic tagging of oceanic whitetip sharks (*Carcharhinus longimanus*) in the Atlantic and Indian oceans between 2011 and 2012: identification (ID) code, total length (TL), sex, location, model of pop-up satellite archival tag used, the period that tags were set to record data (programmed). Tagging: date when a fish was tagged, and location of tagging (latitude [lat] and longitude [long]). Pop-up: date when a tag popped up (was released), location of released tag, and the number of days that the tag had remained on the fish.

						Tagging			Pop-up			
ID	TL (cm)	Sex	Ocean	Tag	Programmed	Date	Lat.	Long.	Date	Lat	Long	Duration
AOCS3	167	M	Atlantic	PAT-Mk10**	180 d	16/01/2011	−0.139	−34.218	10/07/2011	−3.802	−32.466	178 d
AOCS4	197*	F	Atlantic	MiniPAT	140 d	06/12/2011	−3.589	−34.918	25/04/2012	−18.754	−35.771	141 d
AOCS5	180*	F	Atlantic	MiniPAT	140 d	01/03/2012	−0.501	−37.354	20/07/2012	3.215	−41.015	141d***
AOCS6	134	F	Atlantic	MiniPAT	100 d	02/03/2012	−0.736	−37.534	11/06/2012	−0.598	−36.235	101 d
AOCS7	161	F	Atlantic	MiniPAT	100 d	02/03/2012	−0.435	−37.629	14/06/2012	1.306	−35.345	104 d
IOCS1	183*	F	Indian	MiniPAT	100 d	15/04/2011	−13.119	44.967	24/07/2011	−2.522	53.554	100 d

*Mature individuals (size at first maturity: 180 cm TL).
**Recovered tag.
***Tag stopped recording data after 104 d of deployment.

on the daily geolocation estimates from the tags and the NOAA daytime estimation algorithm (NOAA Solar Calculator, website). Day was defined as the period between sunrise and sunset, and night was defined as the period between astronomical dusk and astronomical dawn. Dusk was the hours between sunset and astronomical dusk, and dawn was the hours between astronomical dawn and sunrise. Because sharks made extensive horizontal movements during their monitoring periods, local sunrise and sunset times varied with time for all individuals. The variation, however, was not greater than 50 min. To facilitate graphic representations of aggregated data, day and night and dawn and dusk were depicted by their respective minimum and maximum estimated times. Daytime and nighttime depths were compared with the nonparametric Wilcoxon test at a 95% confidence level. For this analysis, depths corresponding to crepuscular hours (dawn and dusk) were excluded. Mean depths were grouped into 1-h intervals to test for uniformity over the 24-h cycle. The uniformity was tested by using circular statistics (Rao's spacing test), also at a 95% confidence level.

A spectral analysis was carried out with the depth time-series data from the recovered tag of shark AOCS3. This analysis was not feasible for the other tags because of gaps caused by the data transmission. The aim was to identify a potential periodicity in the vertical behavior of this shark and infer possible temporal patterns. A fast Fourier transform algorithm was used in the stats package in R, vers. 3.1.2 (R Core Team, 2014). The function calculates a smoothed periodogram by using Daniell windows, which are modified moving-average filters. The raw periodogram is a widely fluctuating estimate of the spectrum with high variance, and this smoothing method provides a stable estimate (Bloomfield, 2004). The spectral analysis is particularly well suited for long-term and high-resolution time series, including those from archival tagging studies (Shepard et al., 2006).

The depth time-series data were also assessed visually to examine any possible vertical patterns that could have been masked when the data were grouped. This analysis was conducted with the help of a visualization tool, and the window of this software was adjusted on our computer screen to fit 2 d of data at a time. In this analysis, the times of sunrise and sunset did not need to be estimated. Instead, the readings of ambient light from the tags could be simultaneously displayed with the depth readings. The light data were transmitted in the form of 2 daily light curves, representing sunrise and sunset. For the recovered tag, the complete time series of light readings was available. The simultaneous visualization of light curves and the depth time series was created by using the graphing and analysis software program Igor Pro, vers. 6.22A (WaveMetrics Inc., Portland, OR). A suite of data analysis programs (WC-DAP, Wildlife Computers Inc.) was used to export a file formatted for use with Igor Pro, which facilitated the visual analysis. This pairing of light and depth data also increased the precision needed for discerning diel patterns.

Vertical movements and the environment To reconstruct the thermal signature of the water column occupied by the oceanic whitetip sharks during the periods in which they were monitored, the summary data for temperature at depth were used. This data product provides the minimum and maximum temperatures at selected 8-m depth intervals at a user-defined resolution (for this study, the resolution was every 24 h). The average temperatures of depth intervals were interpolated linearly to produce continuous daily temperature

profiles in a grid with a 0.5-m resolution, according to the method described in Bauer et al. (2015). The interpolated temperature profiles were then plotted by using a heat-color scheme and examined in comparison with daily average depths and their standard deviations (SDs). This method was chosen because it has been shown to provide an accurate representation of the thermal signature and, therefore, to be a viable alternative in the absence of temperature time-series data (Bauer et al., 2015).

To identify potential environmental variables that could drive the vertical behavior of oceanic whitetip sharks, we applied generalized additive models (GAMs). This type of model has been used to model habitat preferences of a variety of oceanic species, including sharks (Zagaglia et al., 2004; Damalas and Megalofonou, 2010; Bustamante and Bennett, 2013; Lam et al., 2014). The daily SD of depth records was considered a proxy for the vertical variability (movement amplitude) of sharks and, therefore, was chosen as a response variable. The explanatory variables included environmental variables related to data derived from tag records: geolocation estimates (longitude and latitude), SST, mixed-layer depth (MLD), and shark size. These variables were introduced as smoothing terms (thin-plate regression splines). To assess temporal effects, "month" was included as a factorial variable. Because sharks were tagged in 2 ocean basins (Atlantic and Indian oceans), "ocean" was also included as a factorial variable. Modeling was conducted by using the gam function of the mgcv package, vers. 1.8-12, in R (Wood, 2006), with a Gaussian link function. All possible combinations between variables and factors were tested and yielded 63 models. Models also were run separately for each individual shark to investigate individual variability. In this case, "ocean" and "shark size" were not considered, resulting in 15 models. Model selection was based on the Akaike information criterion and further evaluated with residual analysis.

Results

Vertical movement patterns

Diel cycles Diel changes in vertical behavior were visible across the depth time series of all tagged individuals. However, different patterns also were observed within and between individuals. The strongest signal was observed during crepuscular hours, especially at dawn, when sharks swam at considerably shallower depths (Fig. 1). This pattern was consistent, and it frequently was observed in the time series of all individuals. Circular statistics, applied to the average depth per hour of each individual, revealed a lack of uniformity over a 24-h cycle for the oceanic whitetip sharks (Rao's spacing test: $P>0.001$). Test results highlight the consistency of this crepuscular pattern, which was present even when day and night differences were not observed.

Figure 1 also shows a general pattern of shallower average depths during the day than during night, when tagged sharks appear to move to deeper waters. This pattern was well marked for sharks AOCS4, AOCS5, AOCS7, and IOCS1, for which statistically significant differences were observed between occupied depths during light and dark hours (Suppl. Table 1) (online only). For sharks AOCS3 and AOCS6, a difference between day and night average depths was not evident or statistically significant. As opposed to the averages, SD values in depth records did not vary much across the 24-h cycle (Fig. 1). In contrast, for sharks IOCS1 and AOCS4, SD values were higher during the night than during the day. With SD considered a proxy of vertical amplitude, these sharks appear to explore the water column more extensively during nighttime.

The spectral analysis of high-resolution depth time series from the recovered tag of shark AOCS3 revealed 2 distinct frequency peaks, one at 12 h and another at 24 h (Fig. 2). The sharp 12-h peak might represent the crepuscular pattern described previously. The sharpness of this peak also indicates a high degree of consistency in this diel pattern, i.e., a shift in the vertical behavior frequently occurred around the same time of the day. The 24-h peak indicates that periodic behavioral shifts also occur with daytime and nighttime depths. The broad base of this peak, however, indicates that the shifts in vertical behavior at this scale are less consistent. This result is interesting in that it did not appear when the depth readings were aggregated by hour. In Figure 1 differences between daytime and nighttime average depths of this individual are not presented.

The visual assessment of each depth time series revealed the identification of 3 main types of day and night behavioral patterns. Type-I behavior was characterized by a preference for shallower waters and by some sporadic deep dives during the day and by a preference for deeper waters and regular up-and-down movements during the night. Type-II behavior featured an inverse pattern of that described as type I; sharks occupied deeper waters during the day, as opposed to night, and also made regular up-and-down movements. In contrast, type-III behavior did not show a clear difference between daytime and nighttime depth preferences. Examples of each behavior type can be seen in Figure 3. All individuals exhibited the 3 described behavioral patterns during their monitoring periods, but the frequency of each behavior type varied largely among sharks (Fig. 4). Type II was the least frequent behavior type observed in all time series and occurred most often for shark AOCS3, representing 23.7% of the time series of this individual. Type I dominated the time series of sharks AOCS4 (41.0%) and IOCS1 (61.2%), and type III dominated the time series of sharks AOCS5 (62.8%) and AOCS6 (50.5%). Note that because of gaps in the transmitted depth time-series data, not all 24-h periods could be observed and hence classified.

The temporal distribution of behavior types did not

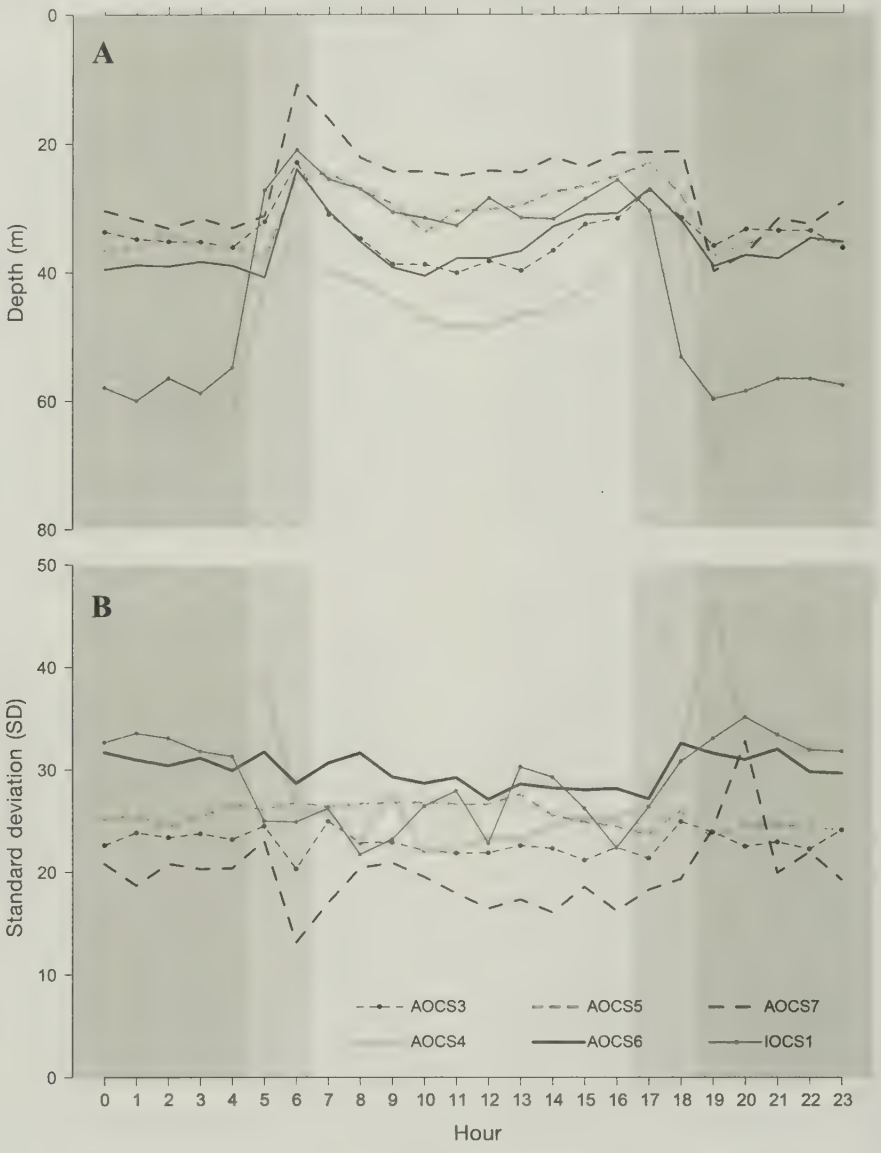

Figure 1

(**A**) Hourly average depth and (**B**) related standard deviation (m) for 6 oceanic whitetip sharks (*Carcharhinus longimanus*) tagged in the Atlantic and Indian oceans between 2011 and 2012. Lightly shaded areas represent crepuscular periods, darker shaded areas represent night, and the white area represents day. The identity codes (e.g., AOCS3) identify individual sharks.

appear to be uniform, nor did they follow any particular pattern (Suppl. Fig. 2) (online only). Shark AOCS3, for instance, exhibited all 3 types of behavior almost in the same proportion (Fig. 4), and these behavior types alternated frequently throughout its time series. Long sequences of the same behavior type were rare for this individual, the maximum being 9 consecutive days for type I. In fact, long sequences of one behavior type were seen only when a particular type was also dominant for an individual, such as type I for shark IOCS1 and type III for shark AOCS5. For all sharks, one isolated day of any behavior type occurred more frequently than any sequence of one type of behavior. Only for one individual, shark AOCS4, was there a clear shift in behavior type with time observed. During its first 50 days of monitoring, this shark almost exclusively exhibited type-I behavior. After this period, shark AOCS4 started to alternate type I with the other behavior types. At the same time, the number of gaps present in the first 50 days of the time series for this shark weakened the veracity of this otherwise constant pattern.

Three sharks (AOCS5, AOCS6, and AOCS7) were

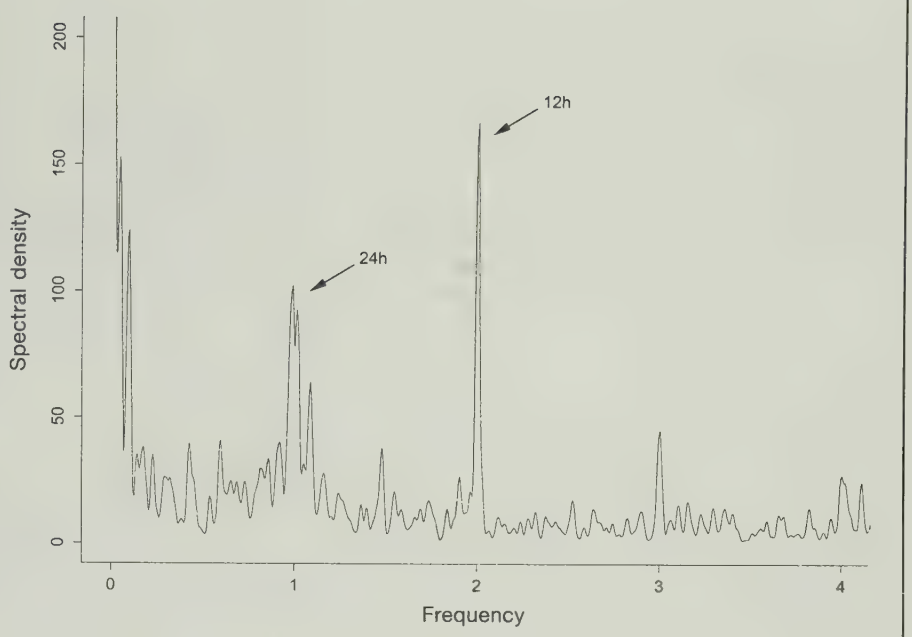

Figure 2

Periodogram generated with fast Fourier transforms of the continuous depth data from an oceanic whitetip shark (*Carcharhinus longimanus*), AOCS3, tagged in the Atlantic Ocean in 2011. The cycles are expressed by 1/(frequency(x)). Spectral density represents the relative magnitude of frequency.

tagged on the same day at similar locations, and the duration of their monitoring period was the same. This unique situation facilitated the incorporation of a spatial aspect in the discussion concerning shifts between behavior types. The proportions of the 3 behavior types were linked across the tracks of these individuals (Fig. 5). Considering that individuals that are simultaneously at the same location typically also experience the same environment, this analysis revealed moments where environmental factors could have been the driver for the behavior of these sharks. At the beginning of May 2012, for example, sharks AOCS5 and AOCS7 were in the same square of latitude and longitude and had a similar behavioral pattern. Shark AOCS6, on the other hand, was in another location and had a different behavioral pattern. In fact, this shark remained in the same area for most of May, but its behavior pattern shifted completely between the first and second half of the month. Again, an environmental factor may have been the driver. However, during the second half of April, sharks AOCS5 and AOCS7 were at the same location exhibiting completely different behavioral patterns. This trend appeared again during the second half of May, indicating that the physical environment might not be the only driver of behavior types.

Spike dives While examining the time series, we noted that all individuals stayed primarily within the top 150 m of water but descended on rare occasions to depths below 150 m. By looking closely at these rare deep diving events, which accounted for only 0.15% of the monitoring periods (Tolotti et al., 2015b), we identified common features. These features, referred to as *spike dives*, were characterized by rapid descents to depths greater than 150 m, followed by considerably slower ascents. Two examples of spike dives can be seen in Supplementary Figure 3 (online only). All individuals performed spike dives during their monitoring period, and estimated descent rates varied from 0.14 to 1.05 m/s and ascent rates varied from 0.08 to 0.26 m/s (Table 2). Most of the spike dives lasted from 30 to 45 min, but spike dives of more than 1 h also were noted. With the exception of movements of shark AOCS7, spike dives occurred primarily during the day (Suppl. Fig. 4 (online only)). Besides performing the great majority of its spike dives during nighttime, shark AOCS7 also exhibited this behavior much more frequently than the other individuals.

Vertical movements and the environment

Daily average depths and SDs were plotted on top of temperature profiles to identify possible links between vertical movements and the thermal structure of the water column. Although some thermal changes were observed, the daily average depths were stable for all sharks (Fig. 6). The daily SD of depth records, on the other hand, indicated some variation. For sharks IOCS1 and AOCS6, for example, higher SD values were ob-

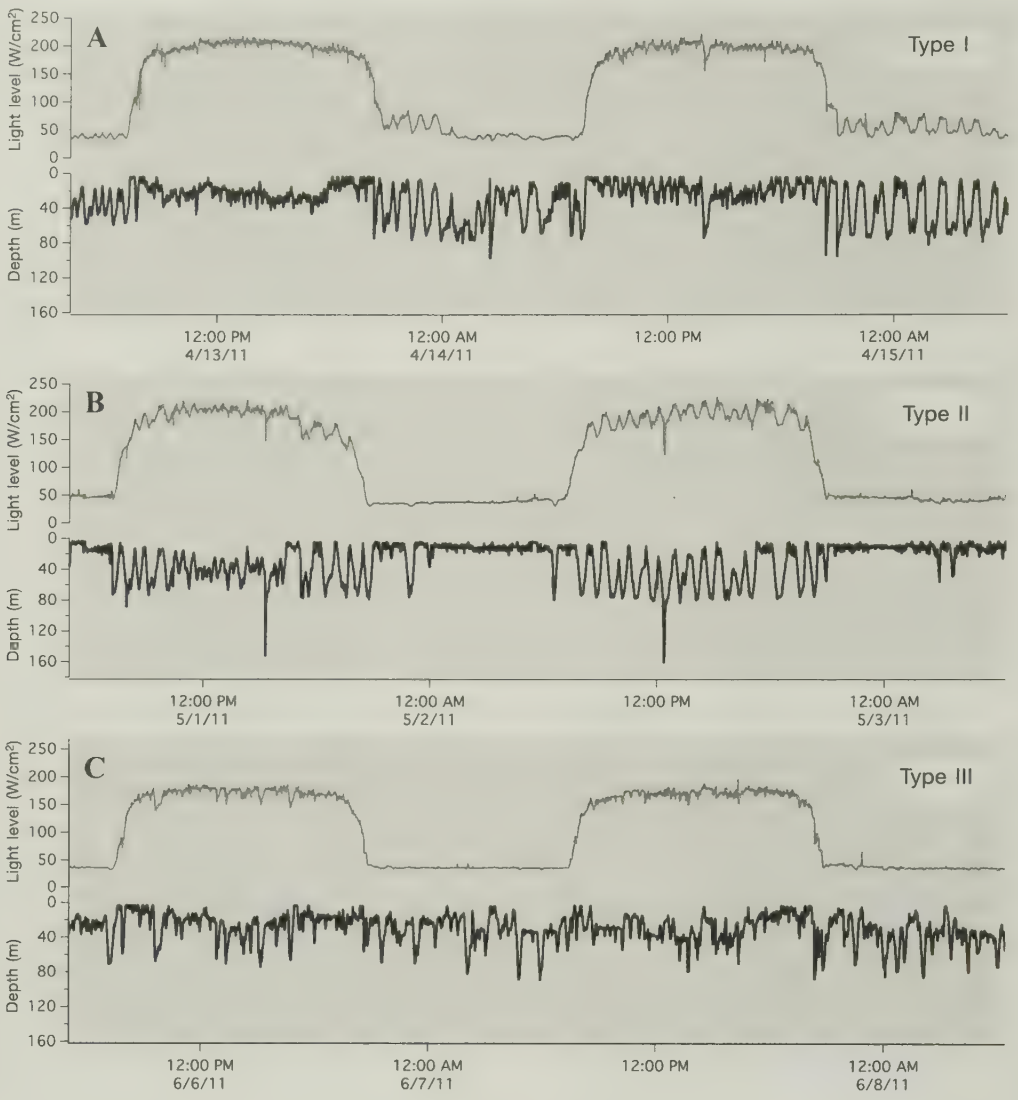

Figure 3

Examples of the 3 behavior types, or patterns of vertical movement, during day and night, of oceanic whitetip sharks (*Carcharhinus longimanus*) identified by visual assessments of depth data from sharks tagged in the Atlantic and Indian oceans between 2011 and 2012: (**A**) type-I, (**B**) type-II, and (**C**) type-III behavior.

served during June–July and early May, respectively, than during other periods. The observation of higher SD values coincided with a larger mixed layer, indicating that oceanic whitetip sharks have a greater depth range when their preferred environment is expanded. Sea-surface temperature also appears to influence vertical behavior. Careful inspection of Figure 6 for sharks AOCS3, AOCS6, and AOCS7 reveals that these individuals explored colder waters during periods of higher SST.

To better understand the influence of environmental conditions on the vertical behavior of the oceanic whitetip sharks in this study, several GAMs were applied. The results from these models were in accordance with the patterns in daily temperature-at-depth profiles estimated from tag data and depth SDs presented in Figure 6. The best models consistently indicated a significant influence of horizontal position (longitude and latitude), MLD, and SST on daily vertical activity (SD of daily depth records). Results from the model with combined data from all sharks indicate an additional effect of shark size and explain 50.1% of the deviance (coefficient of multiple determination [R^2]=0.48, n=685). Results from this model indicate an increase of vertical amplitude with the increase of the MLD and shark size. Sea-surface temperature follows the same trend, but it was the least significant factor

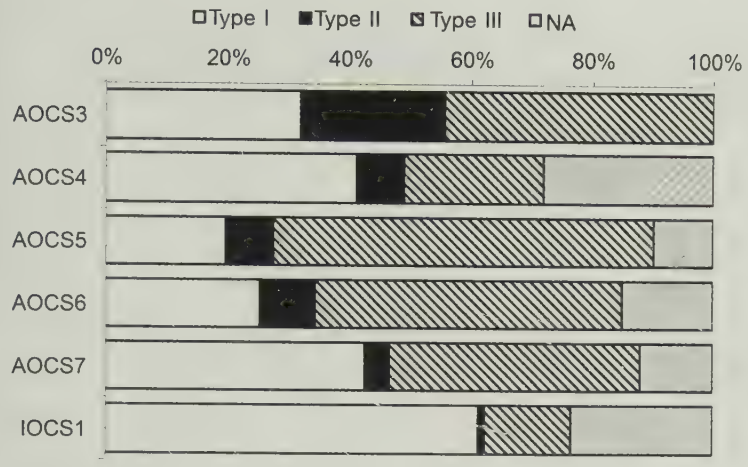

Figure 4

Proportion of the 3 different behavior types of vertical movement during day and night observed on the depth time series of oceanic whitetip sharks (*Carcharhinus longimanus*) tagged in the Atlantic and Indian oceans between 2011 and 2012. The identity codes (e.g., AOCS3) identify individual sharks.

in the model with data from multiple sharks (Fig. 7). The set of explanatory variables in the best models for individual sharks varied slightly between sharks, and horizontal positions, unlike MLD and SST, were always significant (Fig. 7). Summary tables with model results are presented in Supplementary Table 2 and Supplementary Figure 5 (online only).

To assess in detail the effect of environmental factors on variations of vertical movement, the cumulative sums of MLD, SST, and depth SD were plotted for each individual. The cumulative sums were subtracted from the mean and rescaled to highlight periods when values were above or below the mean (Fig. 8). These plots reflect and facilitate understanding of the model results. The results for shark IOCS1 provide an example of the overall observed trend. For this individual, a perfectly aligned correlation between MLD and vertical activity was observed. When MLD was above average and, therefore, the species preferred environment was extended, the SD was also above average. The opposite trend was also true. It is not surprising that the MLD was a highly significant factor in the GAM for this individual; the GAM had a high degree of deviance explained (64.7%). Another interesting case is shark AOCS3. In the beginning of the monitoring period for this shark, the same relationship with MLD and vertical activity (SD), as that found for IOCS1, was observed. Around May, however, a major shift occurred. Instead of decreasing with MLD, vertical activity of this shark started to increase regardless of the reduction of preferred environment. At this time, the SST started to exceed average values; hence, its addition as a significant factor in the model of AOSC3. This same trend was observed for shark AOCS5.

Discussion

Recent studies have shown that the oceanic whitetip shark is an epipelagic predator largely confined to the mixed layer (Musyl et al., 2011; Howey-Jordan et al., 2013; Tolotti et al., 2015b)—a finding that was also confirmed with this study. To date, however, detailed information on how this species occupies the epipelagic environment has been lacking. This study revealed that oceanic whitetip sharks had complex vertical movement patterns, pronounced diel changes and behavioral shifts, and that environmental factors influenced vertical activity. Several statistical approaches were combined to identify these vertical movement patterns. This research represents the first description of satellite archival data from a tag deployed on an oceanic whitetip shark in the Indian Ocean.

Diel patterns

The occurrence of diel behavior has not been reported from previous research on vertical movements of oceanic whitetip sharks (Howey-Jordan et al., 2013). Conversely, diel patterns were observed for all 6 individuals analyzed in our study. Despite some variability, diel patterns occurred at least once during the monitoring period of each tagged shark. Diel vertical movements are very common for fish species with vertical ranges that exceed that of oceanic whitetip sharks, such as the blue shark (*Prionace glauca*), bigeye thresher (*Alopias superciliosus*), swordfish, and bigeye tuna (*Thunnus obesus*) (Musyl et al., 2003, 2011; Abecassis et al., 2012; Lam et al., 2014; Coelho et al., 2015). These species usually occupy deep waters during the day and remain in the mixed layer during the night. They are believed to follow the vertical migration of mesopelagic prey species within the deep scattering layer (Dagorn et al., 2000; Bernal et al., 2009).

Several epipelagic predators have also been reported to display diel patterns in their vertical behavior. For the silky shark (*C. falciformis*) and dolphinfish (*Coryphaena hippurus*) (Merten and Appeldoorn, 2014; Filmalter et al., 2015), for example, vertical movements similar to the type-I behavior described previously for the oceanic whitetip shark have been observed. Although opposite to the general diel migration pattern described for pelagic species with wide vertical ranges, type-I behavior could also be linked to feeding on mesopelagic prey from the deep scattering layer. Filmalter et al. (2015) reported that silky sharks during the night were more vertically active and were observed at depths similar to the nocturnal depth range of pelagic species known to follow the migration of the deep scattering layer. The authors hypothesized that these increased vertical oscillations were associated with feeding activity.

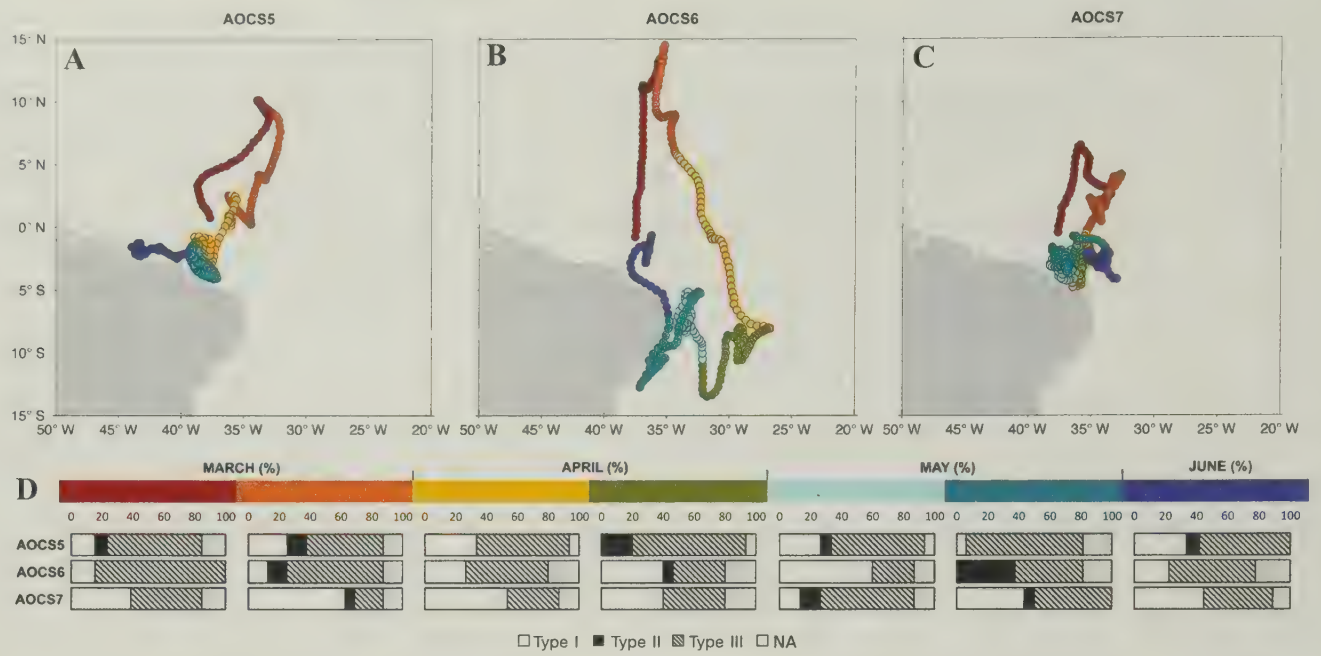

Figure 5

Tracks of 3 oceanic whitetip sharks (*Carcharhinus longimanus*) tagged off northeast Brazil in the Atlantic Ocean at a 24-h interval in March 2012, (**A**) AOCS5, (**B**) AOCS6, and (**C**) AOCS7, and (**D**) the proportion of the 3 behavior types of vertical movement across those tracks. The 2 colors for each month indicate the first and second halves of the month.

Table 2

Summary of data on the spike dives performed by oceanic whitetip sharks (*Carcharhinus longimanus*) during monitoring with pop-up satellite archival tags in the Atlantic and Indian oceans in 2011 and 2012.

ID	Number of deep spike dives	Max depth range (m)	Duration (min)	Descent rate range (m/s)	Ascent rate range (m/s)
AOCS3	4	237–365	21–45	0.55–1.00	0.10–0.24
AOCS4	4	232–340	35–75	0.14–0.49	0.12–0.22
AOCS5	3	154–193	40–55	0.19–0.23	0.08–0.12
AOCS6	2	181–277	45	0.17–0.40	0.09–0.12
AOCS7	18	153–405	30–65	0.44–1.05	0.15–0.26
IOCS1	6	257–317	35–50	0.22–0.89	0.14–0.17

In our study, indication of an increased vertical activity during the night also was found (see Fig. 1). Moreover, oceanic whitetip sharks are known to feed on mesopelagic squids (Backus et al., 1956), and stable isotopes in a recent study have indicated that there is an almost equal importance of squids (44%) and larger pelagic teleosts (47%) in their diet (Madigan et al., 2015). Deep excursions of oceanic whitetip sharks are rare and are, therefore, unlikely to account for such a significant portion of a mesopelagic species in the diet of this shark. This fact indicates that type-I behavior indeed can be linked to feeding on prey from the deep scattering layer during the night.

Variability in vertical movement patterns has also been reported for several pelagic fish species. Blue sharks are known for their marked diel migration to shallower waters during the night, but 5 distinct vertical behavior types have been described recently for that species (Queiroz et al., 2012). These behavior types ranged from the general, known diel pattern to their inverse and included patterns for which no diel differences were apparent, as we have described for

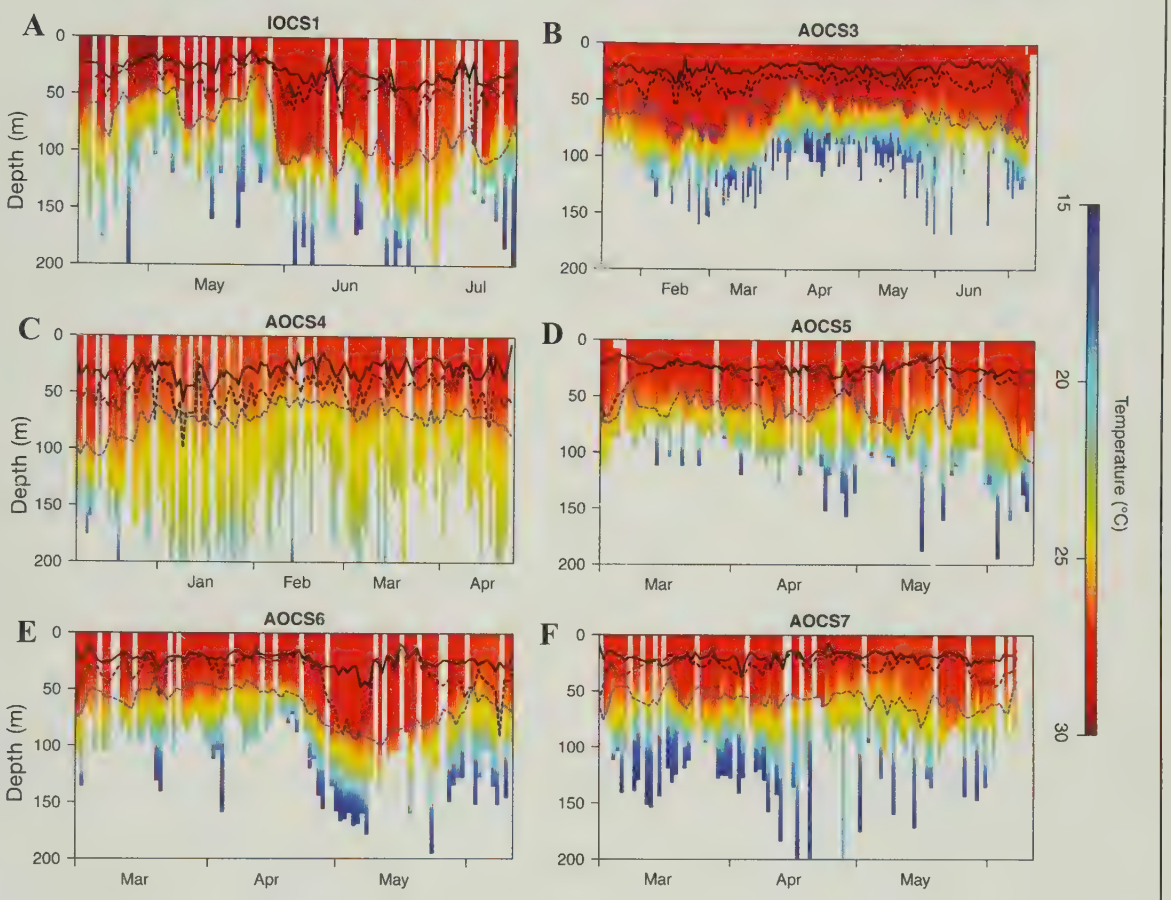

Figure 6

Daily temperature profiles estimated by using transmitted data from pop-up satellite archival tags used to track 6 oceanic whitetip sharks (*Carcharhinus longimanus*) in the Indian and Atlantic oceans between 2011 and 2012: (**A**) IOCS1, (**B**) AOCS3, (**C**) AOCS4, (**D**) AOCS5, (**E**) AOCS6, and (**F**) AOCS7. The continuous and dotted black lines represent the daily average depth and its standard deviation, respectively, for each shark. The dotted blue line represents the mixed-layer depth.

oceanic whitetip sharks in this study (type-III behavior). Contrasting diel vertical behavior types have also been reported for the porbeagle (*Lamna nasus*) and plankton-feeding basking shark (*Cetorhinus maximus*) (Sims et al., 2005; Pade et al., 2009). These behaviors are believed to be linked to prey availability. The studies cited above show that shifts in diel vertical behavior occur when the sharks change their environment, for example, when they move from mixed coastal waters to well-stratified offshore waters (Pade et al., 2009; Queiroz et al., 2012), or when they mirror prey behavior (Sims et al., 2005).

For the oceanic whitetip sharks tagged in our work, it was not possible to identify clear temporal or spatial patterns in the occurrence of the different behaviors. The types of behavior alternated frequently and no pattern was observed across the time series (Fig. 5, Suppl. Fig. 2). Oceanic whitetip sharks are opportunistic predators (Backus et al., 1956; Compagno, 1984), and the variability observed in the vertical movement patterns of the sharks in our study could very well be linked to prey distribution, as has been suggested for other pelagic sharks. Additional research using simultaneous data collection on prey distribution and tagging experiments would be required to verify this hypothesis. A comparison of the vertical behavior of other pelagic sharks tagged in the same areas could also provide useful information.

The fast Fourier transform analysis of depth data from the recovered tag (shark AOCS3) revealed 2 distinct frequency peaks, at 12 and 24 h, indicating a pronounced periodicity in the vertical movements of this shark (Fig. 2). The peak at 24 h confirms the diel behavior, and its broad base indicates a certain degree of variability. Peaks corresponding to a 24-h cycle have been observed for other pelagic shark species, and such peaks are typically interpreted as evidence of diel behavior (Brunnschweiler and Sims, 2012; Filmalter et

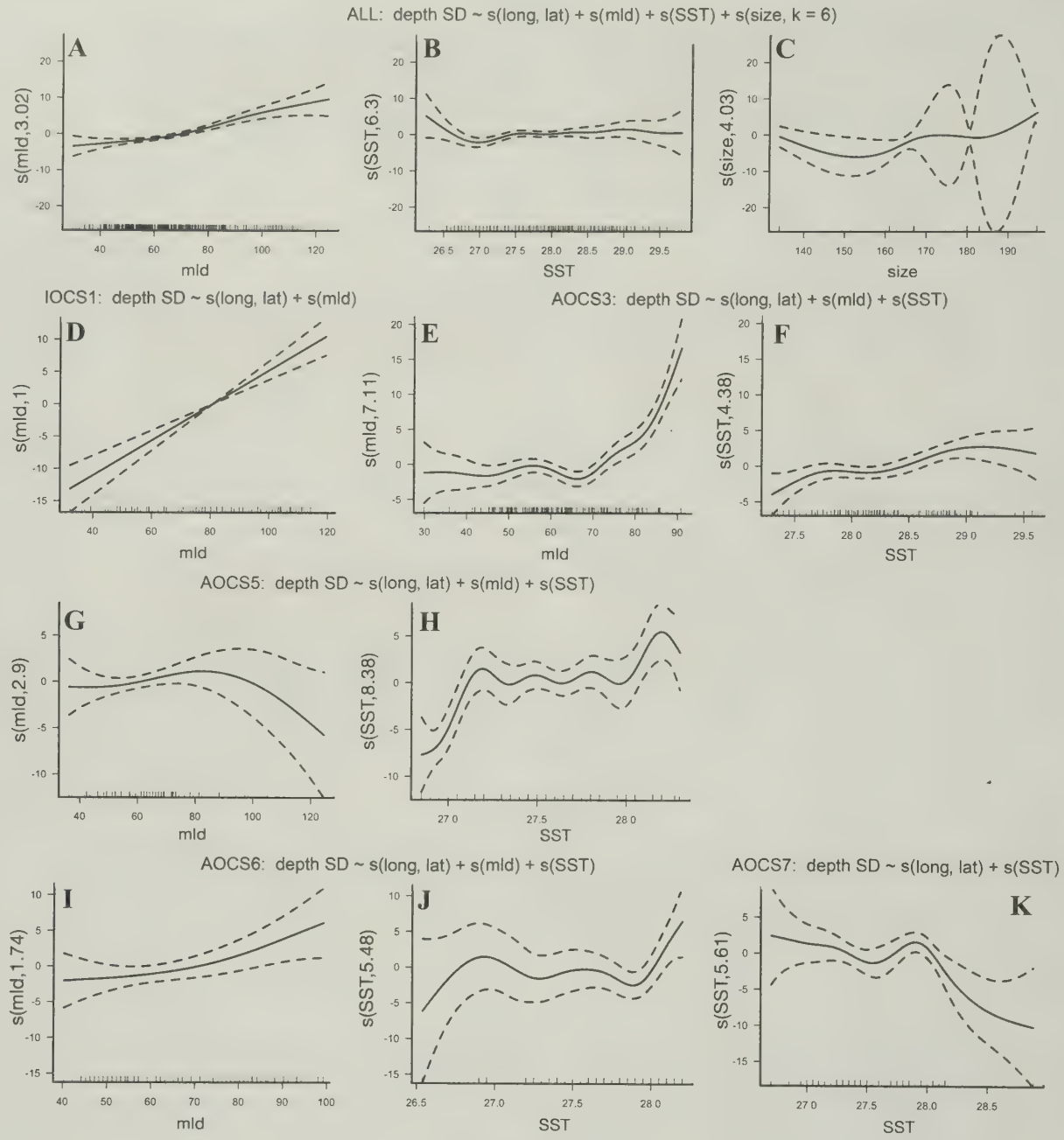

Figure 7

Formulas and corresponding smoothing terms (thin-line regression splines, black lines) with 95% confidence intervals (dotted lines) for the best-fitted generalized additive models used in this study of vertical movements of oceanic whitetip sharks (*Carcharhinus longimanus*). The models were based on data from 6 tagged oceanic whitetip sharks in the Atlantic and Indian oceans between 2011 and 2012, with the daily depth standard deviation (SD) as the response variable. Shown are the splines for (**A**) mixed-layer depth (MLD), (**B**) sea-surface temperature (SST), and (**C**) size for the model that used all 6 sharks, MLD for the model that used the shark tagged in the Indian Ocean (IOCS1) (**D**), MLD and SST for the models that used an individual shark tagged in the Atlantic Ocean—(**E–F**) AOCS3, (**G–H**) AOCS5, (**I–J**) AOCS6—and (**K**) SST for the model that used a shark tagged in the Atlantic Ocean (AOCS7). Splines (s) are not shown for a fourth smoothing term, longitude (long.) and latitude (lat). K=number of individuals.

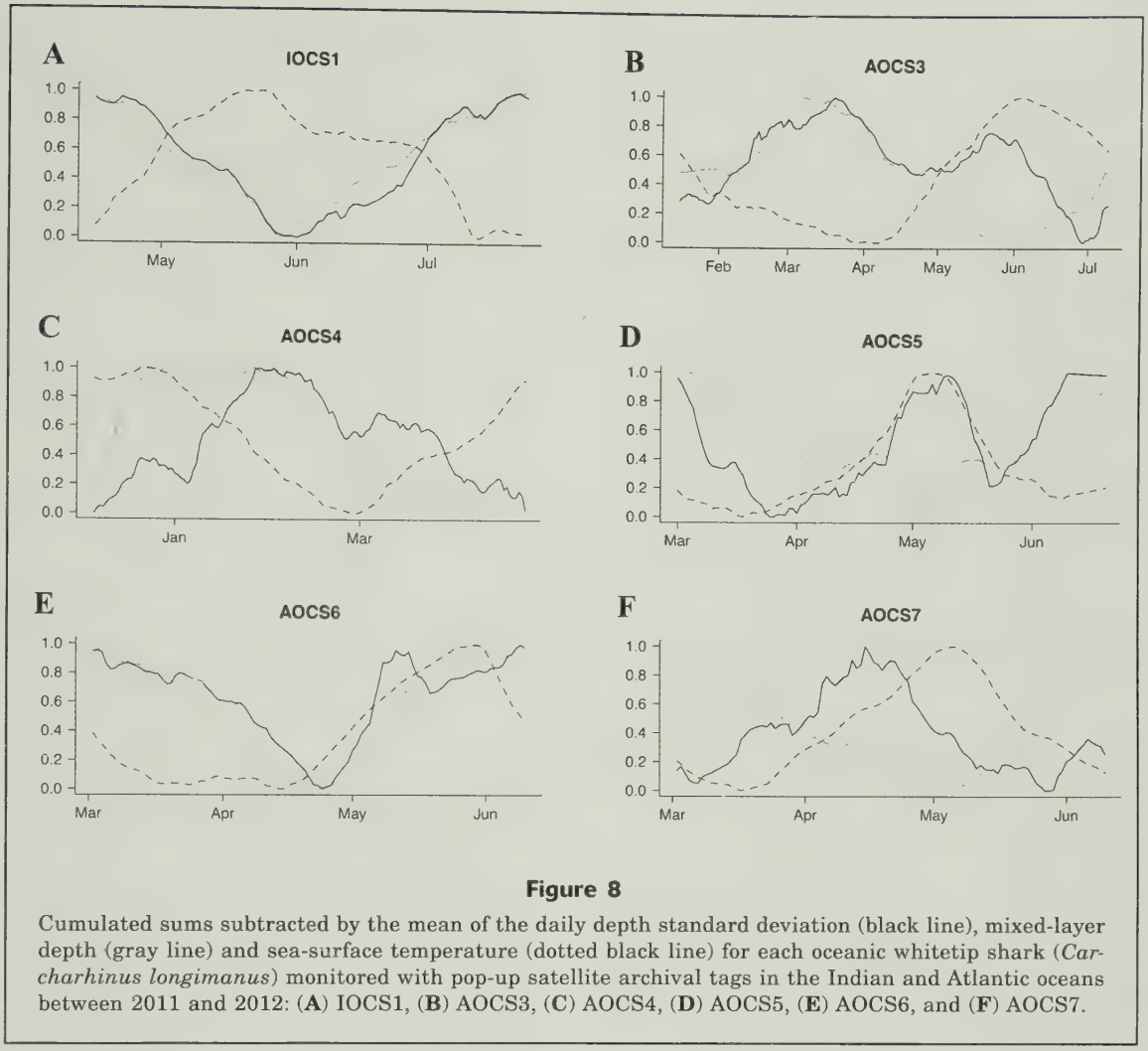

Figure 8

Cumulated sums subtracted by the mean of the daily depth standard deviation (black line), mixed-layer depth (gray line) and sea-surface temperature (dotted black line) for each oceanic whitetip shark (*Carcharhinus longimanus*) monitored with pop-up satellite archival tags in the Indian and Atlantic oceans between 2011 and 2012: (**A**) IOCS1, (**B**) AOCS3, (**C**) AOCS4, (**D**) AOCS5, (**E**) AOCS6, and (**F**) AOCS7.

al., 2015; Tyminski et al., 2015). A 12-h periodicity in vertical behavior, however, has not been reported as often for pelagic species. Typically, a spectral peak at 12 h is observed for coastal species, and such peaks are strongly linked to tidal cycles (Urmy et al., 2012). Similar to the peak observed for shark AOCS3, the strongest spectral peak in the periodogram of a basking shark in another study had a period of 12.35 h (Shepard et al., 2006). The authors associated this peak with the tidal cycle because the shark remained on the continental shelf where there is clearly a tidal influence. In contrast, shark AOCS3 remained in oceanic waters (Suppl. Fig. 1) with a potentially weaker tidal signal. Therefore, it appears unlikely that the 12-h spectral peak observed for this oceanic whitetip shark was linked to any tidal cycle.

Instead, the 12-h peak appears to be related to vertical crepuscular movements. The oceanic whitetip sharks analyzed in this study occupied considerably shallower depths during the hours of dawn and dusk than during other periods of the day (Fig. 1). Coincidentally, at equatorial latitudes, day and night have similar lengths, resulting in a crepuscular event every 12 h (World of Earth Science, 2003). Shark AOCS3 stayed at equatorial latitudes during its entire tracking period, indicating that the 12-h spectral peak of vertical movement matches the crepuscular cycle. This dawn and dusk pattern of vertical movement was consistent throughout the time series of all 6 individuals, and it has been identified also in the behavior of oceanic whitetip sharks tagged in the Pacific Ocean (Musyl et al., 2011). The sharpness of the 12-h peak indicates that this crepuscular pattern represents a frequent and pronounced feature in the oceanic whitetip shark behavioral repertoire. Similar patterns have been reported for other shark species and have been associated with foraging behavior and maintaining a preferred isolume (Nelson et al., 1997; Vianna et al., 2013). In short, the variations in luminosity, characteristic of twilight hours, may represent the cues that regulate the behavioral shifts and feeding activity of this species.

Spike dives

Oceanic whitetip sharks tagged in the North Atlantic Ocean (Bahamas) have been reported to make sporadic deep dives to the mesopelagic zone, down to a depth of 1190 m (Howey-Jordan et al., 2013; Howey et al., 2016). Similar to the deep dives observed in our work, descent rates of dives of oceanic whitetip sharks in the study off the Bahamas were significantly faster than ascent rates. However, unlike most sharks in our study, the sharks in the Bahamas performed deep dives primarily at night and dusk. The difference between the 2 studies in the period during which oceanic whitetip sharks made deep dives could be related to local environmental conditions; however, 1 shark (shark AOCS7) in our study also made spike dives primarily during the night. These contrasting periods and the rarity of these deep dives make it difficult to identify their driving forces. In any case, similarly shaped deep dives are relatively common among pelagic sharks and often are believed to be associated with prey searching (Sepulveda et al., 2004; Hoffmayer et al., 2013; Howey-Jordan et al., 2013; Tyminski et al., 2015). Gleiss et al. (2011) suggested that v-shaped dives might help sharks to efficiently scan the water column for patches of food while expending minimal energy. They also suggested that slower ascent rates might improve the chances of pelagic predators detecting prey because backlighting is improved during ascents.

If searching for prey is the driver behind the occasional spike dives observed for oceanic whitetip sharks in our study, they could have been triggered after sharks remained in less productive surface waters for prolonged periods. It has been hypothesized that deep dives by whale sharks (*Rhincodon typus*) in the Indian Ocean were triggered when individuals were crossing less productive areas (Brunnschweiler and Sims, 2012). Another hypothesis for the occurrence of spike dives is that sharks make these deep dives to search for navigational cues through magnetic gradients (Willis et al., 2009). Seafloor magnetic anomalies associated with bathymetric features form a predictable gridded pattern that is believed to aid navigation (Walker et al., 2002). Sharks can detect magnetic fields (Kalmijn, 1982), and deep dives could represent a mechanism to acquire these magnetic cues (Gleiss et al., 2011; Tyminski et al., 2015). Howey et al. (2016) concluded that foraging or navigation are the only viable hypotheses to explain the reasons for the mesopelagic excursions of oceanic whitetip sharks, but they suggested that foraging is the most likely hypothesis. Nevertheless, the 2 proposed hypotheses are plausible and not mutually exclusive. It is, therefore, possible that isolated spike dives taken by oceanic whitetip sharks can be triggered by both foraging and navigational needs, depending on the circumstances.

Vertical movements and the environment

Water temperature is a limiting factor for ectothermic species whose body temperature is dependent on the external environment, because body temperature is a central factor in the control of their physiological processes (Sims, 2003). For such species, like the oceanic whitetip shark, which occupies the tropical epipelagic niche (Musyl et al., 2011; Howey-Jordan et al., 2013; Tolotti et al., 2015b), variations in the extent and heat content of the warmer mixed layer are expected to play a major role in their vertical movements. Our study confirmed this strong relationship by modeling the SD of daily depth records as a proxy for the amplitude of vertical movements. The GAM results indicate that tagged oceanic whitetip sharks tended to increase their vertical range in the water column as the depth of the mixed layer increased and, consequently, their optimal habitat expanded. A similar relationship was recently observed for another tropical epipelagic species; dolphinfish tagged in the Pacific Ocean extended their vertical depth ranges as the depth of the thermocline increased (Furukawa et al., 2014).

Besides the MLD, other factors were found to influence the vertical movements of tagged oceanic whitetip sharks in our study. Results from the GAM that used data for multiple sharks indicate an effect of shark size, in which larger individuals tended to have wider use of the water column. Values of average depth per hour, displayed in Figure 1, also indicate that vertical behavior might vary with shark size. Such an effect might be linked to the increased thermal inertia that results from a larger body mass, enabling larger individuals to extend their thermal habitat (Neill et al., 1974, 1976; Wilson et al., 2006). A possible effect of size on the vertical movements of oceanic whitetip sharks and silky sharks also has been reported from a tagging study conducted off Hawaii (Musyl et al., 2011). The results of a cluster analysis by Musyl et al. (2011) revealed that the vertical behavior of large individuals (>200 cm in total length) of these 2 closely related species appear to be well separated from that of juveniles.

For oceanic whitetip sharks tagged in the Bahamas, a correlation between average daily depth and SST was observed (Howey-Jordan et al., 2013). The authors reported that the average daily depth increased when individuals experienced warmer SSTs. For the oceanic whitetip sharks that we studied, the results from most GAMs also indicate a positive relationship between vertical movement and SST. Interestingly, for 2 individuals (AOCS3 and AOCS5), this relationship occurred simultaneously with an inverse relationship between MLD and the vertical activity of the sharks. In short, when SST was above average, these 2 sharks increased the amplitude of their vertical movement despite the reduced depth of the mixed layer. This pattern may indicate behavioral thermoregulation. Accordingly, oceanic whitetip sharks could be using the warmer SST to accumulate heat and subsequently explore cooler deep waters or they could be diving below the thermocline to cool down.

Howey-Jordan et al. (2013) also suggested that the correlation between SST and average depth observed for the oceanic whitetips sharks in the Bahamas could

indicate a behavioral thermoregulation mechanism. In fact, the use or active avoidance of heat sources to regulate body temperature has been reported for other shark species (Campana et al., 2011; Speed et al., 2012; Vianna et al., 2013). There is evidence supporting the idea that behaviorally induced thermoregulation optimizes physiological and metabolic processes, reducing metabolic losses and increasing foraging efficiency (Sims, 2003; Campana et al., 2011). Unfortunately, the relatively small sample size of our study hampers a more detailed analysis and discussion concerning behaviorally induced thermoregulation on oceanic whitetip sharks. Although additional data are still required, the results presented here indicate that the accumulation of heat could play an important role in triggering vertical movements. It seems that warmer SST allows oceanic whitetip sharks to tolerate a greater temperature range and, therefore, to temporarily expand their vertical niche.

Longlining is the main gear responsible for the demise of populations of oceanic whitetip shark (Rice and Harley[1]). Given that the depth stratum of this fishing gear considerably overlaps with the vertical distribution of this species (Tolotti et al., 2015b), it is important to continue our efforts to understand the behavioral patterns of sharks and the drivers behind these patterns. It must be noted that when dealing with rare, threatened animals, such as the oceanic whitetip shark, sample size is constrained largely by opportunity. This study was based on only 6 individuals, but the observations over 538 d in the Atlantic Ocean and 100 d in the Indian Ocean provide new information on the behavior of this shark. Nevertheless, the scientific community should direct its efforts to increase the number of tagged individuals, including tagging across a broader geographic region. Electronic tags are resourceful, nonlethal instruments that can significantly improve our knowledge of the ecology of this threatened species and, consequently, can aid its conservation.

Acknowledgments

We thank the crews, observers, and scientists involved in the tagging of oceanic whitetip sharks. We also thank A. Villareal and C. Taylor for returning the tag that was found stranded at a beach in Texas. This study was financed by the Commission of the European Communities Framework Program 7, Theme 2, through the research project "Mitigating adverse ecological impacts of open ocean fisheries." M. Tolotti received doctoral grants from the Coordenação de Aperfeiçoamento de Pessoal de Nível Superior and France Filière Pêche.

Literature cited

Abecassis, M., H. Dewar, D. Hawn, and J. Polovina.
2012. Modeling swordfish daytime vertical habitat in the North Pacific Ocean from pop-up archival tags. Mar. Ecol. Prog. Ser. 452:219–236.

Backus, R. H., S. Springer, and E. L. Arnold Jr.
1956. A contribution to the natural history of the whitetip shark, *Pterolamiops longimanus* (Poey). Deep Sea Res. 3:178–188.

Barker, M. J., and V. Schluessel.
2005. Managing global shark fisheries: suggestions for prioritizing management strategies. Aquat. Conserv. 15:325–347.

Bauer, R. K., F. Forget, and J.-M. Fromentin.
2015. Optimizing PAT data transmission: assessing the accuracy of temperature summary data to estimate environmental conditions. Fish. Oceanogr. 24:533–539.

Baum, J., E. Medina, J. A. Musick, and M. Smale.
2015. *Carcharhinus longimanus*. The IUCN Red List Threatened Species 2015: e.T39374A85699641.

Beerkircher, L. R., E. Cortés, and M. Shivji.
2002. Characteristics of shark bycatch observed on pelagic longlines off the southeastern United States, 1992–2000. Mar. Fish. Rev. 64(4):40–49.

Bernal, D., C. Sepulveda, M. Musyl, and R. Brill.
2009. The eco-physiology of swimming and movement patterns of tunas, billfishes, and large pelagic sharks. *In* Fish locomotion: an etho-ecological perspective (P. Domenici and D. Kapoor, eds.), p. 436–483. Science Publishers, Enfield, New Hampshire.

Bloomfield, P.
2004. Fourier analysis of time series: an introduction, 288 p. John Wiley & Sons Inc., New York.

Bonfil, R., S. Clarke, and H. Nakano.
2008. The biology and ecology of the oceanic whitetip shark, *Carcharhinus longimanus*. *In* Sharks of the open ocean: biology, fisheries and conservation (M. D. Camhi, E. K. Pikitch, E. A. Babcock, eds.), p. 128–139. Blackwell Publishing Ltd., Oxford.

Brunnschweiler, J. M., and D. W. Sims.
2012. Diel oscillations in whale shark vertical movements associated with meso-and bathypelagic diving. Am. Fish. Soc. Symp. 76:457–469.

Bustamante, C., and M. B. Bennett.
2013. Insights into the reproductive biology and fisheries of two commercially exploited species, shortfin mako (*Isurus oxyrinchus*) and blue shark (*Prionace glauca*), in the south-east Pacific Ocean. Fish. Res. 143:174–183.

Camargo, S. M., R. Coelho, D. Chapman, L. Howey-Jordan, E. J. Brooks, D. Fernando, N. J. Mendes, F. H. V. Hazin, C. Oliveira, M. N. Santos, et al.
2016. Structure and genetic variability of the oceanic whitetip shark, *Carcharhinus longimanus*, determined using mitochondrial DNA. PLoS ONE 11(5):e0155623.

Campana, S. E., A. Dorey, M. Fowler, W. Joyce, Z. Wang, D. Wright, and I. Yashayaev.
2011. Migration pathways, behavioural thermoregulation and overwintering grounds of blue sharks in the northwest Atlantic. PLoS ONE 6(2):e16854.

Coelho, R., J. Fernandez-Carvalho, and M. N. Santos.
2015. Habitat use and diel vertical migration of bigeye thresher shark: overlap with pelagic longline fishing gear. Mar. Environ. Res. 112:91–99.

Compagno, L. J. V.
1984. FAO species catalogue, vol . 4. Sharks of the world: an annotated and illustrated catalogue of shark species known to date. Part 1—Hexanchiformes to Lamniformes. FAO Fish. Synop. 125, 249 p. FAO, Rome.

Dagorn, L., P. Bach, and E. Josse.
2000. Movement patterns of large bigeye tuna (*Thunnus obesus*) in the open ocean, determined using ultrasonic telemetry. Mar. Biol. 136:361–371.

Damalas, D., and P. Megalofonou.
2010. Environmental effects on blue shark (*Prionace glauca*) and oilfish (*Ruvettus pretiosus*) distribution based on fishery-dependent data from the eastern Mediterranean Sea. J. Mar. Biol. Assoc. U.K. 90:467–480.

Filmalter, J., P. Cowley, F. Forget, and L. Dagorn.
2015. Fine-scale 3-dimensional movement behaviour of silky sharks *Carcharhinus falciformis* associated with fish aggregating devices (FADs). Mar. Ecol. Prog. Ser. 539:207–223.

Frédou, F. L., M. T. Tolotti, T. Frédou, F. Carvalho, H. Hazin, G. Burgess, R. Coelho, J. D. Waters, P. Travassos, and F. H. V. Hazin.
2015. Sharks caught by the Brazilian tuna longline fleet: an overview. Rev. Fish Biol. Fish. 25:365–377.

Furukawa, S., Y. Tsuda, G. N. Nishihara, K. Fujioka, S. Ohshimo, S. Tomoe, N. Nakatsuka, H. Kimura, T. Aoshima, H. Kanehara, et al.
2014. Vertical movements of Pacific bluefin tuna (*Thunnus orientalis*) and dolphinfish (*Coryphaena hippurus*) relative to the thermocline in the northern East China Sea. Fish. Res. 149:86–91.

Gallagher, A. J., E. S. Orbesen, N. Hammerschlag, and J. E. Serafy.
2014. Vulnerability of oceanic sharks as pelagic longline bycatch. Global Ecol. Conserv. 1:50–59.

Garcia, S. M., and K. L. Cochrane.
2005. Ecosystem approach to fisheries: a review of implementation guidelines. ICES J. Mar. Sci. 62:311–318.

Gleiss, A. C., B. Norman, and R. P. Wilson.
2011. Moved by that sinking feeling: variable diving geometry underlies movement strategies in whale sharks. Funct. Ecol. 25:595–607.

Hall, M., and M. Roman.
2013. Bycatch and non-tuna catch in the tropical tuna purse seine fisheries of the world. FAO Fish. Aquac. Tech. Pap. 568, 249 p. FAO, Rome.

Hoffmayer, E. R., J. S. Franks, W. B. Driggers, and P. W. Howey.
2013. Diel Vertical movements of a scalloped hammerhead, *Sphyrna lewini*, in the northern Gulf of Mexico. Bull. Mar. Sci. 89:551–557.

Howey, L. A., E. R. Tolentino, Y. P. Papastamatiou, E. J. Brooks, D. L. Abercrombie, Y. Y. Watanabe, S. Williams, A. Brooks, D. D. Chapman, and L. K. B. Jordan.
2016. Into the deep: the functionality of mesopelagic excursions by an oceanic apex predator. Ecol. Evol. 6:5290–5304.

Howey-Jordan, L. A., E. J. Brooks, D. L. Abercrombie, L. K. B. Jordan, A. Brooks, S. Williams, E. Gospodarczyk, and D. D. Chapman.
2013. Complex movements, philopatry and expanded depth range of a severely threatened pelagic shark, the oceanic whitetip (*Carcharhinus longimanus*) in the western North Atlantic. PLoS ONE 8(2):e56588.

Joung, S.-J., N.-F. Chen, H.-H. Hsu, and K.-M. Liu.
2016. Estimates of life history parameters of the oceanic whitetip shark, *Carcharhinus longimanus*, in the western North Pacific Ocean. Mar. Biol. Res. 12:758–768.

Kalmijn, A. J.
1982. Electric and magnetic field detection in elasmobranch fishes. Science 218:916–918.

Lam, C. H., B. Galuardi, and M. E. Lutcavage.
2014. Movements and oceanographic associations of bigeye tuna (*Thunnus obesus*) in the northwest Atlantic. Can. J. Fish. Aquat. Sci. 71:1529–1543.

Li, W., X. Dai, Q. Xu, F. Wu, C. Gao, and Y. Zhang.
2016. The complete mitochondrial genome sequence of oceanic whitetip shark, *Carcharhinus longimanus* (Carcharhiniformes: Carcharhinidae). Mitochondrial DNA Part A 27:1775–1776.

Madigan, D. J., E. J. Brooks, M. E. Bond, J. Gelsleichter, L. A. Howey, D. L. Abercrombie, A. Brooks, and D. D. Chapman.
2015. Diet shift and site-fidelity of oceanic whitetip sharks *Carcharhinus longimanus* along the Great Bahama Bank. Mar. Ecol. Prog. Ser. 529:185–197.

Merten, W., R. Appeldoorn., R. Rivera, and D. Hammond.
2014. Diel vertical movements of adult male dolphinfish (*Coryphaena hippurus*) in the western central Atlantic as determined by use of pop-up satellite archival transmitters. Mar. Biol. 161:1823–1834.

Musyl, M. K., R. W. Brill, C. H. Boggs, D. S. Curran, T. K. Kazama, and M. P. Seki.
2003. Vertical movements of bigeye tuna (*Thunnus obesus*) associated with islands, buoys, and seamounts near the main Hawaiian Islands from archival tagging data. Fish. Oceanogr. 12:152–169.

Musyl, M. K., R. W. Brill, D. S. Curran, N. M. Fragoso, L. M. McNaughton, A. Nielsen, B. S. Kikkawa, and C. D. Moyes.
2011. Postrelease survival, vertical and horizontal movements, and thermal habitats of five species of pelagic sharks in the central Pacific Ocean. Fish. Bull. 109:341–368.

Neill, W. H., E. D. Stevens,, F. G. Carey, K. D. Lawson, N. Mrosovsky, and W. Frair.
1974. Thermal inertia versus thermoregulation in "warm" turtles and tunas. Science 184:1008–1010.

Neill, W. H., R. K. C. Chang, and A. E. Dizon.
1976. Magnitude and ecological implications of thermal inertia in skipjack tuna, *Katsuwoaus pelamis* (Lionreus). Environ. Biol. Fish.1:61–80.

Nelson, D. R., J. N. McKibben, W. R. Strong Jr., C. G. Lowe, J. A. Sisneros, D. M. Schroeder, and R. J. Lavenberg.
1997. An acoustic tracking of a megamouth shark, *Megachasma pelagios*: a crepuscular vertical migrator. Environ. Biol. Fish. 49:389–399.

Oliver, S., M. Braccini, S. J. Newman, and E. S. Harvey.
2015. Global patterns in the bycatch of sharks and rays. Mar. Policy 54:86–97.

Pade, N. G., N. Queiroz, N. E. Humphries, M. J. Witt, C. S. Jones, L. R. Noble, and D. W. Sims.
2009. First results from satellite-linked archival tagging of porbeagle shark, *Lamna nasus*: area fidelity, wider-scale movements and plasticity in diel depth changes. J. Exp. Mar. Bio. Ecol. 370:64–74.

Pikitch, E. K., C. Santora, E. A. Babcock, A. Bakun, R. Bonfil, D. O. Conover, P. Dayton, P. Doukakis, D. Fluharty, B. Heneman, et al.
2004. Ecosystem-based fishery management. Science 305:346–347.

Piovano, S., and E. Gilman.
2016. Elasmobranch captures in the Fijian pelagic longline fishery. Aquat. Conserv.

Queiroz, N., N. E. Humphries, L. R. Noble, A. M. Santos, and D. W. Sims.
2012. Spatial dynamics and expanded vertical niche of blue sharks in oceanographic fronts reveal habitat targets for conservation. PLoS ONE 7(2):e32374.

R Core Team.
2014. R: a language and environment for statistical computing. R Foundation for Statistical Computing, Vienna, Austria. [Available from website, accessed November 2014.]

Sepulveda, C. A., S. Kohin, C. Chan, R. Vetter, and J. B. Graham.
2004. Movement patterns, depth preferences, and stomach temperatures of free-swimming juvenile mako sharks, *Isurus oxyrinchus*, in the Southern California Bight. Mar. Biol. 145:191–199.

Shepard, E. L. C., M. Z. Ahmed, E. J. Southall, M. J. Witt, J. D. Metcalfe, D. W. Sims.
2006. Diel and tidal rhythms in diving behaviour of pelagic sharks identified by signal processing of archival tagging data. Mar. Ecol. Prog. Ser. 328:205–213.

Sims, D. W.
2003. Tractable models for testing theories about natural strategies: foraging behaviour and habitat selection of free-ranging sharks. J. Fish Biol. 63:53–73.

Sims, D. W., E. J. Southall, G. A. Tarling, and J. D. Metcalfe.
2005. Habitat-specific normal and reverse diel vertical migration in the plankton-feeding basking shark. J. Anim. Ecol. 74:755–761.

Speed, C. W., M. G. Meekan, I. C. Field, C. R. McMahon, and C. J. A. Bradshaw.
2012. Heat-seeking sharks: support for behavioural thermoregulation in reef sharks. Mar. Ecol. Prog. Ser. 463:231–245.

Tambourgi, M. R. D. S., F. H. V. Hazin, P. G. V. Oliveira, R. Coelho, G. Burgess, and P. C. G. Roque.
2013. Reproductive aspects of the oceanic whitetip shark, *Carcharhinus longimanus* (Elasmobranchii: Carcharhinidae), in the equatorial and southwestern Atlantic Ocean. Braz. J. Oceanogr. 61:161–168.

Tolotti, M. T., P. Travassos, F. L. Frédou, C. Wor, H. A. Andrade, and F. Hazin.
2013. Size, distribution and catch rates of the oceanic whitetip shark caught by the Brazilian tuna longline fleet. Fish. Res. 143:136–142.

Tolotti, M. T., J. D. Filmalter, P. Bach, P. Travassos, B. Seret, and L. Dagorn.
2015a. Banning is not enough: the complexities of oceanic shark management by tuna regional fisheries management organizations. Global Ecol. Conserv. 4:1–7.

Tolotti, M. T., P. Bach, F, Hazin, P. Travassos, and L. Dagorn.
2015b. Vulnerability of the oceanic whitetip shark to pelagic ongline fisheries. PLoS ONE 10(10):e0141396.

Tyminski, J. P., R. de la Parra-Venegas, J. González Cano, and R. E. Hueter.
2015. Vertical movements and patterns in diving behavior of whale sharks as revealed by pop-up satellite tags in the eastern Gulf of Mexico. PLoS ONE 10(11):e0142156.

Urmy, S. S., J. K. Horne, and D. H. Barbee.
2012. Measuring the vertical distributional variability of pelagic fauna in Monterey Bay. ICES J. Mar. Sci. 69:184–196.

Vianna, G. M. S., M. G. Meekan, J. J. Meeuwig, and C. W. Speed.
2013. Environmental influences on patterns of vertical movement and site fidelity of grey reef sharks (*Carcharhinus amblyrhynchos*) at aggregation sites. PLoS ONE 8(4):e60331.

Walker, M. M., T. E. Dennis, and J. L. Kirschvink.
2002. The magnetic sense and its use in long-distance navigation by animals. Curr. Opin. Neurobiol. 12:735–744.

Willis, J., J. Phillips, R. Muheim, F. J. Diego-Rasilla, and A. J. Hobday.
2009. Spike dives of juvenile southern bluefin tuna (*Thunnus maccoyii*): a navigational role? Behav. Ecol. Sociobiol. 64:57–68.

Wilson, S. G., J. J. Polovina, B. S. Stewart, and M. G. Meekan.
2006. Movements of whale sharks (*Rhincodon typus*) tagged at Ningaloo Reef, Western Australia. Mar. Biol. 148:1157–1166.

Wood, S. N.
2006. Generalized additive models: an introduction with R, 410 p. CRC Press, Boca Raton, FL.

World of Earth Science.
2003. Solar illumination: seasonal and diurnal patterns. Encyclopedia.com. [Available from website, accessed January 2016.]

Zagaglia, C. R., J. A. Lorenzzetti, and J. L. Stech.
2004. Remote sensing data and longline catches of yellowfin tuna (*Thunnus albacares*) in the equatorial Atlantic. Remote Sens. Environ. 93:267–281.

National Marine
Fisheries Service
NOAA

Fishery Bulletin
established in 1881

Spencer F. Baird
First U.S. Commissioner
of Fisheries and founder
of *Fishery Bulletin*

Effects of skipped spawning on the reproductive potential of Argentine hake (*Merluccius hubbsi*)

Gustavo J. Macchi[1,2] (contact author)
Karina Rodrigues[1,2]
Marina V. Diaz[1,2]
María I. Militelli[1,2]

Email address for contact author: gmacchi@inidep.edu.ar

[1] Consejo Nacional de Investigaciones Científicas y Técnicas (CONICET)
Instituto de Investigaciones Marinas y Costeras (IIMyC)
Rodríguez Peña 4002-4100
B7602GSD Mar del Plata
Buenos Aires, Argentina

[2] Instituto Nacional de Investigación y Desarrollo Pesquero (INIDEP)
Paseo Victoria Ocampo Nro. 1
B7602HSA Mar del Plata
Buenos Aires, Argentina

Abstract—We analyzed the effect of skipped spawning on the estimates of length and age at maturity and on the reproductive potential of Argentine hake (*Merluccius hubbsi*) from the Patagonian stock during the spawning peaks between 2005 and 2013. The length at first maturity increased by 2–3 cm in total length (TL), and the age at maturity increased by 0.27–0.88 years when the proportion of females that would skip spawning was incorporated in the relationships. In addition, the slopes of the models decreased, suggesting that all individuals reach sexual maturity at a greater size and age than those estimated with the traditional criterion for maturity, which does not consider skipped spawning because fish in the resting stage are classified as mature. The reduction in egg production caused by skipped spawning ranged between 3.56% and 12.12%, when we used the maturity models with age data, or between 2.70% and 6.80%, when we used the models with TL data. Females that would skip spawning were mainly specimens with sizes between 40 and 50 cm TL, and most belonged to the age class of 3-year-old fish.

Manuscript submitted 26 October 2016.
Manuscript accepted 30 May 2017.
Fish. Bull. 115:396–407 (2017).
Online publication date: 13 June 2017.
doi: 10.7755/FB.115.3.9

The views and opinions expressed or implied in this article are those of the author (or authors) and do not necessarily reflect the position of the National Marine Fisheries Service, NOAA.

One of the main assumptions in fishery assessments for iteroparous fish species is that after spawning for the first time, i.e., after reaching maturity, these species reproduce annually. Nevertheless, failure to spawn in consecutive years has been observed in many species, a phenomenon known as skipped spawning (SS) (Rideout et al., 2005). In general, the hypotheses proposed to explain the cause of SS are associated with feeding deficiencies that decrease energy storage before spawning. Such feeding deficiencies may leave the fish in such a poor nutritional condition that they may not have sufficient energy to support egg production in consecutive years (Dutil, 1986; Holmgren, 2003; Jørgensen et al., 2006; Rideout et al., 2006; Rideout and Tomkiewicz, 2011). Failure to consider SS in the reproductive output of a stock could result in an overestimation of spawning stock biomass and reproductive potential (Rideout and Tomkiewicz, 2011). Despite the influence of the SS phenomenon in the estimation of total egg production, this influence has rarely been considered in fishery assessments (Rideout et al., 2005).

The Patagonian stock of Argentine hake (*Merluccius hubbsi*), distributed from 41°S to 55°S at depths between 50 and 500 m, is one of the most important fishery resources for Argentina; the total annual catch reported for 2015 was approximately 260,000 metric tons (Ministerio de Agroindustria[1]). This stock is assessed annually through virtual population analysis with an age-structured model with spawning stock biomass as a biological reference point. The Argentine hake from the Patagonian region is a batch spawner with indeterminate annual fecundity; it reproduces from November to April and peak spawning occurs in January (Macchi et al., 2004). Recently, it was reported that 6–22% of female Argentine hake from Patagonian waters would skip spawning and remain unproductive during the spawning peak (Macchi et

[1] Ministerio de Agroindustria. 2015 Desembarques de capturas marítimas totales—por especie y flota. Subsecretaría de Pesca y Acuicultura, Secretaría de Agricultura, Ganadería y Pesca, Ministerio de Agroindustria, Buenos Aires, Argentina. [Available from website, accessed October 2016.]

Table 1

Number of samples and subsamples of specimens collected from the Patagonian stock of Argentine hake (*Merluccius hubbsi*), as well as the number of ovaries collected for estimation of fecundity. Research surveys were carried out during the spawning peak (January) and the resting period (August) of this stock in the north Patagonian region of Argentina from 2005 through 2013.

Year	Total samples in January	Female samples in January	Female subsamples in January	Female samples in August	Ovaries for fecundity
2005	16250	6810	2322	3228	178
2006	8500	4022	2546		111
2007	8804	5634	2015	4371	78
2008	13,881	7045	1954		110
2009	15,813	7970	1969		101
2010	19,683	9485	2037		105
2011	13,487	6420	1959	5577	731
2012	19,362	9533	3448	3030	82
2013	31,956	14,155	3361	7392	97

al., 2016). These individuals were located mostly on the periphery of the spawning area at depths close to 100 m, and they were mainly young adult females.

We report on our continued study of skipped spawning in Argentine hake. The main purpose of the research described in our study was to establish how this phenomenon affects the reproductive potential of the Patagonian stock of this species. We constructed length- and age-based maturity models by using 2 interpretations of the maturity cycle: 1) females that had skipped spawning were classified as mature (traditional interpretation) and 2) mature females that had not spawned during the reproductive season were classified as functionally immature (revised interpretation). We also examined the relationship between the demographic composition of the stock and the incidence of skipped spawning. We estimated the proportion of the total reproductive potential that was reduced as a result of skipped spawning by analyzing data from research surveys performed during peak spawning of the Patagonian stock of Argentine hake.

Materials and methods

Sample collection and laboratory processing

Most of our samples were collected in the summer during 9 research surveys conducted by the Instituto Nacional de Investigación y Desarrollo Pesquero (INIDEP) in the north Patagonian area off Argentina between 2005 and 2013 (Table 1). These surveys were performed during the peak spawning time for the Patagonian stock of Argentine hake (January) in the area of reproduction, and in the main nursery ground for young-of-the-year individuals in the San Jorge Gulf. Trawling during these surveys was conducted at depths between 50 and 120 m along transects regularly separated by approximately 37 km (20 nmi) and oriented perpendicularly to the coastline (Fig. 1). We also had data from samples of females collected during 5 surveys carried out in the same area (43–47°S and 61–67°W) in August (austral winter) when the Patagonian stock of Argentine hake was in a resting reproductive stage (Table 1). In these 5 surveys, 50–90 stations were sampled by using a stratified random design for the entire study area, at depths between 50 and 200 m. The bottom trawl used for all surveys had a mouth width of approximately 20 m, a height of 4 m, and a net with a 20-mm mesh liner in the codend.

After weighing the catch of Argentine hake, a random sample was taken to determine sex, and the total length (TL, in centimeters) was recorded for each fish. Moreover, the maturity of each specimen was assessed macroscopically on the basis of a 5-stage maturity key: 1) immature, 2) developing, 3) spawning, 4) post-spawning or spent, and 5) resting or recovering. This maturity scale was previously validated for females by histological analysis of the ovaries and was described in Macchi et al. (2016). For this reason, to estimate length and age at maturity (L_{50} and A_{50}, respectively), we used only macroscopic information. To estimate age composition, sagittal otoliths were collected from random subsamples of female Argentine hake collected from different sampling stations during January surveys (Table 1). Ages, based on analysis of these otoliths, were determined by using a method described by Renzi and Pérez (1992).

To estimate models of batch fecundity versus TL and batch fecundity versus age for the Patagonian stock, we collected females classified as spawning (with hydrated oocytes) from different sampling stations, and fixed the ovaries in 10% neutral-buffered formalin for histological analysis (Table 1). The ovaries were weighed to the nearest 0.1 g to obtain gonad weight, and a portion (approximately 2.0 g) of each gonad was then removed,

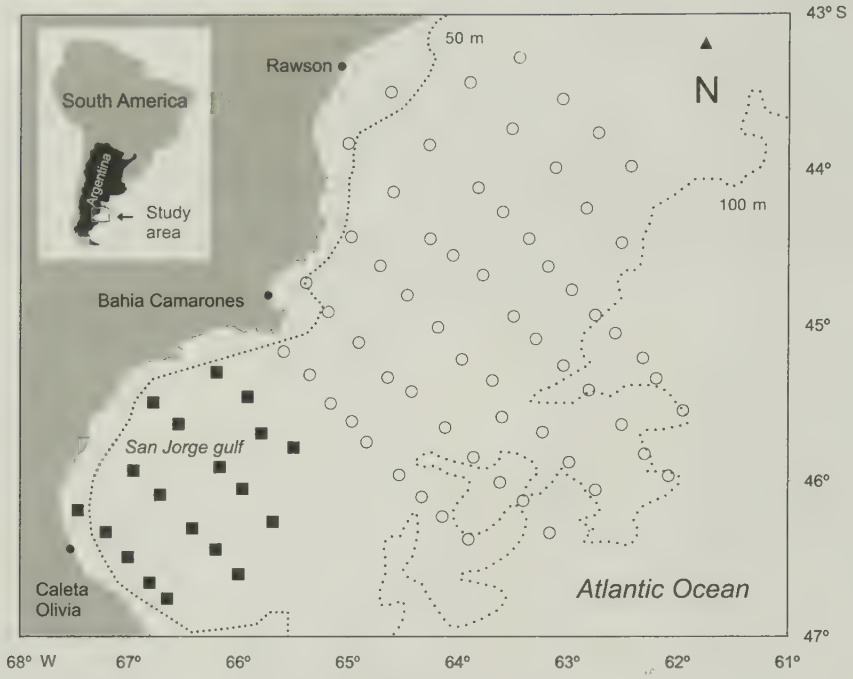

Figure 1

Locations where Argentine hake (*Merluccius hubbsi*) were collected during January for the years 2005 through 2013 in waters of the north Patagonian area off Argentina. Open circles indicate sampling locations in the area where Argentine hake typically spawn, and black squares indicate sampling locations in the nursery area for juvenile Argentine hake in the San Jorge Gulf.

dehydrated in ethanol, cleared in xylol, and embedded in paraffin. From these gonads, 5-µm sections were mounted and stained with Harris hematoxylin followed by eosin counterstain.

Estimation of length and age at maturity

We constructed length- and age-based maturity ogives for female Argentine hake from samples and subsamples collected during the summer spawning peak (January) of the Patagonian stock (Table 1). For estimation of L_{50} and A_{50}, the maximum likelihood method was used to fit the proportion of mature individuals by length class (TL) and age class to a logistic function (Kendall and Stuart, 1967).

The presence of ovaries in fish classified in the resting stage and collected during the main spawning peak of the Patagonian stock was taken as evidence of SS in female Argentine hake (Macchi et al., 2016). These gonads were characterized as having only oocytes in the primary growth phase and as having a thick ovarian tunica, with no evidence of ovary development or recent spawning (Rodgveller et al., 2016). Therefore, when considering SS in estimating the maturity ogives, we classified females in the resting stage as immature individuals.

For this reason, and following the method of Rodgveller et al. (2016), we estimated L_{50} and A_{50} on the basis of the following 2 interpretations of the maturity cycle: 1) the traditional interpretation, in which fish in the resting stage were classified as mature, and 2) the revised interpretation, in which adult females classified as in the resting stage were considered to be functionally immature. We obtained coefficients of the maturity ogives by using both interpretations for each year during the period 2005–2013. The coefficients were compared by using an χ^2 test according to Aubone and Wöhler.[2]

In the case of the August surveys, we had only data for TL and gonad maturity stage from samples of females collected in 2005, 2007, 2011, 2012 and 2013 (Table 1). Using this information, we constructed length-based maturity ogives for August of those years, and the models obtained were compared with the maturity ogives estimated using data from January of the same year, during the previous spawning peak. Coefficients of the logistic relationships obtained in both sampling seasons were compared by using an χ^2 test. It was not possible to identify females that were skipping spawning during August because the majority of the fish during this month were in a resting or immature stage.

[2] Aubone, A., and O. Wöhler. 2000. Aplicación del método de máxima verosimilitud a la estimación de parámetros y comparación de curvas de crecimiento de von Bertalanffy. INIDEP Inf. Téc. 37, 21 p. [Available from Instituto Nacional de Investigación y Desarrollo Pesquero, Paseo Victoria Ocampo Nro. 1, B7602HSA Mar del Plata, Argentina.]

Therefore, to estimate length at first maturity with data from the August survey, only the traditional interpretation of maturity assignment (resting stage as mature female) was employed.

Estimation of size and age distributions of female Argentine hake

The number of females was estimated from data collected during each survey between 2005 and 2013. These cruises covered a wide geographic range from 43°S to 47°S, but to analyze the abundance of females that would skip spawning or would spawn, we used only data from sampling stations located in the area of active reproduction, which covers approximately 65% of the study zone (Fig. 1). The same area, with an extension of about 50,000 km^2, is assessed every year during a fixed-station trawl survey to estimate the potential egg production of the Patagonian stock of Argentine hake (Macchi et al.[3]). Information obtained from sampling the trawl catch was expanded to obtain estimates of the number of individuals per length class, by using the method described by Macchi et al. (2004). The number of mature females for each survey was estimated by multiplying the number of Argentine hake within each length class by the proportion of mature females estimated from the L_{50} ogive obtained for each survey. To obtain the incidence of SS by length class, we compared the length distributions obtained with the estimated maturity ogive with the traditional interpretation and the revised interpretation for each year.

From the age-length keys obtained with data collected in each survey, we estimated the age distributions of female Argentine hake in the sampling area during each January between 2005 and 2013. The number of mature females by age class for each year was estimated by multiplying the number of females in each age class by the proportion of mature females obtained from the A_{50} ogive corresponding to that year. We compared the age distributions of mature females by using the maturity ogive constructed with the traditional and the revised interpretation. In this case, to determine the effect of spawning omission, we estimated the average age distributions obtained after grouping all years sampled during the period 2005–2013.

Estimation of reproductive potential

Because the Argentine hake is a batch spawner with indeterminate annual fecundity, we estimated the batch fecundity (number of oocytes released per spawning) by the hydrated oocyte method of Hunter et al. (1985). After histological diagnosis, we selected only ovaries with hydrated oocytes and without evidence of recent spawning (no postovulatory follicles), and removed 3 pieces of tissue (0.1–0.2 g each) from the anterior, middle and posterior parts of a gonad. These samples were weighed (to the nearest 0.1 mg), and the number of hydrated oocytes was counted to estimate the mean of hydrated oocytes per unit of weight. Batch fecundity value for each female was obtained by multiplying the mean number of hydrated oocytes and the total weight of the ovaries. The relationships of batch fecundity to TL and age were described by using standard regression analysis (Draper and Smith, 1981).

We could not estimate a relationship between spawning frequency and TL or age for each year sampled. For this reason, the index of reproductive potential of the Patagonian stock of Argentine hake in January from 2005 to 2013 was estimated by multiplying the number of mature females in each length class or each age class by the batch fecundity corresponding to that length class or age class. Therefore, this index represents the egg production of the stock during one spawning event.

Estimates of egg production, by TL and age, by using the maturity ogive created with the traditional interpretation and the ogive created with the revised interpretation were compared to obtain the percentage of reduction in egg production attributed to nonreproductive adult females during the spawning season by year.

Results

Length and age at maturity

When we applied the traditional interpretation for maturity diagnosis, the L_{50} estimates for females of Argentine hake during January 2005–2013 ranged between 32.22 and 34.53 cm TL (Table 2). However, when we used the revised interpretation and considered that females in a resting stage were individuals that had skipped spawning, the values of L_{50} increased to range of 34.57–38.01 cm TL. In all cases, the standard error of L_{50} was lower when SS was considered for estimation of the maturity ogives—a result that may be associated with the increase in the number of immature individuals in length classes close to L_{50}. In addition, when SS was included in the L_{50} estimate, the slope of the logistic model decreased (Table 2), suggesting that all females reached sexual maturity at larger sizes than those estimated with the traditional interpretation. Comparison of the maturity ogives estimated by the different interpretations of maturity showed highly significant differences for all years sampled (P<0.001).

The A_{50} curves estimated with samples collected between 2005 and 2013 showed a similar pattern after inclusion of the proportion of females that SS in relationship both to the A_{50} and the slope of the models. The A_{50} values estimated with the traditional inter-

[3] Macchi, G. J., M. Estrada, H. Brachetta, and V. Abachián. 2013. Estructura y producción potencial de huevos del efectivo desovante de merluza (*Merluccius hubbsi*) al sur de 41°S durante enero de 2013. Inf. Téc. 88, 12 p. [Available from Instituto Nacional de Investigación y Desarrollo Pesquero, Paseo Victoria Ocampo Nro. 1, B7602HSA Mar del Plata, Argentina].

Table 2

Length at maturity (L_{50}) and slope (b) determined by the logistic model for female Argentine hake (*Merluccius hubbsi*) from the Patagonian stock. Samples were collected during research surveys conducted off Argentina during the spawning peak (January) and resting period (August) of this stock, 2005–2013. For surveys conducted in January, coefficients of the models were estimated on the basis of the following 2 interpretations of the maturity cycle: 1) the traditional interpretation, in which females in the resting stage were classified as mature, and 2) the revised interpretation, in which females in the resting stage were considered to be functionally immature. Lengths were measured as total length in centimeters. Standard errors of the means are given in parentheses. n=sample size. TI, traditional interpretation; RI, revised interpretation.

Year	Month	L_{50} (cm TL) TI	b TI	L_{50} (cm TL) RI	b RI	n
2005	January	33.88 (1.32)	0.82 (0.032)	35.72 (0.99)	0.32 (0.009)	6783
2006	January	33.44 (1.59)	0.70 (0.033)	35.55 (1.28)	0.25 (0.008)	3984
2007	January	32.69 (2.18)	0.77 (0.051)	34.57 (1.34)	0.16 (0.005)	5582
2008	January	34.53 (1.38)	0.62 (0.025)	38.01 (0.99)	0.22 (0.006)	6988
2009	January	34.26 (1.53)	0.92 (0.041)	37.37 (0.99)	0.27 (0.007)	7900
2010	January	33.19 (1.29)	1.01 (0.039)	36.37 (0.87)	0.21 (0.005)	3437
2011	January	32.22 (1.23)	0.63 (0.024)	35.84 (0.92)	0.23 (0.006)	6377
2012	January	33.04 (1.20)	0.87 (0.031)	35.34 (0.81)	0.29 (0.006)	9501
2013	January	33.13 (0.80)	0.79 (0.019)	36.48 (0.61)	0.26 (0.004)	14136
2005	August	34.45 (1.58)	0.64 (0.029)			3228
2007	August	34.51 (1.81)	0.83 (0.043)			4371
2011	August	32.39 (1.38)	0.91 (0.038)			5577
2012	August	34.26 (1.77)	0.92 (0.047)			3030
2013	August	33.35 (1.32)	0.91 (0.035)			7392

Table 3

Age at maturity (A_{50}) and slope (b) determined with the logistic model for female Argentine hake (*Merluccius hubbsi*) from the Patagonian stock collected during research surveys conducted off Argentina during January for the years 2005–2013. Coefficients of the models were estimated according to the following 2 interpretations: 1) the traditional interpretation, in which females in the resting stage were classified as mature, and 2) the revised interpretation, in which females in the resting stage were considered to be functionally immature. Standard errors of the means are given in parentheses. n=sample size. TI, traditional interpretation; RI, revised interpretation.

Year	A_{50} (years) TI	b TI	A_{50} (years) RI	b RI	n
2005	2.40 (0.11)	4.62 (0.22)	2.74 (0.12)	2.57 (0.11)	2300
2006	2.36 (0.11)	4.74 (0.22)	2.86 (0.12)	1.99 (0.08)	2516
2007	2.32 (0.16)	5.80 (0.44)	3.16 (0.16)	1.07 (0.05)	1961
2008	2.48 (0.14)	4.69 (0.28)	3.36 (0.14)	1.32 (0.06)	1924
2009	2.50 (0.12)	5.60 (0.29)	2.95 (0.14)	2.40 (0.12)	1908
2010	2.43 (0.12)	5.34 (0.26)	2.84 (0.15)	1.49 (0.07)	2027
2011	2.34 (0.14)	3.96 (0.27)	2.79 (0.12)	1.87 (0.08)	1953
2012	2.51 (0.09)	5.02 (0.18)	2.77 (0.11)	2.81 (0.10)	3414
2013	2.47 (0.08)	4.95 (0.17)	2.87 (0.10)	2.21(0.08)	3339

pretation ranged between 2.32 and 2.50 years, while those estimated with the revised criterion increased to 2.74–3.36 years (Table 3).

The length-based maturity ogives estimated with data from January (spawning peak) and by using the traditional interpretation were significantly different ($P<0.05$) from those estimated by using data from August (resting period) of the same year, except for 2013 ($P>0.05$); in general, the L_{50} coefficients were slightly higher in August, but the slopes were similar ($P>0.05$) between months (Table 2, Fig. 2). When we compared the length-based maturity ogives estimated with data

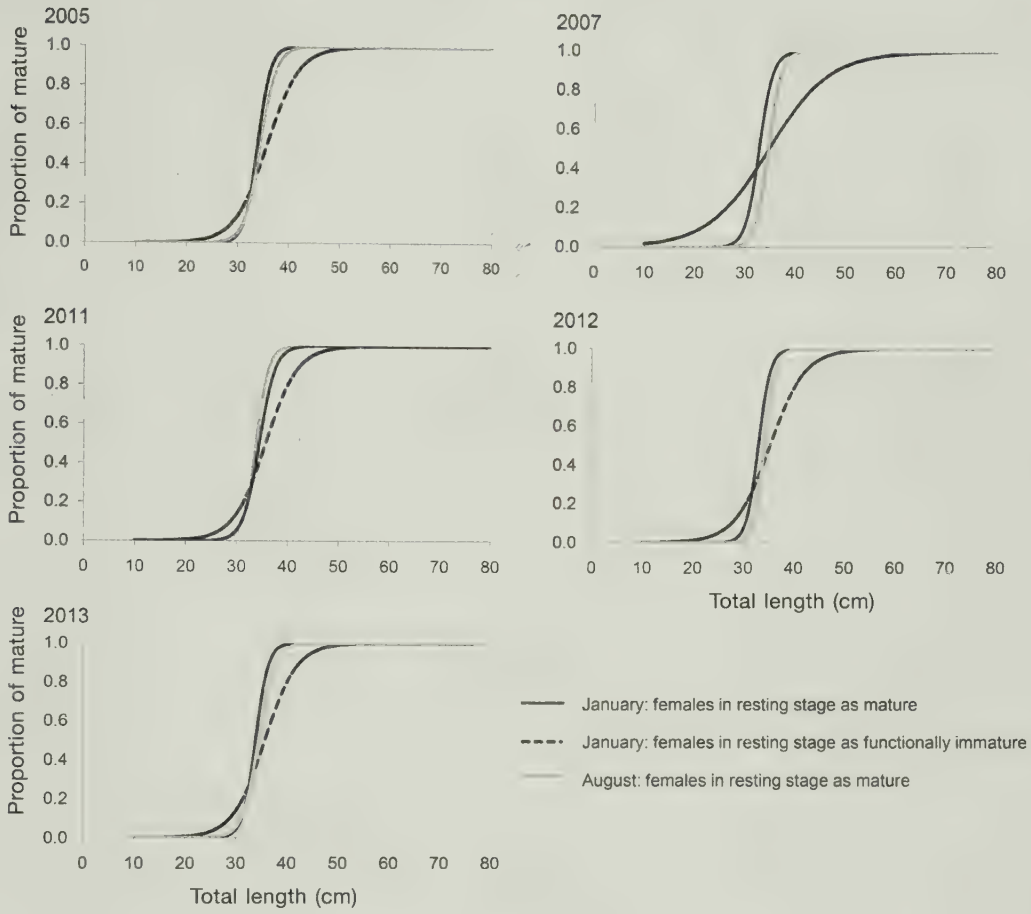

Figure 2

Length-at-maturity curves estimated for female Argentine hake (*Merluccius hubbsi*) collected from the Patagonian stock off Argentina in January and August 2005, 2007, 2011, 2012, and 2013, for which females in the resting stage were considered to be either mature (solid lines) or functionally immature (dashed lines).

from January surveys and using the revised interpretation with those estimated in August of the same year, highly significant differences ($P<0.001$) were observed, mainly in the slopes (Table 2, Fig. 2).

Age and size distributions of females

The length distributions of mature female Argentine hake showed considerable annual variation during the spawning peak in the period 2005–2013, and 1 or 2 modes (Fig. 3). In general, the main group of mature females was composed of individuals between 40 cm and 50 cm TL, but in some years, such as 2007 and 2008, a high frequency of females larger than 50 cm TL was observed (Fig. 3). The latter figure also shows the fraction of the length distributions affected by SS when we used the maturity ogive estimated with the revised interpretation (Table 2). It was observed that females that would skip spawning are mainly specimens smaller than 50 cm TL, and have a modal size between 37 and 40 cm TL (Fig. 3).

Figure 4 shows the average age distributions obtained after grouping all years sampled and by applying the traditional interpretation of maturity and after considering the effect of skipped spawning. This figure confirms that females that would skip spawning were mainly younger specimens. Approximately 70% of females that skipped spawning were 3 years old.

Reproductive potential

Batch fecundity for female Argentine hake sampled in January between 2005 and 2013 ranged from 70,000 to 3,170,000 hydrated oocytes, for fish between 29 cm and 95 cm TL. The relationship of batch fecundity to TL and to age for each sampled year fitted a power model (Table 4).

The number of oocytes produced by batch and by 1-cm

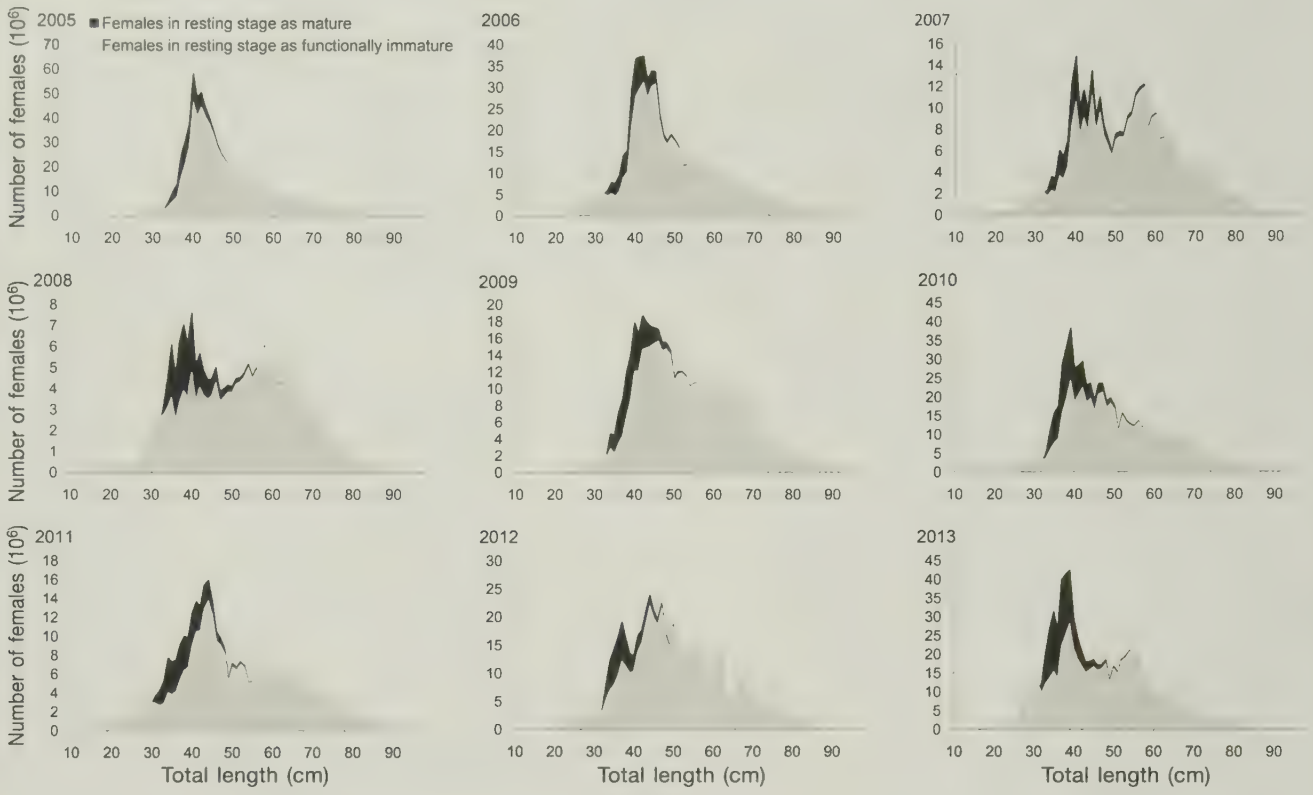

Figure 3

Length-frequency distributions of adult female Argentine hake (*Merluccius hubbsi*) collected from the Patagonian stock off Argentina in January during the years 2005–2013. The black shaded area visible beyond the gray area represents the fraction of females that would skip spawning during the spawning peak of the stock. The length-at-maturity model was applied in 2 ways to create the 2 overlapping areas: females in the resting stage were considered mature (black) or functionally immature (gray).

Table 4

Results of the regression analyses between batch fecundity (BF) and the variables *total length* (TL) and *age* for female Argentine hake (*Merluccius hubbsi*) sampled from the Patagonian stock during research surveys conducted off Argentina in January for the years 2005–2013. The letters a and b indicate the parameters of the equations; r^2=coefficient of determination; n=sample size.

	$BF = a(TL^b)$				$BF = a(age^b)$			
Year	a	b	r^2	n	a	b	r^2	n
2005	0.66	3.39	0.87	90	21,750	1.99	0.70	82
2006	2.32	3.06	0.73	95	26,830	1.83	0.70	89
2007	1.59	3.20	0.84	78	30,169	1.87	0.64	77
2008	1.27	3.24	0.84	81	19,793	2.09	0.68	81
2009	1.58	3.19	0.76	91	21,251	2.04	0.66	89
2010	0.96	3.30	0.78	102	22,492	1.91	0.70	100
2011	2.37	3.07	0.81	80	22,422	1.90	0.68	75
2012	0.31	3.59	0.84	98	17,326	2.02	0.66	98
2013	1.39	3.22	0.85	83	25,350	1.83	0.71	82

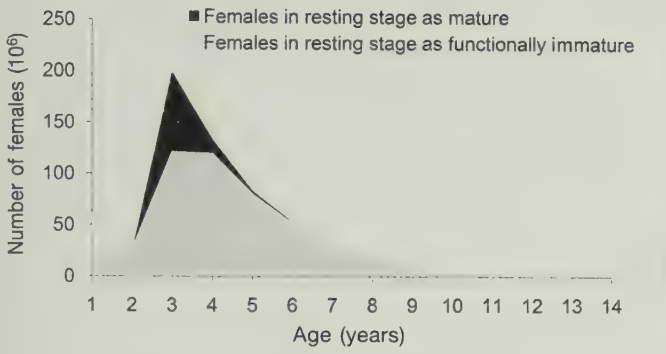

Figure 4

Age-frequency distributions obtained for adult female Argentine hake (*Merluccius hubbsi*) collected from the Patagonian stock off Argentina during January 2005–2013, averaged across years. The black area represents the fraction of females that would skip spawning during the spawning peak of the stock. The age-at-maturity model was applied in 2 ways to create the 2 overlapping areas: females in the resting stage were considered mature (black) or functionally immature (gray).

length classes during the spawning peak in January varied annually during the period 2005–2013 (Fig. 5). During most years, the egg production depended on females larger than 50 cm TL, except in 2005 and 2006, when the abundance of smaller adult individuals was particularly high (Fig. 3). After considering the incidence of SS in the estimate of egg production by length class, it was evident that the SS phenomenon affected mainly females smaller than 50 cm TL (Fig. 5). The reduction in egg production of one batch ranged from 2.70% to 6.80% when we compared egg production by length class (Fig. 6). The lowest value in the reduction of egg production during the period analyzed was observed in 2012, and it was coincident with a low proportion of females that had skipped spawning (Fig. 3).

The analysis of egg production by age class, after both interpretations of maturity were applied, confirmed that SS is observed mainly in young females (Fig. 7). In this case, the reduction in egg production of one batch on account of SS ranged from 3.56% to 12.12%. As found with the comparison by length class, 2012 was the year with the lowest egg production by age class (Fig. 6).

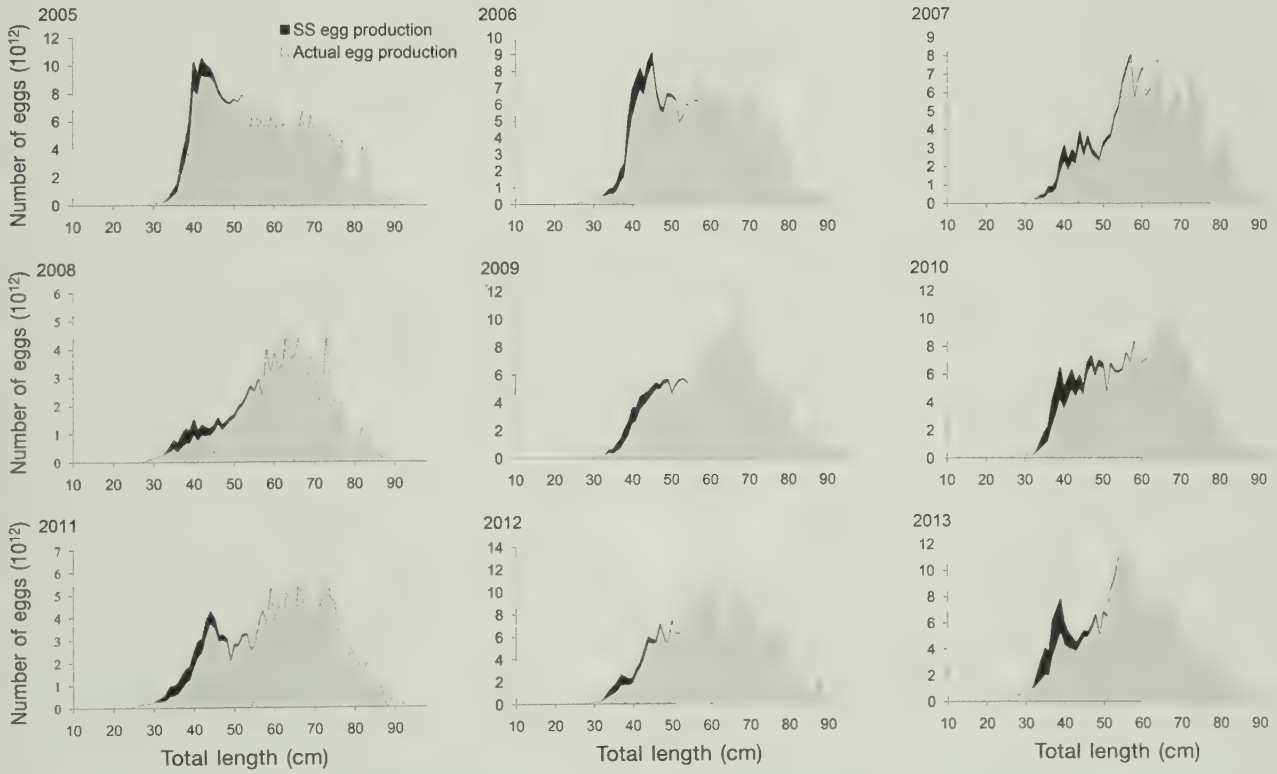

Figure 5

Egg production by length class in one spawning event, estimated for female Argentine hake (*Merluccius hubbsi*) collected from the Patagonian stock off Argentina in January during the spawning peak of 2005–2013. The black area represents the fraction by which the egg production was reduced by females that would skip spawning (SS), and the gray area indicates the actual egg production.

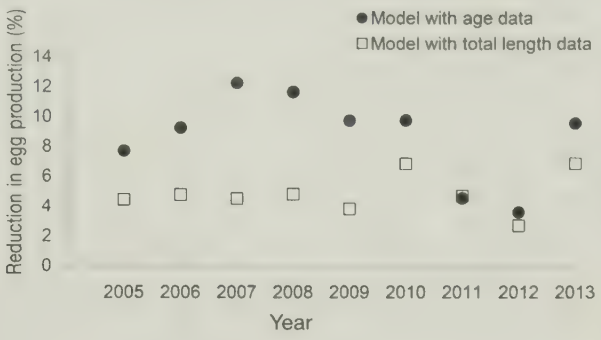

Figure 6

Reduction in egg production (%) caused by female Argentine hake (*Merluccius hubbsi*) that would skip spawning during the spawning peak of the Patagonian stock during the period 2005–2013. The black circles indicate percentages obtained from the model in which age was used, and the open squares indicate percentages from the model in which total length was used.

Discussion

The interruption in gonad maturation during the reproductive cycle has been reported in different fish populations for over 40 years (Rideout et al., 2005), but more recently, SS has been recognized as potentially having important implications for the reproductive output of a population (Livingston et al., 1997; Trippel, 1999; Rideout et al., 2000). Clearly, there is a negative effect on egg production when a proportion of the adult fish does not spawn during an entire year. Therefore, failure to consider females that skip spawning may lead to an overestimation of the actual number of spawning individuals and affect calculations of reproductive potential of a stock.

In the case of Argentine hake, data collected from the primary reproductive area of the Patagonian stock reveal the presence of nonreproductive adult females during the spawning season (Macchi et al., 2004; Pájaro et al., 2005). Recently, Macchi et al. (2016) reported that of the 3 types described for the process of skipped spawning (retaining, reabsorbing, and resting)

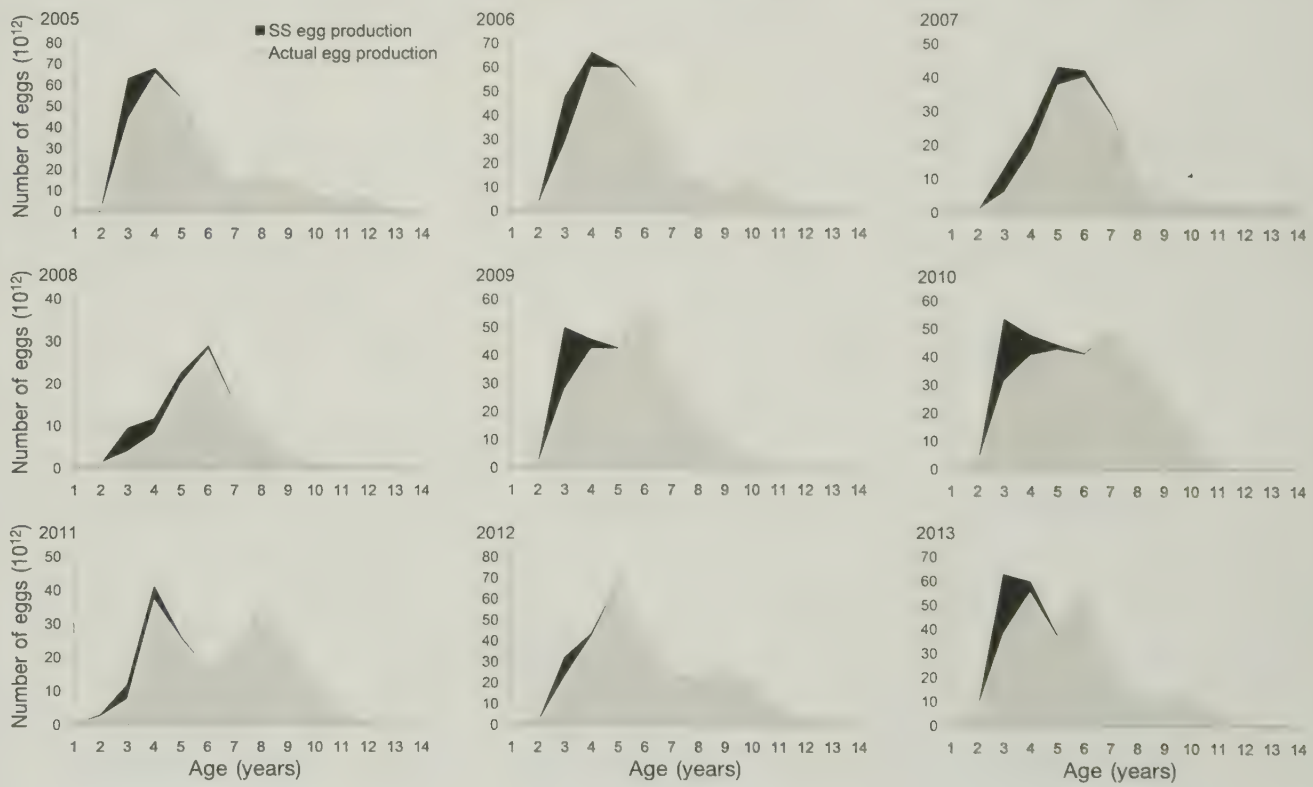

Figure 7

Egg production by age class in one spawning event, estimated for female Argentine hake (*Merluccius hubbsi*) collected from the Patagonian stock off Argentina in January during the spawning peak of 2005–2013. The black area represents the fraction by which the egg production was reduced by females that would skip spawning, and the gray area indicates the actual egg production.

by Rideout et al. (2005), only the resting stage can be found in the Patagonian stock. When SS was included in the estimate of the maturity ogives of Argentine hake, it was shown that both L_{50} and A_{50} were affected by this phenomenon. After accounting for skipped spawning (i.e., considering females at resting stage to be functionally immature individuals), the size at first maturity increased by 2–3 cm TL compared with values obtained with the traditional interpretation of maturity assignment, where females in a resting stage are considered mature individuals. Even so, most L_{50} values estimated with the revised interpretation for the period 2005–2013 were close to 35 cm TL, which is the length class traditionally used to differentiate between juveniles and adults in commercial catches of Argentine hake to define protected areas for this species (Dato et al.[4]).

In the case of age at first maturity, this coefficient increased by 0.27–0.88 years when the proportion of females that would skip spawning was incorporated. This represents an increase between 10% and 25% over the value obtained with the traditional interpretation. However, these differences in A_{50} were low compared with those reported for sablefish (*Anoplopoma fimbria*) by Rodgveller et al. (2016), who estimated an increase of A_{50} of approximately 30% when females that would skip spawning were considered to be functionally immature individuals. The maturity models for Argentine hake, both for size and age, showed a decrease of the slopes when the SS effect was included in the estimations, indicating that the age and size at which 100% of individuals reach sexual maturity are greater than those calculated by the traditional interpretation.

Analysis of the size and age structure of Argentine hake confirms that nonreproductive adult females are mainly young specimens with sizes ranging between 40 and 50 cm TL, corresponding primarily with 3-year-old fish, as was previously reported (Macchi et al., 2016). The 3-year-old age class constitutes approximately 70% of the female Argentine hake that would skip spawning; therefore, it is the main age class affecting the reduction in egg production. If the estimates of A_{50} (Table 3) are taken into account, it is possible that a large proportion of females that have already experienced their first annual spawning could skip the next spawning cycle, probably because of deficiencies in their nutritional condition (Macchi et al., 2016). It is also possible that some females that skip spawning are actually juveniles that had not yet reached sexual maturity. However, for the purposes of estimating L_{50} or A_{50}, this error in determining maturity would generate the same bias as SS because juveniles and adults in the resting stage are both functionally immature. In other cases, when skipped spawning has been reported, it has been observed that this phenomenon affects primarily younger adult individuals, as in the case of Atlantic herring (*Clupea harengus*; Engelhard and Heino, 2005) and Atlantic cod (*Gadus morhua*) from the Arctic (Jørgensen et al., 2006) and from the Atlantic (Rideout and Rose, 2006).

The L_{50} ogives of the Patagonian stock of Argentine hake from the resting period (August) were more similar to those based on the previous spawning peak of January, when fish that would skip spawning were classified as mature, than when fish that would skip spawning were classified as functionally immature. These results indicate that specimens identified as adults in January, during spawning, show the same maturity characteristics 7 months later (August), when the maturity ogive basically differentiates between juveniles and adults at the resting stage. This finding reinforces the idea that females that would skip spawning in January are adults, not juveniles.

The difference in egg production values by age class estimated in January with the traditional criterion, and considering spawning omission, ranged between 3.56% and 12.12% over the period 2005–2013. That is, if the objective is to estimate the reproductive potential of Argentine hake by using the A_{50} ogive, in some years there would be an overestimation close to 12% for this variable. However, when the egg production by length class during January is considered over the same period, the percentages of reductions in egg production resulting from SS were much lower than those estimated from the age-based model, ranging between 2.70% and 6.80%. The differences between the length- and age-based models in the percentages of reduction in egg production caused by SS may be associated with the variability explained by each model. The A_{50} model, which groups different length classes in each age class, embodies greater variability than the maturity relationship with total length. On the other hand, fewer samples were used to estimate the A_{50} curves than the number of samples used to determine L_{50} (Tables 2 and 3) and consequently would be expected to generate a better model fit for length over age.

The relatively low levels of reduction in egg production caused by SS for Argentine hake in our study indicate that the effect of skipped spawning in the Patagonian stock may be less significant than that reported for other species. For example, regarding Atlantic cod, Rideout and Rose (2006) suggested an overestimation of reproductive potential near 40% if the proportion of SS was not taken into account. Kennedy et al. (2014) reported that failure to properly interpret the maturity scale in Greenland halibut (*Reinhardtius hippoglossoides*) could lead to an overestimation of spawning stock biomass between 28% and 92%, depending on areas and years, whereas Núñez et al. (2015) calculated an overestimation of approximately 20% for the same species. In Argentine hake, it seems that the overestima-

[4] Dato, C., G. Álvarez Colombo, and G. J. Macchi. 2013. Evaluación de los juveniles y stock desovante de merluza (*Merluccius hubbsi*) en la zona de cría norpatagónica. Resultados obtenidos en la campaña de enero de 2013 y comparación con los resultados del período 2005–2012. Inf. Téc. Of. 12, 25 p. [Available from Instituto Nacional de Investigación y Desarrollo Pesquero, Paseo Victoria Ocampo Nro. 1, B7602HSA Mar del Plata, Argentina].

tion of reproductive potential could be even lower than expected because in this species, females that would skip spawning are primarily young individuals. Macchi et al. (2006, 2013) suggested that young (<5 years old) female Argentine hake produce eggs of poorer quality than eggs spawned by older females. In addition, it was reported that the extent of the spawning season in young females of this species is shorter than that in old individuals (>5 years old), and a lower number of spawning events occur during the reproductive season (Macchi et al., 2004). Therefore, it is possible that the recruitment success of this stock depends mainly on "big, old, fat, fecund female fish" (BOFFFF hypothesis, Berkeley et al., 2004) rather than on young spawners, as was suggested for many species, including the deepwater hake (*Merluccius paradoxus*) in southern Africa (Field et al., 2008).

Acknowledgments

We wish to thank to the technical staff of the Hake Assessment Group of the INIDEP for age determination. We wish to express our gratitude for the corrections made by reviewers that greatly improved the manuscript. This work was supported by the INIDEP, Consejo Nacional de Investigaciones Científicas y Técnicas (CONICET; PIP 112 201201 00047), and Fondo para la Investigación Científica y Tecnológica (FONCyT; PICT-2013-1484). This article is INIDEP contribution no. 2052.

Literature cited

Berkeley, S. A., M. A. Hixon, R. J. Larson, and M. S. Love.
2004. Fisheries sustainability via protection of age structure and spatial distribution of fish populations. Fisheries 29(8):23–32.

Dutil, J.-D.
1986. Energetic constraints and spawning interval in the anadromous Arctic charr (*Salvelinus alpinus*). Copeia 1986:945–955.

Draper, N. R., and H. Smith.
1981. Applied regression analysis, 2nd ed., 709 p. John Wiley & Sons Inc., New York.

Engelhard, G. H., and M. Heino.
2005. Scale analysis suggests frequent skipping of the second reproductive season in Atlantic herring. Biol. Lett. 1:172–175.

Field, J. G., C. L. Moloney, L. du Buisson, A. Jarre, T. Stroemme, M. R. Lipinski, and P. Kainge.
2008. Exploring the BOFFFF hypothesis using a model of southern African deepwater hake (*Merluccius paradoxus*). *In* Fisheries for global welfare and environment: memorial book of the 5th World Fisheries Congress 2008 (K. Tsukamoto, T. Kawamura, T. Takeuchi, T. D. Beard Jr., and M. J. Kaiser, eds.), p. 17–26. Terrapub, Tokyo, Japan.

Holmgren, K.
2003. Omitted spawning in compensatory-growing perch. J. Fish Biol. 62:918–927.

Hunter, J. R., N. C. H. Lo, and R. J. H. Leong.
1985. Batch fecundity in multiple spawning fishes. *In* An egg production method for estimating spawning biomass of pelagic fish: application to the northern anchovy, *Engraulis mordax* (R. Lasker ed.), p. 67–77. NOAA Tech. Rep. NMFS 36.

Jørgensen, C., B. Ernande, Ø. Fiksen, and U. Dieckmann.
2006. The logic of skipped spawning in fish. Can. J. Fish. Aquat. Sci. 63:200–211.

Kendall, M. G., and A. Stuart.
1967. The advanced theory of statistics, 449 p. Charles Griffin and Co. Ltd., London.

Kennedy, J., R. B. Hedeholm, A. C. Gundersen, and J. Boje.
2014. Estimates of reproductive potential of Greenland halibut (*Reinhardtius hippoglossoides*) in East Greenland based on an update of maturity status. Fish. Res. 154:73–81.

Livingston, M. E., M. Vignaux, and K. A. Schofield.
1997. Estimating the annual proportion of nonspawning adults in New Zealand hoki, *Macruronus novaezelandiae*. Fish. Bull. 95:99–113.

Macchi, G. J., M. Pájaro, and M. Ehrlich.
2004. Seasonal egg production pattern of the Patagonian stock of Argentine hake (*Merluccius hubbsi*). Fish. Res. 67:25–38.

Macchi, G. J., M. Pájaro, M. I. Militelli, N. Radovani, and L. Rivas.
2006. Influence of size, age and maternal condition on the oocyte dry weight of Argentine hake (*Merluccius hubbsi*). Fish. Res. 80:345–349.

Macchi, G. J., E. Leonarduzzi, M. V. Diaz, M. Renzi, and K. Rodrigues.
2013. Maternal effects on the fecundity and egg quality of the Patagonian stock of Argentine hake (*Merluccius hubbsi*). Fish. Bull. 111:325–336.

Macchi, G. J., M. V. Diaz, E. Leonarduzzi, M. I. Militelli, and K. Rodrigues.
2016. Skipped spawning in the Patagonian stock of Argentine hake (*Merluccius hubbsi*). Fish. Bull. 114:397–408.

Núñez, L. A., E. H. Hallfredsson, and I.-B. Falk-Petersen.
2015. Different maturity scales affect estimations of fecundity, TEP and spawning stock size of Greenland halibut, *Reinhardtius hippoglossoides* (Walbaum, 1792). Mar. Biol. Res. 11:824–833.

Pájaro, M., G. J. Macchi, and P. Martos.
2005. Reproductive pattern of the Patagonian stock of Argentine hake (*Merluccius hubbsi*). Fish. Res. 72:97–108.

Renzi M., and M. A. Pérez.
1992. Un criterio para la determinación de la edad en juveniles de merluza (*Merluccius hubbsi*) mediante la lectura de otolitos. Frente Marit. 11:15–31.

Rideout, R. M., and G. A. Rose.
2006. Suppression of reproduction in Atlantic cod *Gadus morhua*. Mar. Ecol. Progr. Ser. 320:267–277.

Rideout, R. M., and J. Tomkiewicz.
2011. Skipped spawning in fishes: more common than you might think. Mar. Coast. Fish. 3:176–189.

Rideout, R. M., M. P. M. Burton, and G. A. Rose.
2000. Observations on mass atresia and skipped spawning in northern Atlantic cod, from Smith Sound, Newfoundland. J. Fish Biol. 57:1429–1440.

Rideout, R. M., G. A. Rose, and M. P. M. Burton.
2005. Skipped spawning in female iteroparous fishes. Fish Fish. 6:50–72.

Rideout, R. M., M. J. Morgan, and G. R. Lilly.
2006. Variation in the frequency of skipped spawning in Atlantic cod (*Gadus morhua*) of Newfoundland and Labrador. ICES J. Mar. Sci. 63:1101–1110.
Rodgveller, C. J., J. W. Stark, K. B. Echave, and P.-J. F. Hulson.
2016. Age at maturity, skipped spawning, and fecundity of female sablefish (*Anoplopoma fimbria*) during the spawning season. Fish. Bull. 114:89–102.
Trippel, E. A.
1999. Estimation of stock reproductive potential: history and challenges for Canadian Atlantic gadoid stock assessments. J. Northwest Atl. Fish. Sci. 25:61–81.

National Marine
Fisheries Service
NOAA

Fishery Bulletin
established in 1881

Spencer F. Baird
First U.S. Commissioner
of Fisheries and founder
of *Fishery Bulletin*

Use of an underwater video system to record observations of black sea bass (*Centropristis striata*) in waters off the coast of Maryland

Daniel W. Cullen (contact author)[1]
Bradley G. Stevens[2]

Email address for contact author: bwtegu@gmail.com

[1] Department of Natural Sciences
University of Maryland Eastern Shore
Henry O. Tanner Airway Sciences Building, Building #915
30806 University Boulevard South
Princess Anne, Maryland 21853

[2] Living Marine Resources Cooperative Science Center
Department of Natural Sciences
University of Maryland Eastern Shore
Henry O. Tanner Airway Sciences Building, Building #915
30806 University Boulevard South
Princess Anne, Maryland 21853

Abstract—A remote underwater video camera system was used to observe black sea bass (*Centropristis striata*) on natural bottom habitats in waters off Maryland. Videos were collected from June to August 2011 at 6 hard bottom sites by deploying a fish trap equipped with multiple cameras. Data obtained from videos included fish counts and general fish behaviors observed around the camera system. We were able to distinguish between 2 categories of fish (i.e., with and without a nuchal forehead hump) and among three different habitat types appearing on videos. Counts of this species differed among habitat types with the highest counts occurring on rocky and reef habitats. Common behaviors exhibited by all fish included resting and aggregating on sand and around structures, whereas fish with nuchal humps exhibited antagonistic and territorial behaviors. On the basis of our results, we conclude that underwater video has the potential to provide useful information about the abundance and behavior of black sea bass in waters off the coast of Maryland.

Manuscript submitted 22 July 2016.
Manuscript accepted 31 May 2017.
Fish. Bull. 115:408–418 (2017).
Online publication date: 22 June 2017.
doi: 10.7755/FB.115.3.10

The views and opinions expressed or implied in this article are those of the author (or authors) and do not necessarily reflect the position of the National Marine Fisheries Service, NOAA.

Located along the U.S. Atlantic coast, the coastal shelf waters of the Mid-Atlantic are characterized by a southward narrowing of shelf width from approximately 150 km off New York to 30 km off Cape Hatteras, NC (Townsend et al., 2006). Dominated by sand, bottom sediments in the Mid-Atlantic also include clay, gravel, silt, and shell. Bottom habitats, known as hard bottom habitats (defined by Steimle and Zetlin (2000) as "multi-dimensional hard structured habitat,") in Mid-Atlantic waters, including those off the coast of Maryland, consist of natural reefs comprising low relief rocky outcroppings, gravel, boulders, stony and sea whip corals, shellfish beds, mud, and peat deposits (Steimle and Zetlin, 2000; Ross et al., 2016). Other hard bottom structures include shipwrecks, artificial reefs, and other manmade objects. Although scarce compared with soft bottoms, hard bottom habitats support a variety of invertebrate and commercially important fish species, including black sea bass (*Centropristis striata*) (Steimle and Zetlin, 2000).

In Mid-Atlantic waters, the black sea bass is migratory and individuals inhabit coastal hard bottom and reef habitats, often at depths of 20 m to 60 m, during spring and summer and offshore shelf waters in late autumn and winter when water temperatures decline (Moser and Shepherd, 2009). Black sea bass are protogynous hermaphrodites that are born female and some change sex to male later in life (Lavenda, 1949). During the spawning season from April to October, mature males may develop a blue nuchal hump anterior to the dorsal fin, making them distinguishable from females and other males (NEFSC[1]). Inshore black

[1] NEFSC (Northeast Fisheries Science Center). 2012. 53rd northeast regional stock assessment workshop (53rd SAW) assessment report. Northeast Fish. Sci. Cent. Ref. Doc. 12-05, 559 p. [Available from website.]

sea bass are primarily targeted by recreational hook-and-line and commercial trap fisheries, and bottom trawls are the chief gear used to harvest fish offshore (Shepherd and Terceiro, 1994). Annual spring bottom trawl surveys conducted by the National Marine Fisheries Service are the primary source of fishery independent data on abundance of black sea bass (NEFSC[1]). The trawl gears used during these surveys generally perform better on softer sediments than on hard bottom habitats occupied seasonally by black sea bass (NEFSC[1]; Ross et al., 2016). Population estimates are based on survey indices, as well as landings from commercial trap and recreational hook-and-line fisheries. However, the effectiveness of traps and other gears to adequately sample black sea bass is poorly understood. The lack of data on abundance of black sea bass in habitats that cannot be trawled effectively is a key uncertainty in assessment and management (NEFSC[1]; Ross et al., 2016). Therefore, fishery-independent data collected for black sea bass on hard bottom habitats with alternative sampling gears (e.g., video, traps) may provide important information for improving both stock assessments and management (NEFSC[1]).

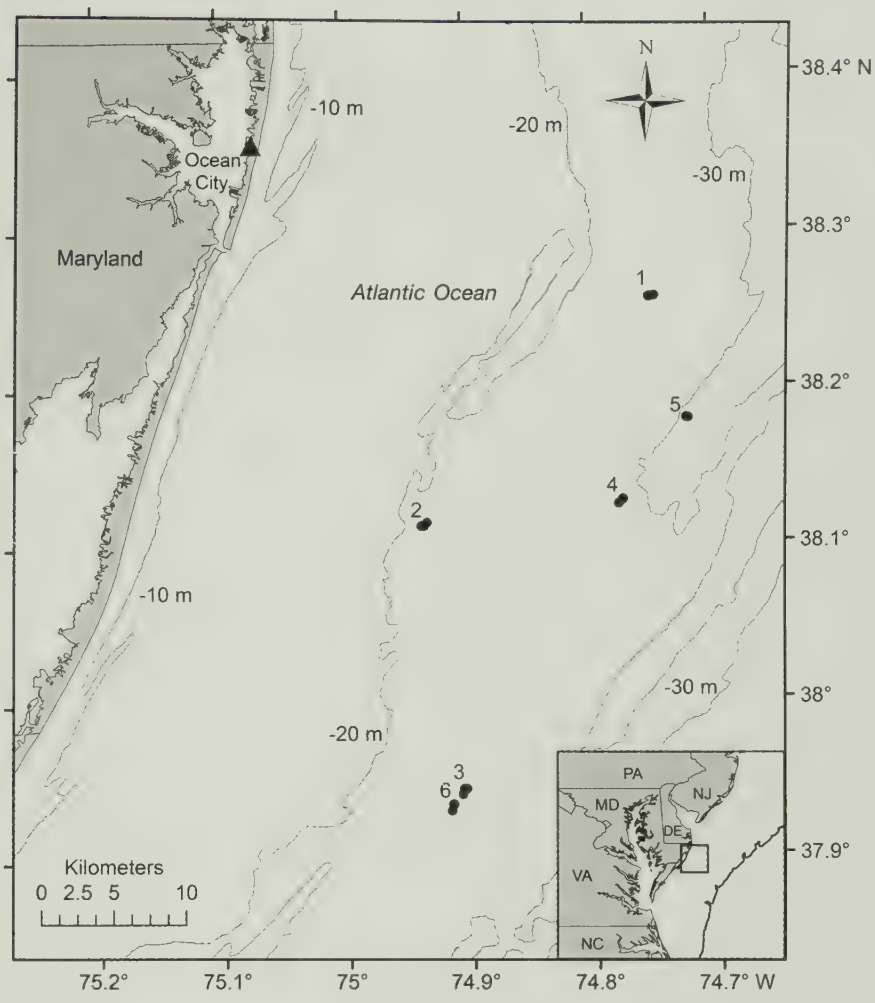

Figure 1

Map of the sampling region depicting the locations of 6 sites (numbered 1–6) off the coast of Maryland, where underwater video of black sea bass (*Centropristis striata*) was collected with a fish trap and camera system from 14 June to 4 August 2011. Overlapping black circles indicate the positions of multiple deployments of the fish trap and camera system per site. The inset shows the location of the sampling region off Maryland along the U.S. Atlantic coast.

Underwater videos, including those that involve remote video camera systems, have been used to assess the abundance of reef fish (Ellis and DeMartini, 1995; Harvey and Shortis, 1996; Burge et al., 2012; Lowry et al., 2012). Remote camera systems typically consist of 1 (single video) or 2 (stereo video) analog or digital video cameras in a waterproof housing fixed to a metal frame in a manner that allows a vertical or horizontal field-of-view (Harvey and Shortis, 1996; Willis and Babcock, 2000; Watson et al., 2005; Cappo et al., 2007; Harvey et al., 2007). We constructed and deployed a remote camera system with a fish trap as a base to collect video recordings of black sea bass *in situ*, to identify important natural bottom habitats, and to determine whether or not male fish with nuchal humps could be distinguished from other life stages. Our camera system included a fish trap as a base because a fish trap was easy to deploy and haul from depth and was simple to modify with a metal frame for attaching multiple cameras. Additionally, it allowed us to collect other information including recordings of behavioral responses of black sea bass to traps (e.g., entries, escapes) which could be used for further analysis (see Cullen and Stevens, 2017). The underwater video collected with the camera system was used to address the following objectives: 1) to observe and count black sea bass on natural hard bottom habitats and 2) to make observations of behavior of black sea bass on natural hard bottom habitats.

Materials and methods

Study area and sampling with video system

The study was conducted in waters off the coast of Maryland (Fig. 1). Sampling occurred on 10 days, during the period from 14 June to 4 August 2011. With-

Table 1

Average values of *MeanCount*, the mean number of fish counted in a sample of frames from a video, for black sea bass (*Centropristis striata*) observed in the 3 classified habitat types (sand, sand+rock, live bottom) in videos collected from 14 June to 4 August 2011 at 6 sampling sites in waters off the coast of Maryland. Values are given for 2 categories: all black sea bass and nuchal black sea bass (or fish that were distinguishable from other individuals by a darker body coloration, a nuchal hump, and white fin stripes). Average values of *MeanCount*, with 95% confidence intervals in parentheses, and mean depths (in meters), with standard deviations (SDs) in parentheses, for all daily deployments (4 per day) are provided for each site and date.

			All black sea bass			Nuchal black sea bass		
Site	Date	Depth (SD)	Sand	Sand+rock	Live bottom	Sand	Sand+rock	Live bottom
1	14 Jun 2011	22.1 (0.3)	0.19 (–0.21–0.40)	0.00 (0.00–0.00)	0.00 (0.00–0.00)	0.01 (–0.01–0.03)	0.00 (0.00–0.00)	0.00 (0.00–0.00)
2	16 Jun 2011	25.9 (2.1)	0.11 (–0.01–0.23)	0.07 (0.00–0.00)	0.00 (0.00–0.00)	0.03 (0.00–0.06)	0.02 (0.00–0.00)	0.00 (0.00–0.00)
3	23 Jun 2011	30.8 (0.5)	0.70 (–0.25–1.65)	0.00 (0.00–0.00)	9.28 (8.84–9.72)	0.43 (–0.17–1.03)	0.00 (0.00–0.00)	1.38 (0.87–1.89)
2	28 Jun 2011	25.9 (2.6)	0.15 (0.07–0.23)	0.00 (0.00–0.00)	0.00 (0.00–0.00)	0.05 (0.00–0.10)	0.00 (0.00–0.00)	0.00 (0.00–0.00)
4	8 Jul 2011	29.1 (2.6)	0.00 (0.00–0.00)	0.20 (0.00–0.00)	12.17 (1.85–22.49)	0.00 (0.00–0.00)	0.08 (0.00–0.00)	1.83 (0.43–3.23)
4	18 Jul 2011	29.1 (2.5)	0.11 (–0.10–0.32)	4.38 (–0.93–9.69)	0.00 (0.00–0.00)	0.03 (–0.04–1.0)	1.05 (0.23–1.87)	0.00 (0.00–0.00)
5	20 Jul 2011	29.7 (2.4)	0.00 (0.00–0.00)	1.02 (–0.07–2.11)	0.00 (0.00–0.00)	0.00 (0.00–0.00)	0.11 (–0.02–0.24)	0.00 (0.00–0.00)
6	26 Jul 2011	30.4 (1.8)	2.12 (0.00–0.00)	3.78 (0.73–6.83)	2.47 (0.00–0.00)	0.00 (0.00–0.00)	0.48 (0.46–0.50)	0.50 (0.00–0.00)
6	1 Aug 2011	30.3 (1.6)	1.85 (1.16–2.45)	0.00 (0.00–0.00)	2.54 (1.48–3.60)	0.47 (0.14–0.80)	0.00 (0.00–0.00)	0.35 (0.12–0.58)
6	4 Aug 2011	30.1 (1.3)	0.00 (0.00–0.00)	8.93 (2.23–15.63)	3.90 (0.00–0.00)	0.00 (0.00–0.00)	0.88 (0.32–1.44)	0.77 (0.00–0.00)

out prior knowledge about the distribution or extent of the bottom topography in the sampling region, we consulted with commercial trap fishermen of black sea bass regarding locations where fish might be observed. Because the goal of this study was to use underwater video to observe and count black sea bass on natural habitats, sampling locations were not selected at random. Instead, 6 hard bottom sites ranging in depth from 22 to 31 m (Table 1, Fig. 1) were chosen because they were primarily characterized by hard bottom substrates or other natural structures that offered the best chance to observe and count fish; sites were visited 1–3 times during the study period.

At each sampling site, videos were collected during daylight hours (0900 to 1500 Eastern Daylight Savings Time) by using a camera system that incorporated a rectangular fish trap as a base (dimensions: 107 cm length×53 cm width×31 cm height; 3.8-cm^2 mesh, 12-gauge plastic coated wire) (Fig. 2). A frame (dimensions: 107 cm length×53 cm width×86 cm height) constructed of galvanized and zinc-plated slotted steel angle was bolted to 15-cm sections of slotted angle positioned inside the trap at each corner. This fixed the frame height at 71 cm above the bottom of the trap and 38 cm from the top. Weight was added to the trap (with 4 bricks weighing ~2.7 kg each) to ensure that it landed flat on the bottom so that the frame stood upright. Five GoPro HD Hero 1[2] digital video cameras (720-pixel resolution, 170° angle of view) were bolted to the steel frame with tripod mounts, 38 cm above the top of the trap. Four cameras faced outward, one on each side at a 45° angle to obtain a standardized view of fish and the bottom habitat near the trap during each deployment. An additional camera looking downward at a 45° angle over the top of the trap was mounted to capture any behavioral responses (e.g., entries, escapes) of black sea bass to the trap that may have occurred during each deployment (Cullen and Stevens, 2017).

Because hard bottom habitats in the coastal waters of Maryland are patchy and sparsely dispersed among soft bottom habitats (e.g., sand), we were concerned that the number of videos depicting black sea bass on these habitats would be limited. Therefore, to account for the potential spatial variation in habitat at sampling sites and to help ensure that we obtained observations of fish on hard bottom habitats, four 60-min continuous deployments of the video camera system were made at a given site per day (n=10 d). Deployment locations for the camera system were based on observations from a fish finder (FCV-582L; Furuno Electric Co. Ltd., Nishinomiya City, Japan) and incorporated a flat bottom area, adjacent to structure. The system was then lowered to the bottom slowly, from the deck of a chartered commercial vessel, with a rope that was attached to a marker buoy and flag at the surface. After 1 h, the system was lifted to the surface with a hydraulic pot-hauler. The vessel was then moved ~200 m to the north, south, east, or west from the deployment site and repositioned over new bottom habitat. The system was then dropped down for the next video sample. After the first 2 deployments, the system was hauled to the vessel where the camera batteries were changed. The final 2 samples of video were collected in the same manner as that described previously, and with a distance of ~200 m between deployment loca-

[2] Mention of trade names or commercial companies is for identification purposes only and does not imply endorsement by the National Marine Fisheries Service, NOAA.

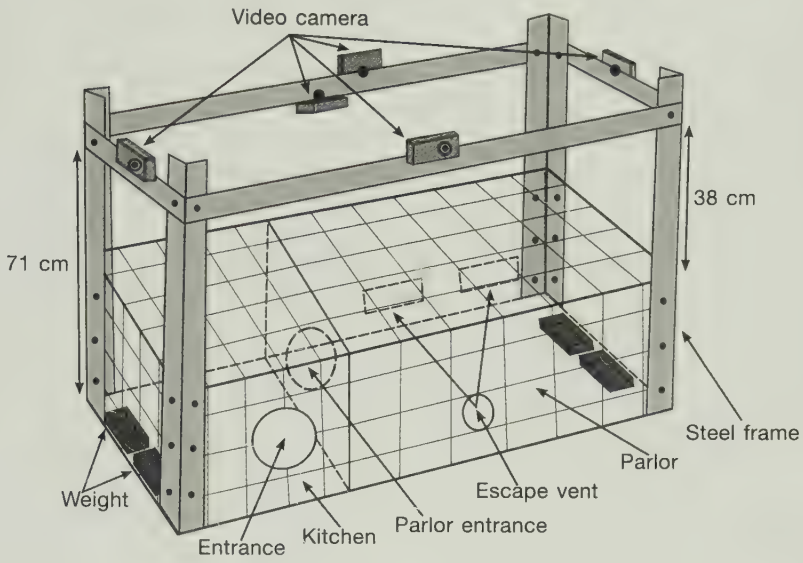

Figure 2

Diagram of the camera system used to collect video of black sea bass (*Centropristis striata*) from 14 June to 4 August 2011 at 6 sampling sites in waters off the coast of Maryland. The system consisted of a rectangular fish trap as a base, with a steel frame equipped with 5 GoPro HD Hero 1 cameras mounted over the top. Four cameras were faced outward at 45° angles to obtain a standardized view of fish and bottom habitat near the trap. A fifth camera was faced downward at a 45° angle over the top of the trap to capture behavioral responses of black sea bass to the trap that may have occurred during each deployment of the fish trap and camera system.

tions. Approximately 20 min were allowed to elapse between each deployment.

With the intention of obtaining observations of responses of black sea bass to the trap, we baited the trap with ~230 g of northern shortfin squid (*Illex illecebrosus*) during the first 2 deployments per day. For these deployments, whole frozen squid were thawed, cut into strips, placed in a plastic mesh bait bag, and hung inside the trap kitchen. The bait bag was removed for the last 2 deployments.

Video analysis

Nearly 160 h of video were collected during the study period. Videos used for analysis were selected randomly. The 4 outward facing cameras were assigned a number 1 to 4 and a random number generator was used to select one camera for each sampling date. Although 4 cameras were used, a single video was chosen from each of the 4 deployments made each day to help reduce recounts of fish moving in and out of multiple camera views. The 40 selected videos were viewed on a wide-screen monitor with standard video editing software (Adobe Premiere Pro CS5; Adobe Systems Inc., San Jose, CA); no videos were excluded from analysis or substituted with others from another camera because all displayed a clear view of the bottom habitat and fish when present. Video processing began ~1 min after the camera view was clear of silt or debris suspended when the camera system landed on the bottom. Habitat appearing on videos was classified into 3 types: 1) sand—smooth or coarse sand and gravel adjacent to structure, bivalve shells were often present but no rocks or boulders (i.e., small cobble to large rocks; sediment types were identified based on definitions from Wentworth [1922]), 2) sand+rock—sand with scattered rocks and boulders but no rocky outcroppings or coral species present, and 3) live bottom—complex reef habitats with boulders, rocky outcroppings, and possibly other structures colonized by gorgonian sea whips (*Leptogorgia* spp.) and stony corals. Bottom habitats were classified as live bottom because they were frequently occupied by other species in addition to black sea bass and corals, including cunner (*Tautogolabrus adspersus*), American lobster (*Homarus americanus*), and crabs (*Cancer* spp.). In video frames where more than sand habitat was present, the habitat was classified as sand+rock only when rocks or boulders were present but no rocky outcroppings or coral species and as live bottom only when corals (sea whips, stony corals) were present in addition to other species and habitat features.

On the basis of the pattern of counts of black sea bass over time (i.e., fish counts generally increased to

a maximum within the first 5–10 min followed by a steady decline in all videos), we chose a 30-min segment from each video for counting fish. Once the camera view was clear of suspended silt and debris, counts were made for 2 categories of black sea bass: all black sea bass and then separately for those with a nuchal hump (i.e., fish that were distinguishable from other individuals by their darker body coloration, a nuchal hump with the usual blue color appearing grayish-white on the videos, and white fin stripes; hereafter referred to as *nuchal black sea bass*) from each video using a variable called *MeanCount*, which is an alternative counting metric to others commonly reported in the literature (e.g., MaxN; maximum number of individuals of a particular species present at one time in any single point on the video) (Schobernd et al., 2014; Bacheler and Shertzer, 2015). *MeanCount* is the mean number of fish counted in a sample of frames from a video (Schobernd et al., 2014). In this case, 60 single frames were sampled systematically, one every 30 s for 30 min of videotaping. Counts from the sampled frames were then averaged to obtain values of *MeanCount*. We chose *MeanCount* because, unlike *MaxN*, it has been shown by Schobernd et al. (2014) to be relatively unbiased and linearly related to true abundance but has similar variation to that of *MaxN*.

Fish behavior during the selected 30 min of a video was evaluated by noting (in minutes) the time of first arrival (TFA) of fish within the camera view followed by general observations of behavior around the camera system. TFA was included as a behavioral measure to examine whether faster arrival times to the camera view could be related to greater densities of fish in the surrounding area. Additionally, we wanted to determine whether the presence of bait in the trap would result in fish appearing on cameras earlier than when bait was not present in the trap. Swimming, resting, and habitat-associating behaviors were recorded by selecting individual fish within the camera field-of-view. Swimming fish were followed until they left the camera view; no more than 3 fish were followed at any one time. Resting and habitat-associating behaviors were recorded if, or when, a swimming fish stopped to rest on the bottom or near structures such as rocky outcroppings or boulders. These behaviors were also noted for fish already resting on the bottom when the camera frame landed. Aggregating behaviors were documented for fish resting on the bottom in groups of 2 or more, and antagonistic behaviors were noted only when nuchal males were observed chasing smaller non-nuchal fish.

Responses to the trap, including entries through the entrance funnel, half entries (entering the entrance funnel but backing out), and exits (exiting the trap through the entrance funnel or through one of the escape vents in the parlor) were noted on videos captured by the camera facing downward over the top of the trap for each deployment (Fig. 2). These data were collected on 9 of the 10 sampling days and were used to examine the influence of trap soak time on catches of black sea bass in fish traps in a complementary manuscript (i.e., Cullen and Stevens, 2017).

Data analysis

We tested for differences in *MeanCount* among the 3 classified habitat types. Because *MeanCount* is a continuous variable and repeated deployments were made at a site on each sampling day, we used linear mixed-effects models to test for differences in *MeanCount* for the categories of all black sea bass and nuchal black sea bass separately among the 3 classified habitat types (sand, sand+rock, live bottom). Linear mixed-effects models can be used as alternatives to methods of repeated-measures analysis of variance (ANOVA) when data are unbalanced, and they allow modeling of covariance structures (Pinheiro and Bates, 2000). In our models, habitat type was treated as a fixed effect; however because of limited knowledge of bottom types at sampling sites, equal replication of habitats across video deployments was not possible *a priori*. Bait method (i.e., baited trap, unbaited trap) was dummy coded (i.e., the categorical variable bait method was converted to a continuous variable by assigning values of 0 for baited trap deployments and values of 1 for unbaited trap deployments) and the continuous variable was included as a covariate in the models to control for its possible influence on values of *MeanCount*. Sampling site was treated as a random effect because consecutive camera system deployments provided multiple, non-independent samples per site (Zurr et al., 2009). This method, which was equal to fitting a model with a compound symmetrical correlation structure, provided a random intercept term for each site, and allowed the variance in values of *MeanCount* within sites to be separated from the residual variance (Pinheiro and Bates, 2000). Linear mixed-effects models with *MeanCount* as the response variable were fitted by using the nlme package, vers. 3.1-129 (Pinheiro et al., 2017) in the R statistical environment, vers. 3.3.2 (R Core Team, 2016). *MeanCount* data were checked for normality and variance homogeneity and log-transformed (by taking a natural logarithm of the variable+1; i.e., $\log_e[MeanCount+1]$, 1 was added to *MeanCount* because the data contained some 0 values) before analysis to help meet the assumptions of the linear mixed-effects models. Corrected Akaike information criterion (AICc), which is recommended for small sample sizes (Burnham and Anderson, 2002) was used to compare 3 model types: models with random effect for site, models without the random effect for site, and weighted models with the random effect for site. The latter models were weighted by using a constant variance function (i.e., weights produced with the varIdent function in the nlme package) to correct for heteroscedasticity or different variances for *MeanCount* data among habitat types (Pinheiro et al., 2017). The constant variance function in weighted models allowed the variance to differ for each level of habitat type.

Table 2

Results from analysis of variance for the best linear mixed-effects (LME) models, determined by using the corrected Akaike information criterion. These results were used to compare the influence of habitat type (sand, sand+rock, live bottom) on values of the counting metric *MeanCount* for black sea bass (*Centropristis striata*) observed on videos collected from 14 June to 4 August 2011 at 6 sampling sites in waters off the coast of Maryland. Results are given for 2 categories: all black sea bass and nuchal black sea bass (the latter fish were distinguishable from other individuals by a darker body coloration, a nuchal hump, and white fin stripes). The standard error (SE) for the random effects represents the variance for each sampling site around the common intercept. *MeanCount* data were log transformed (by taking a natural logarithm of the variable+1; i.e., $\log_e[MeanCount+1]$) before analysis to help meet the assumptions of the LME models. ICC=interclass correlation coefficient, which represents the correlation of observations from the same sampling site.

Category	Parameter	df	*F*-value	*P*-value
All black sea bass	Intercept	1, 31	17.658	<0.001
	Habitat type	2, 31	22.364	<0.001
	Bait method	1, 31	1.318	>0.05
	Random effects	SE	0.142	
	Residuals	Variance	0.028	
		ICC	0.838	
Nuchal black sea bass	Intercept	1, 31	17.447	<0.001
	Habitat type	2, 31	17.973	<0.001
	Bait method	1, 31	0.805	>0.05
	Random effects	SE	0.015	
	Residuals	Variance	0.017	
		ICC	0.469	

All models were first fitted with maximum likelihood estimation and compared with AICc by using the AICcmodavg package, vers. 2.0-3 (Mazerolle, 2016) in R. The AICc best models were refitted with restricted maximum likelihood, which estimates the variance components separately from the fixed effects, thereby providing unbiased estimates for the variance components (Zurr et al., 2009). ANOVA, with type-II sums of squares for unbalanced data, was used to extract *F*-values and Wald test *P*-values for the fixed effect habitat type. Normal quantile-quantile plots, box plots, and scatter plots of the residuals were examined for model validation. Tukey's honestly significant difference tests, with *P*-values adjusted by using a Bonferroni correction, were conducted for multiple comparisons if the ANOVA indicated a significant difference in values of *MeanCount* between habitat types for either category of black sea bass. Results were obtained by using the multcomp package, vers. 1.4-6 in R, which provides multiple comparisons tests for linear mixed-effects models (Torsten et al., 2008).

Additional analyses included Spearman's rank correlation analysis to examine the relationship between *MeanCount* for nuchal and non-nuchal black sea bass (without nuchal humps) and between *MeanCount* and TFA for both categories of black sea bass with deployments as samples (n=40). Further, separate correlations were calculated between *MeanCount* and TFA for both categories of black sea bass for deployments with bait (n=20) in the trap and without (n=20). Correlations were obtained by using the stats package in R (R Core Team).

Results

Habitat appearing in the camera view during deployments (n=40) consisted primarily of smooth and coarse sand, rock, corals (i.e., sea whips, stony corals), and shell. In total, 19 (47.5%) deployments were made in sand, 13 (32.5%) in sand+rock, and 8 (20.0%) in live bottom habitats. In general, values of *MeanCount* were greatest in the first 5–10 min of video followed by a variable decline. Values of *MeanCount* varied by site and date and were highest for both categories of black sea bass in sand+rock and live bottom habitats (Table 1). The proportion of nuchal black sea bass observed in the 3 classified habitats were 31.2% in sand, 15.1% in sand+rock, and 18.2% in live bottom. A total of 9 black sea bass, of which 5 had nuchal humps, were caught in the trap, 6 during baited trap deployments and 3 during unbaited trap deployments.

Weighted linear mixed-effects models (i.e., with the random effect for sampling site) that included a constant variance function that allowed the variance to differ for each level of habitat type were identified by AICc as the best models for the categories of all black sea bass and nuchal black sea bass. The variance for

the residuals and the standard error (SE) of the random effects around the population intercept were relatively small for each model (Table 2). However, intraclass correlation coefficients (ICC=[Intercept SE]/[Intercept SE+Residual variance]; Zurr et al., 2009) were fairly high, indicating moderate to strong correlations between *MeanCount* observations from the same sampling sites. On average, untransformed values of *MeanCount* and their associated variances (all black sea bass, sand=0.51, sand+rock=19.21, live bottom=27.07; nuchal black sea bass, sand=0.05, sand+rock=0.25, live bottom=0.57) were greatest in live bottom habitats (Fig. 3). Log-transformed values of *MeanCount* were significantly different between habitat types for both categories of black sea bass (Table 2; Fig. 3); bait method was not significant ($P>0.05$). Results from pairwise Tukey's honestly significant difference tests with a Bonferroni correction indicated that log-transformed values of *MeanCount* differed significantly between sand and sand+rock habitats (all black sea bass, $P=0.004$; nuchal black sea bass, $P=0.016$) and between sand and live bottom habitats (all black sea bass, $P=0.003$; nuchal black sea bass, $P=0.002$) but not between sand+rock and live bottom habitats ($P>0.05$).

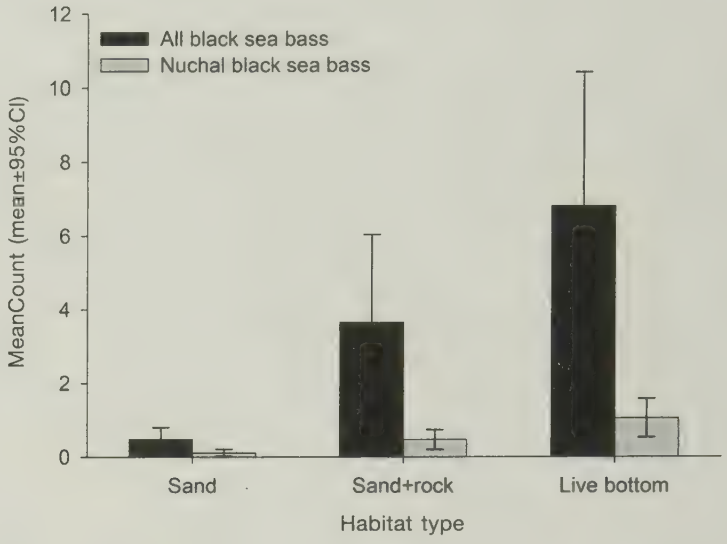

Figure 3

Average values of *MeanCount*, the mean number of fish counted in a sample of frames from a video, for black sea bass (*Centropristis striata*) observed in the 3 classified habitat types (sand, sand+rock, live bottom) on videos collected from 14 June to 4 August 2011 at 6 sampling sites in waters off the coast of Maryland. Average values are given for 2 categories: all black sea bass and nuchal black sea bass, (the latter fish were distinguishable from other individuals by a darker body coloration, a nuchal hump, and white fin stripes). The error bars indicate the 95% confidence intervals.

Results of Spearman's rank correlation analysis indicated that values of *MeanCount* for nuchal black sea bass were significant and positively correlated with those for non-nuchal black sea bass ($\rho=0.829$, $P<0.001$). Time of first arrival, ranging from 0.5 to 27.5 min, was latest in sand habitats and earliest in live bottom habitats for both categories of black sea bass. The range of TFA was 0.5–21.5 min for baited trap deployments, with a mean of 2.9 min (95% confidence interval [CI]: 1.7–5.1), and 0.5–27.5 min for unbaited trap deployments, with a mean of 3.8 min (95% CI: 0.8–6.8). *MeanCount* was significantly and negatively correlated with TFA for all black sea bass ($\rho=-0.397$, $P=0.011$) but not for nuchal black sea bass ($P>0.05$). Black sea bass also arrived earliest in live bottom habitats and latest in sand habitats when the trap was baited. Mean TFA was 3.4 min (95% CI: −0.3–7.1) in sand, 2.7 min (95% CI: −0.2–5.6) in sand+rock, and 0.5 min (95% CI: 0.0–0.0) in live bottom and 8.6 min (95% CI: 2.2–15.0) in sand, 0.6 min (95% CI: 0.4–0.8) in sand+rock, and 0.5 min (95% CI: 0.0–0.0) in live bottom for baited and unbaited trap deployments, respectively. TFA was significantly and negatively correlated with *MeanCount* for the category of all black sea bass during baited trap deployments ($\rho=-0.738$, $P<0.001$) but not for unbaited trap deployments or for nuchal black sea bass for either baited or unbaited trap deployments ($P>0.05$).

It was clear from processing videos that general behaviors observed around the camera system depended on the type of habitat in the camera view regardless of whether bait was present in the trap or not. On sand habitats, fish swam past quickly or entered the view slowly by moving short distances of 1 m or so before stopping and resting on the bottom; some fish would lie on the bottom without moving for up to 10 min or more. Infrequently, antagonistic behaviors were observed when large nuchal males chased smaller fish out of the camera view. Fish also aggregated when nuchal and non-nuchal fish would lie next to each other in groups of 2 or more. Other behaviors included nipping at the sediment and 'back rubbing' when fish turned over and rubbed their dorsal surface or head on the sand. On structured (e.g., rocks, boulders) and live bottom habitats, fish were generally present when the camera system landed on the bottom. Occasionally black sea bass approached the camera system, however they spent the majority of the time swimming around and above structures or resting on the bottom next to or under rocks and in holes or crevices of outcroppings. Approximately 20–30% of the behaviors displayed by nuchal black sea bass were antagonistic and territorial. For example, in one case, a large nuchal male continuously returned to and swam around the same rocky outcropping after repeatedly chasing other nuchal and non-nuchal fish away.

Discussion

We used our analysis of video collected with a remote underwater camera system to observe and count black sea bass, examine behavior, and distinguish between life stages (i.e., black sea bass with and without nuchal humps) and bottom types. Our camera system allowed a comparison of values of *MeanCount* among sand, sand+rock, and live bottom habitats, as well as an examination of behavioral responses to fish traps. We found values of *MeanCount* to be significantly higher in live bottom and sand+rock habitats than in sand habitats. An important aspect of this study was that we were able to observe and discriminate between nuchal and non-nuchal black sea bass. Values of *MeanCount* for nuchal black sea bass were positively correlated with those for non-nuchal black sea bass, which may be an indication that greater numbers of male fish were present when densities of black sea bass were higher. However, a method to identify individual fish would be necessary to avoid recounts in order to verify whether values of *MeanCount* are an adequate index for the number of mature males available for spawning on different habitats. For most deployments, bottom types and black sea bass were relatively easy to observe despite variability among sites in factors such as water depth, turbidity, and cloud cover that resulted in reduced visibility around the camera system. On most days (7 of 10), bottom visibility was ~10 m or more but on others it was as little as ~5–6 m. Low visibility as a factor limiting the quality of videos has been reported in other studies using an underwater video technique as a sampling method (Pratt et al., 2005; Bacheler et al., 2014). For example, in the south Atlantic, Bacheler et al. (2014) examined the influence of environmental factors and habitat features on trap and video detection probabilities for reef fish and found that black sea bass and 2 other species were more likely to be observed on videos as water clarity increased. In our study, sampling was conducted during daylight hours to help ensure that natural bottom lighting was adequate. The use of artificial lighting may have increased visibility during periods of low light (~30% of videos in our study); however, our camera system did not include lights because it was not known if or how lights would affect fish behavior.

Habitat type was the most significant factor for observing black sea bass. This result was not surprising given the species strong affinity for structurally complex habitats during their inshore residency. Ross et al. (2016) examined fish communities on soft, natural hard, and shipwreck habitats near Norfolk Canyon, off the coast of Virginia, and observed black sea bass on both soft and hard bottom habitats although they were found primarily on the latter. Despite fish being observed on soft bottoms, Ross et al. (2016) noted that, like other dominant hard bottom species, they were generally not observed far from reef structures. In another study, Fabrizio et al. (2013) examined habitat associations and dispersal of black sea bass with acoustic telemetry at a temperate reef off the coast of New Jersey and found that throughout the summer and fall fish primarily used shallow areas (depths <27 m) with coarse grain materials. Similarly, we observed the majority of black sea bass on hard and rocky bottoms at depths from 19 to 31 m. Conversely, despite the lack of bottom structure, we did observe fish on sand habitats, possibly because fish were attracted to the camera system as an additional or novel source of habitat because black sea bass are regularly caught by the commercial fishery using unbaited traps (Shepherd et al., 2002). Another reason for this finding may be related to feeding activities. Steimle and Figley (1996) examined diets of black sea bass in coastal waters off New Jersey and found that sandy bottom areas adjacent to artificial reefs were very important for feeding. They concluded that much of the diet of black sea bass consists of prey items that are not closely affiliated with reef structure. Lastly, the high percentage of nuchal males that we observed on sand habitats may be related to movements between adjacent hard bottom sites (Bacheler and Ballenger, 2015). Fabrizio et al. (2013) reported on the dispersal of black sea bass from a reef off the coast of New Jersey and found that fish, mostly nuchal males, began to leave the site in early summer, possibly for other reef areas.

Arrival time at a camera system may be related to densities of fish in the surrounding area. Ellis and DeMartini (1995), Willis and Babcock (2000), and Stoner et al. (2008) compared the TFA of fish species in the camera view with their metric for relative abundance and found moderate to strong negative correlations between the 2 metrics. In our study, TFA was moderately correlated with *MeanCount* for all black sea bass—a finding that is in agreement with results from Ellis and DeMartini (1995) and Willis and Babcock (2000) and suggests that faster arrival times for black sea bass are likely due to higher densities of fish in the area. This was the case in our study with fish appearing on cameras earlier for videos collected in live bottom and sand+rock habitats. Fish also arrived earlier in sand habitats when the trap was baited.

Compared with other serranids that have been reported to primarily use their caudal fin while swimming (Fulton, 2007), the main swimming mode of black sea bass appeared to involve the use of both the caudal and pectoral fins for propulsion. In all habitats, black sea bass swam both with and against the current, although fish were often observed swimming close to the bottom and stopping or resting next to rocks or in the crevices of outcroppings when the current appeared to be particularly strong. Resting by black sea bass may be a type of station-holding behavior where fish use substrates as a refuge from flow at higher current speeds (Gerstner, 1998). In high-current flows, black sea bass might seek refuge next to or between bottom structures—a strategy that could possibly reduce the number observed on videos although this may not be the case because Bacheler et al. (2014) found that the likelihood of observing black sea bass on videos

increased, although only marginally, from low to high relief habitats in their study. Additionally, guarding territory was a behavior exhibited by nuchal black sea bass around rocky outcroppings and may be an indication that outcroppings, along with other structures, are important for activities such as spawning (Fabrizio et al., 2013).

There was one key limitation to our sampling approach, which involved the use of bait only during the first 2 deployments on each sampling day. It is possible that the bait may have attracted black sea bass to the area, where they remained for some time afterward, and may have resulted in recounts on videos from subsequent deployments despite the ~200 m distance between each deployment. Additionally, the re-use of bait after the first baited drop may have reduced its quality and ability to produce an adequate odor plume for attracting fish to the trap. Nevertheless, the earlier TFA of fish to the camera system, as well as higher trap entries and catches when the trap was baited compared with the period when it was unbaited (Cullen and Stevens, 2017), may be an indication that bait would improve underwater video sampling for black sea bass. Because of the high variability in deployment locations in relation to habitat structure at each site and the small sample size (n=20 deployments with bait, n=20 without bait), a statistically significant result for bait method was not found; a power analysis (power=0.8) indicated that, when the trap was either baited or unbaited, only a 200% change in *MeanCount* could be detected with a 2-tailed test for our sample size. Exploratory plots of *MeanCount* for baited and unbaited trap deployments and for bait methods (i.e., baited, unbaited) within each habitat type provided no indication that the use of bait resulted in higher counts. However, we believe that the influence of bait on video counts of black sea bass in coastal waters off Maryland and the Mid-Atlantic coast should be investigated once a method is developed for identifying habitats before sampling. We recommend that samples be collected over a greater temporal and spatial scale with a paired design with equal replication of habitat types across deployments. Unbaited deployments should be conducted first, followed by baited deployments with fresh bait to ensure independence of samples and bait quality (Harvey et al., 2007; Bernard and Götz, 2012). Further, a stand-alone camera system with a clear view of the bait should be used in place of a baited trap (Harvey et al., 2007). Lastly, because fish and crustaceans have been shown to be the most important components of diets of black sea bass (Byron and Link, 2010), the use of an oily fish such as Atlantic menhaden (*Brevoortia tyrannus*) (Wells et al., 2008; Bacheler et al., 2013) or crushed crabs (*Cancer* spp.) may be more effective at attracting black sea bass to the camera system.

Our results indicate that underwater video has the potential to provide information on the abundance of black sea bass during their inshore residency on hard bottom habitats. However, we suggest that changes be made to the sampling method to help reduce variability in abundance estimates. Despite the efforts of the captain to position the vessel directly over bottom structure, it was not possible to determine where the camera system landed in relation to structure after it was deployed. The high variation between successive deployments in relation to habitat appearing in the camera field-of-view resulted in less samples in sand+rock and live bottom habitats than in sand habitats. We suggest, on the basis of the higher values of *MeanCount* for both categories of black sea bass observed for sand+rock and live bottom habitats than in sand habitats, that efforts to reduce the inconsistency related to deployment locations should include the use of a sampling scheme with sites stratified by habitat type. Methods to identify habitats before sampling may include the use of a remotely operated vehicle or camera sled (Harvey et al., 2007). Scuba divers may also be used to identify suitable locations for deployment and arrange the system so that the camera(s) has a sufficient view of the reef or other habitat (Burge et al., 2012). Further, a system with live video feed to the surface would allow a view of deployment locations where the investigator could make adjustments to the position of the vehicle or camera system if necessary (Stoner et al., 2008).

Acknowledgments

We thank captains C. Townsend and W. Townsend of the FV *Andrew G* for their invaluable help in the field. We also thank C. McGeachy and other students for their assistance with data collection and E. Babcock for her critical review of the manuscript. Additional thanks to anonymous reviewers whose comments greatly improved the manuscript. This project was funded by the NOAA Living Marine Resources Cooperative Science Center at the University of Maryland Eastern Shore.

Literature cited

Bacheler, N. M., and J. C. Ballenger.
2015. Spatial and temporal patterns of black sea bass sizes and catches in the southeastern United States inferred from spatially explicit nonlinear models. Mar. Coast. Fish. 7:523–536.

Bacheler, N. M., and K. W. Shertzer.
2015. Estimating relative abundance and species richness from video surveys of reef fishes. Fish. Bull. 113:15–26.

Bacheler, N. M., Z. H. Schobernd, D. J. Berrane, C. M. Schobernd, W. A. Mitchell, and N. R. Geraldi.
2013. When a trap is not a trap: converging entry and exit rates and their effect on trap saturation of black sea bass (*Centropristis striata*). ICES J. Mar. Sci. 70:873–882.

Bacheler, N. M., D. J. Berrane, W. A. Mitchell, C. M. Schobernd, Z. H. Schobernd, B. Z. Teer, and J. C. Ballenger.
2014 Environmental conditions and habitat characteristics influence trap and video detection probabilities for reef fish species. Mar. Ecol. Prog. Ser. 517:1–14.

Bernard, A. T. F., and A. Götz.
2012. Bait increases the precision in count data from remote underwater video for most subtidal reef fish in the warm-temperate Agulhas region. Mar. Ecol. Prog. Ser. 471:235–252.

Burnham, K. P., and D. R. Anderson.
2002. Model selection and multimodal inference: a practical information-theoretic approach, 2nd ed., 488 p. Springer-Verlag, New York.

Burge, E. J., J. D. Atack, C. Andrews, B. M. Binder, Z. D. Hart, A. C. Wood, L. E. Bohrer, and K. Jagannathan.
2012. Underwater video monitoring of groupers and the associated hard-bottom reef fish assemblage of North Carolina. Bull. Mar. Sci. 88:15–38.

Byron, C. J., and J. S. Link.
2010. Stability in the feeding ecology of four demersal fish predators in the US Northeast shelf large marine ecosystem. Mar. Ecol. Prog. Ser. 406:239–250.

Cappo, M., G. De'ath, and P. Speare.
2007. Inter-reef vertebrate communities of the Great Barrier Reef Marine Park determined by baited remote underwater video stations. Mar. Ecol. Prog. Ser. 350:209–221.

Cullen, D. W., and B. G. Stevens.
2017. Examination of black sea bass trap catches in relation to soak time in the Middle Atlantic Bight. N. Am. J. Fish. Manage. 37:9–15.

Ellis, D. M., and E. E. DeMartini.
1995. Evaluation of a video camera technique for indexing abundances of juvenile pink snapper, *Pristipomoides filamentosus*, and other Hawaiian insular shelf fishes. Fish. Bull. 93:67–77.

Fabrizio, M. C., J. P. Manderson, and J. P. Pessutti.
2013. Habitat associations and dispersal of black sea bass from a mid-Atlantic Bight reef. Mar. Ecol. Prog. Ser. 482:241–253.

Fulton, C. J.
2007. Swimming speed performance in coral reef fishes: field validations reveal distinct functional groups. Coral Reefs 26:217–228.

Gerstner, C. L.
1998. Use of substratum ripples for flow refuging by Atlantic cod, *Gadus morhua*. Environ. Biol. Fish. 51:455–460.

Harvey, E., and M. Shortis.
1996. A system for stereo-video measurements of sub-tidal organisms. Mar. Tech. Soc. J. 29:10–22.

Harvey, E. S., M. Cappo, J. J. Butler, N. Hall, and G. A. Kendrick.
2007. Bait attraction affects the performance of remote underwater video stations in assessment of demersal fish community structure. Mar. Ecol. Prog. Ser. 350:245–254.

Lavenda, N.
1949. Sexual differences and normal protogynous hermaphroditism in the Atlantic sea bass, *Centropristis striatus*. Copeia 3:185–194.

Lowry, M., H. Folpp, M. Gregson, and I. Suthers.
2012. Comparison of baited remote underwater video (BRUV) and underwater visual census (UVC) for assessment of artificial reefs in estuaries. J. Exp. Mar. Biol. Ecol. 416–417:243–253.

Mazerolle, M. J.
2016. AICcmodavg: model selection and multimodal inference based on (Q)AIC(c). R package vers. 2.0-3. [Available from website, accessed January 2017.]

Moser, J., and G. R. Shepherd.
2009. Seasonal distribution and movement of black sea bass (*Centropristis striata*) in the northwest Atlantic as determined from a mark-recapture experiment. J. Northwest Atl. Fish. Sci. 40:17–28.

Pinheiro, J. C., and D. M. Bates.
2000. Mixed-effects models in S and S-PLUS, 528 p. Springer-Verlag, New York.

Pinheiro, J., D. Bates, S. DebRoy, D. Sarkar, and R Core Team.
2017. nlme: linear and nonlinear mixed effects models. R package vers. 3.1-129. [Available from: website, accessed January 2017.]

Pratt, T. C., K. E. Smokorowski, and J. R. Muirhead.
2005. Development and experimental assessment of an underwater video technique for assessing fish-habitat relationships. Arch. Hydrobiol. 164:547–571.

R Core Team.
2016. R: a language and environment for statistical computing. R Foundation for Statistical Computing, Vienna, Austria. [Available from Article, accessed November 2016.]

Ross, S. W., M. Rhode, S. T. Viada, and R. Mather.
2016. Fish species associated with shipwreck and natural hard-bottom habitats from the middle to outer continental shelf of the Middle Atlantic Bight near Norfolk Canyon. Fish. Bull. 114:45–57.

Schobernd, Z. H., N. M. Bacheler, and P. B. Conn.
2014. Examining the utility of alternative video monitoring metrics for indexing reef fish abundance. Can. J. Fish. Aquat. Sci. 71:464–471.

Shepherd, G. R., and M. Terceiro.
1994. The summer flounder, scup, and black sea bass fishery of the Middle Atlantic Bight and southern New England waters. NOAA Tech. Rep. NMFS 122, 13 p.

Shepherd, G. R., C. W. Morre, and R. J. Seagraves.
2002. The effect of escape vents on the capture of black sea bass, *Centropristis striata*, in fish traps. Fish. Res. 54:195–207.

Steimle, F. W., and W. Figley.
1996. The importance of artificial reef epifauna to black sea bass diets in the Middle Atlantic Bight. N. Am. J. Fish. Manage. 16:433–439.

Steimle, F. W., and C. Zetlin.
2000. Reef habitats in the Middle Atlantic Bight: abundance, distribution, associated biological communities, and fishery resource use. Mar. Fish. Rev. 62(2):24–42.

Stoner, A. W., B. J. Laurel, and T. P. Hurst.
2008. Using a baited camera to assess relative abundance of juvenile Pacific cod: field and laboratory trials. J. Exp. Mar. Biol. Ecol. 354:202–211.

Torsten, H., F. Bretz, and P. Westfall.
2008. Simultaneous inference in general parametric models. Biometrical J. 50:346–363.

Townsend, D. W., A. C. Thomas, L. M. Mayer, M. A. Thomas, and J. A. Quinlan.
2006. Oceanography of the northwest Atlantic continental shelf. *In* The sea, volume 14A: the global coastal ocean (A. R. Robinson and K. H. Brink, eds.), p. 119–168. Harvard Univ. Press, Cambridge, MA.

Watson, D. L., E. S. Harvey, M. J. Anderson, and G. A. Kendrick.
2005. A comparison of temperate reef fish assemblages recorded by three underwater stereo-video techniques. Mar. Biol. 148:415–425.

Wells, R. J. D., K. M. Boswell, J. H. Cowan Jr., and W. F. Patterson III.
2008. Size selectivity of sampling gears targeting red snapper in the northern Gulf of Mexico. Fish. Res. 89:294–299.

Wentworth, C. K.
1922. A scale of grade and class terms for clastic sediments. J. Geol. 30:377–392.

Willis, T. J., and R. C. Babcock.
2000. A baited underwater video system for the determination of relative density of carnivorous reef fish. Mar. Freshw. Res. 51:755–763.

Zurr, A., E. N. Ieno, N. Walker, A. A. Saveliev, and G. M. Smith.
2009. Mixed effects models and extensions in ecology with R, 574 p. Springer-Verlag, New York.

National Marine Fisheries Service
NOAA

Fishery Bulletin
established in 1881

Spencer F. Baird
First U.S. Commissioner of Fisheries and founder of *Fishery Bulletin*

Fish assemblages associated with red grouper pits at Pulley Ridge, a mesophotic reef in the Gulf of Mexico

Stacey L. Harter (contact author)[1]
Heather Moe[1]
John K. Reed[2]
Andrew W. David[1]

Email address for contact author: stacey.harter@noaa.gov

[1] Southeast Fisheries Science Center
National Marine Fisheries Service, NOAA
3500 Delwood Beach Road
Panama City, Florida 32408
[2] Harbor Branch Oceanographic Institute
Florida Atlantic University
5600 U.S. 1 North
Fort Pierce, Florida 34946

Abstract—Red grouper (*Epinephelus morio*) modify their habitat by excavating sediment to expose rocky pits, providing structurally complex habitat for many fish species. Surveys conducted with remotely operated vehicles from 2012 through 2015 were used to characterize fish assemblages associated with grouper pits at Pulley Ridge, a mesophotic coral ecosystem and habitat area of particular concern in the Gulf of Mexico, and to examine whether invasive species of lionfish (*Pterois* spp.) have had an effect on these assemblages. Overall, 208 grouper pits were examined, and 66 fish species were associated with them. Fish assemblages were compared by using several factors but were considered to be significantly different only on the basis of the presence or absence of predator species in their pit (no predators, lionfish only, red grouper only, or both lionfish and red grouper). The data do not indicate a negative effect from lionfish. Abundances of most species were higher in grouper pits that had lionfish, and species diversity was higher in grouper pits with a predator (lionfish, red grouper, or both). These results may indicate that grouper pits are a favorable habitat for both lionfish and native fish species or that the presence of lionfish is too recent to have caused changes to fish community structure.

Manuscript submitted 15 August 2016.
Manuscript accepted 2 June 2017.
Fish. Bull. 115:419–432 (2017).
Online publication date: 23 June 2017.
doi: 10.7755/FB.115.3.11

The views and opinions expressed or implied in this article are those of the author (or authors) and do not necessarily reflect the position of the National Marine Fisheries Service, NOAA.

The red grouper (*Epinephelus morio*) has been harvested in the United States since the 1880s and is currently the most common grouper species landed in both commercial and recreational fisheries of the Gulf of Mexico (Fisheries Statistics Division, National Marine Fisheries Service, Annual Commercial Landing Statistics, website, and Saltwater Recreational Data and Statistics, website). Like other grouper species, the red grouper is a slow growing, late maturing, relatively stationary, and long lived fish (Moe[1]; Jory and Iversen[2]). Adult red grouper inhabit the deeper waters (>70 m) of the shelf edge and have been known to modify their habitat by excavating sediment to expose rocky depressions (or pits) on the seafloor in areas where vertical relief is not already present (Coleman et al., 2010). Red grouper use these pits as their home territories (Scanlon et al., 2005). These excavations increase the architectural complexity of the habitat, attracting many reef-associated species and providing shelter for juveniles of some economically important species and, thereby, increasing biodiversity (Coleman et al., 2010). By excavating the sediments, red grouper act as "ecological engineers" and may play an important role in influencing community dynamics (Jones et al., 1994; Coleman and Williams, 2002; Coleman et al., 2010).

Grouper pits have been described for 2 marine protected areas (MPAs) in the northeastern Gulf of Mexico: Madison-Swanson and Steamboat Lumps MPAs, which were established in 2000 on the shelf break (at

[1] Moe, M. A., Jr. 1969. Biology of the red grouper *Epinephelus morio* (Valenciennes) from the eastern Gulf of Mexico. Fla. Dep. Nat. Resour. Mar. Res. Lab. Prof. Pap. Ser. 10, 95 p.
[2] Jory, D. E., and E. S. Iversen. 1989. Species profiles: life histories and environmental requirements of coastal fishes and invertebrates (South Florida)—black, red, and Nassau groupers, 21 p. U.S. Fish Wildl. Serv. Biol. Rep. 82(11.110). U.S. Army Corps Eng., TR EL-82-4. [Available from website.]

depths of 50–120 m) to alleviate fishing pressure on aggregations of gag (*Mycteroperca microlepis*). Grouper pits at Steamboat Lumps consist of carbonate rocks that have been scoured out from a thick veneer of carbonate-derived sediment. The pits are on average 5–6 m in diameter but can become as large as 25 m in diameter and 1–2 m deep with a density of about 250 pits/km^2 (Scanlon et al., 2005; Coleman et al., 2010; Wall et al., 2011). Pits in the Madison-Swanson MPA differ in their level of relief; some have a thin veneer of carbonate-derived sediments and some have more relief (Coleman et al., 2010).

Our study area was at Pulley Ridge, a mesophotic coral ecosystem (MCE) in the northeastern Gulf of Mexico, which has large populations of red grouper and a high density of grouper pits. This geological feature is a carbonate ridge that extends for nearly 300 km along the southwestern shelf of Florida and lies about 250 km west of the Florida coastline (Hine et al., 2008). The southern end of Pulley Ridge supports an MCE at depths of 60–100 m and covers an area of ~600 km^2 (Fig. 1; Jarrett et al., 2005; Cross et al.[3]; USGS[4]; Hine et al., 2008; Reed, 2016). Mesophotic coral ecosystems are characterized by the presence of light-dependent corals and their associated communities, and Pulley Ridge is the deepest MCE on the U.S. continental shelf (Halley et al.[5]). The hard-bottom substrate along this ridge consists of rock and coral pavements and cemented conglomerates of carbonate rubble and cobble rock (5–15 cm in diameter) that provide habitat for hermatypic corals (primarily *Agaricia* spp., great star coral [*Montastraea cavernosa*], and *Madracis* spp.), macroalgae, sponges, and a large variety of species of tropical fish (Phillips et al., 1990; Halley et al.[5]; Reed, 2016). The Pulley Ridge Habitat Area of Particular Concern (HAPC) was established in 2005 by the Gulf of Mexico Fishery Management Council[6] to provide protection from bottom longlines and trawls. Hook-and-line fishing, however, is still allowed. The established HAPC provides protection for 348 km^2, an area that is roughly half the total MCE area (Reed, 2016).

Structural complexity has often been shown to positively influence abundance and diversity of fish species (McClanahan, 1994; Öhman and Rajasuriya, 1998; Gratwicke and Speight, 2005; Harter et al., 2009). Most of Pulley Ridge is a low relief, low rugosity, rock and rubble habitat. The highest densities of fish reside on 2 biologically derived habitat features that provide more structural complexity: mounds of rock rubble and cobble created by sand tilefish (*Malacanthus plumieri*) and grouper pits (Halley et al.[7]). The grouper pits are large enough (8–15 m in diameter and 1–2 m deep) to be visible in high-resolution bathymetric images collected with a multibeam sonar during a research cruise in September 2011 (NOAA[8]), and up to 340 pits/km^2 are visible in those images. Approximately 90 species of fish, both shallow-water and deepwater species, have been observed on Pulley Ridge (Jaap et al., 2015). The fish communities of Pulley Ridge have been characterized previously, but communities associated with the grouper pits specifically have not.

Species of lionfish (*Pterois* spp.) first were discovered on Pulley Ridge during submersible dives in 2010 (Reed and Rogers[9]) when 6 fish were observed. Since then, exponential increases in the abundance of this population of lionfish have been observed (Andradi-Brown et al., 2016). It is unknown at this time whether red lionfish (*P. volitans*), devil firefish (*P. miles*), or both species exist at Pulley Ridge. At this time, positive identification can be achieved only through genetic analysis; therefore, lionfish were identified only to genus level for this study. The invasion of lionfish is regarded as one of the most successful colonizations of a marine species ever documented (Albins and Hixon, 2008; Green and Côte, 2009; Albins, 2013). Lionfish first were recorded in waters of the Atlantic Ocean in the mid-1980s, but their range has expanded to include the Gulf of Mexico, Caribbean, and much of the tropical and subtropical western Atlantic Ocean (Schofield, 2009, 2010). Over the years, densities of lionfish in the western Atlantic Ocean have expanded rapidly to the point that they are nearly 5 times more abundant in the invaded range (Green and Côte, 2009) than in the Pacific Ocean (Kulbicki et al., 2012). High individual growth and reproductive rates (Morris and Whitfield, 2009) have contributed to the rapid increase of the population in the western Atlantic Ocean. Many stud-

[3] Cross, V., D. C. Twichell, R. B. Halley, K. T. Ciembronowicz, B. D. Jarrett, E. S. Hammar-Klose, A. C. Hine, S. D. Locker, and D. F. Naar. 2005. GIS compilation of data collected from the Pulley Ridge deep coral reef region. U.S. Geol. Surv. Open-File Rep. 2005-1089. [Available from website.]

[4] USGS (U.S. Geological Survey). 2005. Recently discovered reef is deepest known off continental U.S. ScienceDaily, 5 January 2005. [Internet press release available from website.]

[5] Halley, R. B., V. E. Garrison, K. T. Ciembronowicz, R. Edwards, W. C. Jaap, G. Mead, S. Earle, A. C. Hine, B. Jarret, S. D. Locker, et al. 2003. Pulley Ridge—The United States' deepest coral reef? *In* U.S. Geological Survey Greater Everglades Science Program: 2002 biennial report. U. S. Geol. Surv. OFR-03-54, 153–154 p. [Available from website.]

[6] Gulf of Mexico Fishery Management Council (GMFMC). 2005. Essential Fish Habitat Amendment 3. Addressing essential fish habitat requirements, habitat areas of particular concern, and the adverse effects of fishing on fishery management plans of the Gulf of Mexico.

[7] Halley, R., G. P. Dennis, D. Weaver, and F. Coleman. Halley, R., G. P. Dennis, D. Weaver, and F. Coleman. 2005. Part II: characterization of the Pulley Ridge coral and fish fauna. Final report to the National Oceanic and Atmospheric Administration Coral Reef Conservation Grant Program, 25 p. [Available from website.]

[8] NOAA. 2011. Multibeam sonar bathymetry data collected aboard Nancy Foster (NF-11-09-CIOERT). NOAA National Centers for Environmental Information. [Available from website.]

[9] Reed, J. K., and S. Rogers. 2011. Final cruise report. Florida Shelf-Edge Expedition (FLoSEE), Deepwater Horizon oil spill response: survey of deepwater and mesophotic reef ecosystems in the eastern Gulf of Mexico and southeastern Florida. R/V Seward Johnson and Johnson-Sea-Link submersible, July 9–August 9, 2010, 16 p. [Available from website.]

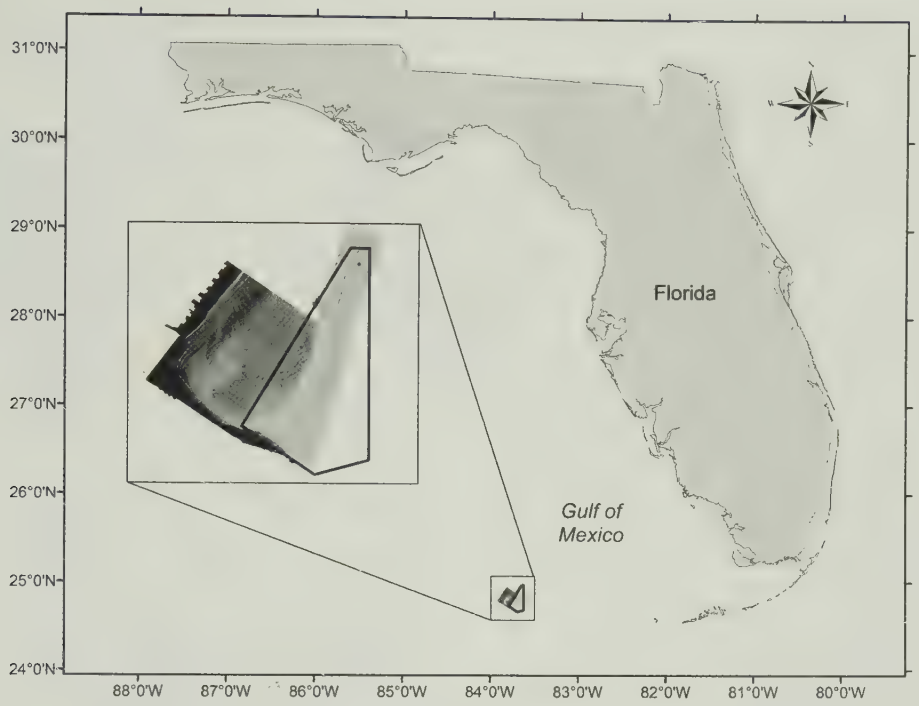

Figure 1

Map of the Pulley Ridge mesophotic coral ecosystem off southwestern Florida in the Gulf of Mexico where video surveys were conducted with a remotely operated vehicle during 2012–2015. The polygon outlined in black represents the Pulley Ridge Habitat Area of Particular Concern. The extent of the survey area includes the entire area of available multibeam bathymetric imagery.

ies have revealed deleterious effects of the invasion of lionfish on abundances and species richness of native fish through predation and competition (Albins and Hixon, 2008; Green et al., 2012; Albins, 2013). In addition, studies of MCEs in the Bahamas found that predation by lionfish on herbivorous fish has caused a shift in the benthic fauna, and an increase in the proportion of algae to the proportion of corals (Lesser and Slattery, 2011).

Because the grouper pits of Pulley Ridge have not been characterized previously, particularly since the invasion of lionfish, our objectives for this study were 1) to quantify and characterize fish populations associated with grouper pits at Pulley Ridge, 2) to estimate the spatial distribution and abundance of key economically and ecologically important reef fish species, and 3) to examine the effect of lionfish on the abundance and composition of fish communities of the grouper pits.

Materials and methods

Data collection

Information on the fish community in the grouper pits was collected annually from 2012 to 2015 by using underwater video cameras attached to remotely operated vehicles (ROVs) that were deployed from the RV *F. G. Walton Smith*. Video surveys were conducted with 2 different ROVs: the *Phantom S-2* in 2012–2013 and the *Mohawk* in 2014–2015. Both vehicles are operated by the Undersea Vehicles Program of the University of North Carolina at Wilmington. To keep the ROV near the seafloor during dives, a "down weight" (145 kg) was tethered to its umbilical cable at a distance of 25–30 m behind the ROV. The configuration of the down weight allowed the ROV to traverse just above the seafloor (<1 m) at a mean speed-over-ground of approximately 0.13 m/s (range: 0.13 to 0.28 m/s). The precise location of the ROV was recorded constantly throughout each dive with a tracking system linked to the GPS of the RV *F. G. Walton Smith*.

The *Phantom* ROV was equipped with a standard-definition Sony[10] color video camera (Sony Corp., Tokyo, Japan) with more than 460 lines of resolution, and the *Mohawk* ROV had a Mini Zeus II high-definition video camera (Insite Pacific Inc., Solana Beach, CA). Both cameras provided continuous video data recorded on external hard drives. On both ROVs, the camera typically was angled down ~30° to capture the view both

[10]Mention of trade names or commercial companies is for identification purposes only and does not imply endorsement by the National Marine Fisheries Service, NOAA.

near to and far from the horizon in video recordings of fish aggregations and habitat. An on-screen display system recorded and superimposed time, date, ROV heading (direction), and ROV depth on the video taken with the cameras. The ROVs also had high-resolution digital cameras that captured still images of fish and habitats within the study area. The still cameras were mounted on the ROV in a fixed, downward-looking orientation for images of habitat cover. Both cameras were equipped with parallel lasers (10 cm) to calculate scale. Two 250-W halogen lights (DeepSea Power & Light, San Diego, CA) were mounted on top of the ROV tilt platform and provided illumination for the video cameras on the *Phantom*, and the *Mohawk* ROV had two 3700-lm SeaLite Sphere 3100 LED lights (DeepSea Power & Light). Water clarity and natural light, however, usually allowed visibility in excess of 20 m. When available, an SBE 39 temperature and depth recorder (Sea-Bird Scientific, Bellevue, WA) was attached to the ROV for each dive.

A statistically rigorous sampling protocol was used to select the ROV survey sites at Pulley Ridge. In ArcGIS, vers. 10.1 (Esri, Redlands, CA), a grid of blocks, each 1×1 km, was overlaid on maps created with multibeam bathymetric imagery collected by NOAA[7] (Fig. 1). Blocks were selected randomly to be surveyed quantitatively by the ROV over the 4 years, and the pooling of blocks for selection targeted both the Pulley Ridge HAPC and areas adjacent to the HAPC that appeared to be mesophotic habitat from the bathymetric maps. Areas outside the HAPC had been mapped previously, but the bathymetric maps have not yet been verified by direct observations, or ground-truth; therefore, areas interpreted as hard-bottom habitat from the bathymetric data were used in the selection of blocks. Once a block had been examined, it was not resampled in subsequent years. Each dive of the ROV lasted approximately 3–4 h during daylight hours and covered an average distance of 1.85 km (standard error [SE] 0.11). The direction of each dive within a block was selected haphazardly on the basis of a flip of a coin and the maneuverability of the ship, which is affected by wind and current, but the direction was not altered to target grouper pits.

Video reading

All fish were counted and identified in each encountered grouper pit, including species that were both inside the pit and swimming in the water column above (1–3 m) the pit. Individual fish were identified to the lowest taxonomic level possible, and fish counts for each taxon were made by using a tally system. Still images of single frames of video were used to identify and count fish when multiple species were present and when areas had high fish abundance. If confident identifications could not be made, individuals were recorded as *unknown*. Random segments of video were analyzed by a second reader to confirm identification of fish and accuracy of the primary reader's counts. Counts for large schools of fish (>100 individuals) were estimated by counting a group of 25 fish and then extrapolating that count for the size of the entire school. To avoid recounting fish, unique color patterns, body markings, and attraction behaviors (i.e., schooling of fish around the ROV) were noted. Fish abundances were recorded for each taxon observed in every grouper pit. Because pits were of relatively similar sizes, averaging ~10 m in diameter (as measured from high-resolution, multibeam bathymetric imagery) and 1–2 m in depth, fish abundance per pit, rather than density, was used. Coleman et al. (2010) found no relationship between pit diameter and either fish density or species abundance in the Madison-Swanson and Steamboat Lumps MPAs in the northeastern Gulf of Mexico.

Analyses of multivariate fish communities

Multivariate analyses were conducted by using PRIMER, vers. 6 (PRIMER-E, Auckland, New Zealand) to compare fish communities in the grouper pits. Each grouper pit was defined and characterized by the following 4 factors: year, predator presence or absence, region, and HAPC. Year indicated the year the grouper pit was sampled: 2012–2015 (Fig. 2A). Red grouper and lionfish are the 2 top-level predators that inhabit the grouper pits. To test the effect of predator presence or absence on community structure, grouper pits were categorized as 1) having either no predators (no lionfish or red grouper), 2) lionfish only, 3) red grouper only, or 4) both (red grouper and lionfish present) (Fig. 2B). Although in some cases on shallow reefs lionfish have been observed to move more than 1 km (Akins et al., 2014; Tamburello and Côté, 2015), both lionfish and red grouper are known for their site fidelity (Coleman et al., 2010; Jud and Layman, 2012; Bachelor et al., 2015). Coleman et al. (2010) examined the movement patterns of red grouper in pits specifically and found that they exhibit high site fidelity, remaining in the same pit for long periods of time (>1 year). Other predators around the grouper pits, such as other grouper species and species of snapper, are more roving predators. The region factor indicated the location of the grouper pits in relation to the geological features of the Pulley Ridge MCE, primarily on the basis of bathymetric maps. Four geological regions were used to categorize the location of each grouper pit: main ridge, off main ridge (area east of the main ridge), central basin, and west ridge (Fig. 2C). The HAPC factor indicated whether the pit was located inside or outside the HAPC.

Four multivariate routines in PRIMER were employed to examine fish communities by using the factors described previously. They were nonmetric multidimensional scaling (MDS), analysis of similarity (ANOSIM), similarity percentages (SIMPER), and biodiversity indices (DIVERSE) routines. For these analyses, taxa that composed less than 1% of the total abundance were removed to minimize the disproportionate effect they can have on the data. Data were averaged by factor and fourth-root transformed—a calculation

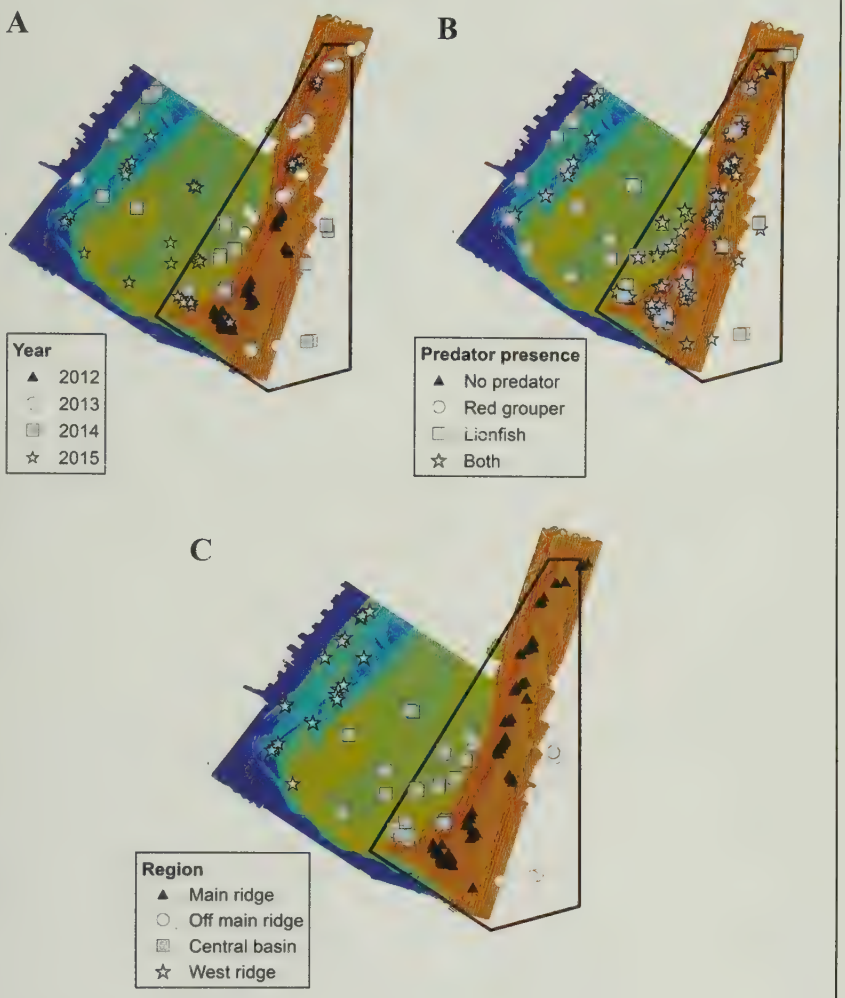

Figure 2

Locations of each grouper pit surveyed during 2012–2015 in the Gulf of Mexico, characterized by 3 of the factors used to compare fish assemblages at pits: (**A**) year, (**B**) predator presence, and (**C**) region. The polygon outlined in black represents the Pulley Ridge Habitat Area of Particular Concern, which is located off southwestern Florida. Predator presence or absence categories were no predator, red grouper (*Epinephelus morio*) only, species of lionfish (*Pterois* spp.) only, or both predators.

that "down-weighs" the dominance of highly abundant species, allowing species with intermediate density to exert some influence on the calculation of similarity (Clarke and Warwick, 2001).

An MDS routine based on Bray–Curtis similarity coefficients and a dendrogram with group-average linking were created to depict the results of a concurrent similarities profile (SIMPROF routine in PRIMER). The MDS routine is an ordination technique in which points that are located closer together in multivariate space are considered more similar than points further away. The stress values shown in MDS plots reflect the accuracy of the representation of community structure; lower stress values indicate that the plots are increasingly representative of the community structure. Stress values less than 0.20 generally indicate that plots provide an accurate representation of the data rather than that the points have been placed arbitrarily in the 2-dimensional ordination space.

We also tested for differences in community structure among pits with one-way ANOSIM tests based on the Bray-Curtis similarity coefficients. Significant differences among groups were defined in our study when $P \leq 0.05$, but for those pairwise tests that showed significant difference, we further examined the ANOSIM R-statistic. Unlike the P-value, the R-statistic reflects the absolute difference in community structure between treatments (i.e., it reflects the size of the effect) (Clarke et al., 2006). The R-statistic typically ranges from 0 to 1, with values closer to 1 representing more significant separation among groups and values closer to 0 representing no difference among groups. It is possible to obtain a significant P-value with an R-statistic that is very low when there are many replicates at each site, and obtaining a significant P-value in such a case would indicate little biologically significant separation among groups (Clarke, 1993). Negative R-values denote unusual situations where replicates among groups are more similar than within a group. Analysis of similarity percentages was then used to determine which species contributed to the dissimilarities between the group pairs.

Biodiversity indices derived with the DIVERSE routine were compared among grouper pits for each factor. Parameters examined included total number, diversity, and evenness of species in the community. The Shannon-Weiner function (H') was used to estimate pit diversity as $\Sigma_i\, p_i \log(p_i)$, where p_i is the proportion of the total count arising from the ith species. Pielou's evenness was estimated as $H'/\log(S)$, where S is the total number of taxa at a pit (Pielou, 1977).

Analyses of univariate fish abundance

Fish associated with grouper pits were divided into 3 categories: small fish, schooling fish, and large fish. This classification was needed because several of the species (primarily the economically important species)

Table 1

Summary information from video surveys conducted with a remotely operated vehicle during 2012–2015 at the Pulley Ridge mesophotic coral ecosystem off southwestern Florida in the Gulf of Mexico. N/A indicates that information was not available for that year.

Year	No. of 1-km^2 blocks surveyed	Average distance surveyed (km)	No. of grouper pits surveyed	Dates of survey	Depth range (m)	Bottom temperature range (°C)
2012	10	35.2	80	14–25 Aug	62.8–75.5	N/A
2013	15	29.4	41	12–27 Aug	60.3–93.9	N/A
2014	17	23.8	35	14–28 Aug	63.1–86.1	18.1–29.2
2015	28	33.4	52	23 Aug–2 Sept	59.3–105.5	19.0–22.52

were not abundant enough to examine individually. For all analyses, the replicate was each grouper pit, and average abundances (with standard errors) for each factor were calculated and compared. Significant differences existed when $P \leq 0.05$.

The small fish group consisted of taxa of small, benthic fish that typically reside inside the pit to use the structural complexity it offers. Taxa in the small fish category were cardinalfish (*Apogon* spp.); damselfish (*Chromis* spp.); small sea basses (Serranidae), including anthiids (Anthiinae); wrasses (*Halichoeres* spp.); and parrotfish (Labridae). Not only do these species use the grouper pits in the same manner, but they are all possible prey of lionfish and red grouper. Abundances of small fish were $\log_e$ transformed to correct for normality and then tested with one-way analysis of variance (ANOVA) to examine the effects of year, predator presence or absence, region, and HAPC. Categories for each factor were the same as the multivariate analyses: year was 2012–2015; predator presence or absence was either no predator, lionfish only, red grouper only, or both; region was main ridge, off main ridge, central basin, or west ridge; and HAPC was either inside or outside the protected area.

Taxa in the schooling fish category hover just above a grouper pit and usually travel in schools of greater than 50 individuals. This group included the striped grunt (*Haemulon striatum*), the school bass (*Schultzea beta*), and bonnetmouths (Haemulidae). Because of the nature of the abundance data for the schooling group (large variances among pits) and because transformations did not correct for normality, nonparametric Kruskal–Wallis tests were used to test for effects of year, predator presence, region, and HAPC on the abundances of taxa in the schooling group.

The final category, large fish, consisted of the larger taxa, most of which are managed by the Gulf of Mexico Fishery Management Council. This group included grunts (*Haemulon* spp.), except for the striped grunt; snapper (*Lutjanus* spp.); grouper (*Mycteroperca* spp., *Epinephelus* spp., and the graysby, *Cephalopholis cruentata*), except for the red grouper; triggerfish (*Balistes* spp.); and the hogfish (*Lachnolaimus maximus*). Again, transformations did not correct for non-normality this time because of low abundances; therefore, nonparametric Kruskal–Wallis tests were used to test the effects of the 4 factors (year, predator presence, region, and HAPC) on the abundance of taxa in the large fish group.

Results

In August of each year between 2012 and 2015, 70 random blocks (each 1 km^2) were surveyed over the entire Pulley Ridge MCE region (Table 1). Within those blocks, 208 grouper pits were encountered and analyzed. The number of grouper pits observed by year was 80 in 2012, 41 in 2013, 35 in 2014, and 52 in 2015. The average distance surveyed per year was 30.5 km (SE 2.5). The temperature range was 18.1–29.2°C in 2014 and 19.0–22.5°C in 2015; however, these data were not available for 2012 and 2013 because a conductivity, temperature, and depth profiler was not on the ROV during those years. Depths sampled were slightly shallower in 2012 because dives that year were conducted primarily on the main ridge, which is shallower than the other regions. The central basin and west ridge areas of the Pulley Ridge MCE are slightly deeper (10–30 m) and were sampled during the remaining years of the surveys (Fig. 2).

Grouper pits were distributed throughout the sampling region. Their locations are shown in Figure 2 by year, region, predator presence, and HAPC. In general, all the regions surveyed have very similar habitat, except the off main ridge region, which is east of the main ridge and is a predominately soft-bottom substrate mixed with rock rubble and cobble. The other regions (main ridge, central basin, and west ridge) all have low relief (0–1 m) and a substrate consisting primarily of rock pavement (probably old, dead coral plates), and rock rubble and cobble (5–20 cm rock), or a combination of the latter 2 substrate types.

Bathymetric maps show grouper pits 8–15 m in diameter, 1–2 m deep, and evenly spaced about 100 m apart over much of the area. Up to 340 grouper pits were visible in a single 1-km^2 block on high-resolution bathymetric maps of main Pulley Ridge (NOAA[7]).

Table 2

Annual mean abundances of all taxa, observed during video surveys conducted with a remotely operated vehicle at Pulley Ridge, in the Gulf of Mexico, from 2012 through 2015. The overall mean is the average of the 4 annual values for each taxon. Taxa are listed in order from highest to lowest overall mean. Commercially or recreationally harvested species are noted in bold.

Scientific name	2012	2013	2014	2015	Overall mean
Haemulidae	124.09	4.05	0.00	0.00	32.04
Haemulon striatum	0.00	64.86	21.77	12.15	24.70
Schultzea beta	0.00	13.51	32.17	33.00	19.67
Apogon spp.	0.63	31.24	5.40	32.73	17.50
Chromis scotti	9.74	2.46	0.97	26.25	9.85
Pterois volitans	3.06	4.70	13.97	6.65	7.10
Hemanthias vivanus	0.00	0.00	26.37	0.00	6.59
Chromis enchrysura	2.50	7.35	10.51	2.46	5.71
Serranidae	0.05	21.62	0.00	0.00	5.42
Chromis spp.	2.73	4.68	0.00	7.10	3.62
Chromis insolata	2.48	2.41	4.63	4.17	3.42
Anthiinae	7.13	4.05	0.49	1.92	3.40
Apogon affinis	0.00	0.00	13.43	0.00	3.36
Coranthias tenuis	0.25	0.00	0.11	11.54	2.98
Apogon maculatus	4.44	2.97	0.71	0.00	2.03
Holocentrus spp.	0.50	3.65	2.34	1.02	1.88
Bodianus pulchellus	0.43	0.38	1.14	1.10	0.76
Chromis cyanea	1.81	0.68	0.17	0.31	0.74
Chaetodon sedentarius	0.35	0.73	0.71	0.58	0.59
Equetus lanceolatus	0.00	0.24	1.97	0.04	0.56
Centropyge argi	0.28	0.57	0.17	0.87	0.47
Canthigaster rostrata	0.08	0.03	1.29	0.31	0.42
Epinephelus morio	0.38	0.49	0.46	0.35	0.42
Holacanthus tricolor	0.38	0.16	0.26	0.46	0.31
Serranus tortugarum	0.06	0.03	0.00	1.15	0.31
Mycteroperca phenax	0.44	0.05	0.23	0.52	0.31
Sparisoma atomarium	0.13	0.00	0.49	0.27	0.22
Liopropoma eukrines	0.03	0.19	0.23	0.37	0.20
Holacanthus bermudensis	0.19	0.11	0.31	0.10	0.18
Chaetodon ocellatus	0.00	0.11	0.23	0.29	0.16
Stegastes partitus	0.06	0.14	0.00	0.38	0.15
Pronotogrammus martinicensis	0.00	0.16	0.26	0.13	0.14
Apogon pseudomaculatus	0.00	0.14	0.20	0.08	0.10
Halichoeres spp.	0.08	0.00	0.06	0.25	0.10
***Lutjanus* spp.**	0.01	0.00	0.20	0.15	0.09

Table Continued

These pits represent the only areas of Pulley Ridge that provide a diversity of structural habitat. Whereas most of Pulley Ridge is relatively flat and consists of rubble and pavement and little rugosity, the grouper pits provide moderate relief (1–2 m), slopes of 5–30°, and high-rugosity habitat. Rugosity here is defined as a degree of ruggedness of the rock bottom in relation to the size of rock ledges, holes, and crevices, which tend to provide the most structurally complex habitat for reef fish. The grouper pits provide habitat for a large variety and density of small reef fish, and the exposed rock provides habitat for sessile benthic biota. Although rugosity of the grouper pits was not measured quantitatively, it differed visually only for those grouper pits that were not actively being maintained by a predator. These abandoned pits tended to be filled with sediment and lack exposed rock ledges.

Overall, 66 fish taxa were observed in the grouper pits of Pulley Ridge, 16 of which are managed species (Table 2). Schooling species, such as bonnetmouths and the striped grunt, had the highest overall mean abundances (84.40 individuals/pit [SE 25.30]), but the species that composed the schooling category varied among years. Bonnetmouths dominated in 2012, but the striped grunt and the school bass were more abundant during 2013–2015. Of the small, benthic fish that

Table 2 ***Continued***

Scientific name	2012	2013	2014	2015	Overall mean
Holacanthus ciliaris	0.08	0.05	0.11	0.12	0.09
Cephalopholis cruentata	0.14	0.00	0.09	0.08	0.08
Holocentrus adscensionis	0.11	0.11	0.00	0.00	0.06
Seriola rivoliana	0.03	0.08	0.09	0.00	0.05
Halichoeres bathyphilus	0.00	0.00	0.14	0.04	0.05
Muraenidae	0.01	0.05	0.03	0.08	0.04
Pomacanthus paru	0.09	0.00	0.03	0.04	0.04
Rypticus saponaceus	0.10	0.03	0.00	0.02	0.04
Mycteroperca interstitialis	0.11	0.03	0.00	0.00	0.03
Mycteroperca bonaci	0.06	0.00	0.00	0.08	0.03
Pseudupeneus maculatus	0.03	0.00	0.11	0.00	0.03
Acanthurus spp.	0.00	0.03	0.09	0.02	0.03
Pomacanthus arcuatus	0.00	0.05	0.03	0.04	0.03
Haemulon album	0.11	0.00	0.00	0.00	0.03
Gymnothorax moringa	0.03	0.00	0.09	0.00	0.03
Myripristis jacobus	0.10	0.00	0.00	0.00	0.03
Aulostomus maculatus	0.01	0.00	0.03	0.04	0.02
Epinephelus adscensionis	0.01	0.00	0.00	0.06	0.02
Balistes vetula	0.01	0.03	0.03	0.00	0.02
Epinephelus guttatus	0.03	0.00	0.00	0.04	0.02
Haemulon melanurum	0.00	0.05	0.00	0.00	0.01
Lutjanus analis	0.05	0.00	0.00	0.00	0.01
Priacanthus arenatus	0.00	0.03	0.00	0.02	0.01
Seriola dumerili	0.01	0.00	0.03	0.00	0.01
Lachnolaimus maximus	0.00	0.00	0.00	0.04	0.01
***Seriola* spp.**	0.00	0.00	0.00	0.04	0.01
Acanthurus coeruleus	0.00	0.00	0.03	0.00	0.01
Lutjanus buccanella	0.00	0.00	0.03	0.00	0.01
Lutjanus campechanus	0.00	0.00	0.03	0.00	0.01
Lutjanus griseus	0.00	0.00	0.03	0.00	0.01
Monacanthus tuckeri	0.00	0.00	0.03	0.00	0.01
Opsanus spp.	0.00	0.00	0.03	0.00	0.01
Serranus phoebe	0.00	0.00	0.03	0.00	0.01
Epinephelus itajara	0.00	0.03	0.00	0.00	0.01
Haemulon spp.	0.00	0.03	0.00	0.00	0.01
***Balistes* spp.**	0.03	0.00	0.00	0.00	0.01
Neoniphon marianus	0.03	0.00	0.00	0.00	0.01
Balistes capriscus	0.00	0.00	0.00	0.02	0.00
Paranthias furcifer	0.00	0.00	0.00	0.02	0.00
Serranus annularis	0.00	0.00	0.00	0.02	0.00
Mycteroperca venenosa	0.01	0.00	0.00	0.00	0.00
Scarus coelestinus	0.01	0.00	0.00	0.00	0.00

used the grouper pits, cardinalfish, damselfish, and anthiids were the most abundant taxa (mean: 54.70 individuals/pit [SE 6.70]). The red grouper and scamp (*Mycteroperca phenax*) were the most abundant economically important species (mean: 0.40 individuals/pit [SE 0.04] for red grouper and 0.35 individuals/pit [SE 0.07] for scamp). Average abundance of unidentifiable fish was 13.91 individuals/pit (SE 3.60).

The percentage of grouper pits with red grouper in them was 37.5% in 2012, 46.3% in 2013, 45.7% in 2014, and 34.6% in 2015—proportions that were not significantly different (one-way ANOVA: P=0.61). There were never multiple red groupers in any one pit, and they were distributed evenly inside and outside the HAPC, as well as across the various regions. Frequency of occurrence for red grouper was 40.6% inside and 35.1% outside the HAPC, proportions that were not significantly different (one-way ANOVA: P=0.54). Their frequency of occurrence was 40.4% on the main ridge, 37.5% at off main ridge, 37.5% in the central basin, and 44% on the west ridge. These values were also not significantly different (one-way ANOVA: P=0.97). Of red grouper that could be measured from the lasers mounted on the ROV, total length ranged from 50 to 80 cm (average: 60 cm).

In contrast, lionfish were observed in 72.5% of grou-

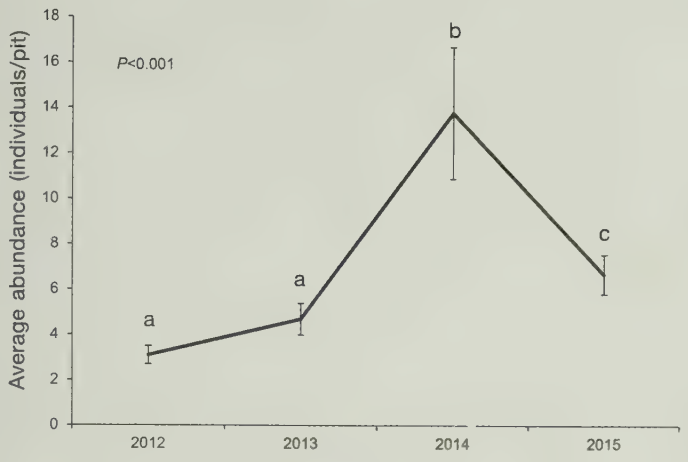

Figure 3

Average abundance of lionfish (*Pterois volitans* or *P. miles*) measured as number of individuals by year from surveys conducted from 2012 through 2015 at Pulley Ridge off southwestern Florida. The *P*-value is given for the results from one-way ANOVA. Statistically significant differences are noted with different letters (a–c); for years with the same letter, the difference is not significant. Error bars indicate standard errors of the mean.

per pits in 2012, 73.2% in 2013, 91.4% in 2014, and 86.5% in 2015. Although the maximum number of lionfish observed in a single pit was 74, the average abundance was 6.10 individuals/pit (SE 0.60), and the average abundance increased significantly over time ($P<0.0001$) (Fig. 3). Abundance of lionfish throughout the sampling area and presence of red grouper are displayed in Figure 4. Both species were distributed throughout the region, but the highest abundances of lionfish were located primarily outside the HAPC on the west ridge as well as a few places along the main ridge inside the HAPC.

Analyses of multivariate fish communities

Fish species composition associated with grouper pits was not significantly different for year, region, or HAPC factors. It did, however, differ depending on the predator species present (R-statistic=0.402, $P<0.01$). Three significantly different groups resulted from the SIMPROF test ($P< 0.05$), indicated by the letters on the MDS plot (Fig. 5). Grouper pits with lionfish only and with both predators formed one group, which meant that their fish assemblages were not significantly different from one another. Grouper pits with red grouper only formed their own group, as did those with no predators, which meant that their fish assemblages were significantly different from all other groups. The groups clustered together in this fashion at 80% similarity—a result that meant that the species composition of grouper pits with lionfish only and with both predators was 80% similar. Pairwise tests with the SIMPER routine indicated that the primary species responsible for the groups clustering in this way were cardinalfish and 3 damselfish species, including the sunshinefish (*Chromis insolata*), the purple reeffish (*Chromis scotti*), and the yellowtail reeffish (*Chromis enchrysura*). These species, as well as several others, including the scamp, striped grunt, and school bass, had higher abundances in grouper pits with either both predators or lionfish only than in grouper pits with no predators or red grouper only. Because the scamp was the most abundant economically important species observed (with the exception of red grouper), we needed to test the potential effect this species, as a predator, could have on fish assemblages in grouper pits through predation. The results of tests with the ANOSIM routine support the assertion that the presence of scamp did not affect fish assemblages of the grouper pits (R-statistic=0.169).

Species diversity and evenness did not differ considerably by HAPC or region but were different by year and predator presence (Table 3). All sampling years had similar species di-

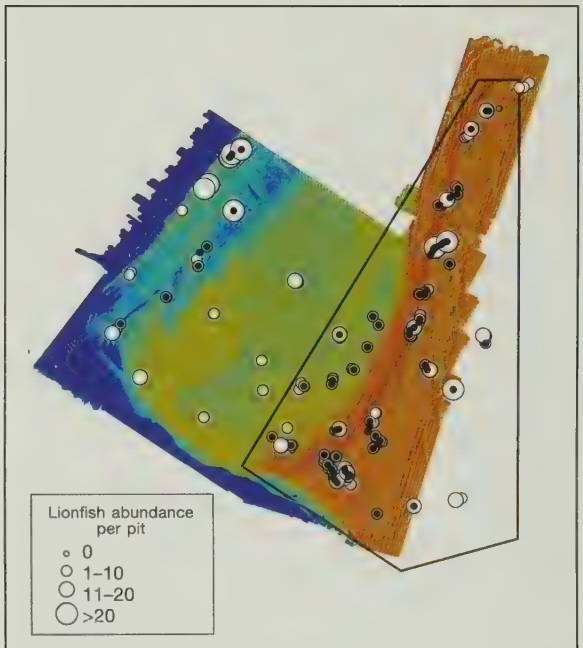

Figure 4

Average abundance of lionfish (*Pterois volitans* or *P. miles*) measured as number of individuals per grouper pit, for each pit surveyed during 2012–2015 off southwestern Florida. The size of the white circles indicates the level of abundance. Small black circles indicate the presence of a red grouper (*Epinephelus morio*). The polygon outlined in black represents the Habitat Area of Particular Concern at Pulley Ridge.

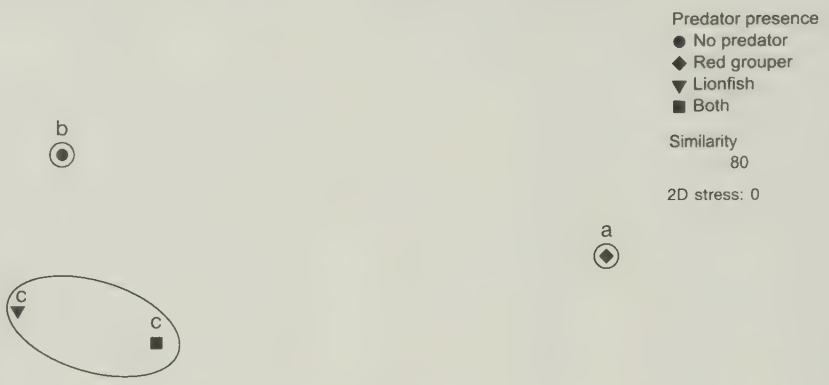

Figure 5

Plot of nonmetric multidimensional scaling ordination, derived from the Bray–Curtis similarity matrix constructed by using fourth-root transformed fish abundances averaged for each predator presence or absence category: no predator; red grouper (*Epinephelus morio*) only; species of lionfish (*Pterois* spp.) only; or both predators. Groups of fish assemblages surveyed at grouper pits during 2012–2015 off southwestern Florida are shown at 80% similarity. The closer 2 groups are in space, the more similar they are to each other. The letters (a–c) above the group symbols represent the results of the test with the SIMPROF routine in PRIMER software, and statistically different fish assemblage groups are indicated by different letters.

versity and evenness, with the exception of 2012, when those values were lower than those of other years. The lower species diversity in 2012 may have been observed because only the main ridge was sampled in that year. Species diversity and evenness were very similar for grouper pits with both predators, lionfish only, and red grouper only but were considerably lower for pits with no predators. In contrast, the highest number of species was observed in 2012 (again, this observation of a higher number of species may have occurred because only the main ridge was sampled in 2012), in grouper pits with either lionfish only or with both predators, inside the HAPC, and on the main ridge.

Analyses of univariate fish abundance

Average abundances of small fish associated with grouper pits were significantly different among years and predator groups (Fig. 6). Abundances significantly increased from 2012 to 2015 ($P<0.0001$) and species were more abundant in grouper pits with a predator present ($P=0.006$). Average abundances of small fish were not significantly different among regions or HAPC groups ($P>0.05$). In contrast, average abundances of schooling fish were not significantly different for any of the factors analyzed ($P>0.05$). Average abundances of large fish associated with the grouper pits were significantly different only among predator groups, where higher abundances were observed in grouper pits with either red grouper only or with both predators ($P<0.001$; Fig. 7). As with the multivariate analyses, we tested whether presence of scamp had an effect on abundances of

Table 3

Biodiversity indices for fish communities observed during video surveys conducted with a remotely operated vehicle at the Pulley Ridge mesophotic coral ecosystem in the Gulf of Mexico. Values are shown for each factor: year; predator presence; inside the Pulley Ridge Habitat Area of Particular Concern (HAPC) (area protected from fishing) and outside the HAPC (unprotected area); and the region of Pulley Ridge. *S*=total number of species; *H'*=Shannon-Wiener function of species diversity; *J'*=Pielou's evenness.

	S	*H'*	*J'*
Year			
2012	50	1.15	0.29
2013	41	2.09	0.56
2014	46	2.33	0.61
2015	43	2.26	0.60
Predator			
No predator	32	0.64	0.18
Red grouper only	24	2.10	0.66
Lionfish only	64	2.56	0.62
Both predators	56	2.48	0.62
HAPC			
Inside	65	2.38	0.57
Outside	42	2.36	0.63
Pulley Ridge			
Main ridge	61	2.05	0.50
Central basin	43	2.16	0.57
West ridge	40	2.26	0.61
Off main ridge	25	1.98	0.61

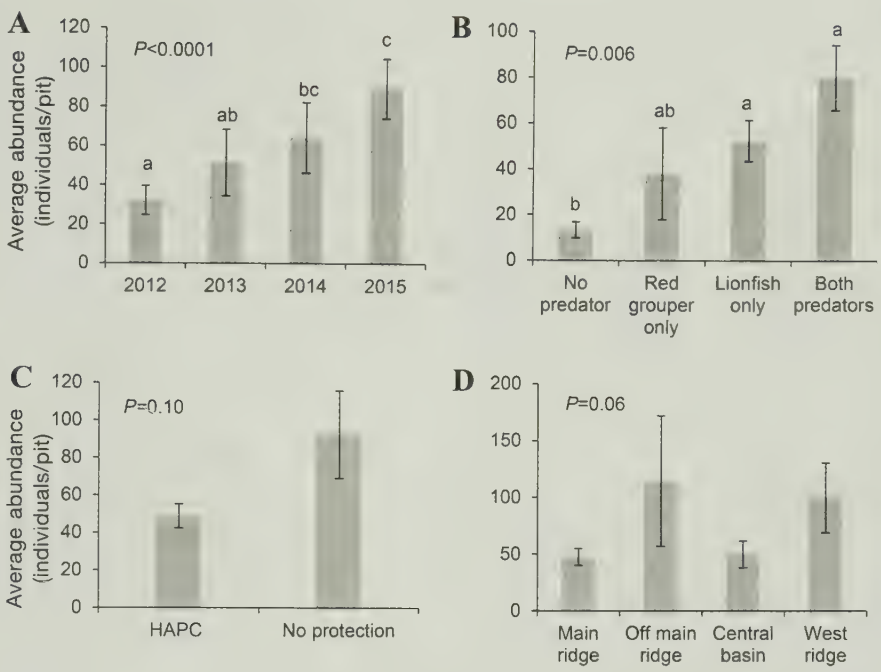

Figure 6

Average abundance measured as number of individuals of small benthic fish, including cardinalfish (*Apogon* spp.), damselfish (*Chromis* spp.), small sea basses (Serranidae), wrasses (*Halichoeres* spp.), and parrotfish (Labridae), associated with grouper pits surveyed during 2012–2015 off southwestern Florida, shown by the factor used to compare fish assemblages at pits: (**A**) year, (**B**) predator presence or absence, (**C**) inside or outside Pulley Ridge Habitat Area of Particular Concern (HAPC), and (**D**) region. Predators included the red grouper (*Epinephelus morio*) and species of lionfish (*Pterois* spp.). *P*-values are given for the results from one-way analysis of variance. Statistically significant differences are noted with different letters (a–c). Error bars indicate standard errors of the mean.

small and schooling fish through predation, possibly confounding other results observed. The results of tests with one-way ANOVA indicate that the presence of scamp did not have an effect on average abundances of either small fish (P=0.442) or schooling fish (P=0.244).

Discussion

Grouper pits inhabited by red grouper were observed to have greater species diversity and fish abundances compared with the levels observed at pits not inhabited by red grouper. These higher levels likely occurred because pits with red grouper are actively maintained, with the resident grouper of a pit using its fins and mouth to keep the pit scoured down to the rock ledges. The structural complexity of a pit remains intact, providing habitat for other fish species. Once a pit loses its grouper (to fishing capture in fisheries or for another reason), the pit begins to fill in with sediment, and the exposed ledges are covered. Average abundances of both small, benthic species and larger, managed species were significantly higher in pits with a red grouper present than in those with no predator. Some of the most abundant taxa in pits with red grouper present were the striped grunt, bonnetmouths, the school bass, cardinalfish, damselfish, and anthiids. Coleman et al. (2010) also observed higher species diversity in actively maintained grouper pits in the Steamboat Lumps and Madison-Swanson MPAs, which are 358 km north of Pulley Ridge. They found the most common species observed in those pits were the yellowtail reeffish, tomtate (*Haemulon aurolineatum*), the vermilion snapper (*Rhomboplites aurorubens*), the roughtongue bass (*Pronotogrammus martinicensis*), and a scad (*Decapterus* sp.).

An unusual observation from this study is the lack of a negative effect from lionfish on fish assemblages in the grouper pits that were analyzed. Most studies that have examined the effect of the invasion of lionfish on native fish species have been conducted in shallow water and have reported that lionfish adversely affect indigenous fish species (Albins and Hixon, 2008, 2013). In a study that is analogous to our work and

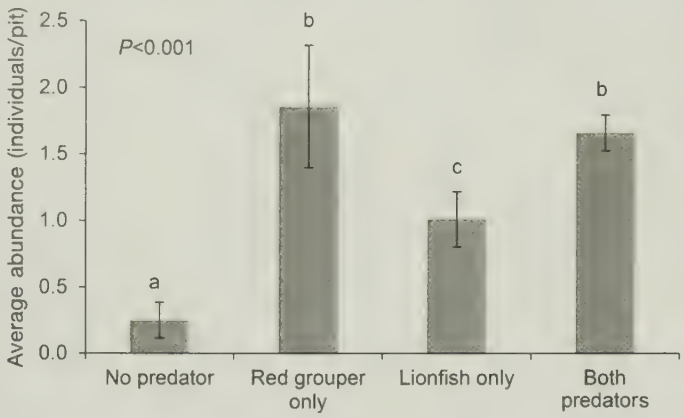

Figure 7

Average abundance, measured as number of individuals per grouper pit, of large fish, including large grunts such as the margate (*Haemulon album*) and cottonwick (*Haemulon melanurum*), snapper (*Lutjanus* spp.), grouper (*Mycteroperca* spp, *Epinephelus* spp., and the graysby, *Cephalopholis cruentata*), triggerfish (*Balistes* spp.), and the hogfish (*Lachnolaimus maximus*), associated with grouper pits surveyed during 2012–2015 off southwestern Florida, shown for each predator presence or absence category: no predator; red grouper (*Epinephelus morio*) only; species of lionfish (*Pterois* spp.) only; or both predators. The *P*-value is given for results from the Kruskal–Wallis test. Statistically significant differences are noted with different letters (a–c). Error bars indicate standard errors of the mean

was conducted by Albins (2013), native fish communities on shallow-water patch reefs in the Bahamas were compared when a native grouper (the coney [*Cephalopholis fulva*]), the lionfish, both predators together, and neither predator was present. Lionfish were found to cause a reduction in abundance of small, native coral-reef fishes 2.5 times greater than the reduction caused by the native piscivore. Lionfish also caused a reduction in the species richness of small coral-reef fishes, whereas the native piscivorous grouper had no significant effect. We observed no negative effects of presence of lionfish on the fish communities associated with mesophotic red grouper pits. Instead, pits with lionfish had both greater species diversity and species richness, and they had higher abundances of some fish species.

Although limited in number, other studies also have reported no negative effect from the invasion of lionfish. Elise et al. (2015), for example, found no significant change in the structure of the native fish assemblage or in species richness and density of potential lionfish prey, predators, and competitors over time with the arrival of lionfish in the Archipelago Los Roques National Park, Venezuela. In fact, species richness of predators and competitors of lionfish and density of predators of lionfish were higher where lionfish were present. They attributed this result to habitat characteristics and good abiotic conditions supporting high species richness and density of prey. Lionfish may therefore actively select areas where species richness and prey density are highest. Areas where lionfish are found may reflect not only favorable habitat for lionfish but also for native predators.

This explanation could also apply to Pulley Ridge. The effect of lionfish has not been documented previously for a habitat type such as grouper pits. These pits are essentially the only feature on the ridge with enough structural complexity to provide suitable habitat for both large predators and small reef fish. If high abundances of fish are actively recruiting to these pits, it is conceivable that an effect from lionfish would not be observed. An alternative explanation for the lack of a lionfish effect could be the length of time since lionfish have colonized the location. In the Albins (2013) study, during which a negative effect from lionfish was observed, data were collected 4 years after the presence of lionfish had been confirmed. In contrast, Elise et al. (2015) collected data just 1 year after lionfish were first sighted, and we began collecting data at Pulley Ridge just 2 years after lionfish were detected.

Red grouper, through their manipulation of the substrate of their habitat form structurally complex pits that play an important role in the dynamics of fish communities. Overexploitation of red grouper because of its economic value could have negative effects on biodiversity (Coleman and Williams, 2002), especially in an area like Pulley Ridge where the pits are one of the only features providing habitat refuge for any number of fish species. Although Pulley Ridge is protected, because of its status as an HAPC, the regulations (ban on longlines, trawling, and anchoring) primarily protect coral and sessile invertebrates and not any of the 12 economically valuable fish species. Conversely, hook-and-line fishing is still allowed in this otherwise protected area. The occurrence of hook-and-line fishing may explain why differences in abundance of red grouper were not observed inside versus outside the HAPC.

The presence of fish in grouper pits is significant for fisheries management because a change in pit activity and numbers may indicate the presence and abundance of economically important fish. Over time, a change in pit density may indicate changes in fish populations and could be used to either evaluate health of a stock or the effectiveness of a fishery closure. Wall et al. (2011), for example, recorded an increase in the number and density of pits from 2006 to 2009 in Steamboat Lumps MPA by mapping habitat with acoustic sonar. Gathering additional information on the variety and number of fish associated with the pits could be used to evaluate their populations as well (Scanlon et al., 2005). The data reported here on pits uninhabited and habited by red grouper will be useful for management and could be used to assess the long-term health and status of the important fish communities found in grouper pits.

Acknowledgments

This research was funded by the National Centers for Coastal Ocean Science (NOAA) under award NA-11NOS4780045 to the Cooperative Institute for Marine and Atmospheric Studies and by the Office of Ocean Exploration and Research (NOAA) under awards NA09OAR4320073 and NA14OAR4320260 to the Cooperative Institute for Ocean Exploration, Research, and Technology. We are grateful to the crews of the RV *F. G. Walton Smith* (University of Miami) and the ROV *Mohawk* (Underwater Vehicles Program, University of North Carolina at Wilmington) for their operational support.

Literature cited

Akins, J. A., J. A. Morris Jr, and S. J. Green.
2014. In situ tagging technique for fishes provides insight into growth and movement of invasive lionfish. Ecol. Evol. 4:3768–3777.

Albins, M. A.
2013 Effects of invasive Pacific red lionfish *Pterois volitans* versus a native predator on Bahamian coral-reef fish communities. Biol. Invasions 15:29–43.

Albins, M. A., and M. A. Hixon.
2008. Invasive Indo-Pacific lionfish *Pterois volitans* reduce recruitment of Atlantic coral-reef fishes. Mar. Ecol. Prog. Ser. 367:233–238.
2013. Worst case scenario: potential long-term effects of invasive predatory lionfish (*Pterois volitans*) on Atlantic and Caribbean coral-reef communities. Environ. Biol. Fish. 96:1151–1157.

Andradi-Brown, D., J. Laverick, I. Bejarano, T. Bridge, P. L. Colin, G. Eyal, R. Jones, S. E. Kahng, J. Reed, T. B. Smith, et al.
2016. Threats to mesophotic coral ecosystems and management options. *In* Mesophotic coral ecosystems—a lifeboat for coral reefs? (E. K. Baker, K. A. Puglise, and P. T. Harris, eds.), p. 67–82. The United Nations Environment Programme and GRID, Arendal, Nairobi and Arendal.

Bachelor, N. M., P. E. Whitfield, R. C. Muñoz, B. B. Harrison, C. A. Harms, and C. A. Buckel.
2015. Movement of invasive adult lionfish *Pterois volitans* using telemetry: importance of controls to estimate and explain variable detection probabilities. Mar. Ecol. Prog. Ser. 527:205–220.

Clarke, K. R.
1993. Non-parametric multivariate analyses of changes in community structure. Aust. J. Ecol. 18:117–143.

Clarke, K. R., and R. M. Warwick.
2001. Change in marine communities: an approach to statistical analysis and interpretations, 2nd ed., 172 p. PRIMER-E Ltd., Plymouth, UK.

Clarke, K. R., P. J. Somerfield, and M. G. Chapman.
2006. On resemblance measures for ecological studies, including taxonomic dissimilarities and a zero-adjusted Bray–Curtis coefficient for denuded assemblages. J. Exp. Mar. Biol. Ecol. 330:55–80.

Coleman, F. C., and S. L. Williams.
2002. Overexploiting marine ecosystem engineers: potential consequences for biodiversity. Trends Ecol. Evol. 17:40–44.

Coleman, F. C., C. C. Koenig, K. M. Scanlon, S. Heppell S. Heppel, and M. W. Miller.
2010. Benthic habitat modification through excavation by red grouper, *Epinephelus morio*, in the northeastern Gulf of Mexico. Open Fish Sci. J. 3:1–15.

Elise, S., I. Urbina-Barreto, H. Boadas-Gil, M. Galindo-Vivas, and M. Kulbicki.
2015. No detectable effect of lionfish (*Pterois volitans* and *P. miles*) invasion on a healthy reef fish assemblage in Archipelago Los Roques National Park, Venezuela. Mar. Biol. 162:319–330.

Gratwicke, B. and M. R. Speight.
2005. The relationship between fish species richness, abundance and habitat complexity in a range of shallow tropical marine habitats. J. Fish Biol. 66:650–667.

Green, S. J., and I. M. Côté.
2009. Record densities of Indo-Pacific lionfish on Bahamian coral reefs. Coral Reefs 28:107.

Green, S. J., J. L. Akins, A. Maljković, and I. M. Côté .
2012. Invasive lionfish drive Atlantic coral reef fish declines. PLoS One 7(3): e32596.

Harter, S. L., M. M. Ribera, A. N. Shepard, and J. K. Reed.
2009. Assessment of fish populations and habitat on Oculina Bank, a deep-sea coral marine protected area off eastern Florida. Fish. Bull. 107:195–206.

Hine, A. C., R. B. Halley, S. D. Locker, B. D. Jarrett, W. C. Jaap, D. J. Mallinson, K. T. Ciembronowicz, N. B. Ogden, B. T. Donahue, and D. F. Naar.
2008. Coral reefs, present and past, on the west Florida shelf and platform margin. *In* Coral reefs of the USA (B. Riegl and R. E. Dodge, eds.), p. 127–173. Springer Science+Business Media, Dordrecht, Netherlands.

Jaap, W. C., S. W. Ross, S. Brooke, and W. S. Arnold.
2015. Factors affecting coral reef fisheries in the eastern Gulf of Mexico. *In* Interrelationships between corals and fisheries (S. A. Bortone, ed.), p. 83–112. CRC Press, Boca Raton, FL.

Jarrett, B. D., A. C. Hine, R. B. Halley, D. F. Naar, S. D. Locker, A. C. Neumann, D. Twichell, C. Hu, B. T. Donahue, W. C. Jaap, et al.
2005. Strange bedfellows—a deep-water hermatypic coral reef superimposed on a drowned barrier island; southern Pulley Ridge, SW Florida platform margin. Mar. Geol. 204:295–307.

Jones, C. G., J. H. Lawton, and M. Shachak.
1994. Organisms as ecosystem engineers. Oikos 69:373–386.

Jud, Z. R., and C. A. Layman.
2012. Site fidelity and movement patterns of invasive lionfish, *Pterois* spp., in a Florida estuary. J. Exp. Mar. Biol. Ecol. 414–415:69–74.

Kulbicki, M., J. Beets, P. Chabanet, K. Cure, E. Darling, S. R. Floeter, R. Galzin, A. Green, M. Harmelin-Vivien, M. Hixon, et al.
2012. Distributions of Indo-Pacific lionfishes *Pterois* spp. in their native ranges: implications for the Atlantic invasion. Mar. Ecol. Prog. Ser. 446:189–205.

Lesser, M. P., and M. Slattery.
2011. Phase shift to algal dominated communities at mesophotic depths associated with lionfish (*Pterois volitans*) invasion on a Bahamian coral reef. Biol. Invasions 13:1855–1868.

McClanahan, T. R.
1994. Kenyan coral reef lagoon fish: effects of fishing, substrate complexity, and sea urchins. Coral Reefs 13:231–241.

Morris, J. A., Jr, and P. E. Whitfield.
2009. Biology, ecology, control and management of the invasive Indo-Pacific lionfish: an updated integrated assessment. NOAA Tech. Memo. NOS-NCCOS-99, 57 p.
Öhman, M. C., and A. Rajasuriya.
1998. Relationships between habitat structure and fish communities on coral. Environ. Biol. Fish. 53:19–31.
Phillips, N. W., D. A. Gettleson, and K. D. Spring.
1990. Benthic biological studies of the southwest Florida shelf. Am. Zool. 30:65–75.
Pielou, E. C.
1977. Mathematical ecology, 385 p. John Wiley & Sons, New York.
Reed, J. K.
2016. Pulley Ridge, Gulf of Mexico, USA. *In* Mesophotic coral ecosystems—A lifeboat for coral reefs? (E. K. Baker, K. A. Puglise, and P. T. Harris, eds.), p. 23–25. The United Nations Environment Programme and GRID, Arendal, Nairobi and Arendal.
Scanlon, K. M., F. C. Coleman, and C. C. Koenig.
2005. Pockmarks on the outer shelf in the northern Gulf of Mexico: gas-release features or habitat modifications by fish? Am. Fish. Soc. Symp. 41:301–312.
Schofield, P. J.
2009. Geographic extent and chronology of the invasion of non-native lionfish (*Pterois volitans* [Linnaeus 1758] and *P. miles* [Bennett 1828]) in the Western North Atlantic and Caribbean Sea. Aquat. Invasions 4:473–479.
2010. Update on the geographic spread of invasive lionfishes (*Pterois volitans* [Linnaeus, 1758] and *P. miles* [Bennett, 1828]) in the Western North Atlantic Ocean, Caribbean Sea and Gulf of Mexico. Aquat. Invasions 5:S117–S122.
Tamburello, N., and I. M. Côté.
2015 Movement ecology of Indo-Pacific lionfish on Caribbean coral reefs and its implications for invasion dynamics. Biol. Invasions 17:1639–1653.
Wall, C. C., B. T. Donahue, D. F. Naar, and D. A. Mann.
2011. Spatial and temporal variability of red grouper holes within Steamboat Lumps Marine Reserve, Gulf of Mexico. Mar. Ecol. Prog. Ser. 431:243–254.

Fishery Bulletin

Guidelines for authors

Contributions published in *Fishery Bulletin* describe original research in marine fishery science, fishery engineering and economics, as well as the areas of marine environmental and ecological sciences (including modeling). Preference will be given to manuscripts that examine processes and underlying patterns. Descriptive reports, surveys, and observational papers may occasionally be published but should appeal to an audience outside the locale in which the study was conducted.

Although all contributions are subject to peer review, responsibility for the contents of papers rests upon the authors and not on the editor or publisher. *Submission of an article implies that the article is original and is not being considered for publication elsewhere.*

Plagiarism and double publication are considered serious breaches of publication ethics. To verify the originality of the research in papers and to identify possible previous publication, manuscripts may be screened with plagiarism-detection software.

Manuscripts must be written in English; authors whose native language is not English are strongly advised to have their manuscripts checked by English-speaking colleagues before submission.

Once a paper has been accepted for publication, online publication takes approximately 3 weeks.

There is no cost for publication in *Fishery Bulletin.*

Types of manuscripts accepted by the journal

Articles generally range from 20 to 30 double-spaced typed pages (12-point font) and describe an original contribution to fisheries science, engineering, or economics. Tables and figures are not included in this page count, but the number of figures should not exceed one figure for every four pages of text. Articles contain the following divisions: abstract, introduction, methods, results, and discussion.

Short contributions are generally less than 15 double spaced typed pages (12-point font) and, like articles, describe an original contribution to fisheries science. They follow the same format as that for articles: abstract, introduction, results and discussion, but the results and discussion sections may be combined. They are distinguished from full articles in that they report a noteworthy new observation or discovery—such as the first report of a new species, a unique finding, condition, or event that expands our knowledge of fisheries science, engineering or economics—and do not require a lengthy discussion.

Companion articles are presented together and published together as a scientific contribution. Both articles address a closely related topic and may be articles that result from a workshop or conference. They must be submitted to the journal at the same time.

Review articles generally range from 40 to 60 double-spaced typed pages (12-point font) and address a timely topic that is relevant to all aspects of fisheries science. They should be forward thinking and address novel views or interpretations of information that encourage new avenues of research. They can be reviews based on the outcome from thematic workshops, or contributions by groups of authors who want to focus on a particular topic, or a contribution by an individual who chooses to review a research theme of broad interest to the fisheries science community. A review article will include an abstract, but the format of the article per se will be up to the authors. Please contact the Scientific Editor to discuss your ideas regarding a review article before embarking on such a project.

Preparation of manuscript

Title page should include authors' full names, mailing addresses, and the senior author's e-mail address.

Abstract should be limited to 200 words (one-half typed page), state the main scope of the research, and emphasize the authors conclusions and relevant findings. Do not review the methods of the study or list the contents of the paper. Because abstracts are circulated by abstracting agencies, it is important that they represent the research clearly and concisely.

General text must be typed in 12-point Times New Roman font throughout. A brief introduction should convey the broad significance of the paper; the remainder of the paper should be divided into the following sections: Materials and methods, Results, Discussion, and Acknowledgments. Headings within each section must be short, reflect a logical sequence, and follow the rules of subdivision (i.e., there can be no subdivision without at least two subheadings). The entire text should be intelligible to interdisciplinary readers; therefore, all acronyms, abbreviations, and technical terms should be written out in full the first time they are mentioned. Abbreviations should be used sparingly because they are not carried over to indexing databases and slow readability for those readers outside a discipline. They should never be used for the main subject (species, method) of a paper.

For general style, follow the U.S. *Government Printing Office Style Manual* (2008) [available at website] and *Scientific Style and Format: the CSE Manual for Authors, Editors, and Publishers* (2014, 8th ed.) published by the Council of Science Editors. For scientific nomenclature, use the current edition of the American Fisheries Society's *Common and Scientific Names of*

Fishes from the United States, Canada, and Mexico and its companion volumes (*Decapod Crustaceans, Mollusks, Cnidaria and Ctenophora*, and *World Fishes Important to North Americans*). For species not found in the above mentioned AFS publications and for more recent changes in nomenclature, use the Integrated Taxonomic Information System (ITIS) (available at website), or, secondarily, the California Academy of Sciences *Catalog of Fishes* (available at website) for species names not included in ITIS. Common (vernacular) names of species should be lowercase. Citations must be given of taxonomic references used for the identification of specimens. For example, "Fishes were identified according to Collette and Klein-MacPhee (2002); sponges were identified according to Stone et al. (2011)."

Dates should be written as follows: 11 November 2000. Measurements should be expressed in metric units, e.g., 58 metric tons (t); if other units of measurement are used, please make this fact explicit to the reader. Use numerals, not words, to express whole and decimal numbers in the general text, tables, and figure captions (except at the beginning of a sentence). For example: We considered 3 hypotheses. We collected 7 samples in this location. Use American spelling. Refrain from using the shorthand slash (/), an ambiguous symbol, in the general text.

Word usage and grammar that may be useful are the following:

- *Aging* For our journal, the word *aging* is used to mean both age determination and the aging process (senescence). Authors should make clear which meaning is intended where ambiguity may arise.

- *Fish and fishes* For papers on taxonomy and biodiversity, the plural of *fish* is *fishes,* by convention. In all other instances, the plural is *fish.*

  Examples:
  The fishes of Puget Sound [biodiversity is indicated];
  The number of fish caught that season [no emphasis on biodiversity];
  The fish were caught in trawl nets [no emphasis on biodiversity].
  The same logic applies to the use of the words *crab* and *crabs, squid* and *squids,* etc.

- *Sex* For the meaning of male and female, use the word *sex*, not *gender.*

- *Participles* As adjectives, participles must modify a specific noun or pronoun and make sense with that noun or pronoun.

  Incorrect:
  Using the recruitment model, estimates of age-1 recruitment were determined. [Estimates were not using the recruitment model.]

  Correct:
  Using the recruitment model, we determined age-1 estimates of recruitment. [The participle now modifies the word *we,* i.e., those who were using the model.]

  Incorrect:
  Based on the collected data, we concluded that the mortality rate for these fish had increased. [*We* were not based on the collected data.]

  Correct:
  We concluded, on the basis of the collected data, that the mortality rate for these fish had increased. [Eliminate the participle and replace it with the adverbial phrase *on the basis of.*]

Equations and mathematical symbols should be set from a standard mathematical program (MathType) and tool (Equation Editor in MS Word). LaTex is acceptable for more advanced computations. For mathematical symbols in the general text (α, χ^2, π, $\pm$, etc.), use the symbols provided by the MS Word program and italicize all variables, except those variables represented by Greek letters. Do not use photo mode when creating these symbols in the general text and do not cut and paste equations and letters or symbols of variables from a different software program.

Number equations (if there are more than 1) for future reference by scientists; place the number within parentheses at the end of the first line of the equation.

Literature cited section comprises published works and those accepted for publication in peer-reviewed journals (in press). Follow the name and year system for citation format in the "Literature cited" section (that is to say, citations should be listed alphabetically by the authors' last names, and then by year if there is more than one citation with the same authorship. A list of abbreviations for citing journal names can be found at website.

Authors are responsible for the accuracy and completeness of all citations. Literature citation format: Author (last name, followed by first-name initials). Year. Title of article. Abbreviated title of the journal in which it was published. Always include number of pages. For a sequence of citations in the general text, list chronologically: (Smith, 1932: Green. 1947; Smith and Jones, 1985).

Acknowledgments should be no more than 6 lines of text. Only those who have contributed in an outstanding way should be acknowledged by name. For recognition of other persons or groups, use a general term, such as "crew," "observers," "research coordinators," and do not include names with these terms.

Digital object identifier (doi) code ensures that a publication has a permanent location online. Doi code should be included at the end of citations of published litera-

ture. Authors are responsible for submitting accurate doi codes. Faulty codes will be deleted at the page-proof stage.

Cite all software, special equipment, and chemical solutions used in the study within parentheses in the general text: e.g., SAS, vers. 6.03 (SAS Inst., Inc., Cary, NC).

Footnotes are used for all documents that have not been formally peer reviewed and for observations and personal communications. These types of references should be cited sparingly in manuscripts submitted to the journal.

All reference documents, administrative reports, internal reports, progress reports, project reports, contract reports, personal observations, personal communications, unpublished data, manuscripts in review, and council meeting notes are footnoted in 9 pt font and placed at the bottom of the page on which they are first cited. Footnote format is the same as that for formal literature citations. A link to the online source (e.g., [http://www/..... , accessed July 2007.]), or the mailing address of the agency or department holding the document, should be provided so that readers may obtain a copy of the document.

Tables are often overused in scientific papers; it is seldom necessary to present all the data associated with a study. Tables should not be excessive in size and must be cited in numerical order in the text. Headings should be short but ample enough to allow the table to be intelligible on its own.

All abbreviations and unusual symbols must be explained in the table legend. Other incidental comments may be footnoted with italic numeral footnote markers. Use asterisks only to indicate significance in statistical data. Do not type table legends on a separate page; place them above the table data. *Do not submit tables in photo mode.*

- Note probability with a capital, italic *P*.
- Provide a zero before all decimal points for values less than one (e.g., 0.07).
- Round all values to 2 decimal points.
- Use a comma in numbers of five digits or more (e.g., 13,000 but 3000).

Figures must be cited in numerical order in the text. Graphics should aid in the comprehension of the text, but they should be limited to presenting patterns rather than raw data. Figures should not exceed one figure for every four pages of text and must be labeled with the number of the figure. Place labels **A, B, C,** etc. within the upper left area of graphs and photos. Avoid placing labels vertically (except for the y axis).

Figure legends should explain all symbols and abbreviations seen in the figure and should be double-spaced on a separate page at the end of the manuscript.

Line art and halftone figures should be saved at a resolution of >800 dpi (dots per inch) and >300 dpi, respectively. Color is allowed in figures to show morphological differences among species (i.e., for species identification), to show stain reactions, and to show gradations, such as those of temperature and salinity within maps. Color is discouraged in graphs. For the few instances where color is allowed, the use of color will be determined by the Managing Editor. Figures approved for color should be saved in CMYK format.

All figures must be submitted as either PDF of EPS files.

- Capitalize the first letter of the first word in all labels within figures.
- Do not use overly large font sizes in maps and for axis labels in graphs.
- Do not use bold fonts or bold lines in figures.
- Do not place outline rules around graphs.
- Place a North arrow and label degrees latitude and longitude (e.g., 170°E) in all maps.
- Use symbols, shadings, or patterns (not clip art) in maps and graphs.

Supplementary materials that are considered essential, but are too large or impractical for inclusion in a paper (e.g., metadata, figures, tables, videos, websites), may be provided at the end of an article. These materials are subject to the editorial standards of the journal. A URL to the supplementary material and a brief explanation for including such material should be sent at the time of initial submission of the paper to the journal.

- **Metadata, figures, and tables** should be submitted in standard digital format (Word docx) and should be cited in the general text as (Suppl. Table, Suppl. Fig., etc.).
- **Websites** should be cited as (Suppl. website) in the general text and be made available with doi code (if possible) at the end of the article.
- **Videos** must not be larger than 30 MB to allow a swift technical response for viewing the video. Authors should consider whether a short video uniquely captures what text alone cannot capture for the understanding of a process or behavior under examination in the article. Supply an online link to the location of the video.

Copyright law does not apply to *Fishery Bulletin,* which falls within the public domain. However, if an author reproduces any part of an article from *Fishery Bulletin*, reference to source is considered correct form (e.g., Source: Fish. Bull. 97:105).

Failure to follow these guidelines and failure to correspond with editors in a timely manner will delay publication of a manuscript.

Submission of manuscript

Submit manuscript online at the ScholarOne website. Commerce Department authors should submit papers under a completed NOAA Form 25-700. For further details on electronic submission, please contact the Associate Editor, Kathryn Dennis, at

kathryn.dennis@noaa.gov

When requested, the text and tables should be submitted in Word format. Figures should be sent as separate PDF or EPS files. Send a copy of figures in the original software if conversion to any of these formats yields a degraded version of the figure.

Questions? If you have questions regarding these guidelines, please contact the Managing Editor, Sharyn Matriotti, at

sharyn.matriotti@noaa.gov

Questions regarding manuscripts under review should be addressed to Kathryn Dennis, Associate Editor.

Fishery Bulletin

Subscription form

Superintendent of Documents **Publications** Order Form

*5178

☐ YES, please send me the following publications:

____ Subscriptions to *Fishery Bulletin*
for $32.00 per year ($44.80 foreign)

The total cost of my order is $ _____ . Prices include regular domestic postage and handling and are subject to change.

_____
(Company or Personal Name) (Please type or print)

_____
(Additional address/attention line)

_____
(Street address)

_____
(City, State, ZIP Code)

_____
(Daytime phone including area code)

_____
(Purchase Order No.)

Charge your order. IT'S EASY!

VISA

MasterCard

Please Choose Method of Payment:

☐ Check payable to the Superintendent of Documents

☐ GPO Deposit Account ☐☐☐☐☐☐☐–☐

☐ VISA or MasterCard Account

☐☐☐☐☐☐☐☐☐☐☐☐☐☐☐☐

☐☐☐☐ (Credit card expiration date)

To fax your orders (202) 512-2104

_____
(Authorizing Signature)

Mail to: Superintendent of Documents
P.O. Box 979050, St. Louis, Missouri 63197
Tel. no. (U.S. callers): 866-512-1800
Tel. no. (International callers): 1-202-512-1800

Thank you for your order!

Also available online at
http://bookstore.gpo.gov/actions/GetPublication.do?stocknumber=703-023-00000-2
email: ContactCenter@gpo.gov